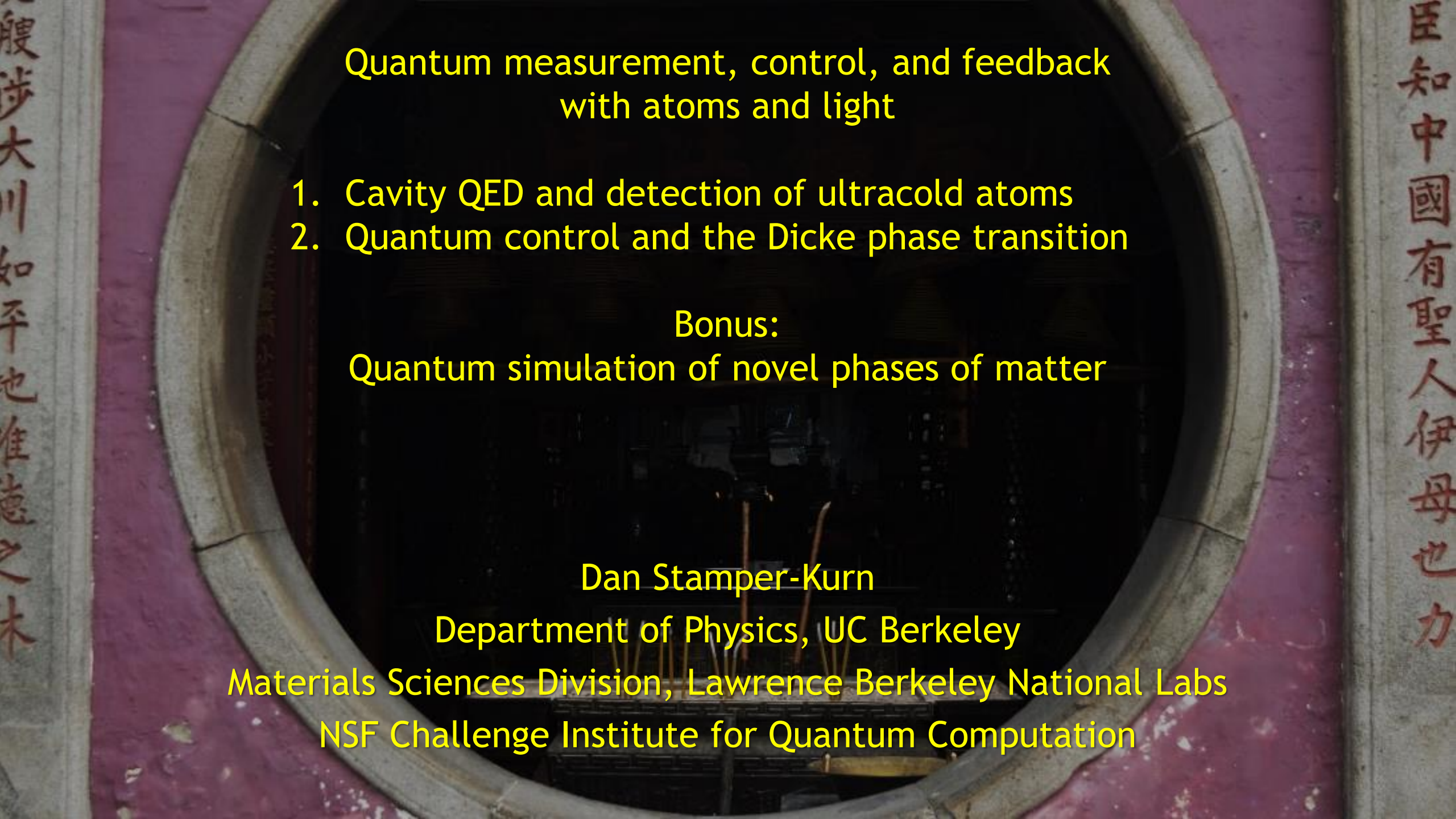


Quantum measurement, control, and feedback with atoms and light

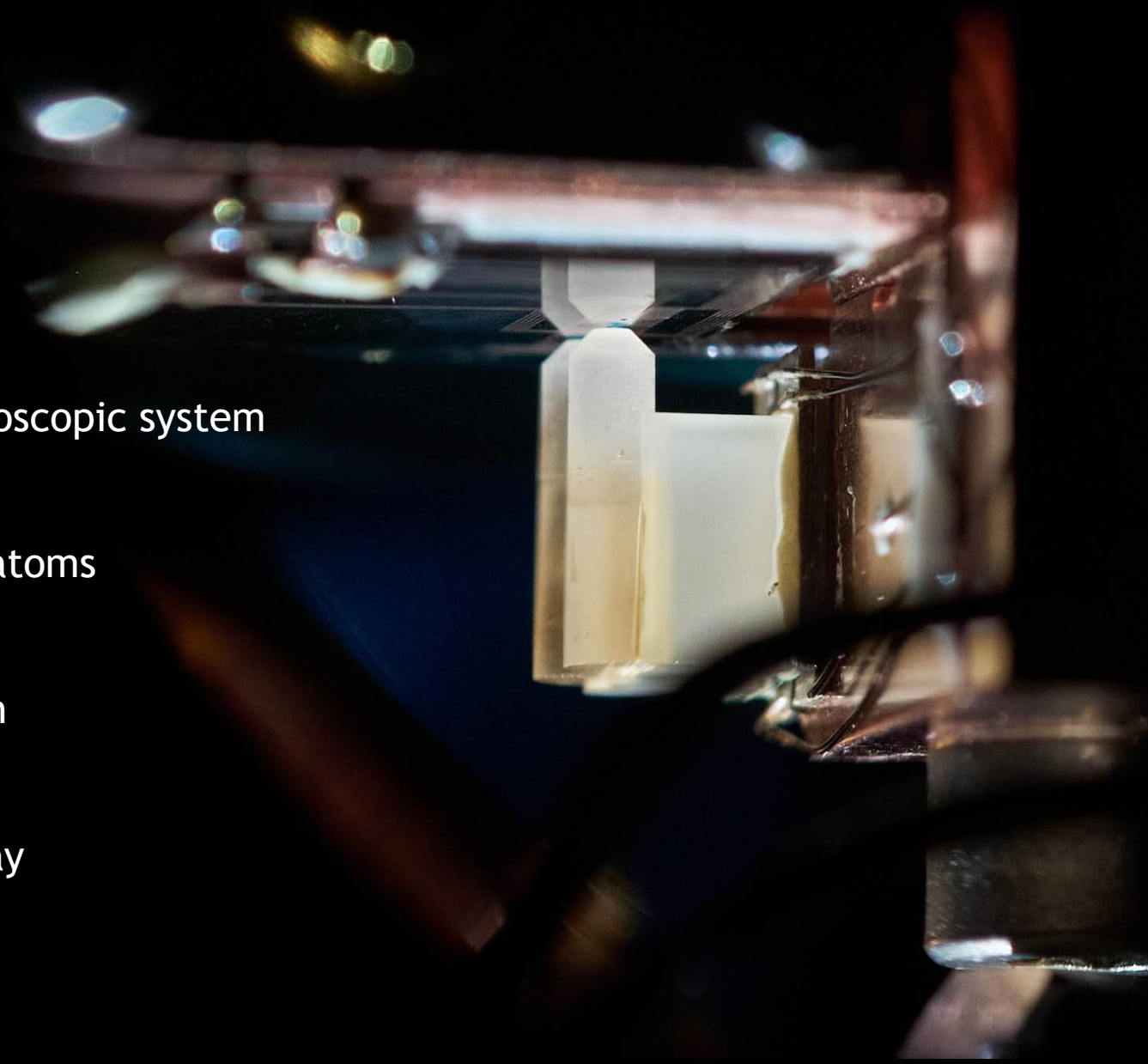
1. Cavity QED and detection of ultracold atoms
2. Quantum control and the Dicke phase transition

Bonus:
Quantum simulation of novel phases of matter

Dan Stamper-Kurn
Department of Physics, UC Berkeley
Materials Sciences Division, Lawrence Berkeley National Labs
NSF Challenge Institute for Quantum Computation

Cavity QED and detection of ultracold atoms

- Primer on cavity QED
- How to position atoms in an optical cavity
- Cavity-enhanced detection of atom number
  - Non-equilibrium thermodynamics in a mesoscopic system
- Cavity-enhanced detection of atomic position
  - Quantum cavity optomechanics with cold atoms
- Cavity-enhanced detection of atomic spin
  - Coherent and incoherent cavity backaction
- Cavity-enhanced detection of single atoms:
  - Mid-circuit measurement in a tweezer array



Quantum mechanics: then

first appearance of the term
“quantum mechanics”

Born, Z. Physik **26**, 379 (1924)

Über Quantenmechanik.

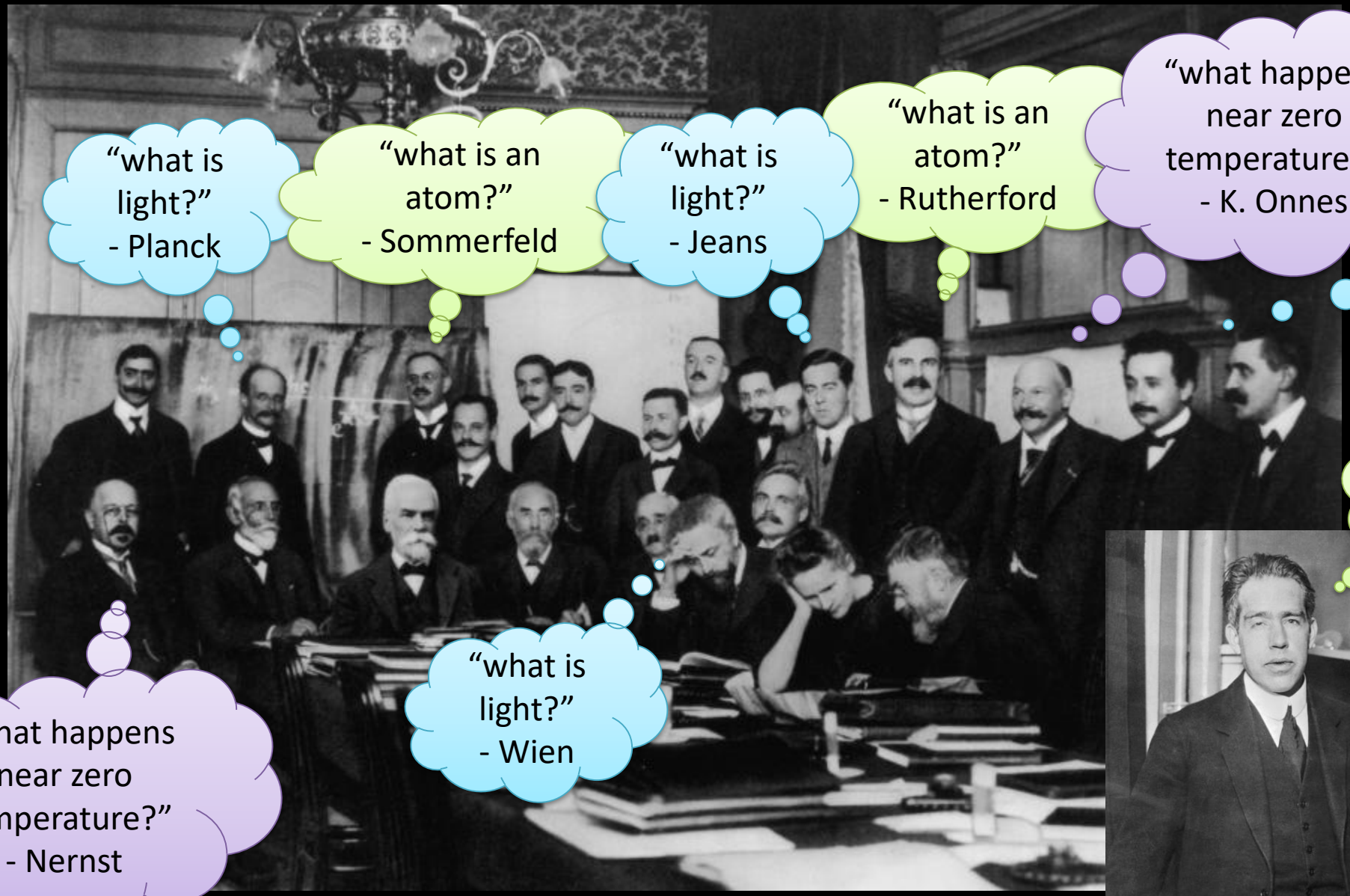
Von **M. Born** in Göttingen.

(Eingegangen am 13. Juni 1924.)

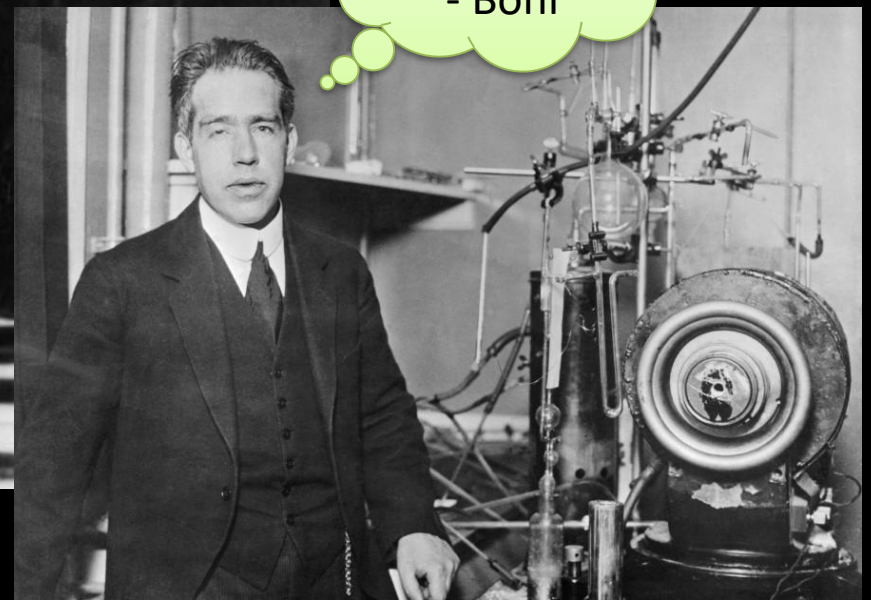
Die Arbeit enthält einen Versuch, den ersten Schritt zur Quantenmechanik der Kopplung aufzustellen, welcher von den wichtigsten Eigenschaften der Atome (Stabilität, Resonanz für die Sprungfrequenzen, Korrespondenzprinzip) Rechenschaft gibt und in natürlicher Weise aus den klassischen Gesetzen entsteht. Diese Theorie enthält die Dispersionsformel von Kramers und zeigt eine enge Verwandtschaft zu Heisenbergs Formulierung der Regeln des anomalen Zeemaneffekts.

Einleitung. Das Versagen der Quantentheorie in allen Fällen, wo es sich um Bewegungen mehrerer Elektronen handelt (z. B. beim Helium), ist schon mehrfach darauf zurückgeführt worden, daß dabei auf jedes Elektron ein Wechselfeld wirkt, dessen Frequenz von derselben Größenordnung ist wie bei einer Lichtwelle. Da man nun weiß, daß die Atome auf Lichtwellen unter Umständen gänzlich „unmechanisch“ reagieren (nämlich zu Quantensprüngen angeregt werden), so wird man auch nicht erwarten dürfen, daß die Wechselwirkung zwischen Elektronen desselben Atoms nach den Gesetzen der klassischen Mechanik erfolgt; damit wird die Anwendung der durch Quantenregeln ergänzten klassischen Störungstheorie zur Berechnung der stationären Bahnen hinfällig. Solange man die Gesetze der Einwirkung des Lichtes auf Atome, also den Zusammenhang der Dispersion mit dem Atombau und den Quantensprüngen, nicht kennt, wird man erst recht über die Gesetze der Wechselwirkung zwischen mehreren Elektronen eines Atoms im Dunkeln sein.

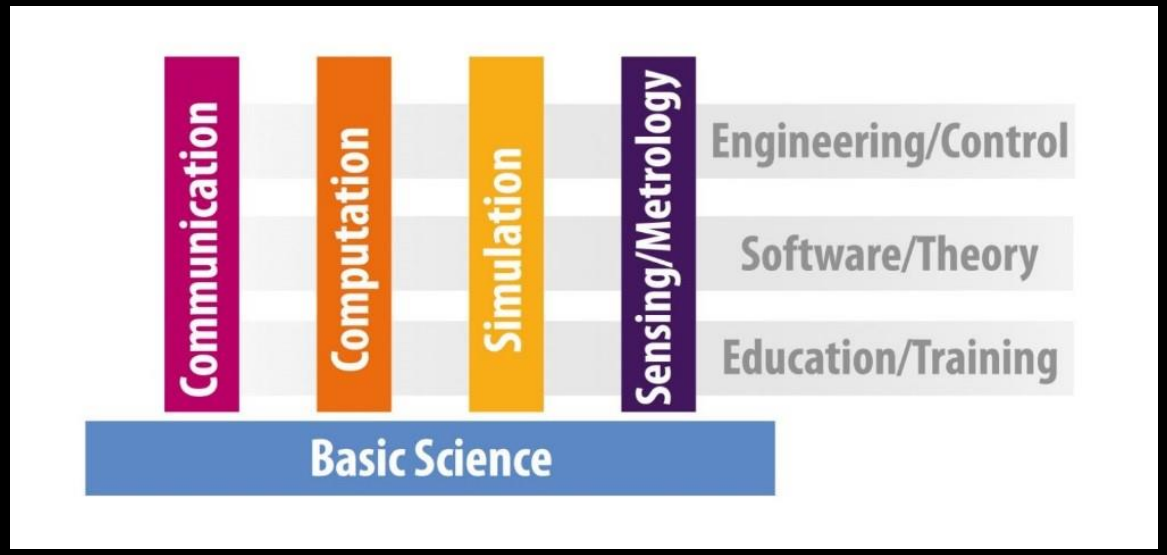
Quantum mechanics: then



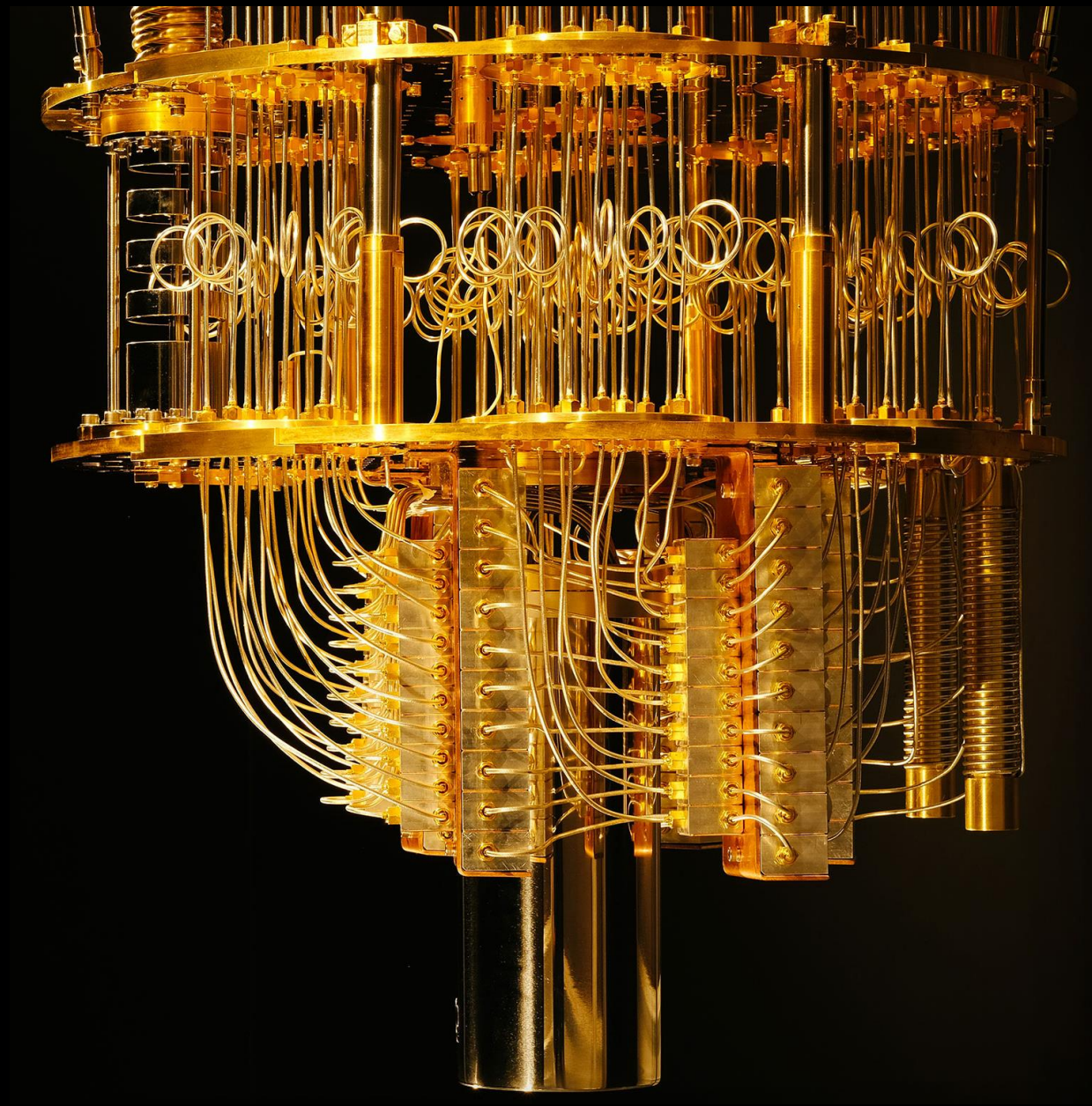
First Solvay Conference on Physics, 1911



Quantum mechanics: now

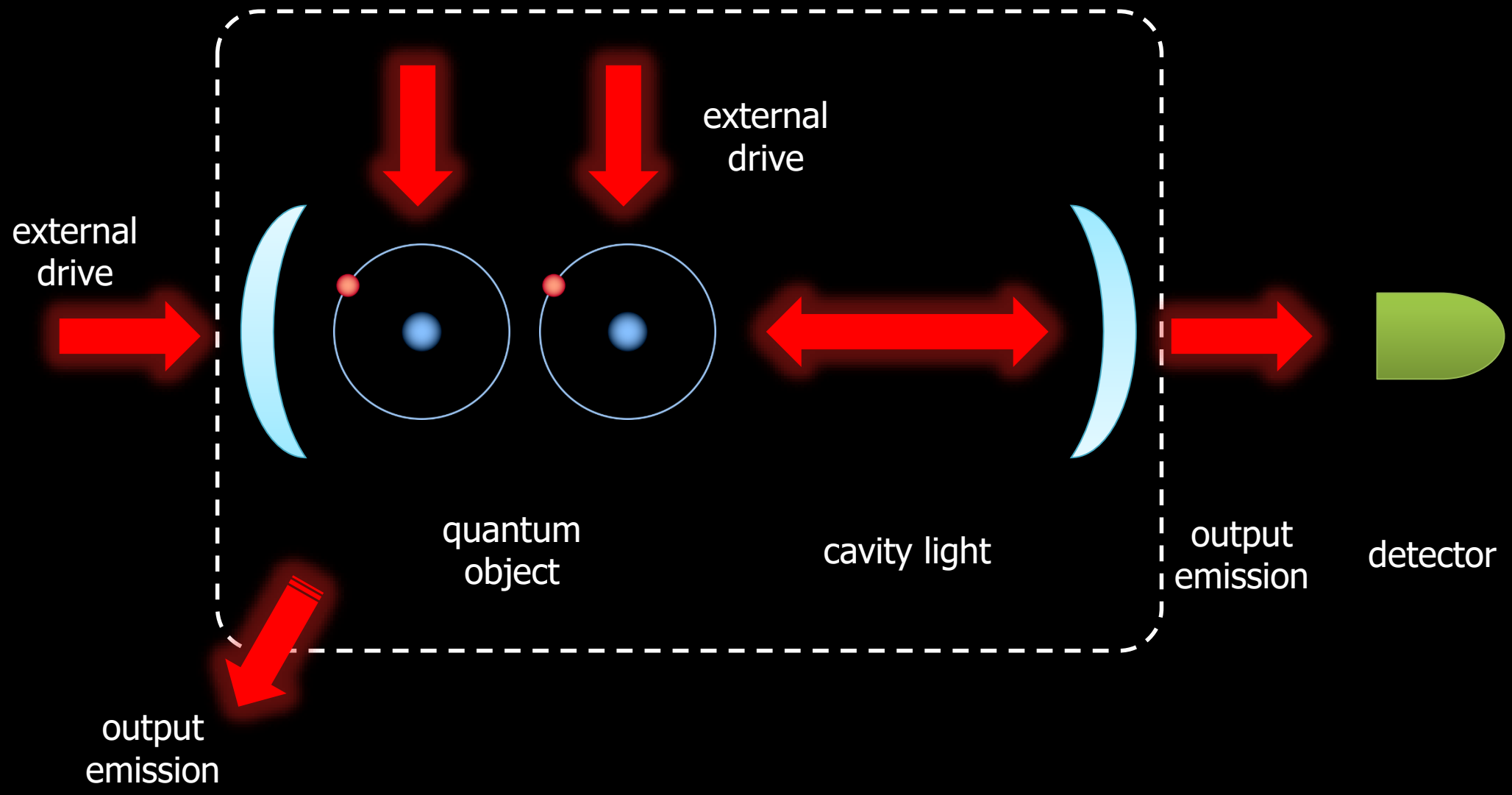


European Commission,
“Quantum technologies flagship final report,” 2017

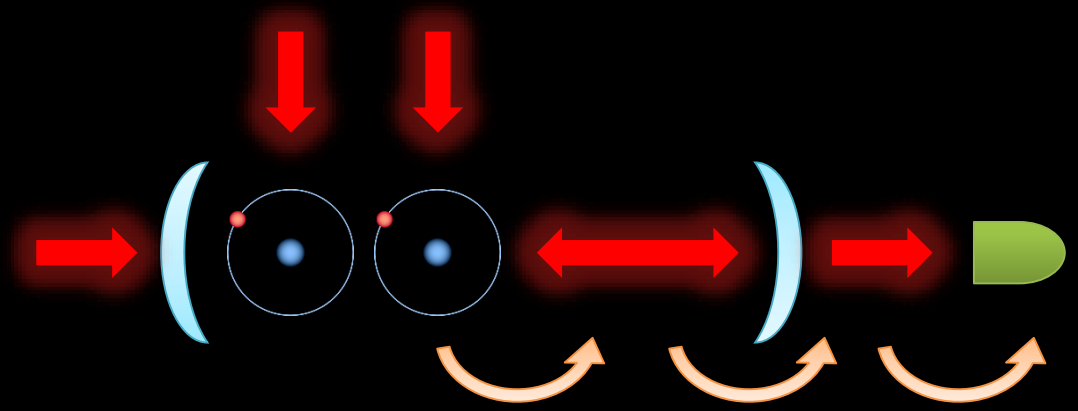


Building quantum systems and devices with ultracold atoms and light

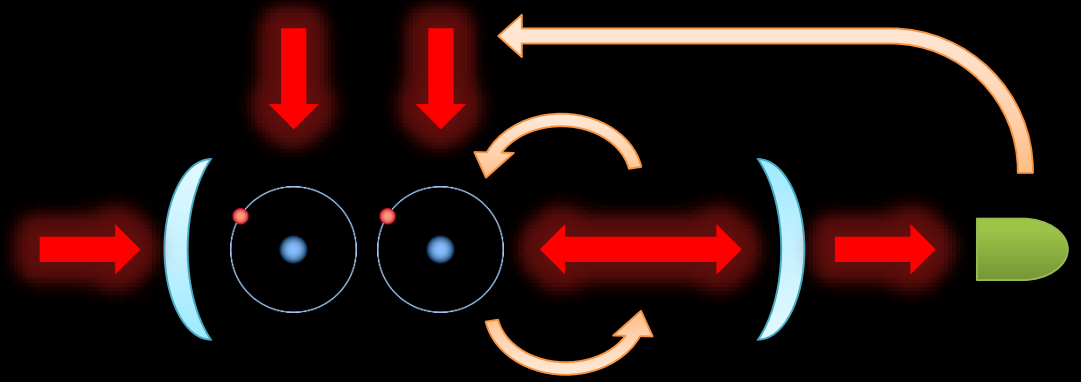
Cavity quantum electrodynamics (QED)



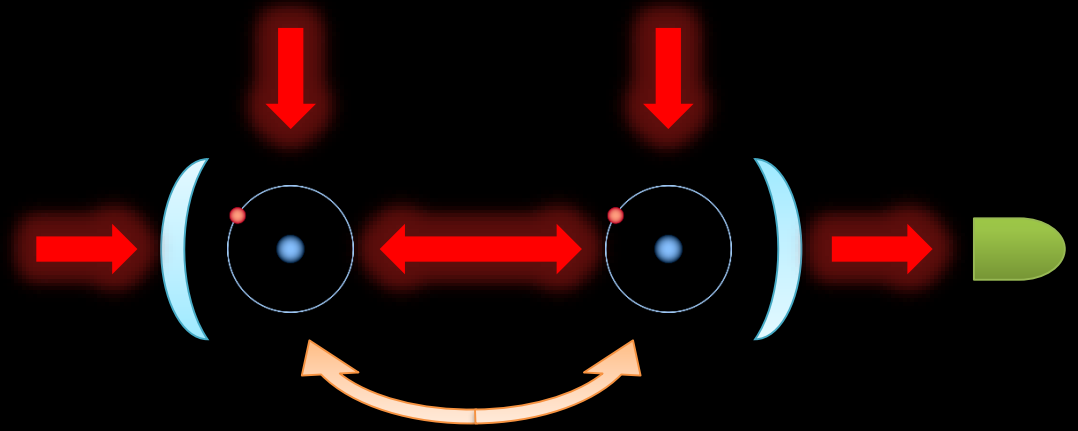
detection of quantum systems



feedback control



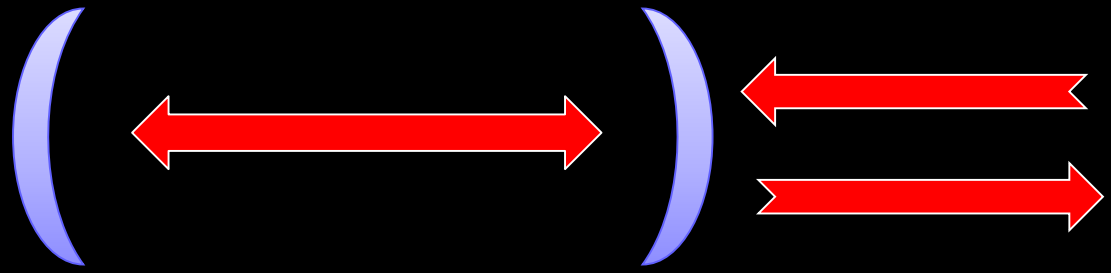
interactions/entanglement/gates by photon exchange



… and much more!

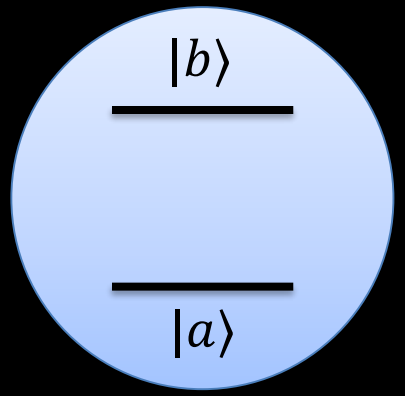
- entangled matter -> entangled light
- quantum networks
- …

A primer on cavity quantum electrodynamics



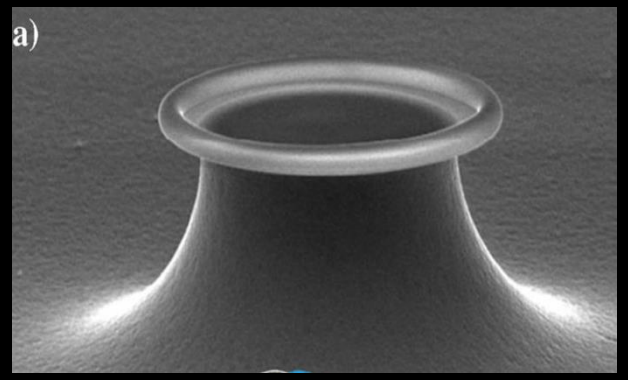
electromagnetic resonator
coupled weakly to continuum of outside modes

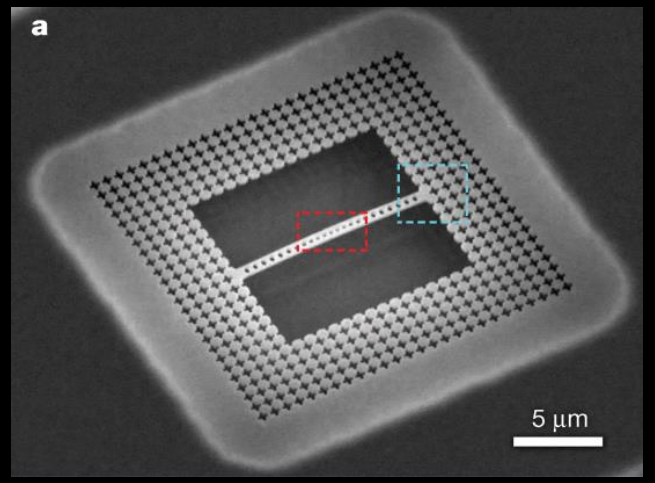


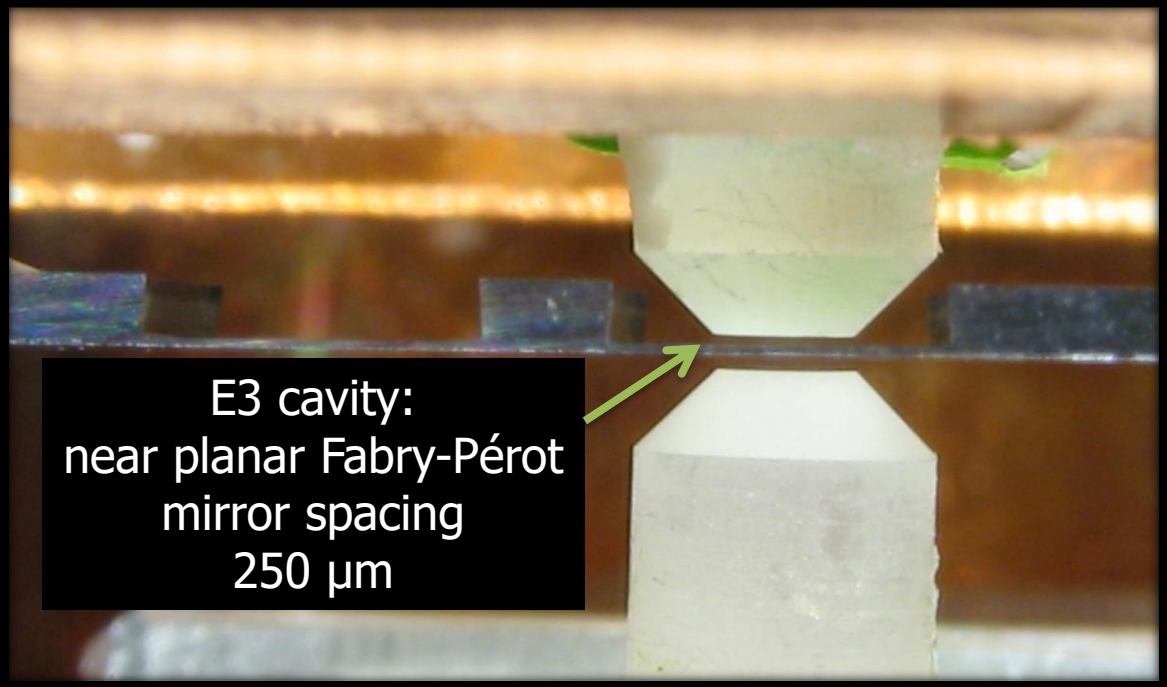


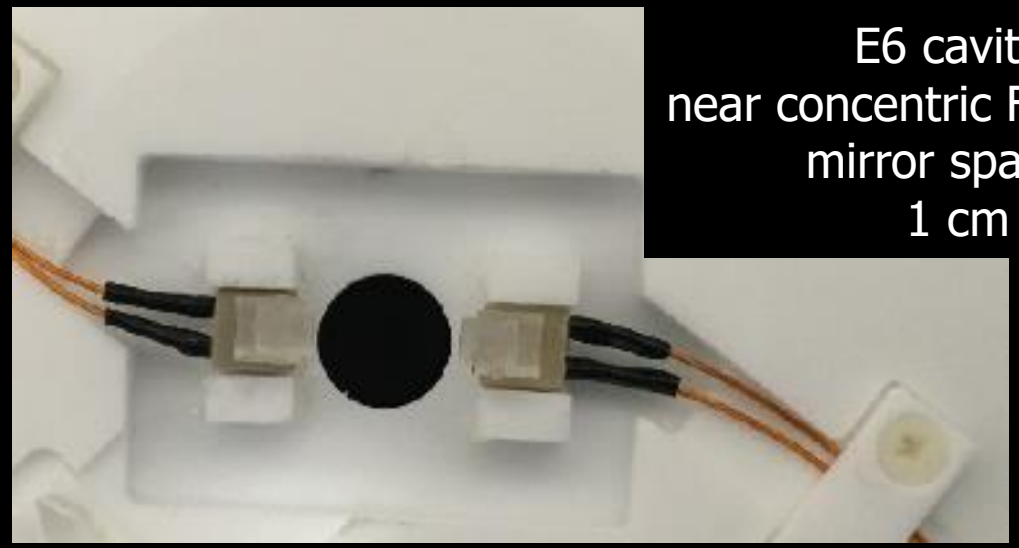
quantum emitter

Real resonators





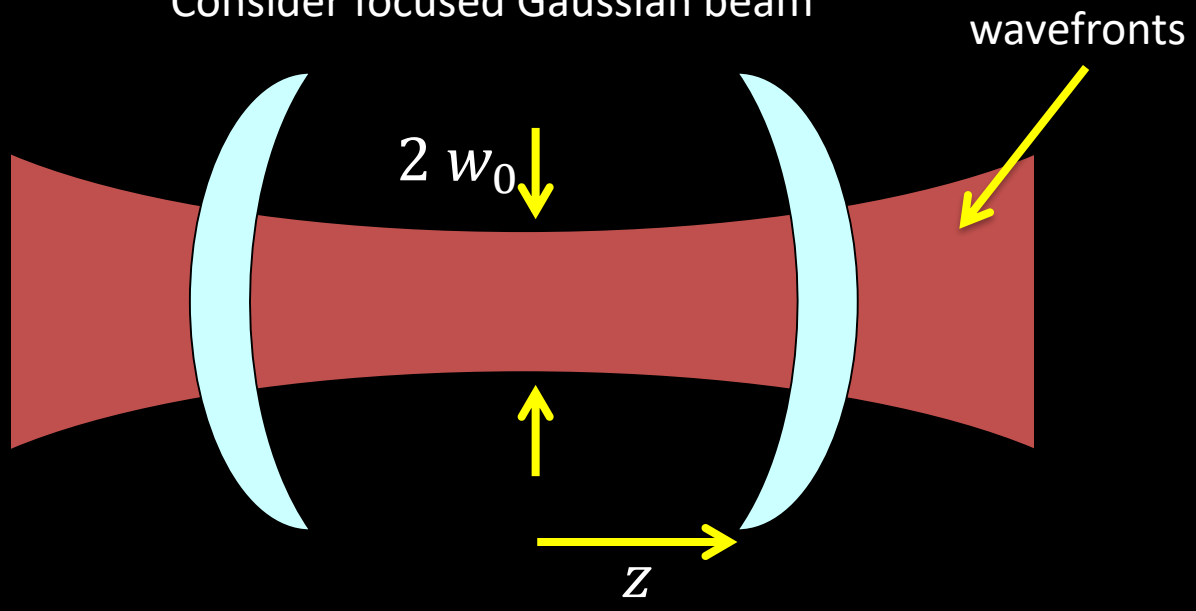




E6 cavity:
near concentric Fabry-Pérot
mirror spacing
1 cm

Fabry-Pérot optical resonator

Consider focused Gaussian beam



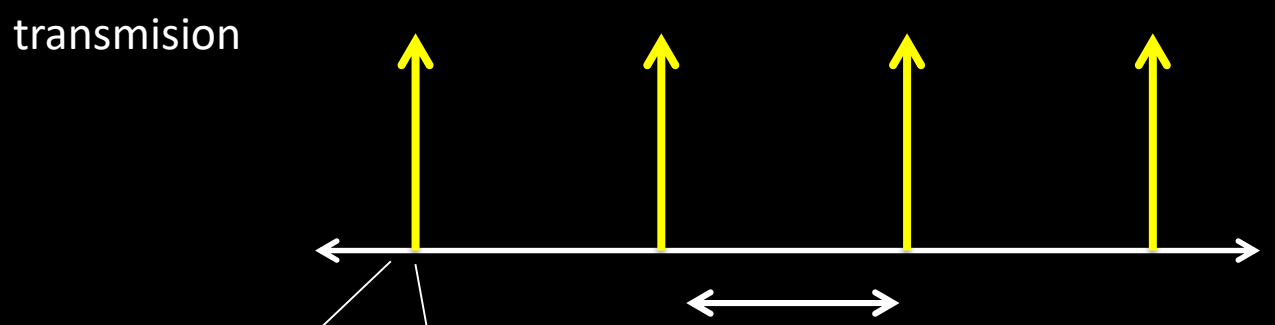
Cavity mode: wavefronts match mirror curvature

$$R(z) = \frac{1}{z}(z^2 + z_0^2) \qquad z_0 = \frac{\pi w_0^2}{\lambda}$$

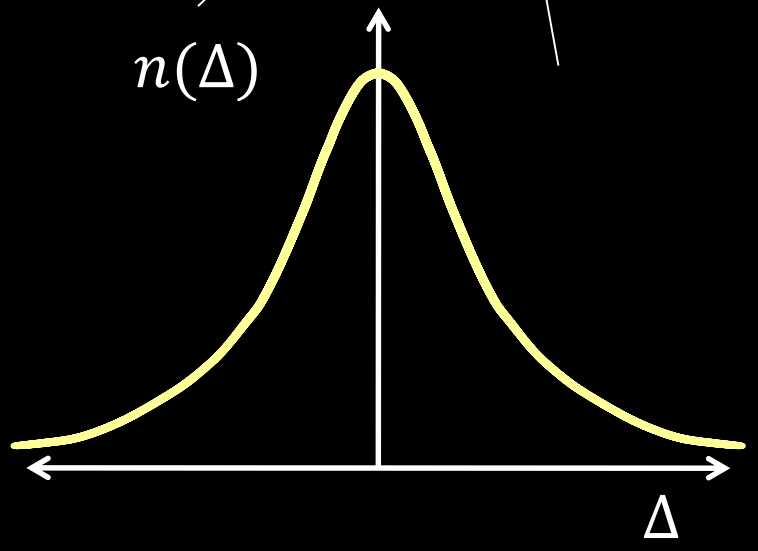
E3 cavity: 5 cm radius of curvature, 250 µm spacing: z_0 = 2.5 mm, w_0 = 25 µm at λ = 780 nm

E6 cavity: 5 mm radius of curvature, (1 cm – 500 µm) spacing: z_0 = 1.1 mm, w_0 = 16 µm at λ = 780 nm

Fabry-Pérot optical resonator



$$FSR = \frac{c}{2l} = 300 \text{ GHz}$$



$$n(\Delta) = n_{max} \frac{1}{1 + \Delta^2/\kappa^2}$$

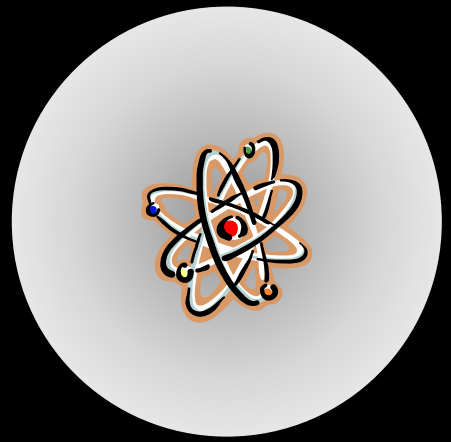
$$\kappa = \text{FSR} \times (round\ trip\ loss)$$

Example E3: transmission = (1.5, 12) ppm
scattering loss = 25 ppm (oops)

$$\kappa = 2\,\pi \times 1.8 \text{ MHz}$$

Quantum emitter = atom

real complicated atom



$\simeq$



electron on spring

dipole matrix element: $e\sqrt{\frac{\hbar}{2\,m\,\omega_0}}$

spontaneous emission rate: $\Gamma = \frac{1}{2}\left(\frac{e^2}{3\,\pi m}\frac{\omega_0^3}{c^3}\right) = 2\,\pi \times 3$ MHz

Single atom + single photon coupling

electron on spring

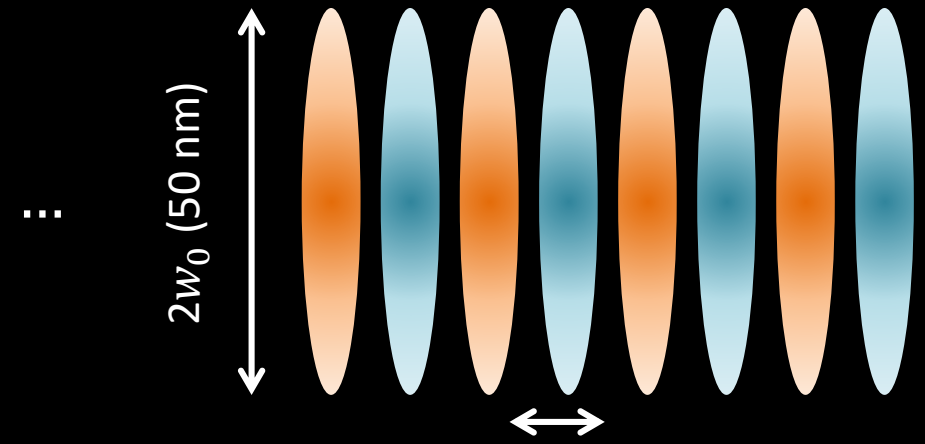
$$g_{CQED} = \frac{1}{\hbar} d\, E$$

electric field that puts one photon energy into cavity mode

near cavity center:

$$E = \sqrt{\frac{\hbar\omega_0}{\epsilon_0\, Vol}} \exp\left(\frac{x^2+y^2}{w_0^2}\right) \cos kz$$

$g_{CQED}(\vec{r})$

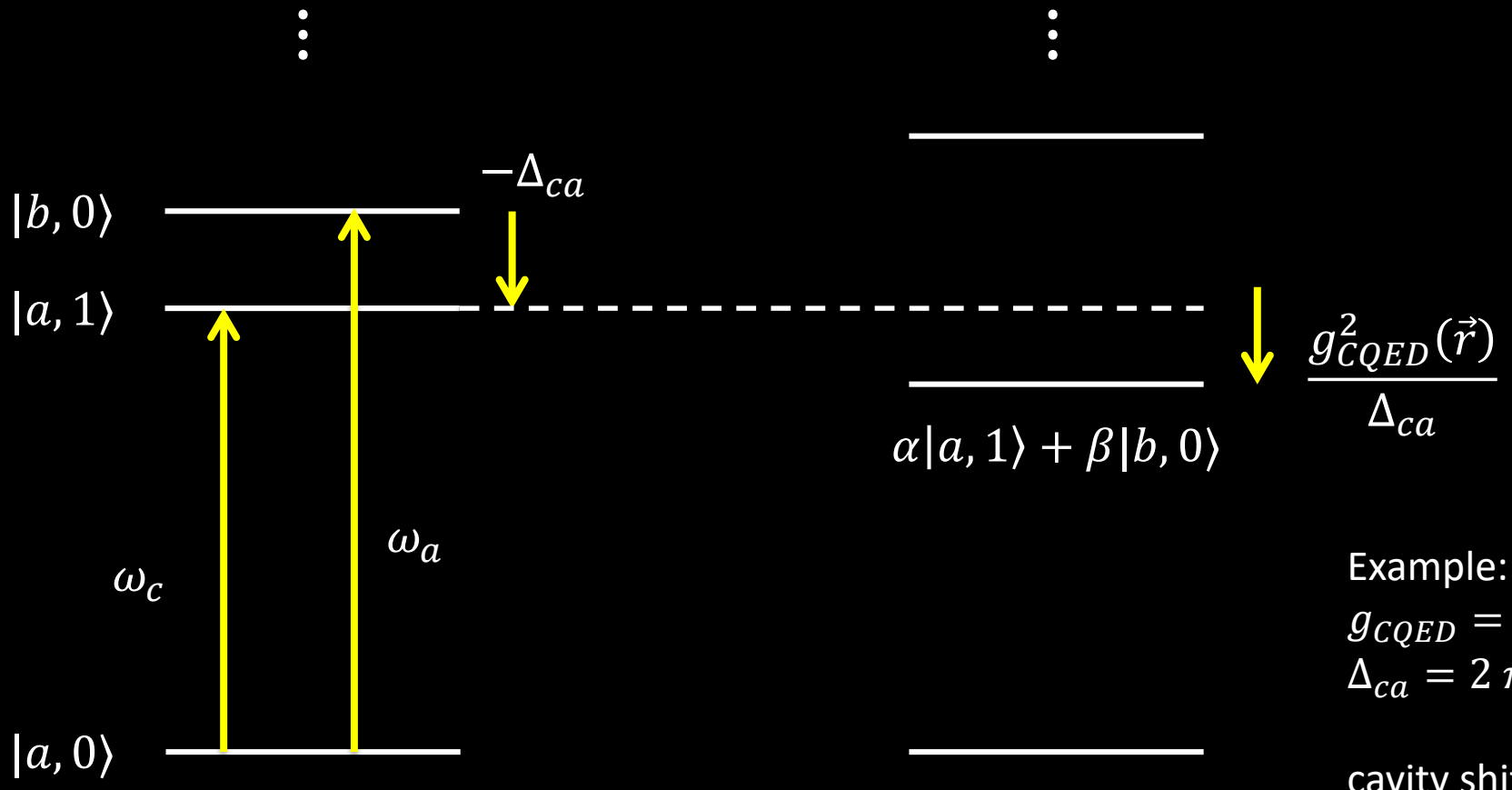


peak magnitude:

$$\frac{1}{\hbar}\left(\frac{e^2}{m\,\epsilon_0 Vol}\right)^{\frac{1}{2}}$$

$$= 2\,\pi \times 13 \text{ MHz}$$

Dispersion by a single atom



no atom-cavity coupling

with atom-cavity coupling

Example:

$g_{CQED} = 2\pi \times 13$ MHz

$\Delta_{ca} = 2\pi \times 30$ GHz

cavity shift per atom:

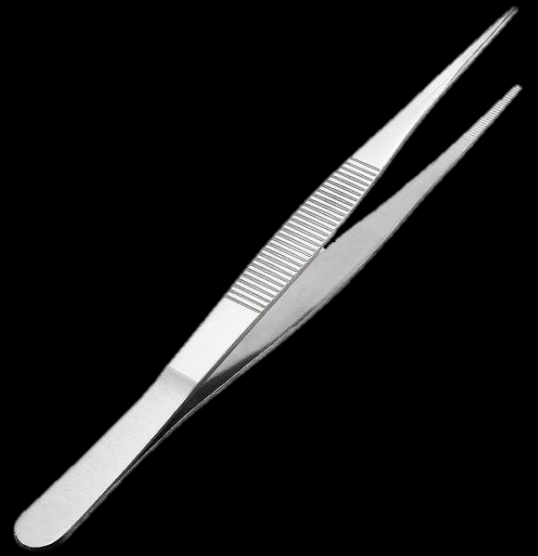
$\frac{g_{CQED}^2}{\Delta_{ca}} = 2\pi \times 5.6$ kHz

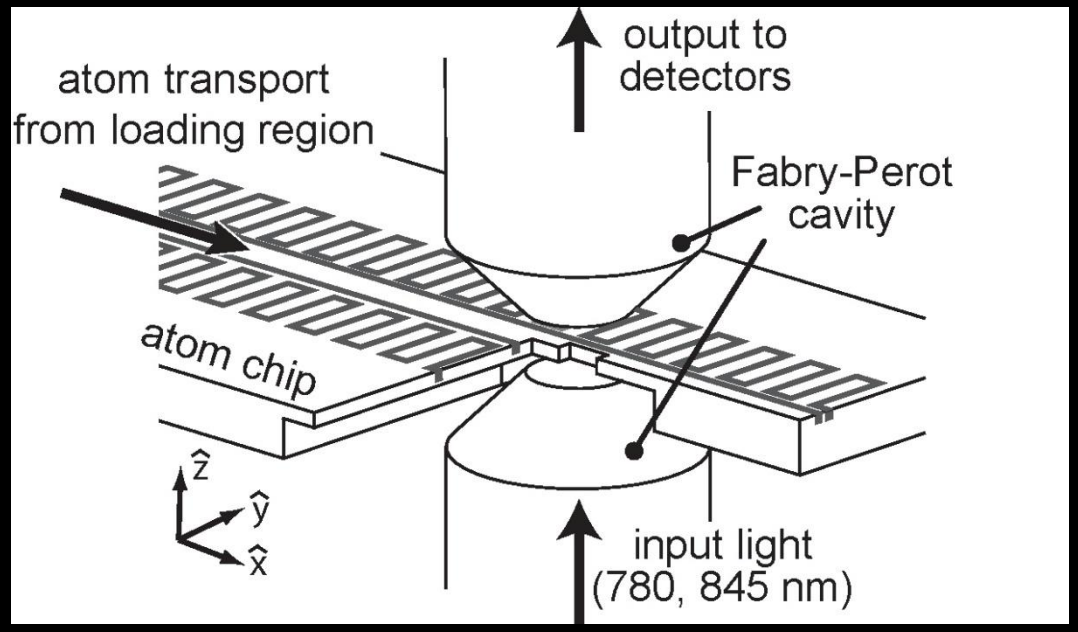
How to position atom(s) in an optical cavity

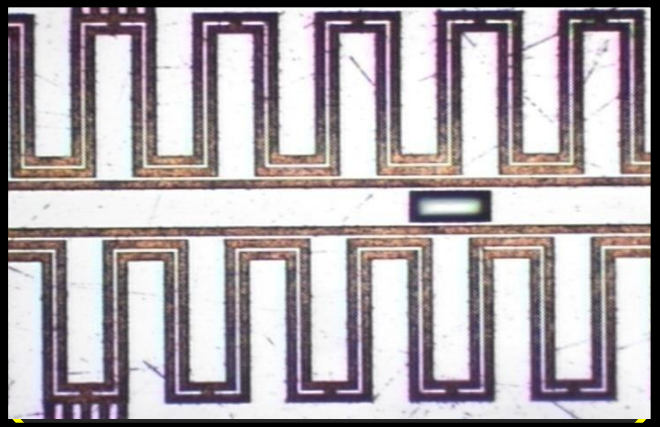
- The old way: atomic ensembles in magnetic or optical traps
  (roughly 1990 – 2020)

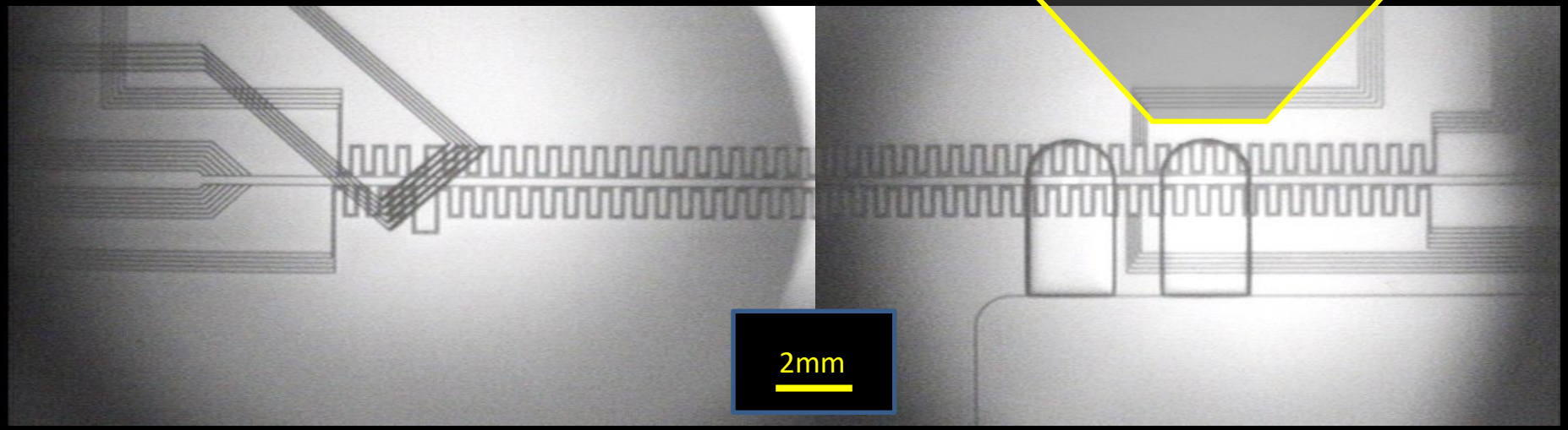


- The new way: single atoms in optical tweezers
  (roughly 2020 - present)





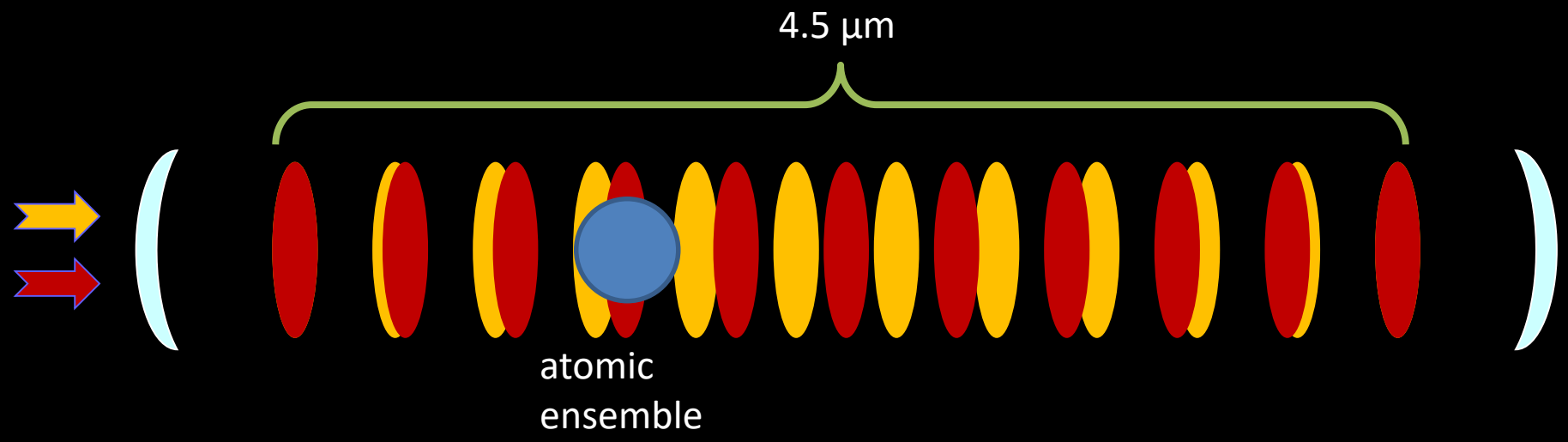




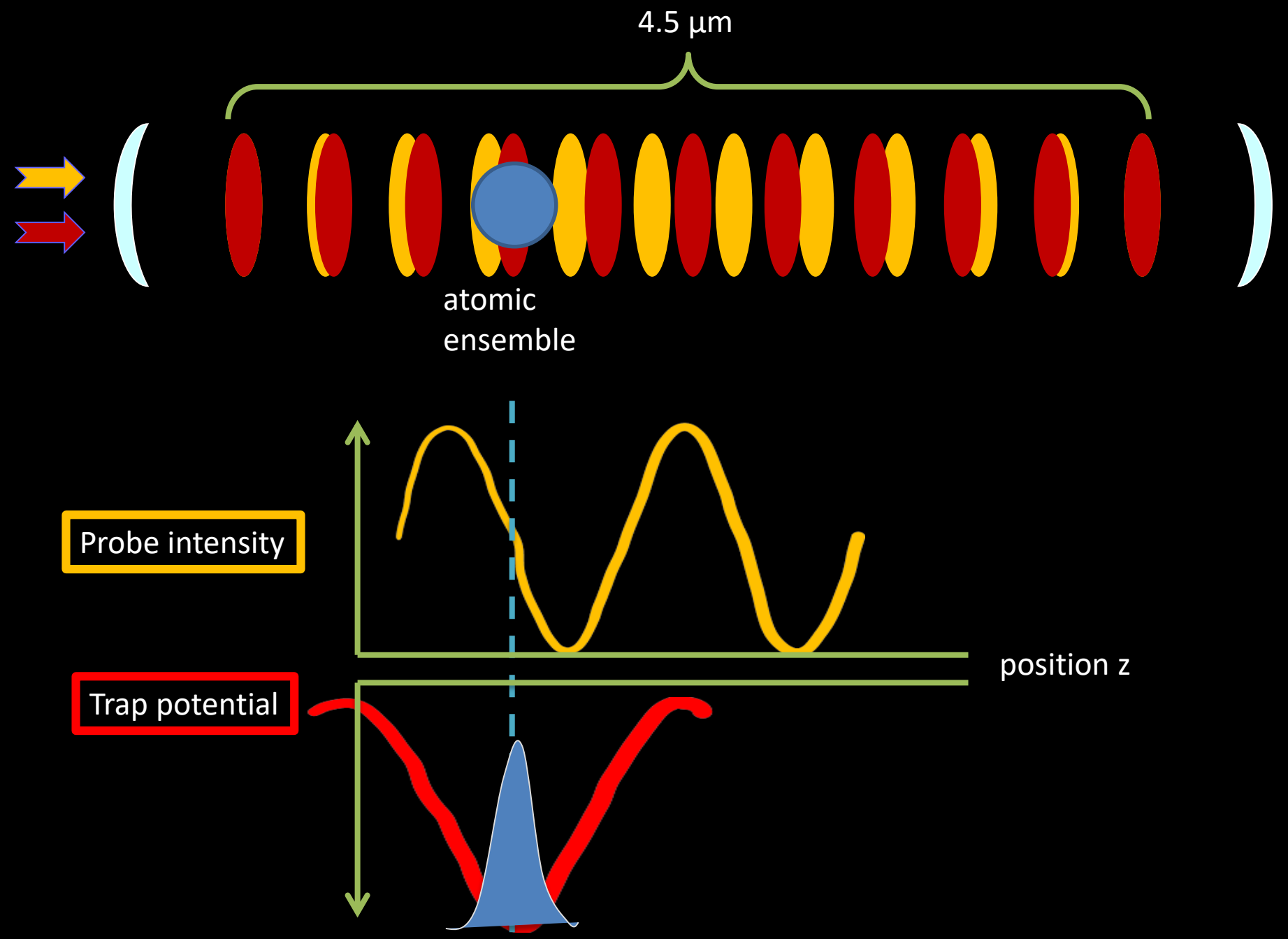
MOT Loading

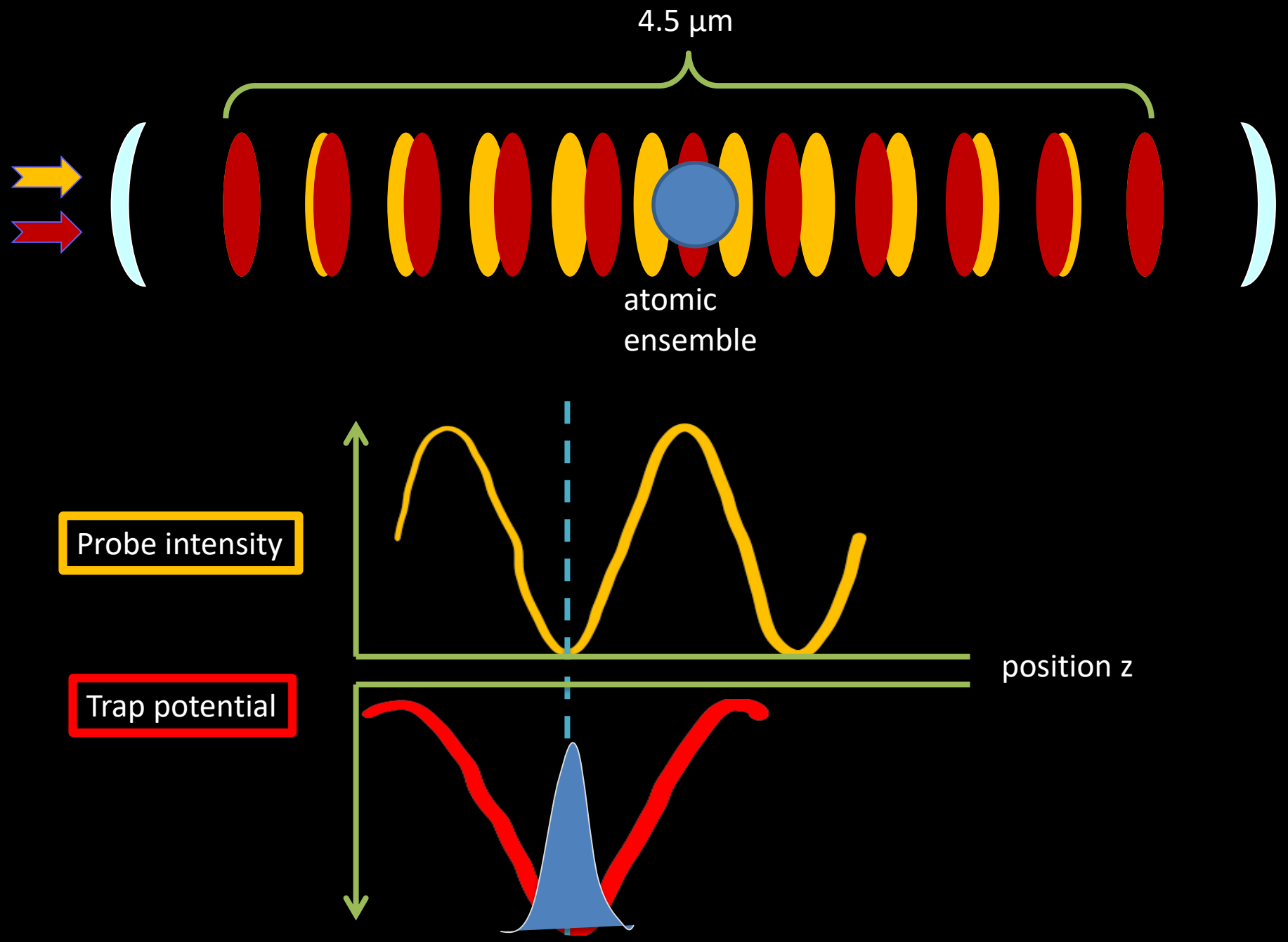
Conveyor Belt

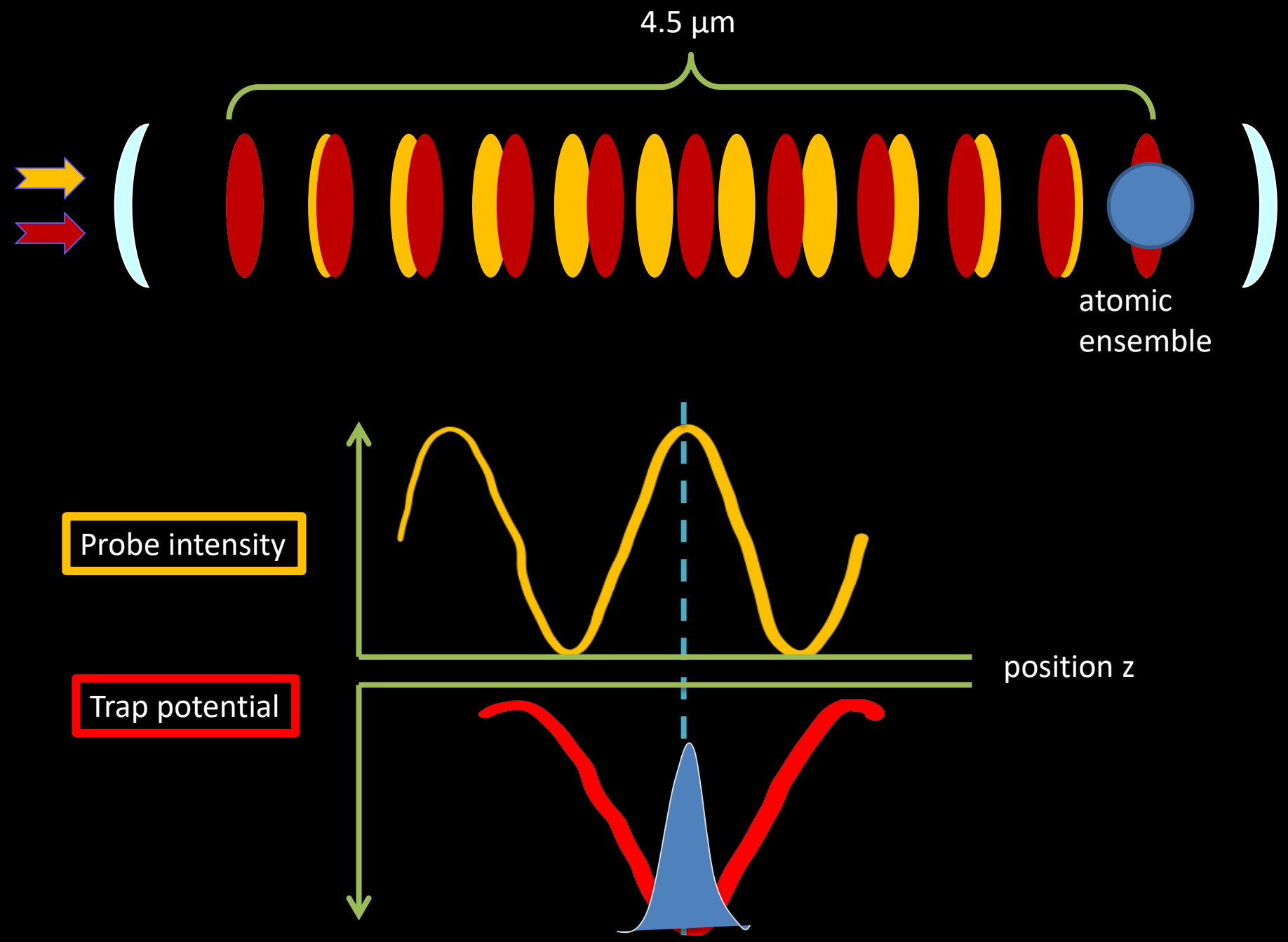
Cavity Locations



- pre-position with magnetic trap
- load into 845 nm optical trap
- probe with 780 nm light
  (either red [attractive] or blue [repulsive] detuned)
- Note TWO color superlattice
  Long spatial beatnote makes it easy to tune the optomechanical coupling


4.5 µm
atomic
ensemble
Probe intensity
Trap potential
position z


4.5 µm
atomic
ensemble
Probe intensity
Trap potential
position z


4.5 µm
atomic
ensemble
Probe intensity
Trap potential
position z

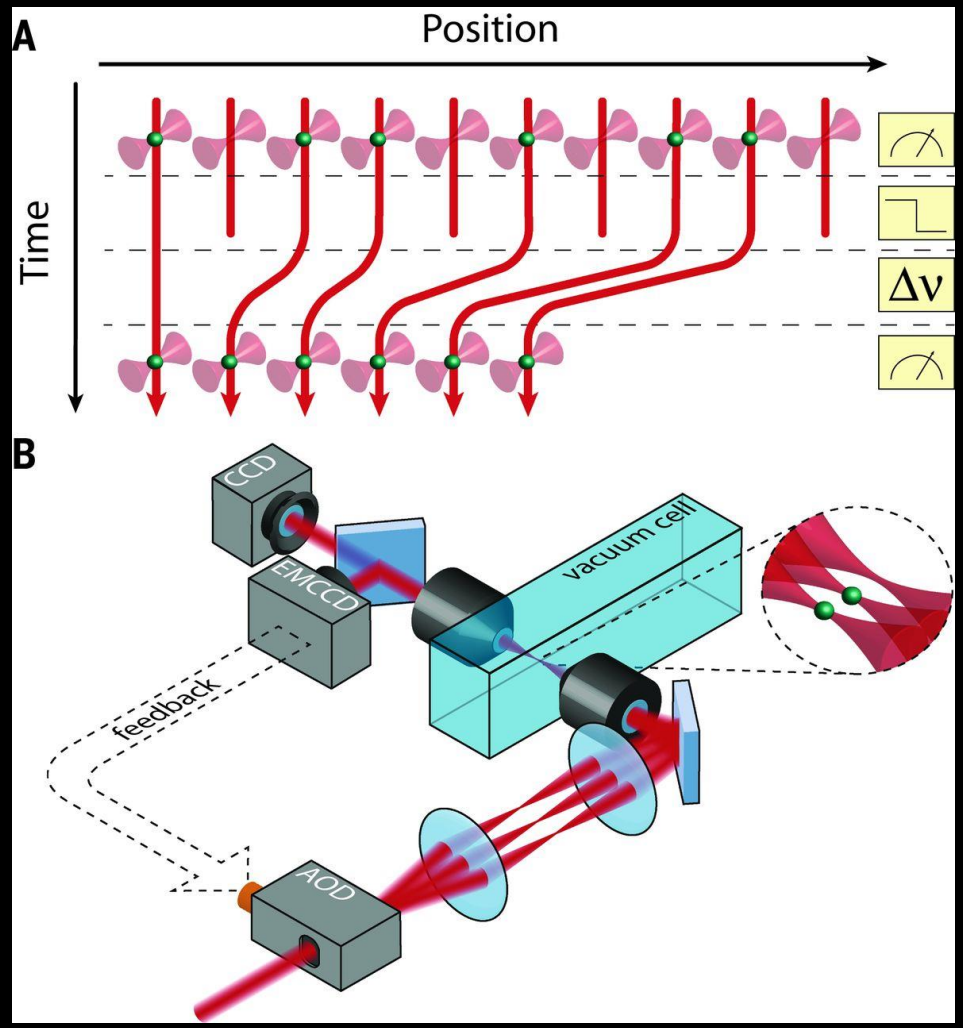
Atom tweezer arrays: A revolutionary new approach to atomic physics

Tweezer array experimental sequence:

1. Load tweezers
2. Image to find filled tweezers (10's ms)
3. Sort
4. Science

16 non-deterministically loaded tweezers

6 deterministically loaded tweezers



atom number reduced to 0, 1 by light-induced atom loss

PRL 89, 023005 (2002)

Barredo et al., Science 354, 1021 (2016)
Endres et al., Science 354, 1024 (2016)

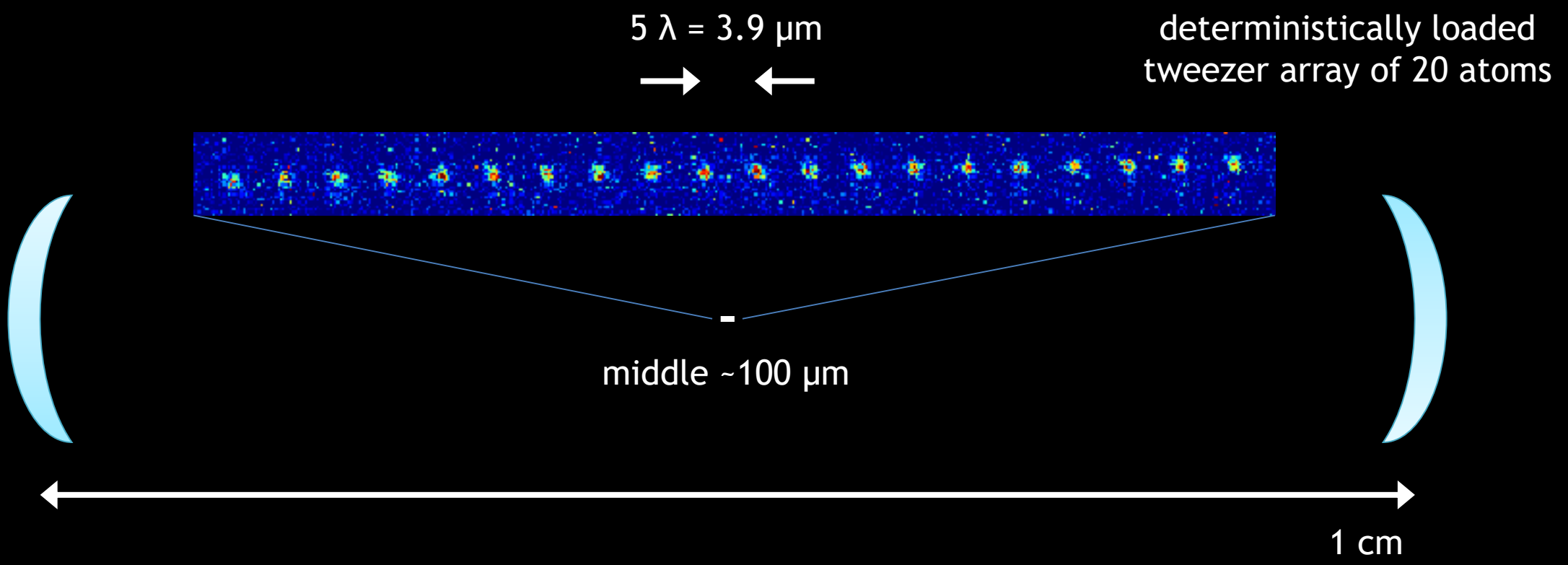
Integrating cavity QED with a tweezer array (E6)

Cavity QED for tweezers

- Photon-mediated coupling
- Fast, local, efficient measurement
- Transduction to photons

Tweezers for cavity QED

- Deterministic loading
- Nanometer positioning
- Assembling optical metamaterial atom by atom

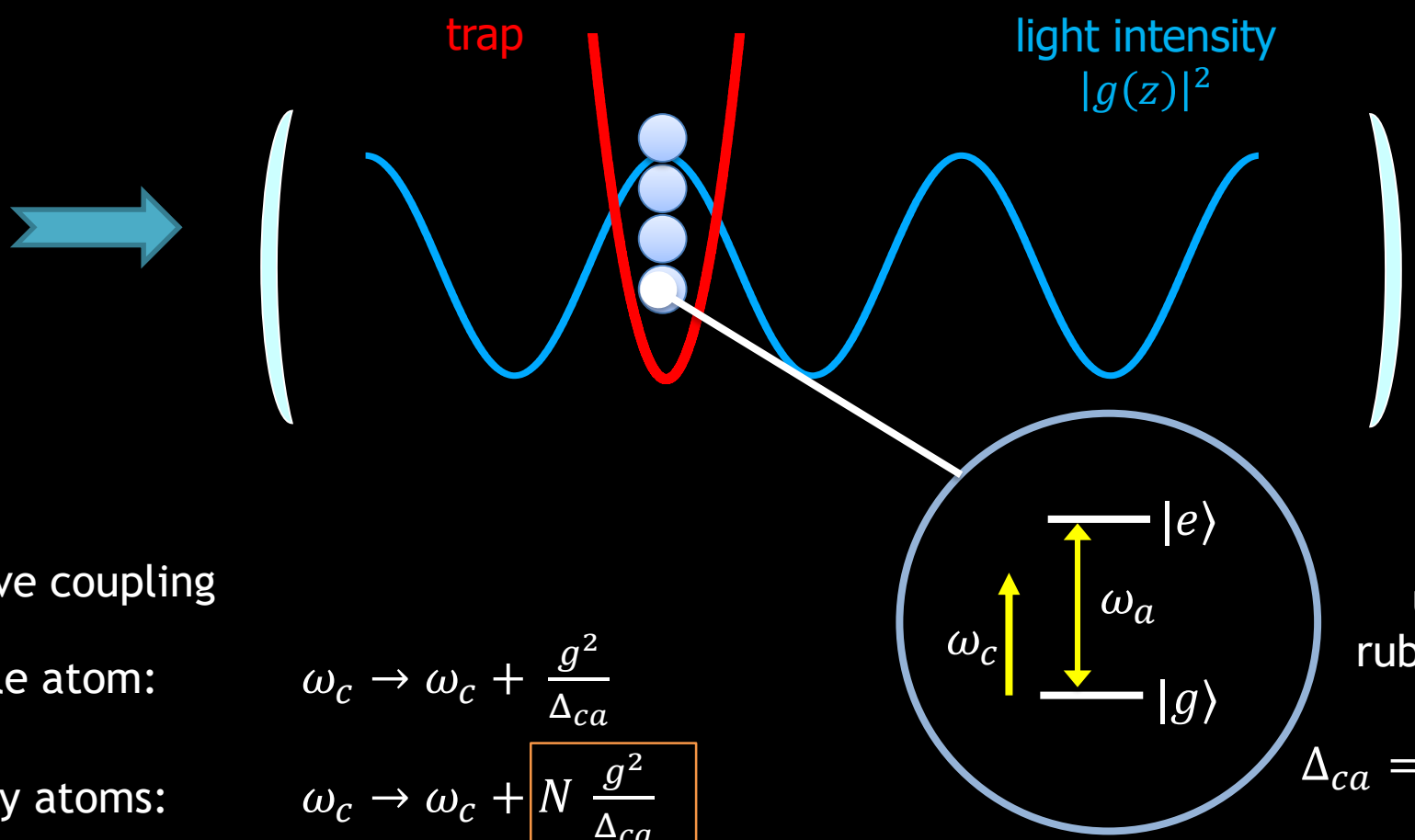


Cavity-enhanced detection of atom number:

Non-equilibrium thermodynamics in a mesoscopic system

“Tracking evaporative cooling of a mesoscopic atomic quantum gas in real time,”
Physical Review X 11, 041017 (2021).

Cavity-enhanced detection of atom number



ultracold rubidium atom

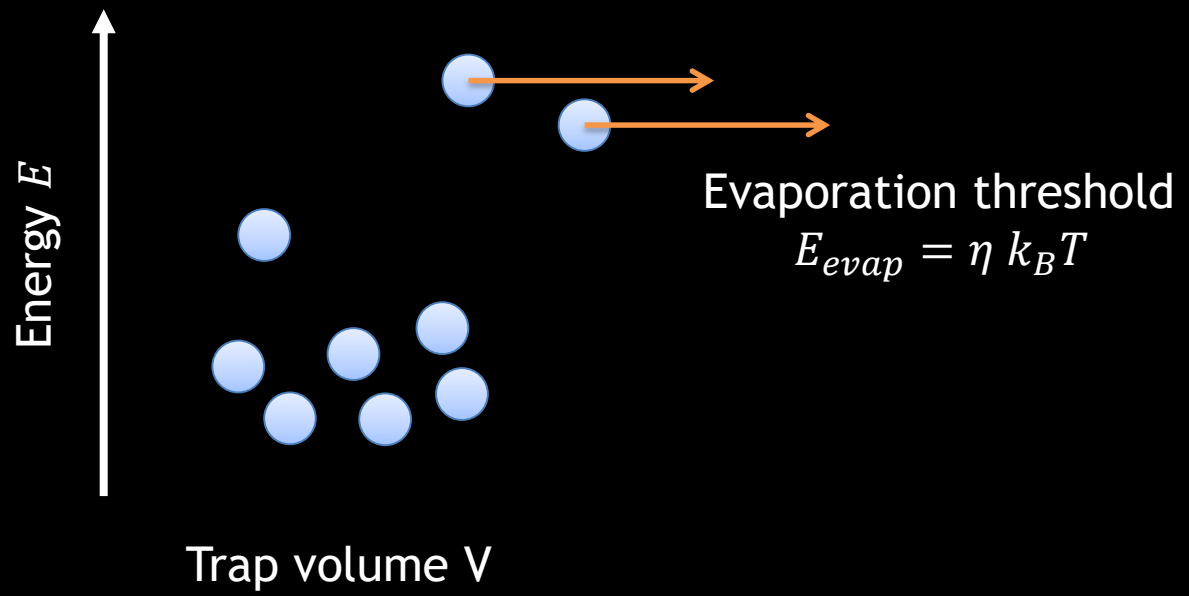
$\Delta_{ca} = \omega_c - \omega_a$

- Dispersive coupling
  - single atom: $\omega_c \rightarrow \omega_c + \frac{g^2}{\Delta_{ca}}$
  - many atoms: $\omega_c \rightarrow \omega_c + \boxed{N \frac{g^2}{\Delta_{ca}}}$

(scalar) shift allows for real-time monitoring (and stabilization) of atom number

"Tracking evaporative cooling of a mesoscopic atomic quantum gas in real time," PRX 11, 041014 (2021)

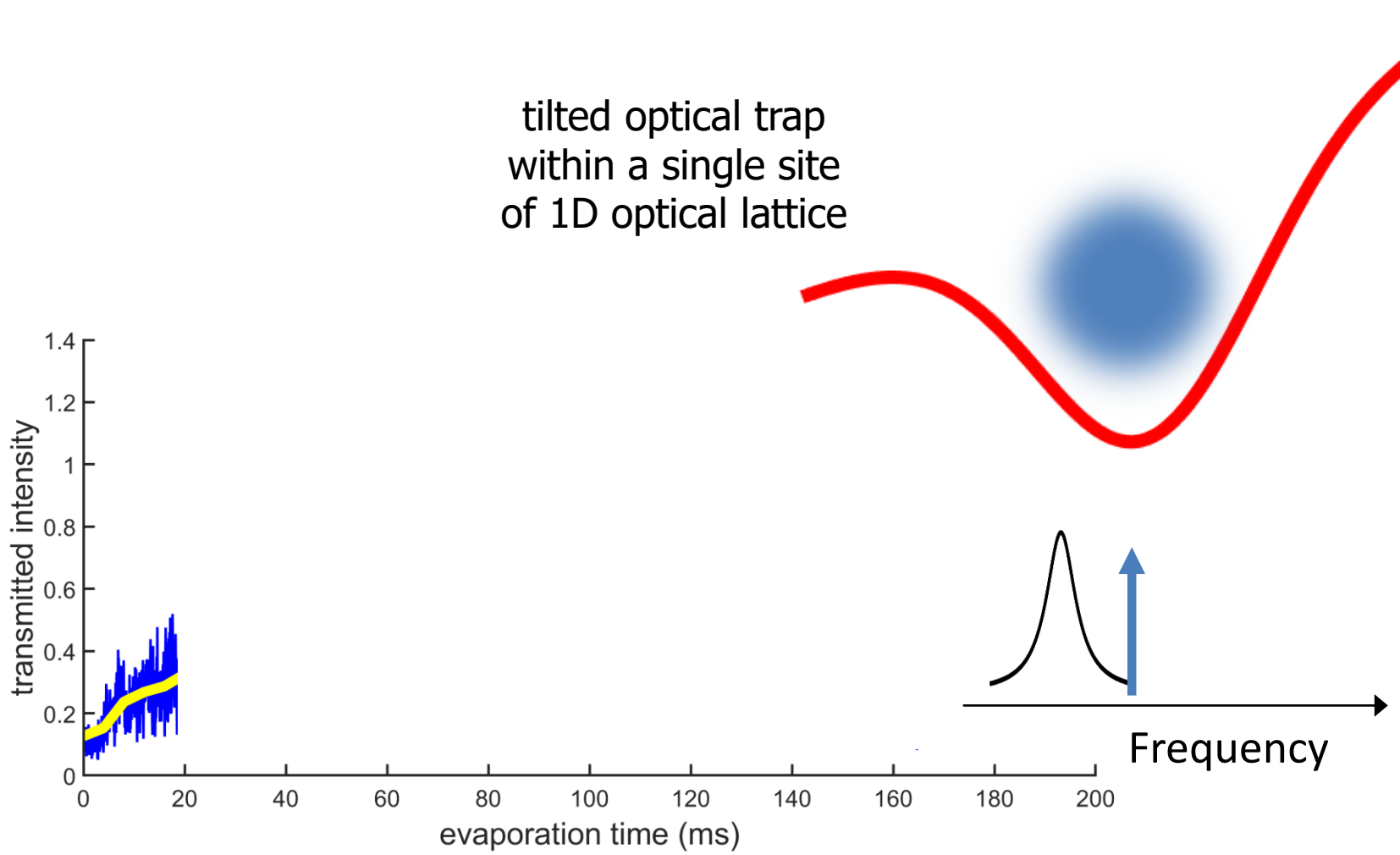
Non-equilibrium thermodynamics of evaporation



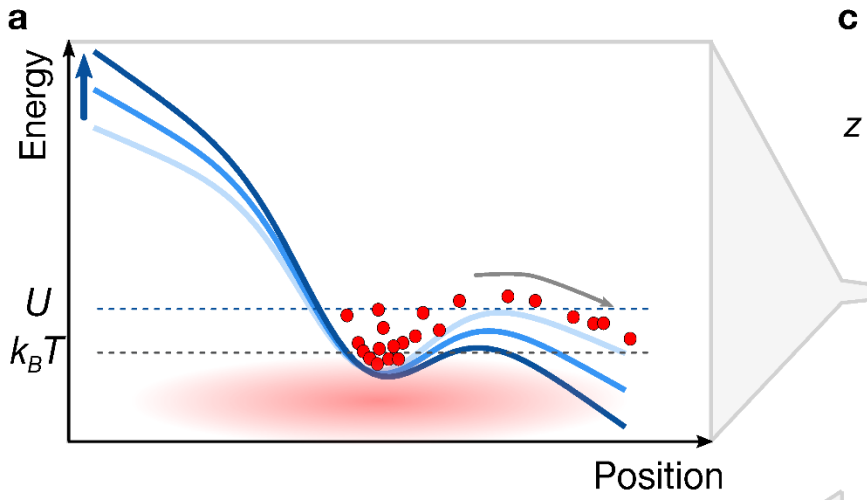
- Non-equilibrium thermodynamics describes
  - average evaporated number/rate
  - variations in evaporated number

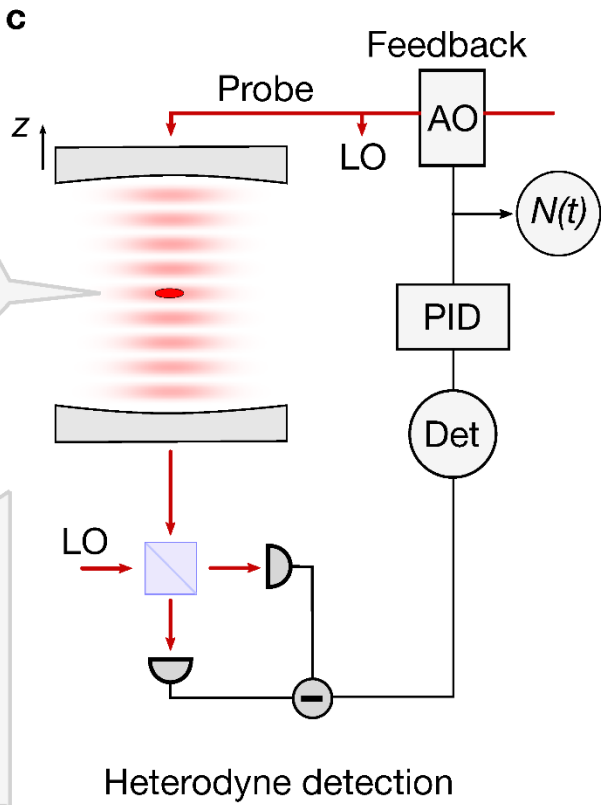
Ketterle *et al.*, Adv in At and Mol Phys 37, 181 (1996)
Luiten *et al.*, PRA 53, 381 (1996)
Sacket et al., PRA 55, 3797 (1997)

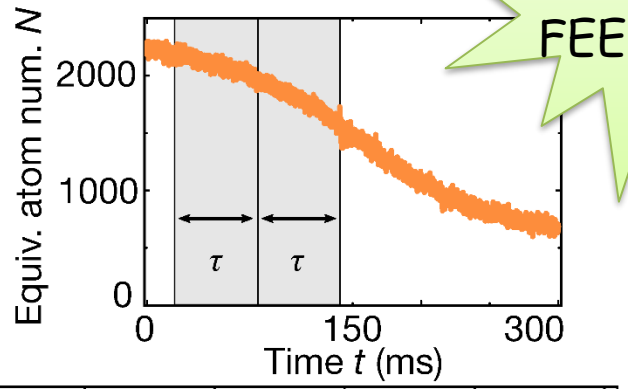
Real-time dispersive measurement of atom number during evaporation

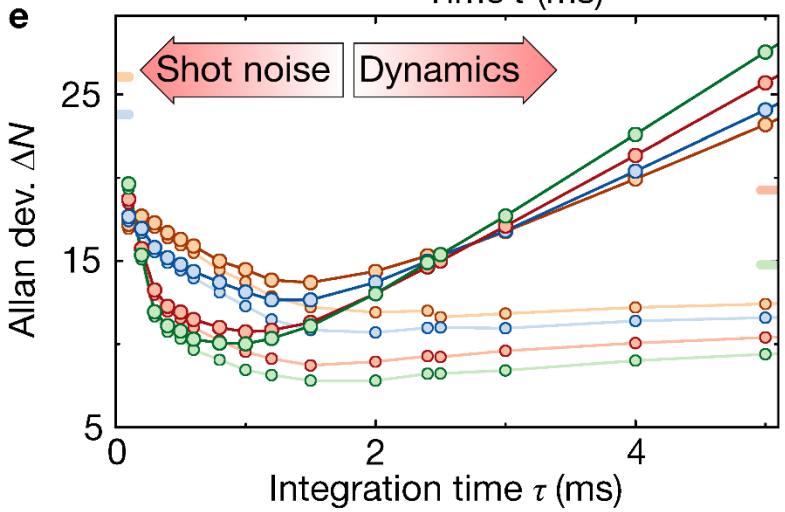


Real-time dispersive measurement of atom number during evaporation



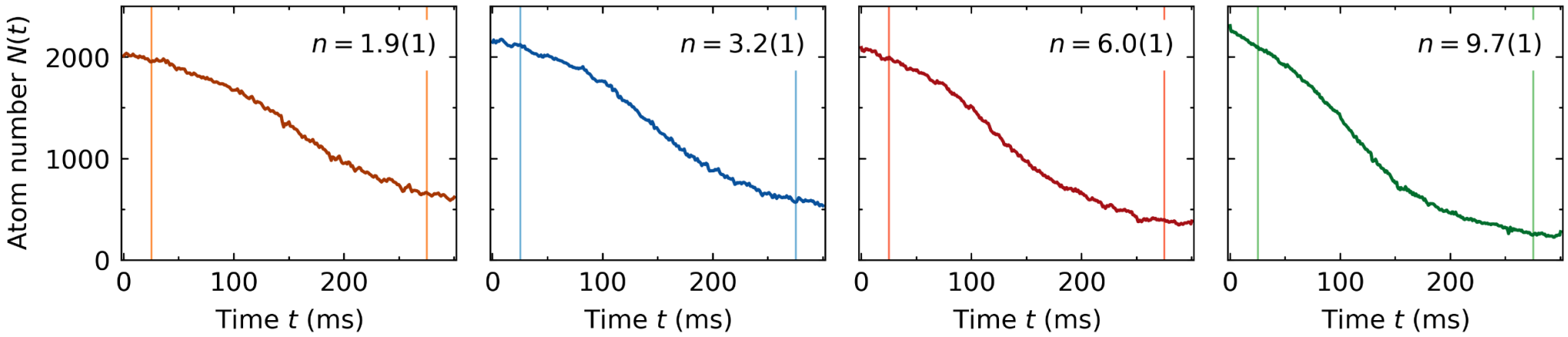






NOW WITH FEEDBACK!

Two- (or more) time correlations from continuous measurement

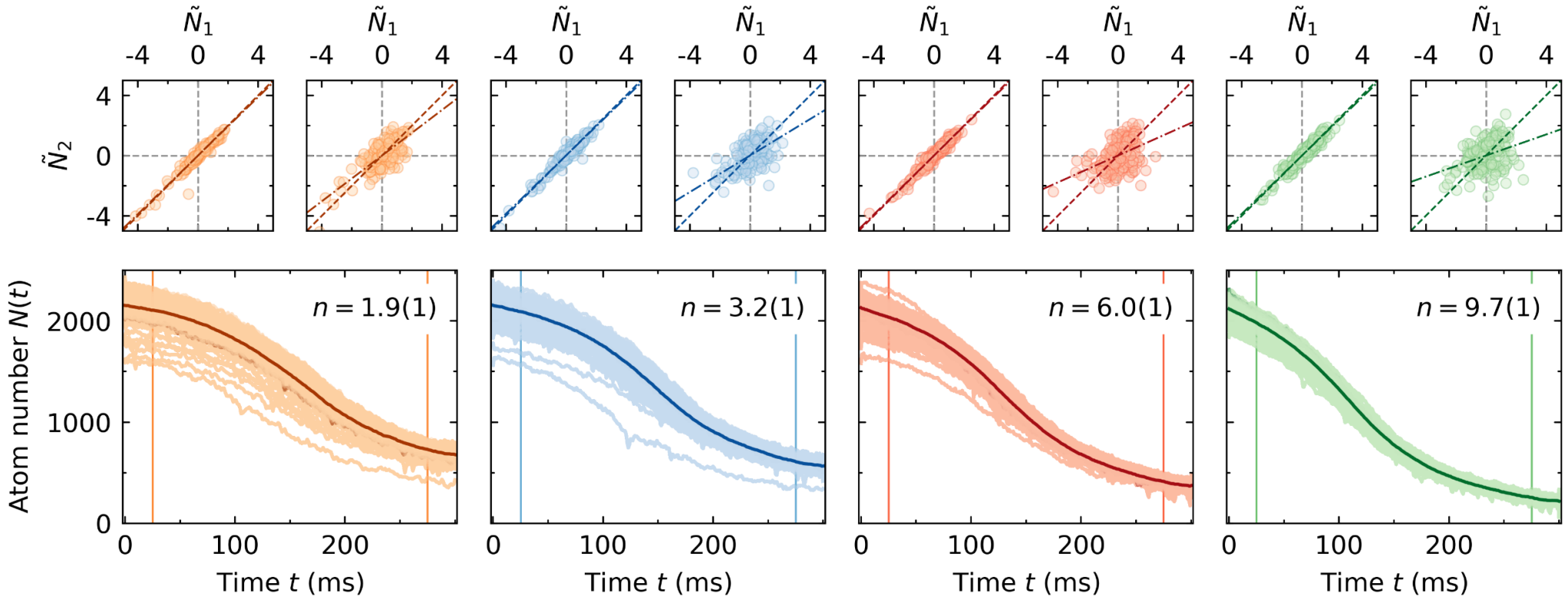


Note: $\bar{n} = 1$ corresponds to 2.9 pW

Two- (or more) time correlations from continuous measurement

N_1= number at early time t_1

N_2= number at late time t_2



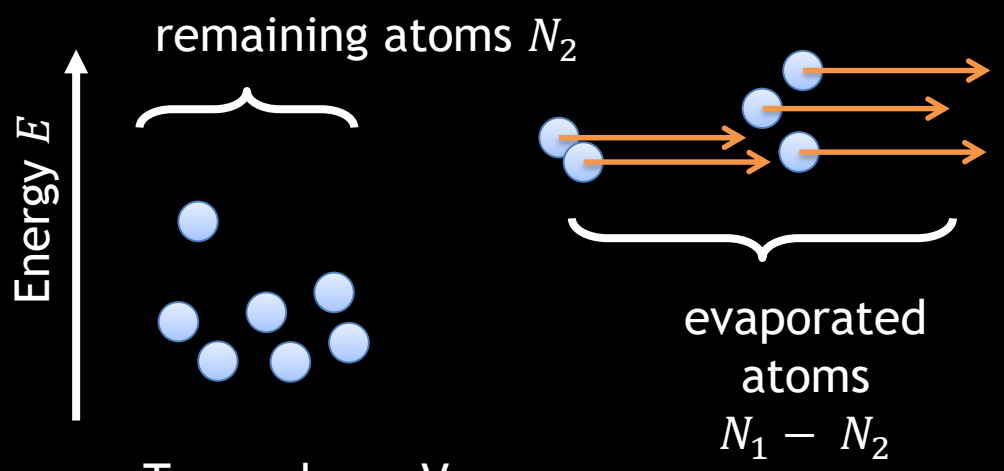
Numbers scaled by standard deviation

Note: $\bar{n} = 1$ corresponds to 2.9 pW

Fluctuations in mesoscopic non-equilibrium thermodynamics

- Consider evaporation from time t_1 to time t_2

$$\langle N_2 \rangle = \; g(\langle N_1 \rangle)$$



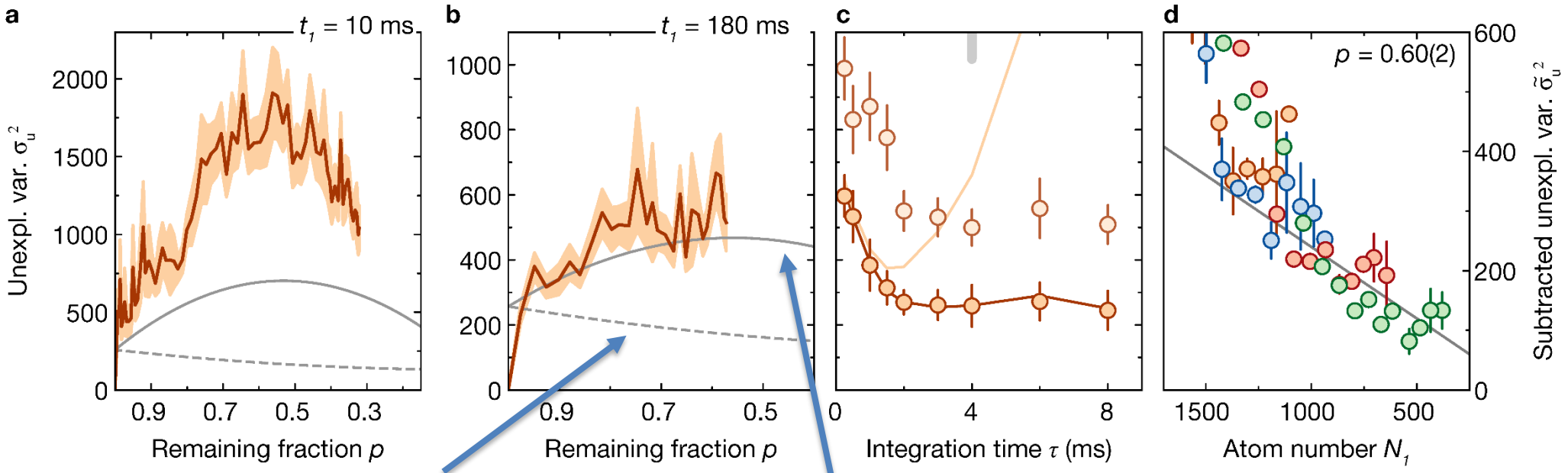
Added fluctuations in N_2 (not predicted by variations in N_1)

- Measurement noise
- Binomial distribution: $Var(N_2) = N_1\, p\, (1-p)$
- Higher order atom loss: $Var(N_2) \times= M$
- Amplification/damping of fluctuations
- Thermodynamics – compressibility: $\frac{Var(N)}{N} = \kappa_T\, k_B T\, \frac{V}{N}$
- Transport - lessons from mesoscopic electronics

Measured added variance

$t_1 = 10$ ms
dominated by early temperature fluctuations

$t_1 = 180$ ms
shows natural behavior of evaporative cooling



measurement (optical shot) noise

measurement + binomial noise

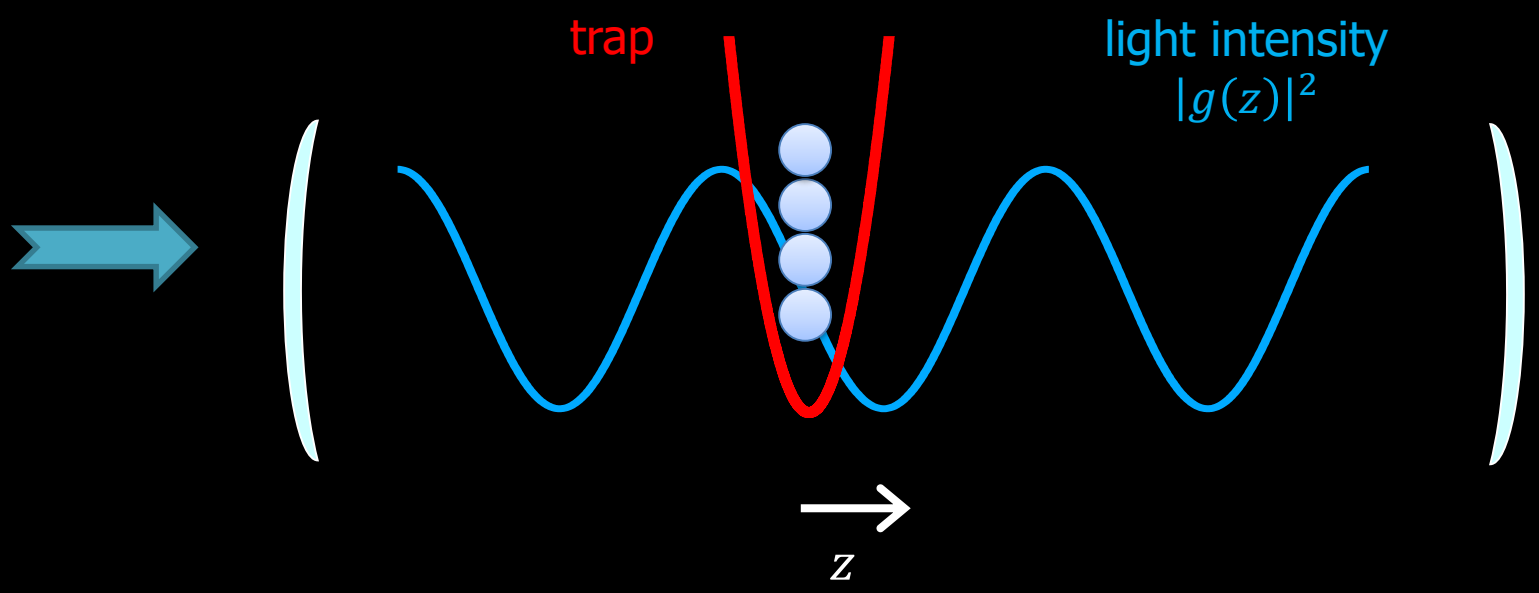
scaling with atom number shows mesoscopic fluctuation limit

Cavity-enhanced detection of atomic position:

Quantum cavity optomechanics with cold atoms

Cavity nonlinearity at sub-zero photon number	PRL **99**, 213601 (2007)
Observation of measurement backaction / radiation-pressure shot noise	Nat. Phys. **4**, 561 (2008)
Quadratic optomechanical coupling	PRL **105**, 133602 (2010)
Ponderomotive squeezing of light	Nature **488**, 476 (2012)
Quantization of collective atomic motion	PRL **108**, 133601 (2012)
Quantum optomechanical arrays	PRL **110**, 153001 (2013)
Quantum-limited force detection	Science **344**, 1486 (2014)
Backaction-limited coupling of mechanical oscillators	Nat. Phys. **12**, 27 (2016)

Cavity-enhanced detection of atomic motion (cavity optomechanics)

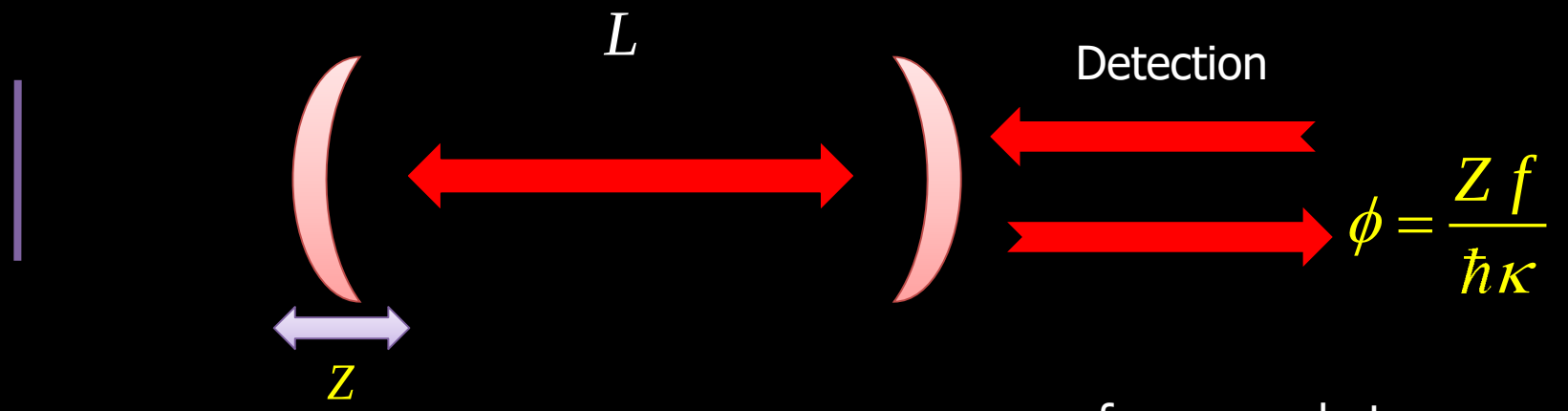


- Dispersive coupling
  - many atoms: $\omega_c \rightarrow \omega_c + \sum \frac{g^2(z_i)}{\Delta_{ca}} \simeq \omega_c + \Delta_N + \boxed{\frac{g_0^2 \sqrt{N}\, k}{\Delta_{ca}} z_{com}}$

Quantum cavity optomechanics with an ultracold-atom mechanical oscillator

"Cavity optomechanics with cold atoms," in Cavity Optomechanics: Nano-and Micromechanical Resonators Interacting with Light (Springer Berlin Heidelberg, 2014).

Cavity optomechanics paradigm



$$\phi = \frac{Z f}{\hbar \kappa}$$

$$H = H_{osc} + H_{cav} + H_{in/out} - Z f n$$

force per photon:

$$f = \frac{hc}{\lambda L}$$

Cavity frequency shift due to oscillator displacement

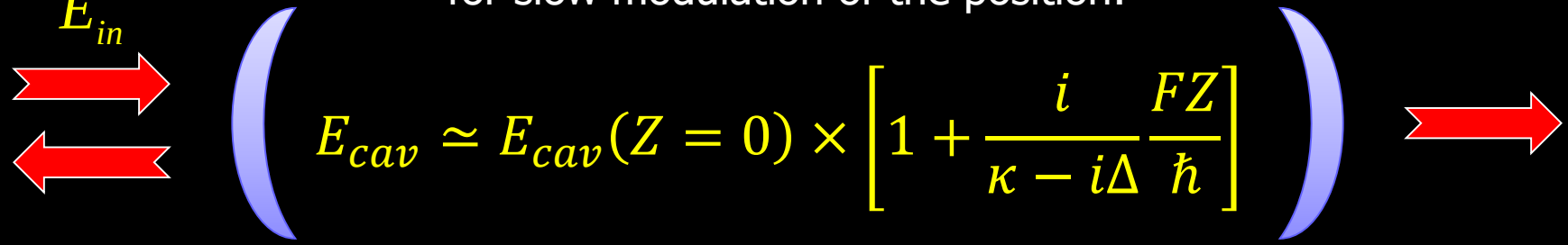
(sensitivity to oscillator motion)

Optical force on oscillator

(optical back-action on oscillator)

How motion affects the cavity field

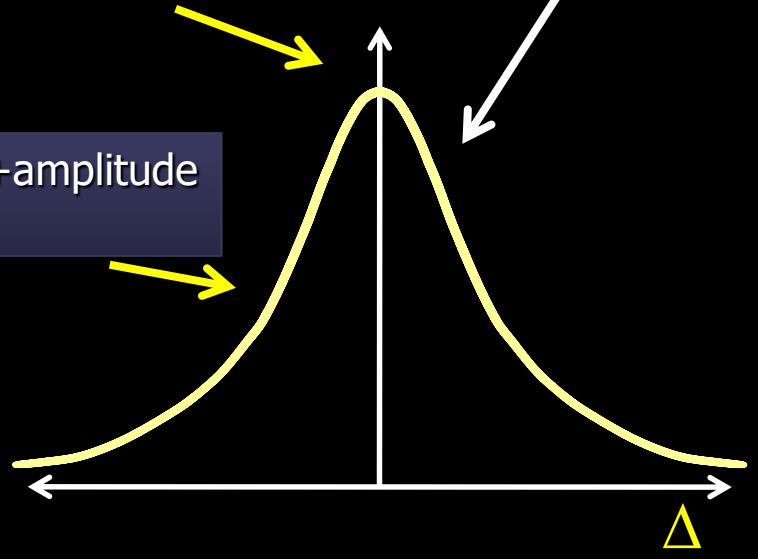
for slow modulation of the position:



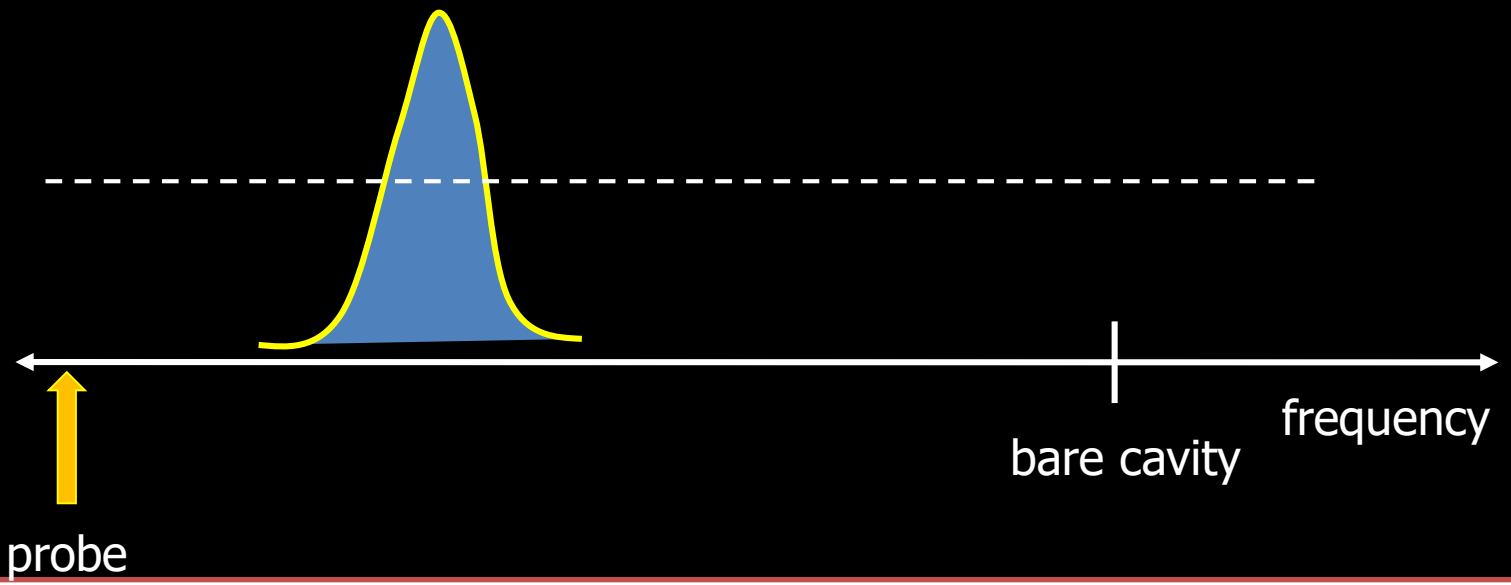
Information/photon re: position $\left| \frac{i}{\kappa - i\Delta} \frac{F}{\hbar} \right|^2$

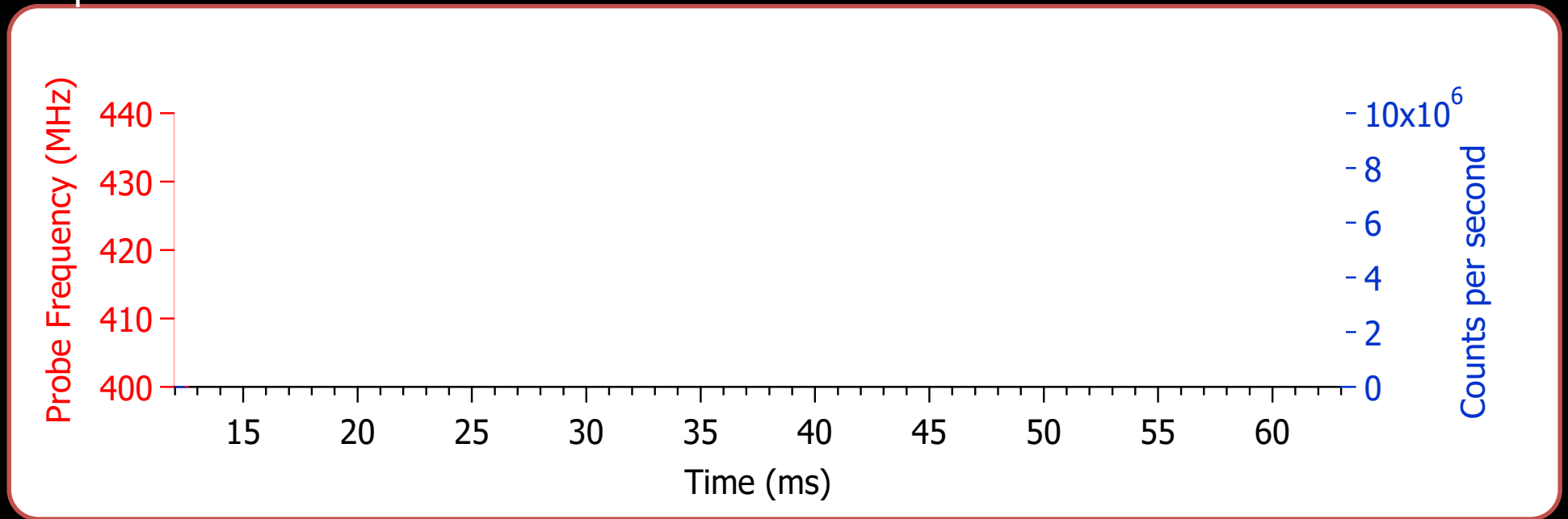
Position read out as phase modulation

Position read out as phase+amplitude modulation

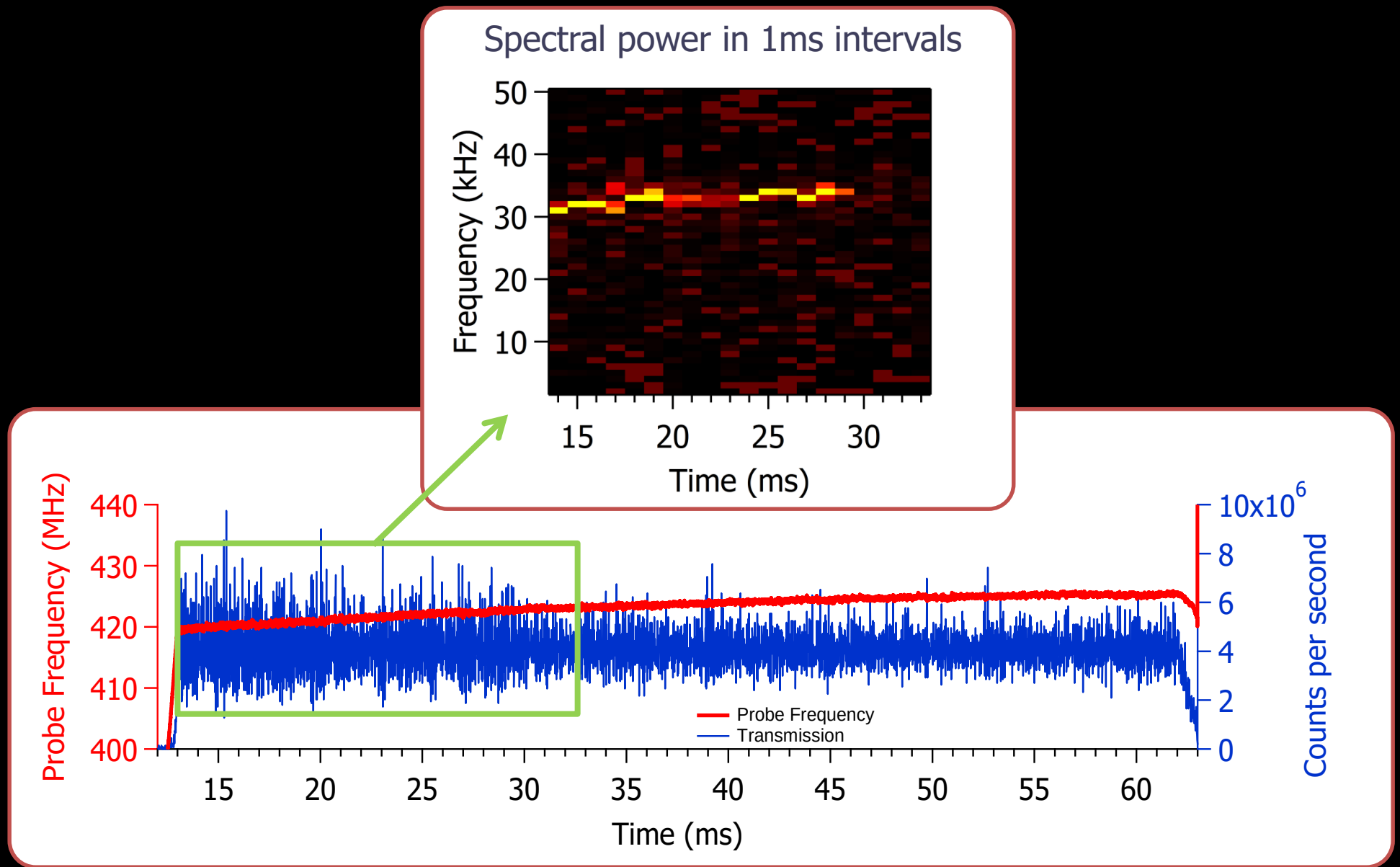


Direct observation of collective atomic motion: probe side-lock

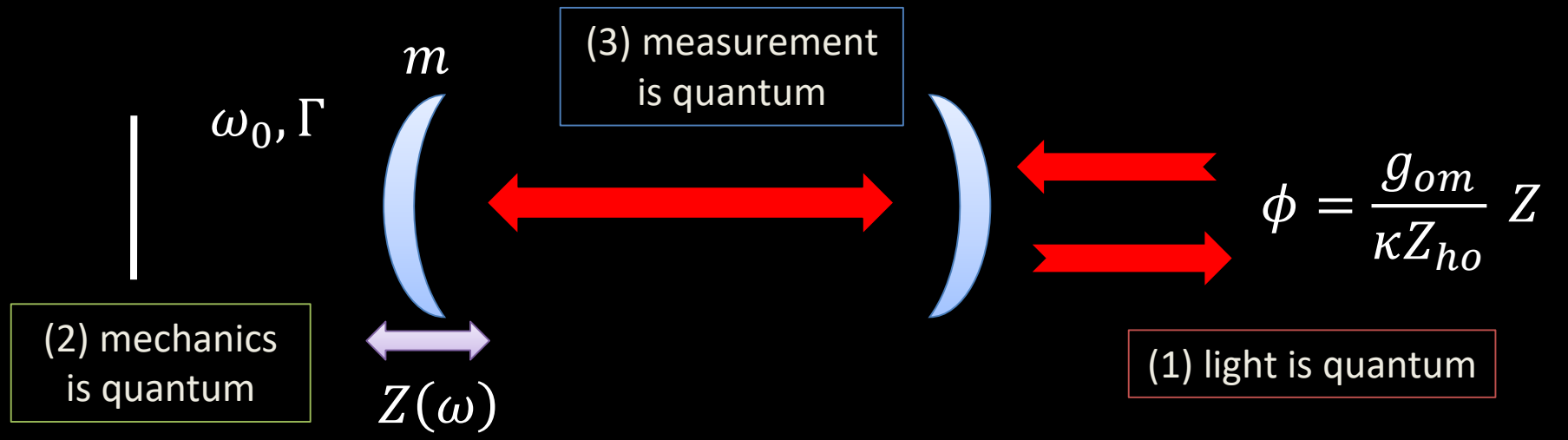


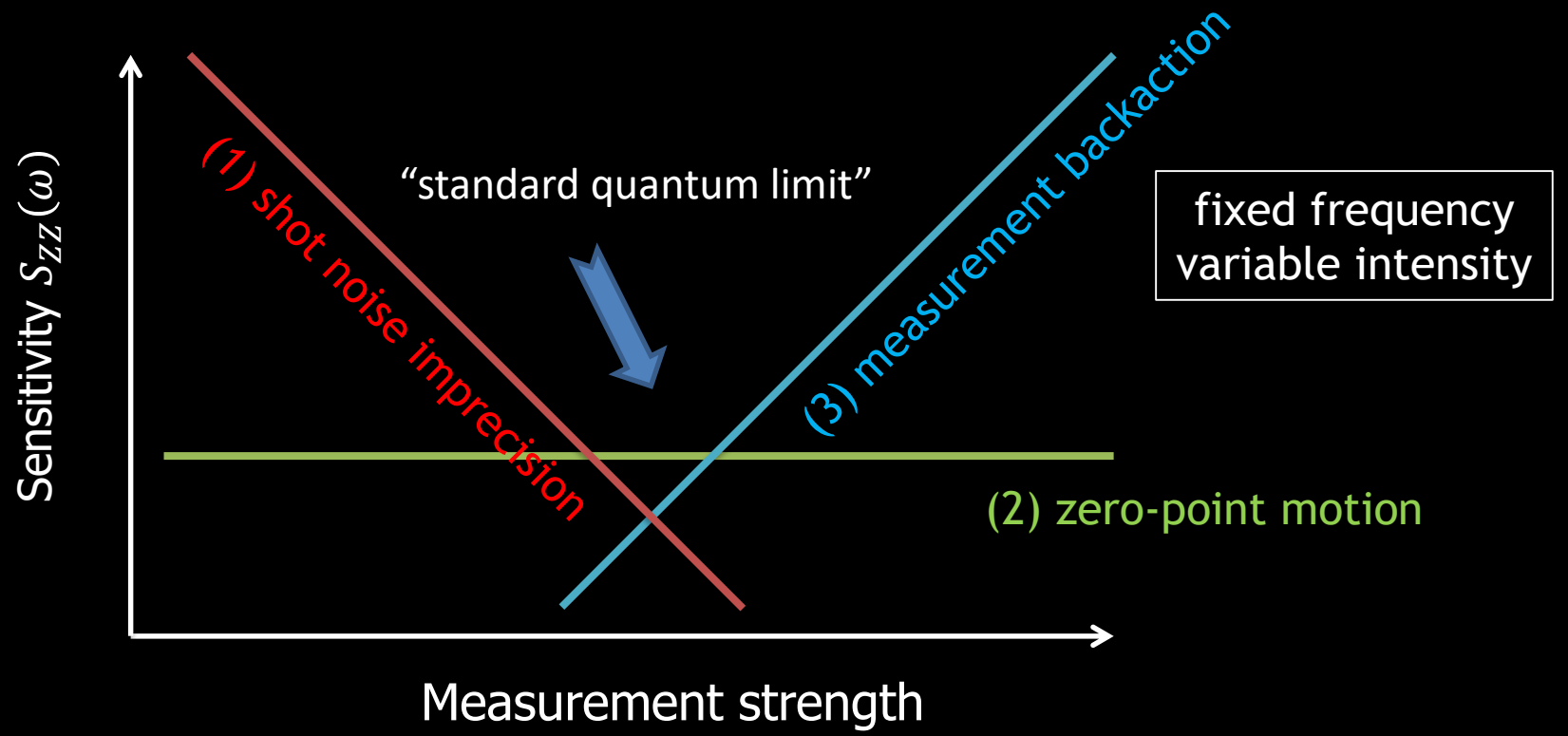


Direct observation of collective atomic motion: probe side-lock



Force/position sensing: Quantum mechanics sets the limit

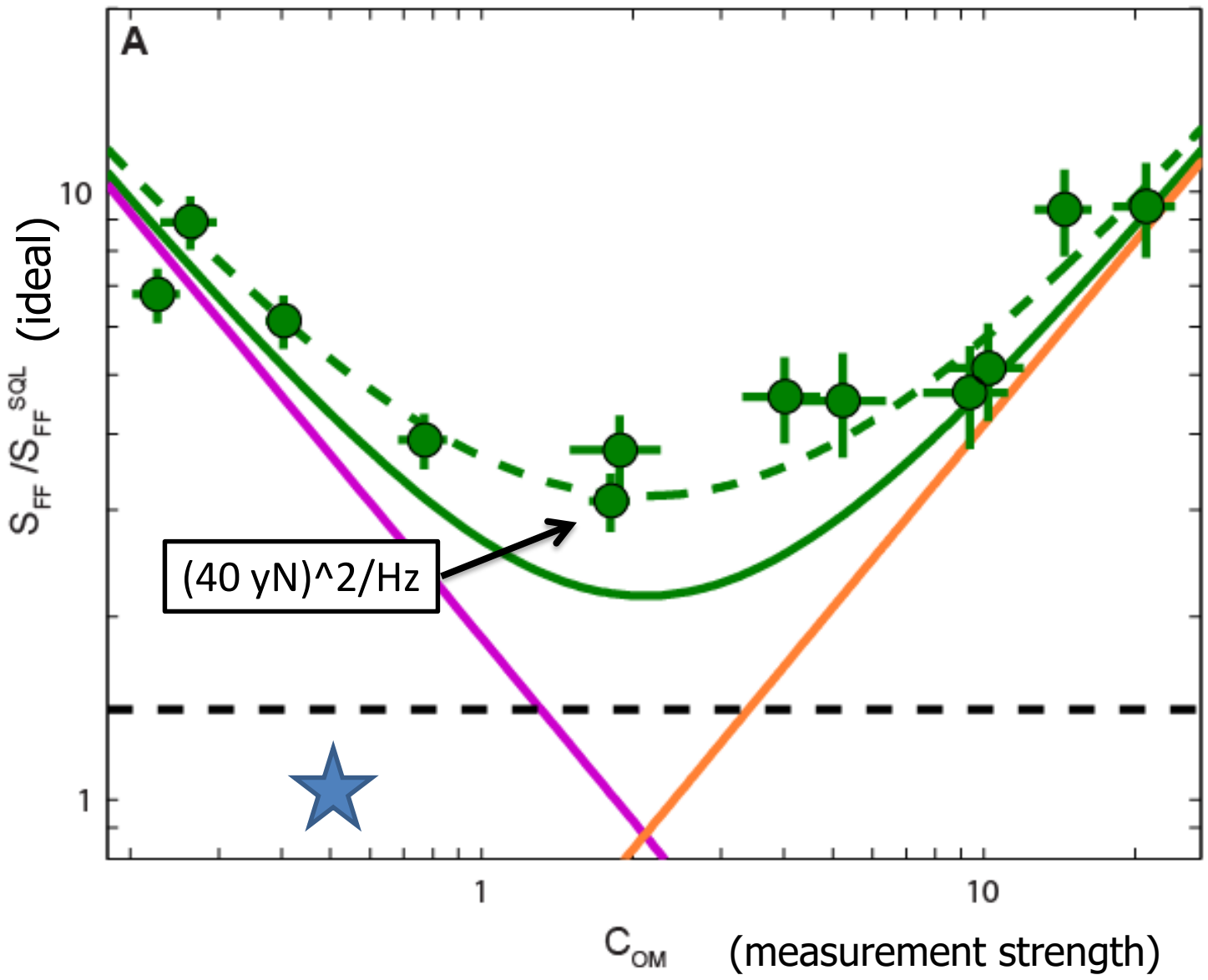




SQL force detection experiment

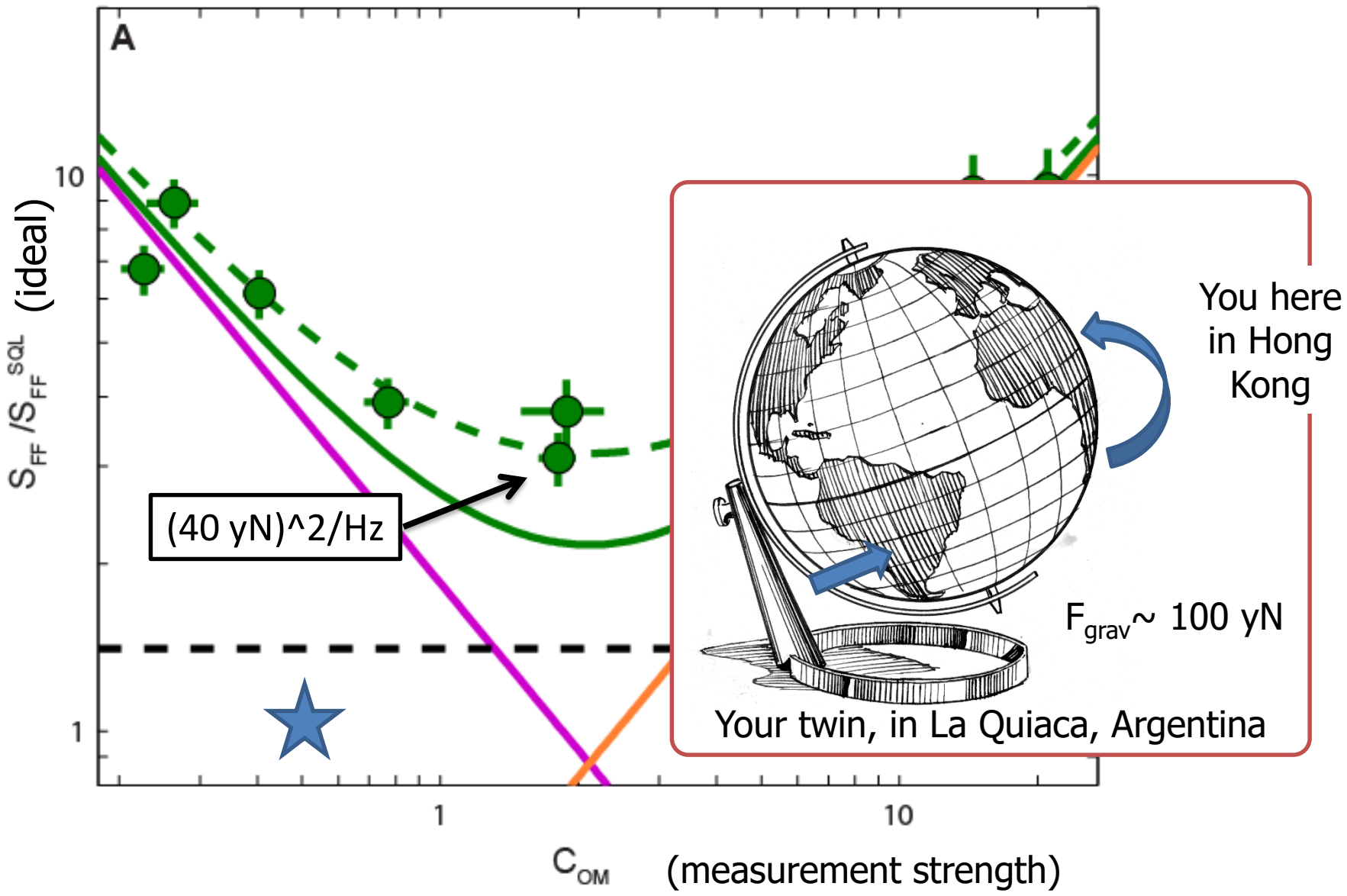
- Load atoms mostly into single lattice site, cool to near ground state
- Modulate one color of optical superlattice to apply known force
- Lock probe to resonance, raise to desired light level, measure heterodyne signal (between 1 ms and 5 ms), extract phase modulation off-line
- Repeat 1000’s of times over many days

Comparison to standard quantum limit

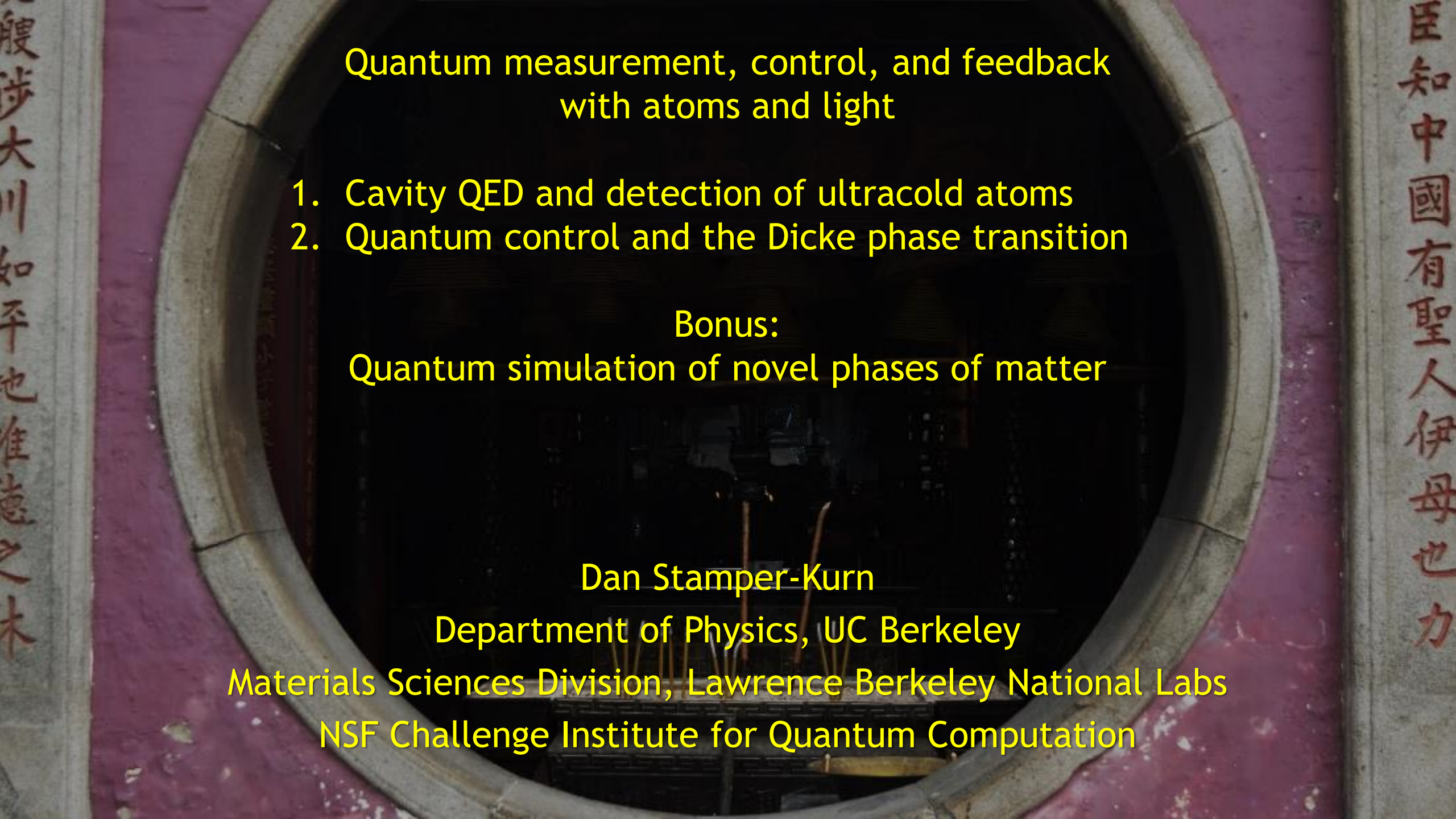


"Optically measuring force near the SQL," Science **344**, 1486 (2014)

Comparison to standard quantum limit



"Optically measuring force near the SQL," Science **344**, 1486 (2014)



Quantum measurement, control, and feedback with atoms and light

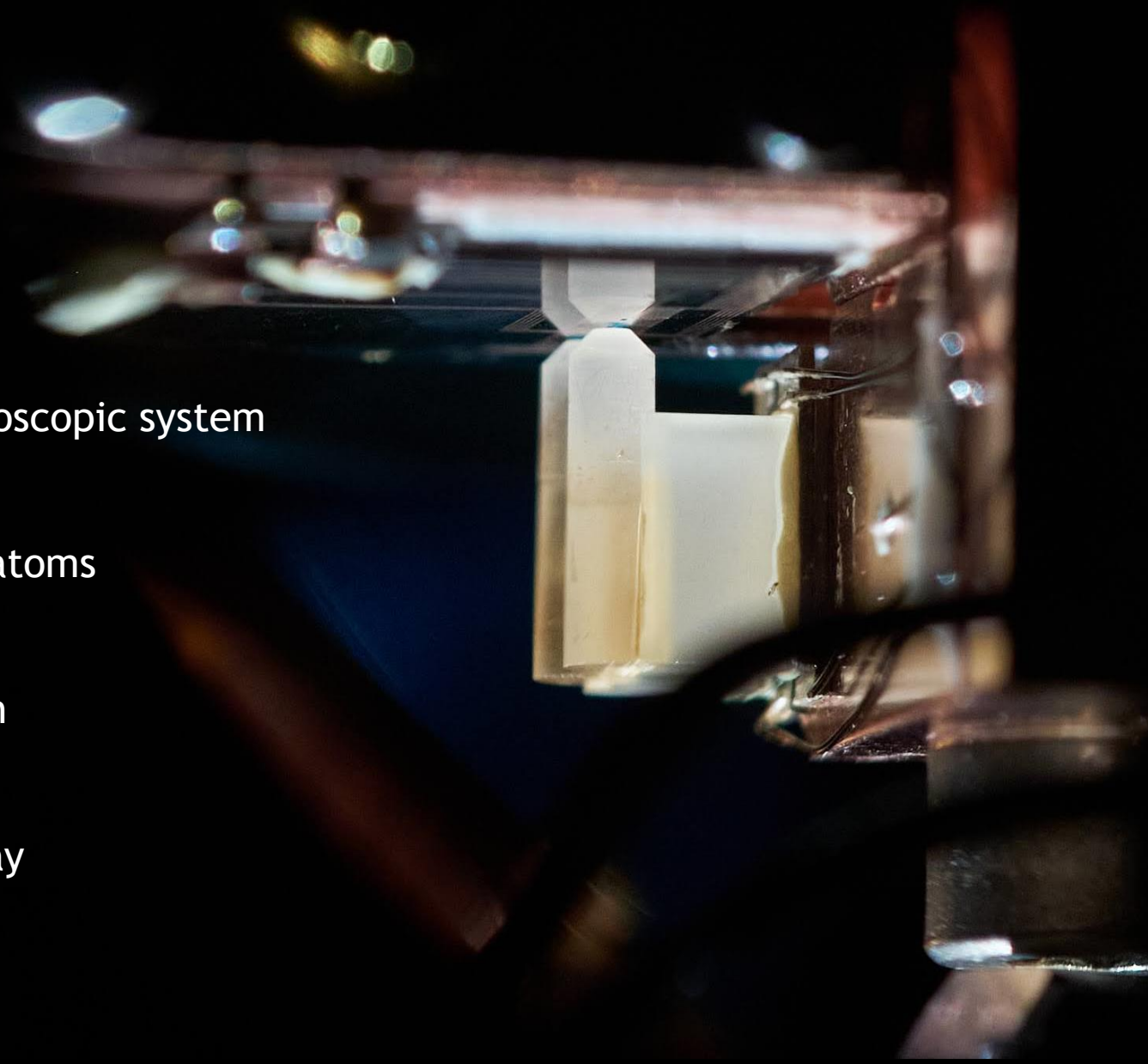
1. Cavity QED and detection of ultracold atoms
2. Quantum control and the Dicke phase transition

Bonus:
Quantum simulation of novel phases of matter

Dan Stamper-Kurn
Department of Physics, UC Berkeley
Materials Sciences Division, Lawrence Berkeley National Labs
NSF Challenge Institute for Quantum Computation

Cavity QED and detection of ultracold atoms

- Primer on cavity QED
- How to position atoms in an optical cavity
- Cavity-enhanced detection of atom number
  - Non-equilibrium thermodynamics in a mesoscopic system
- Cavity-enhanced detection of atomic position
  - Quantum cavity optomechanics with cold atoms
- Cavity-enhanced detection of atomic spin
  - Coherent and incoherent cavity backaction
- Cavity-enhanced detection of single atoms:
  - Mid-circuit measurement in a tweezer array



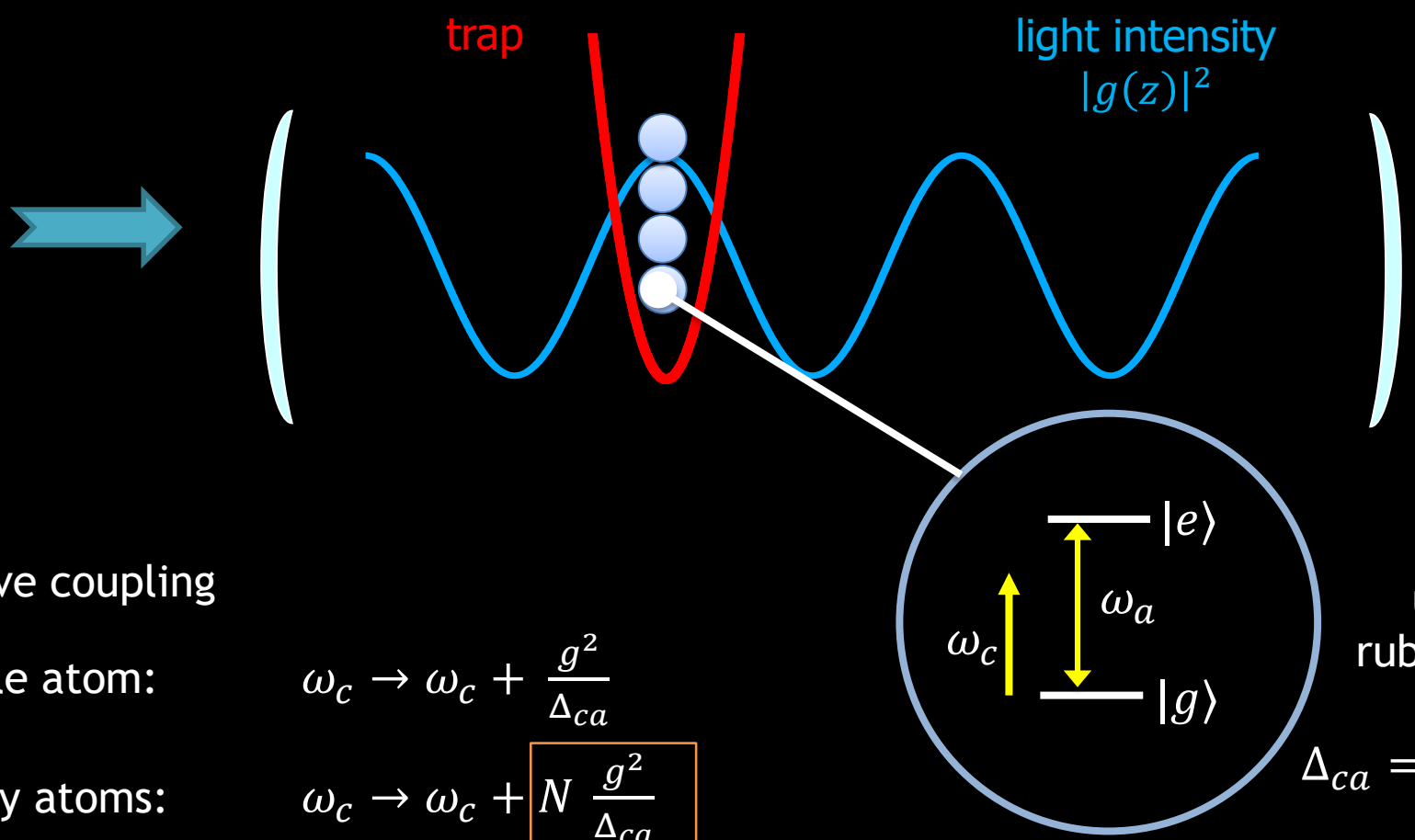
Cavity-enhanced detection of atomic spin:

Coherent and incoherent cavity backaction

"Spin optodynamics analog of cavity optomechanics," PRA **82**, 041804(R) (2010)

"Cavity-assisted measurement and coherent control of collective atomic spin oscillators," PRL **118**, 063604 (2017)

Cavity-enhanced detection of atom number



ultracold rubidium atom

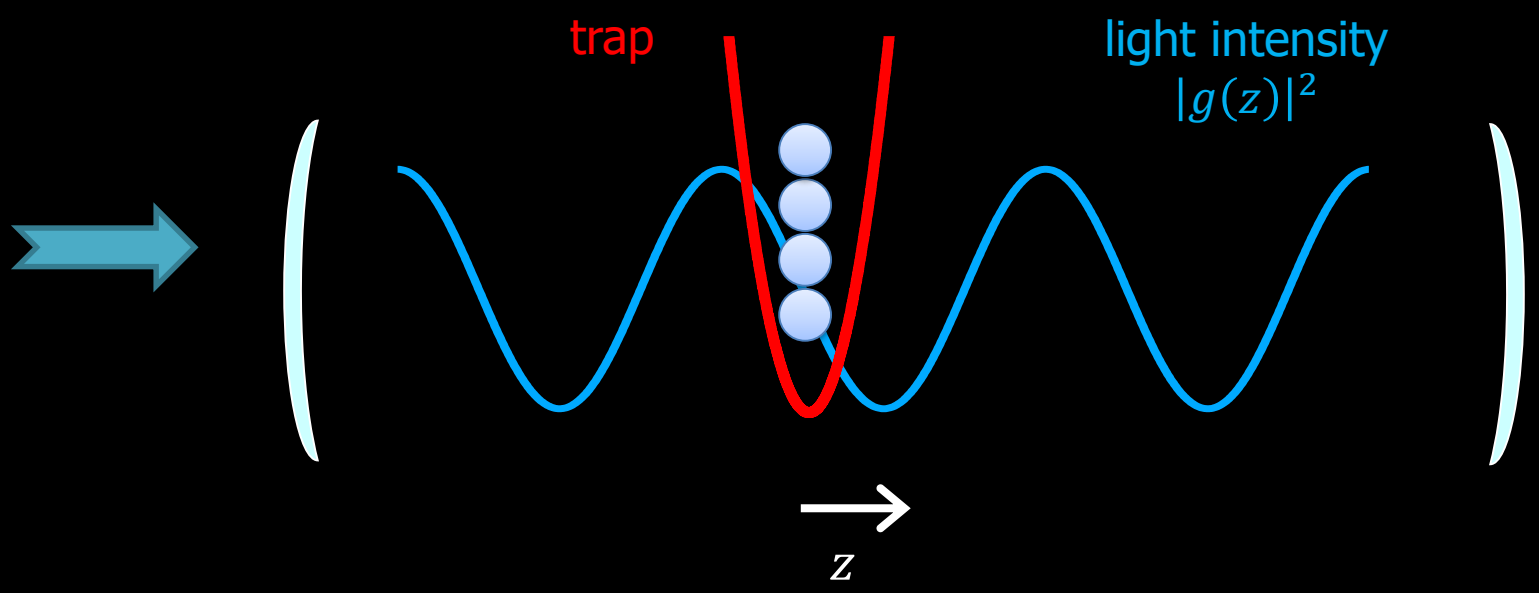
$\Delta_{ca} = \omega_c - \omega_a$

- Dispersive coupling
  - single atom: $\omega_c \rightarrow \omega_c + \frac{g^2}{\Delta_{ca}}$
  - many atoms: $\omega_c \rightarrow \omega_c + \boxed{N \frac{g^2}{\Delta_{ca}}}$

(scalar) shift allows for real-time monitoring (and stabilization) of atom number

"Tracking evaporative cooling of a mesoscopic atomic quantum gas in real time," PRX 11, 041014 (2021)

Cavity-enhanced detection of atomic motion (cavity optomechanics)



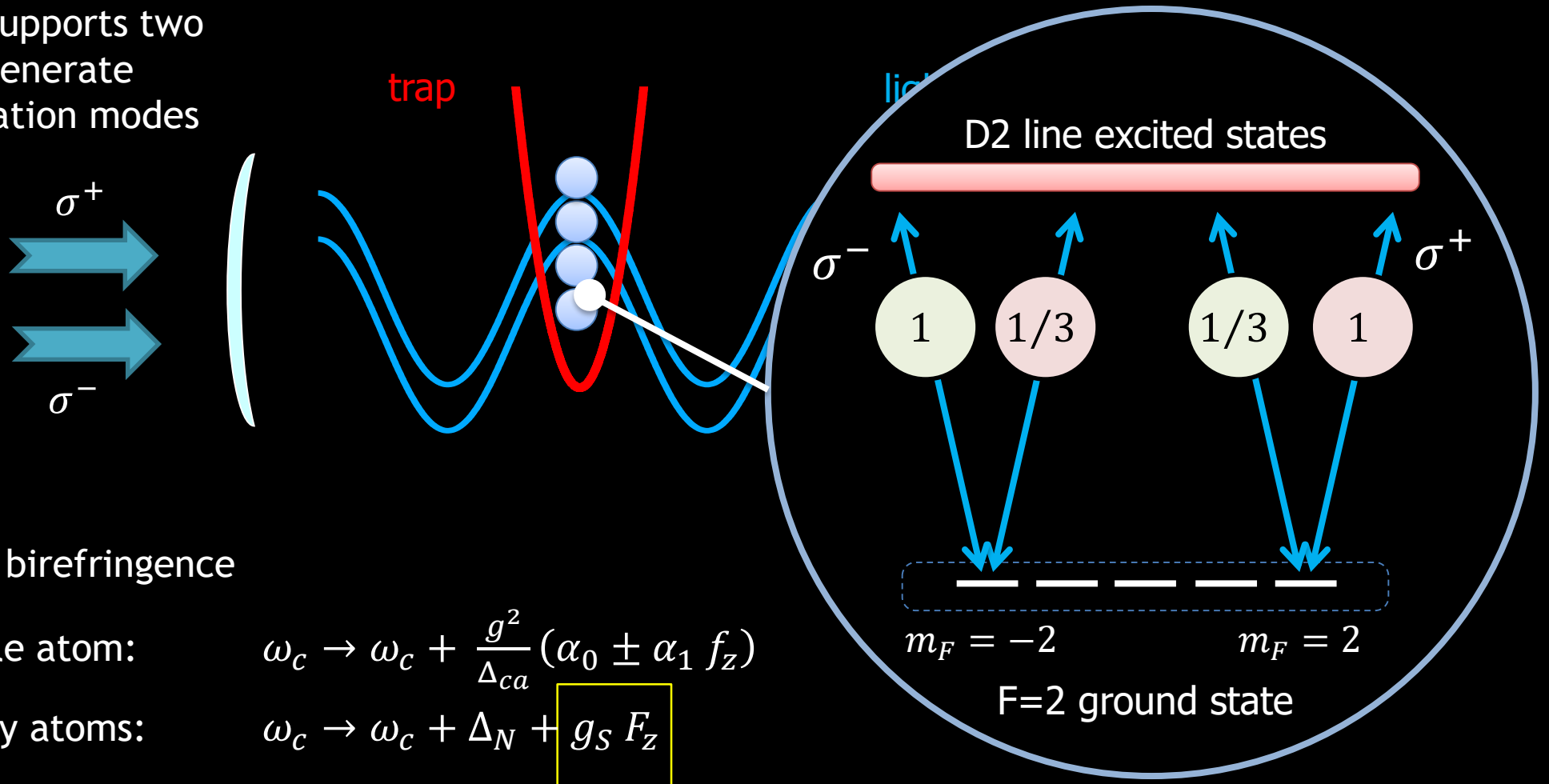
- Dispersive coupling
  - many atoms: $\omega_c \rightarrow \omega_c + \sum \frac{g^2(z_i)}{\Delta_{ca}} \simeq \omega_c + \Delta_N + \boxed{\frac{g_0^2 \sqrt{N}\, k}{\Delta_{ca}} z_{com}}$

Quantum cavity optomechanics with an ultracold-atom mechanical oscillator

"Cavity optomechanics with cold atoms," in Cavity Optomechanics: Nano-and Micromechanical Resonators Interacting with Light (Springer Berlin Heidelberg, 2014).

Atom(s) coupled to light in a cavity

cavity supports two degenerate polarization modes



- Circular birefringence
  - single atom: $\omega_c \rightarrow \omega_c + \frac{g^2}{\Delta_{ca}}(\alpha_0 \pm \alpha_1 f_z)$
  - many atoms: $\omega_c \rightarrow \omega_c + \Delta_N + g_S F_z$

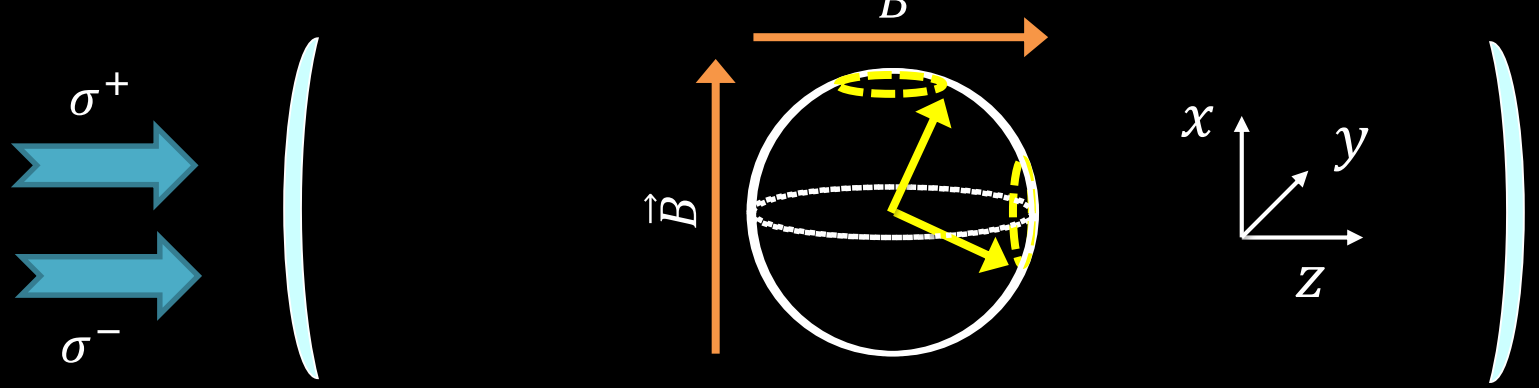
(vector) shift allows for real-time monitoring (and stabilization) of collective atomic spin

"cavity opto-magnonics"

Spin optodynamics analog of cavity optomechanics," PRA **82**, 041804(R) (2010)

Optical spin detection

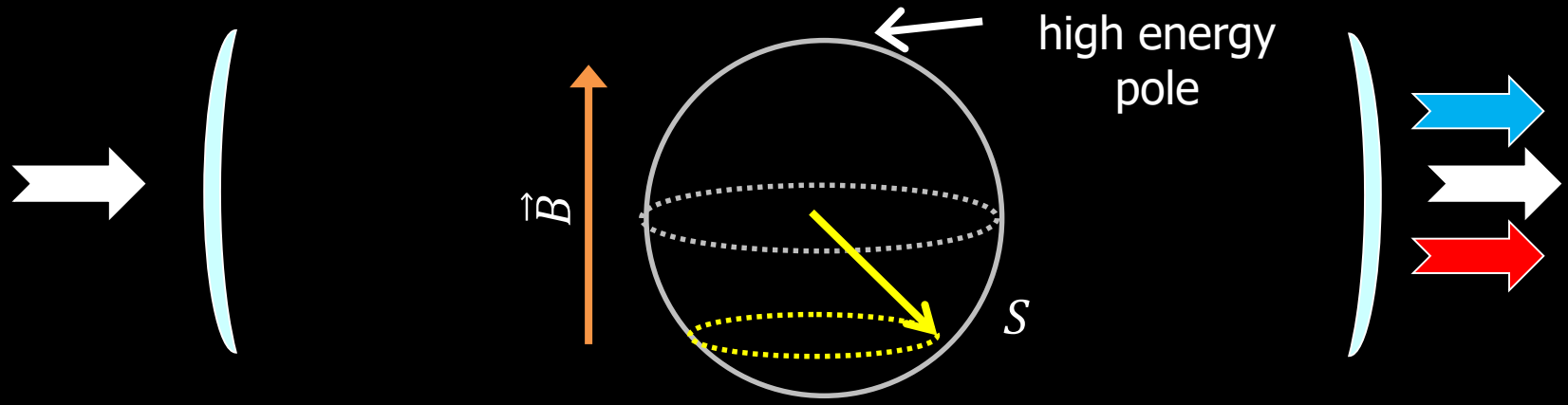
$$H = \gamma \vec{B} \cdot \vec{S}_{coll} \pm \hbar g_S \left(\hat{c}_+^\dagger \hat{c}_+ + \hat{c}_-^\dagger \hat{c}_- \right) \hat{S}_{coll,z}$$

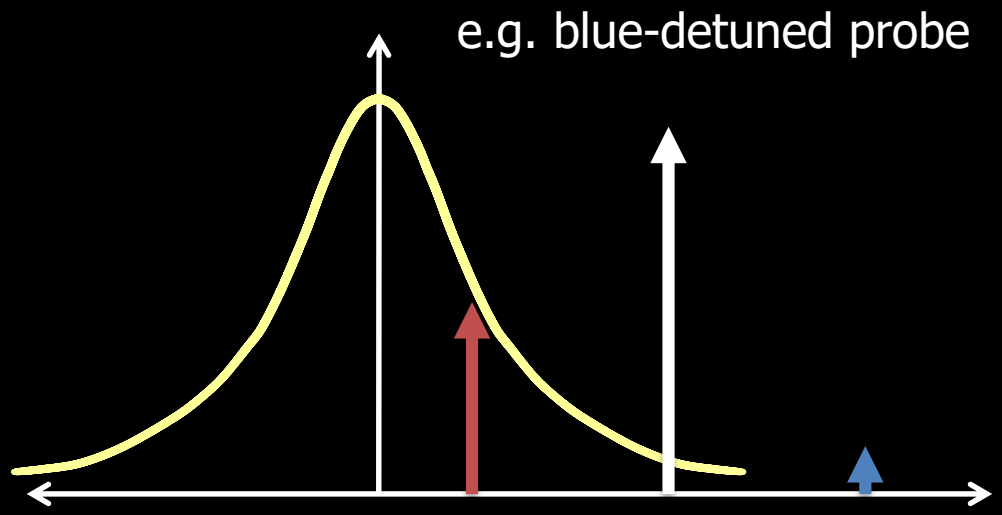


- Longitudinal field:
  - Continuous QND spin detection ($\hat{S}_{coll,z}(t)$ is const. of motion)
  - Measurement back-action does not affect measured signal

- Transverse field:
  - Continuous non-QND spin detection ($\hat{S}_{coll,z}(t)$ is not const. of motion)
  - Back-action enters measured signal ⇒ standard quantum limits
  - Cavity feeds measurement back onto dynamics ⇒ autonomous feedback

Coherent back-action as autonomous feedback



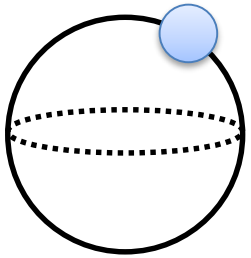


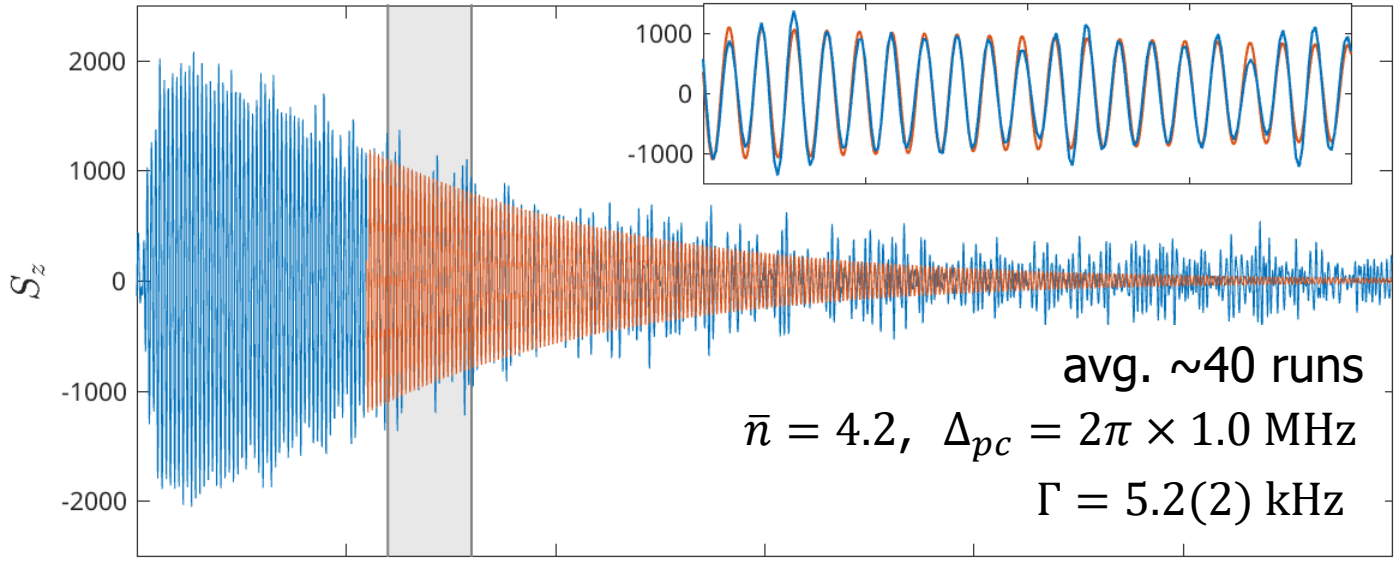
Larmor precession sidebands
cavity promotes anti-Stokes line,
extracts energy

- Dynamics observed through cavity emission:
  - phase coherent signal
  - sideband asymmetry

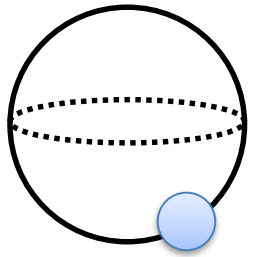
Autonomous feedback cooling toward high-energy pole

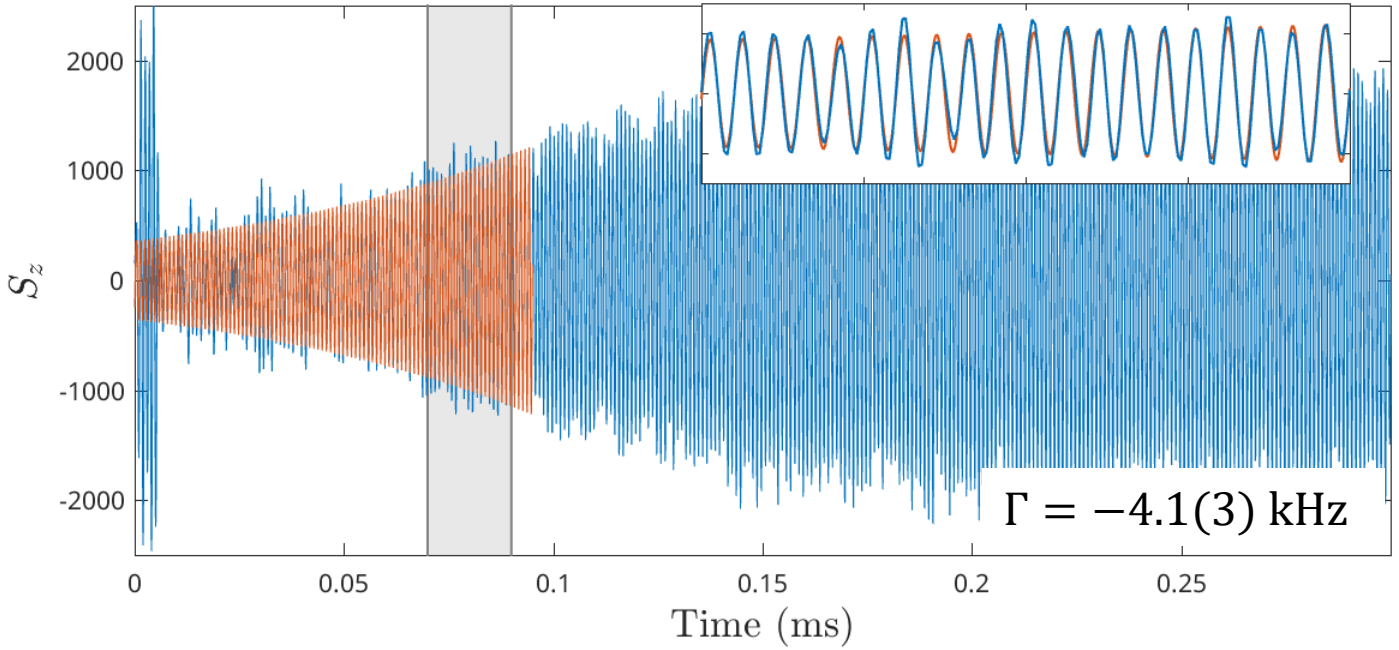
starting near high-energy pole





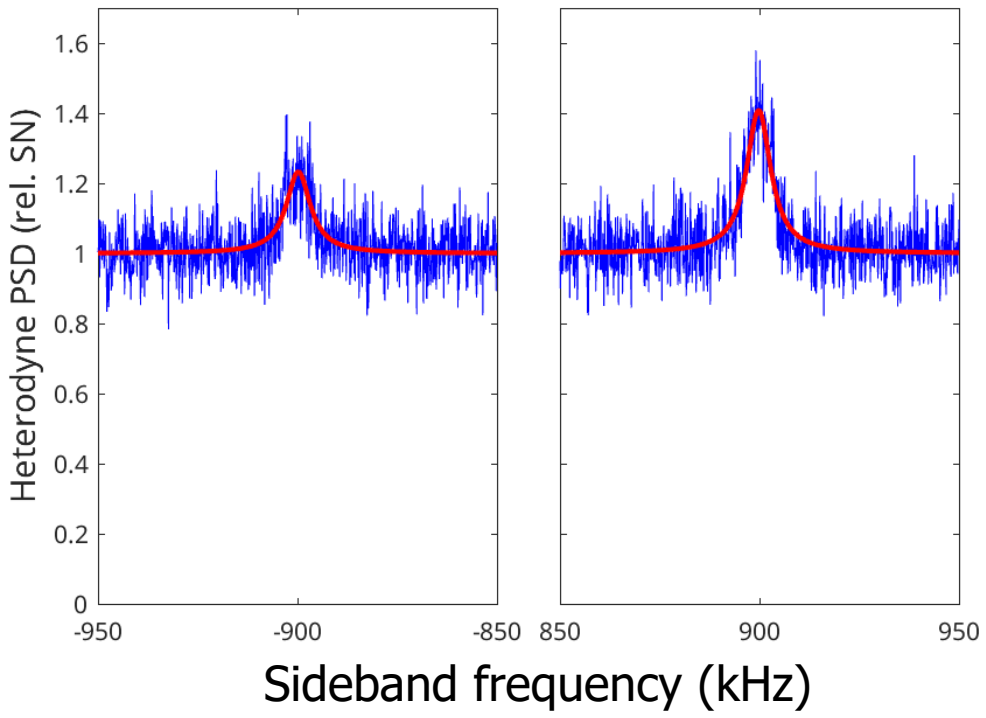
starting near low-energy pole

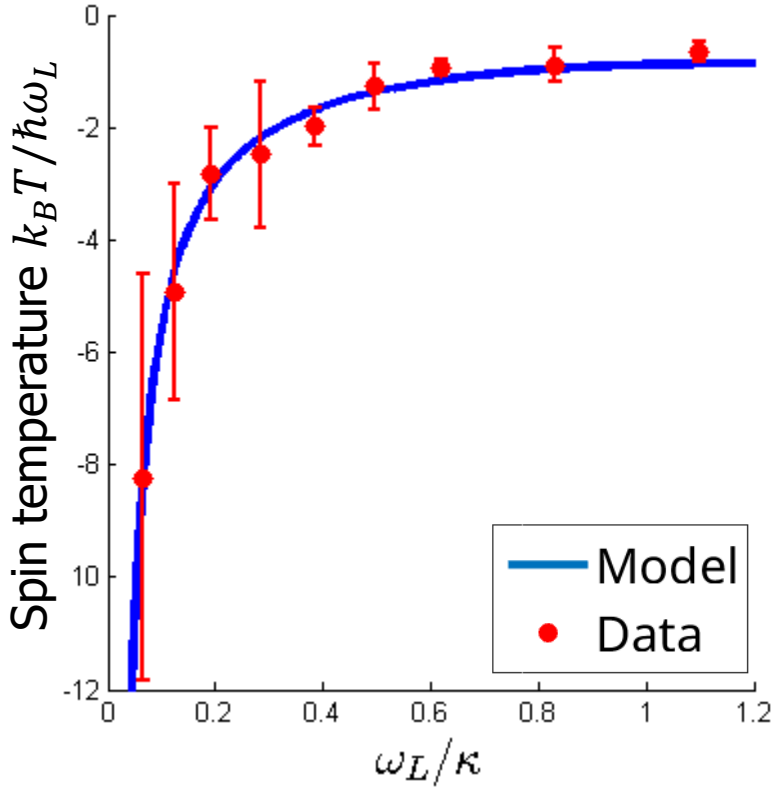




“Cooling” toward high-energy pole

- Sideband asymmetry
  - Cooling to negative spin temperature

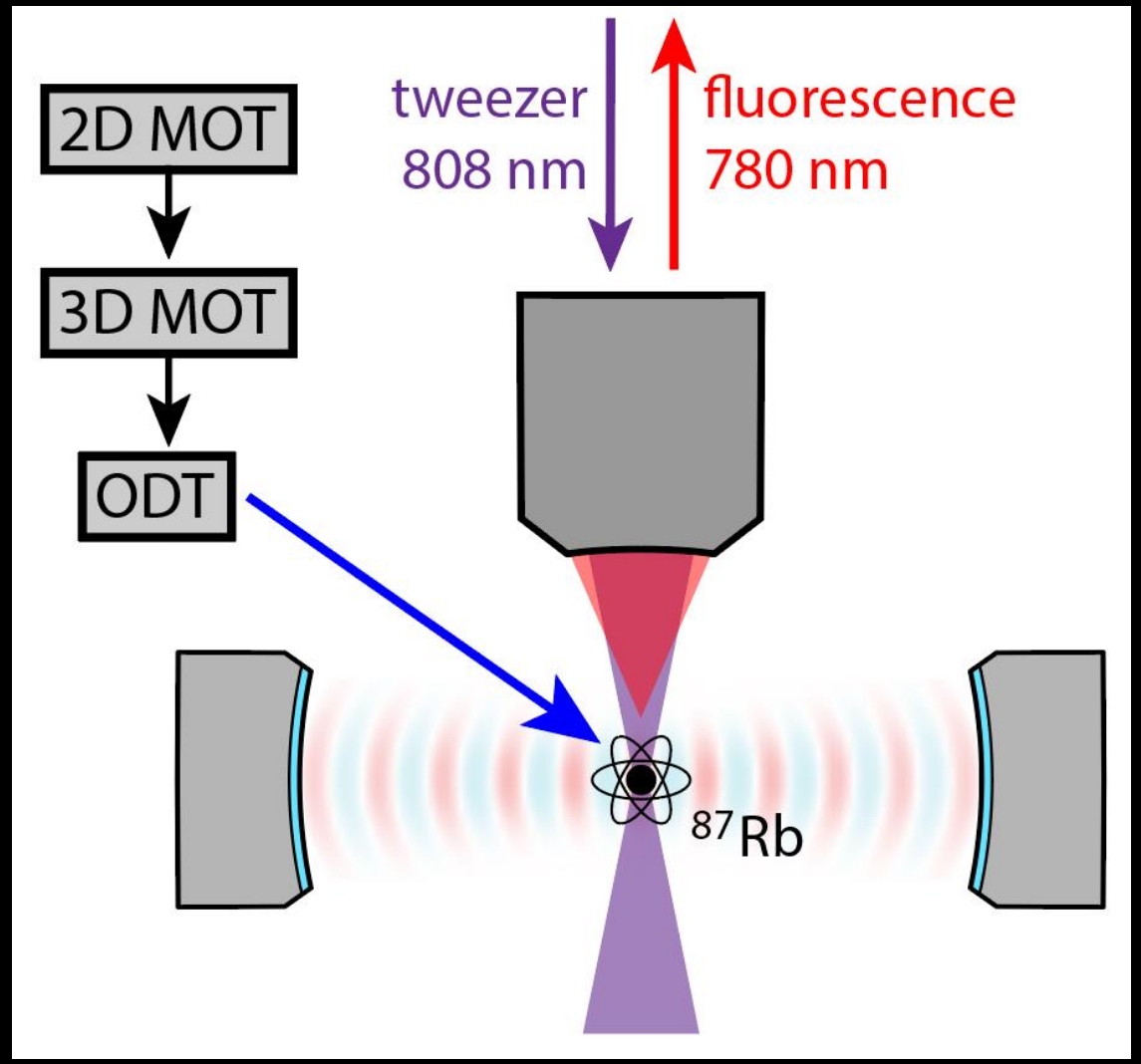




Cavity-enhanced detection of single atoms

"Super-resolution microscopy of optical fields using tweezer-trapped single atoms,"
Physical Review Letters **128**, 083201 (2022)

Cavity QED with a tweezer array (E6)



High-resolution lens

- 1D AOD-generated tweezer array
- Single atom fluorescence imaging
- Mitutoyo 0.5-NA objective
- Detection efficiency $\eta \sim .015$

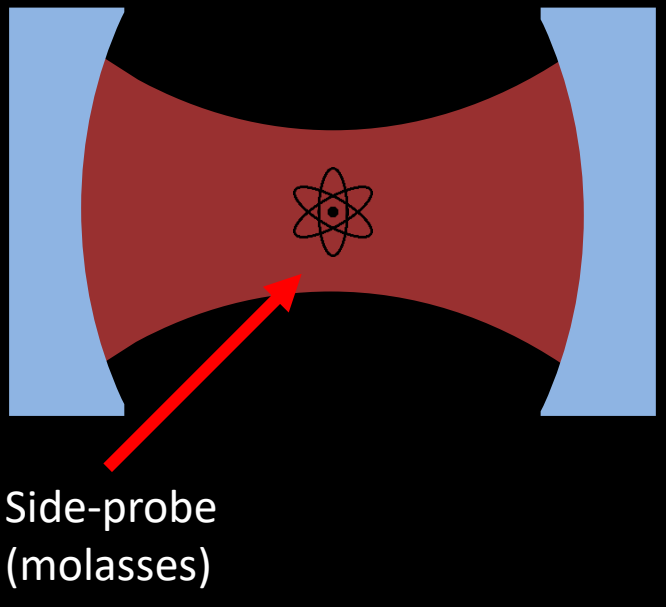
Near-concentric cavity

- Finesse @780 nm: ~15,000
- L ~ 1 cm
- $g_{\max} \sim 2\pi \times 2.7$ MHz
- $\kappa \sim 2\pi \times 1.2$ MHz
- $\Gamma \sim 2\pi \times 6.07$ MHz
- Cooperativity $4g^2/\kappa\Gamma \sim 4$
- Detection efficiency $\eta \sim .25$
- Also high finesse @1560 nm

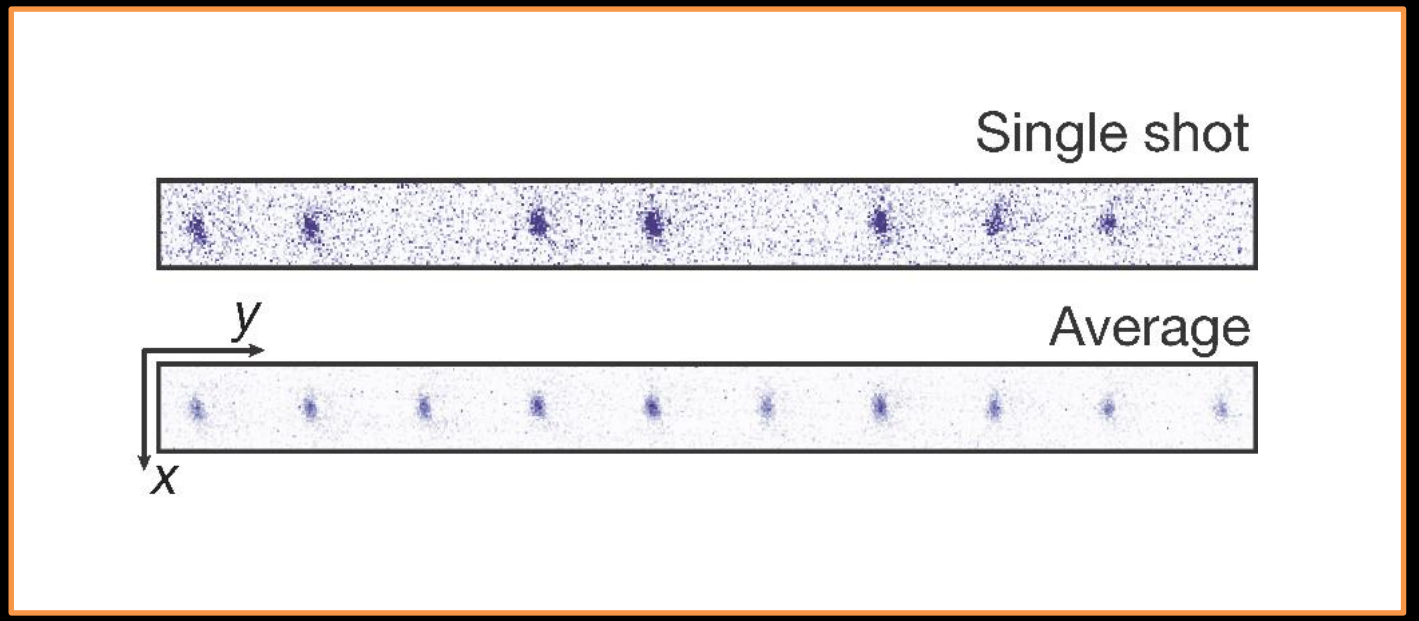
Fluorescence detection

camera

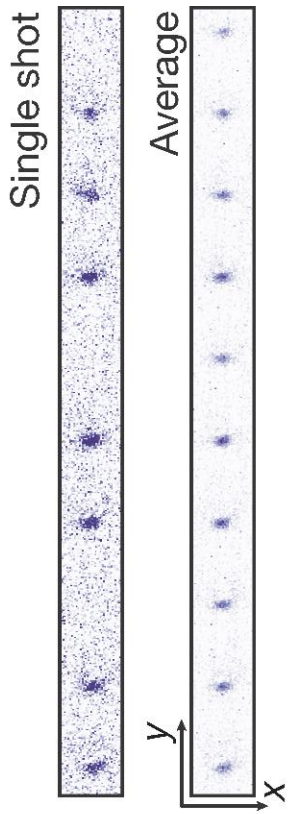


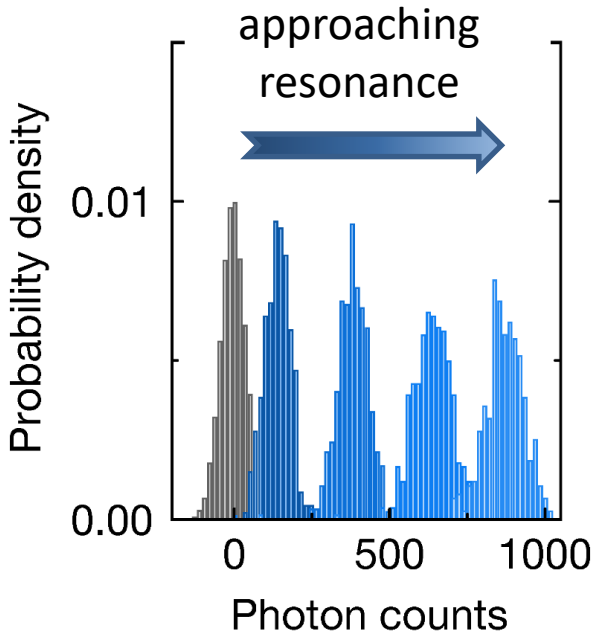


Side-probe
(molasses)



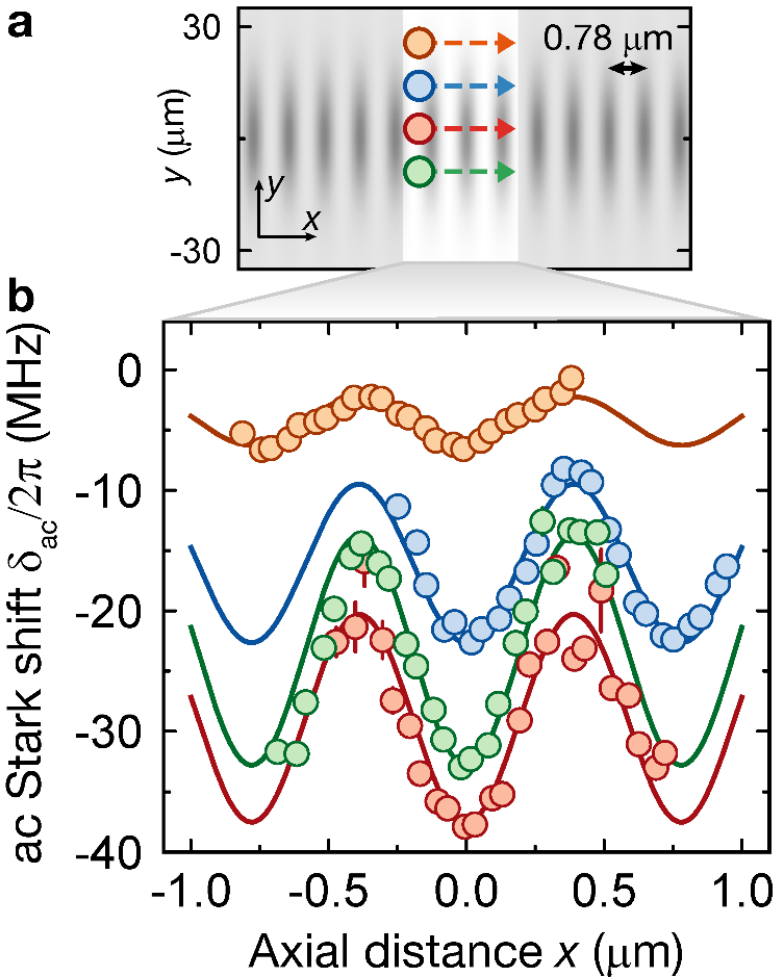
Scanning probe microscopy with single atoms





Fluorescence intensity varies with imaging light detuning

$$\Gamma_{scat} \propto (\omega_L - \omega_0 - \delta_{ac})^{-2}$$



"Sparrow resolution"
$r = 2\,\sigma = 300$ nm

"Super-resolution microscopy of optical fields using tweezer-trapped single atoms,"
Physical Review Letters 128, 083201 (2022)

Mid-circuit measurement in a tweezer array

“cavity QED for tweezers”

“Mid-circuit cavity measurement in a neutral atom array,”
Physical Review Letters **129**, 203602 (2022)

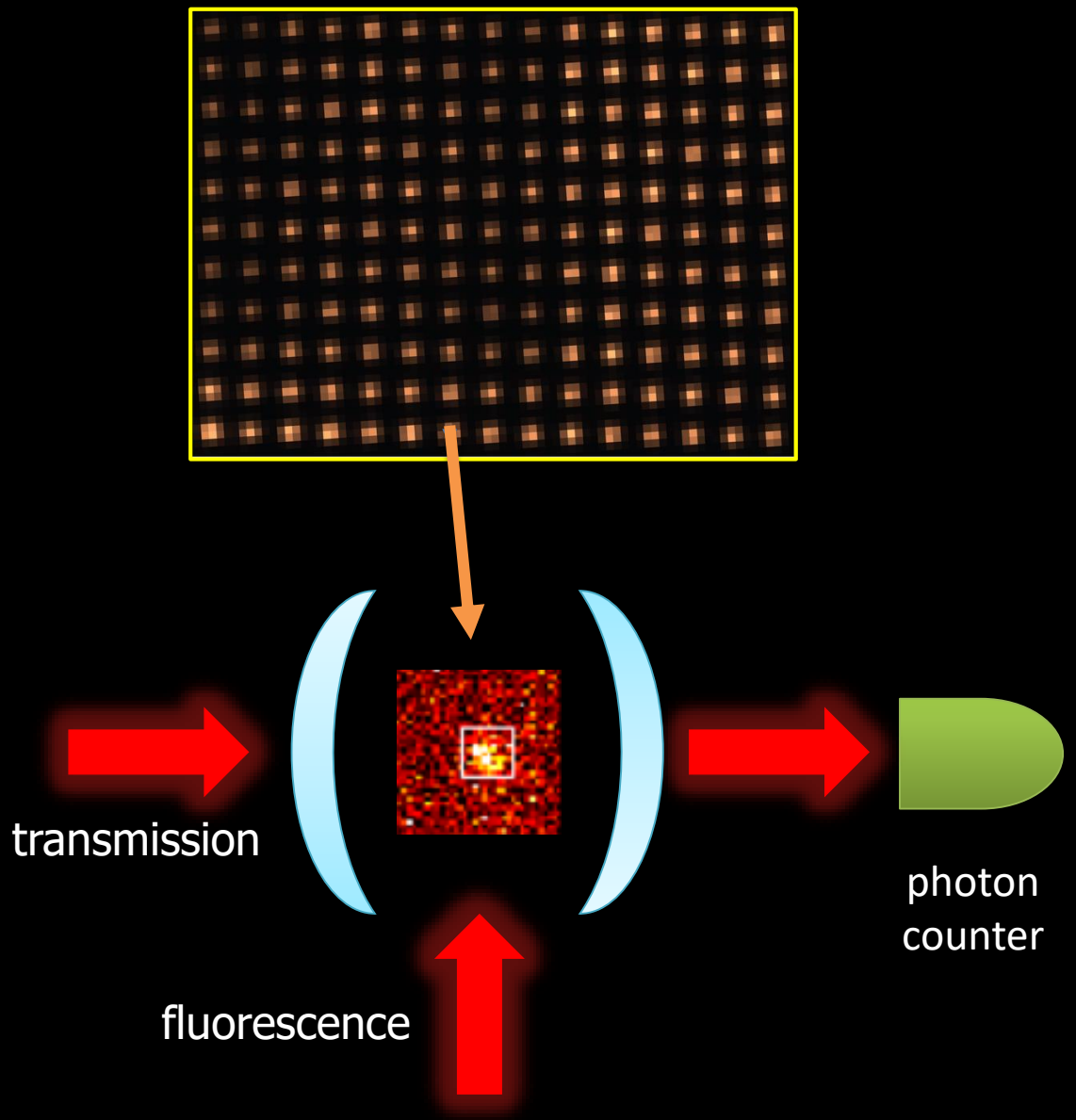
Cavity detection of a single tweezer-trapped atom

Tweezer array experimental sequence:

1. Load tweezers
2. Image filled/empty tweezers
3. Sort
4. Quantum interactions/gates/sensing
5. Image state of each tweezer

Possible improvements:

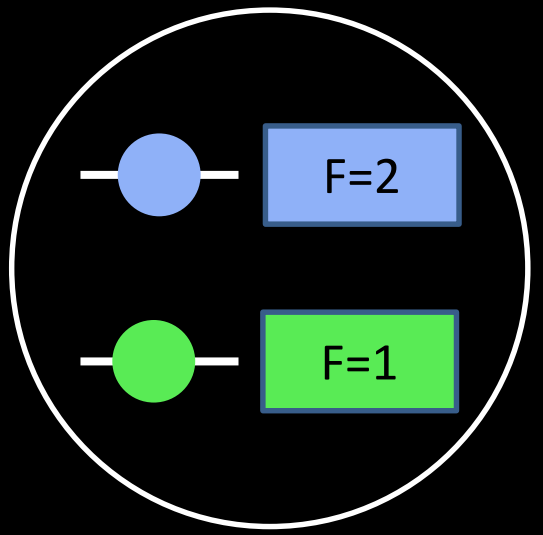
- Faster readout
  - Currently takes 10's of ms. Limits cycle time.
- Atom(s) specific, non-global readout
  - Feedback on live quantum system, error correction.
  - Cluster state quantum computing, sensing



Cavity-based single-atom state detection

Goal: fast, high fidelity detection of three states

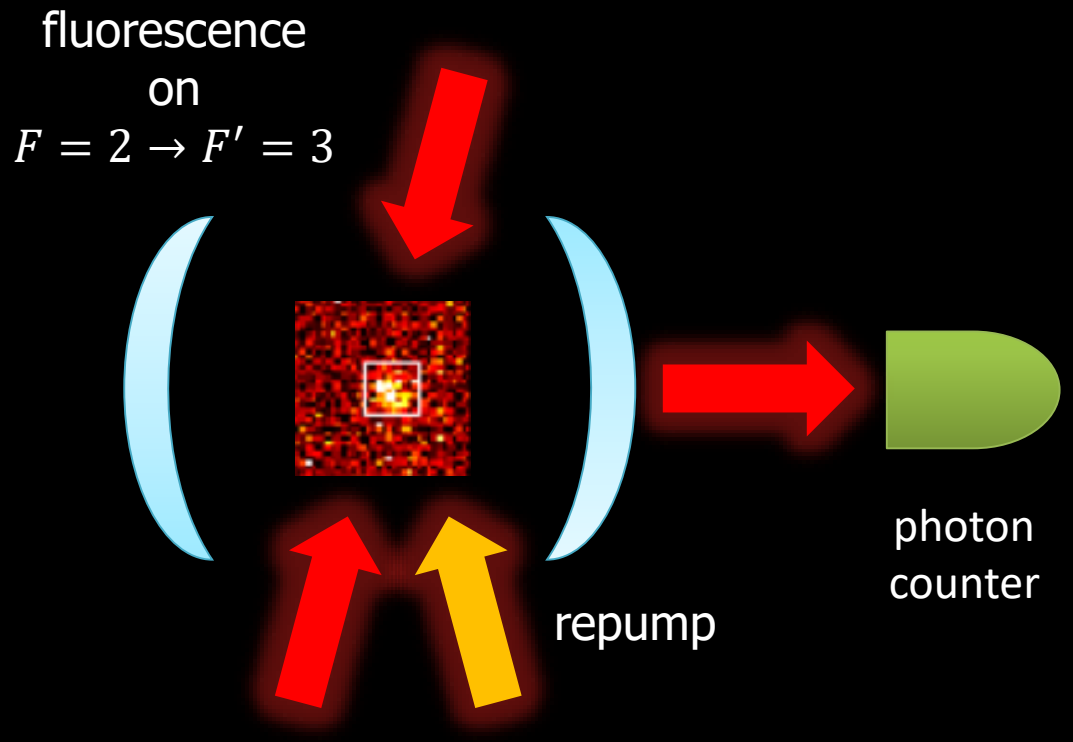
^{87}Rb hyperfine qubit

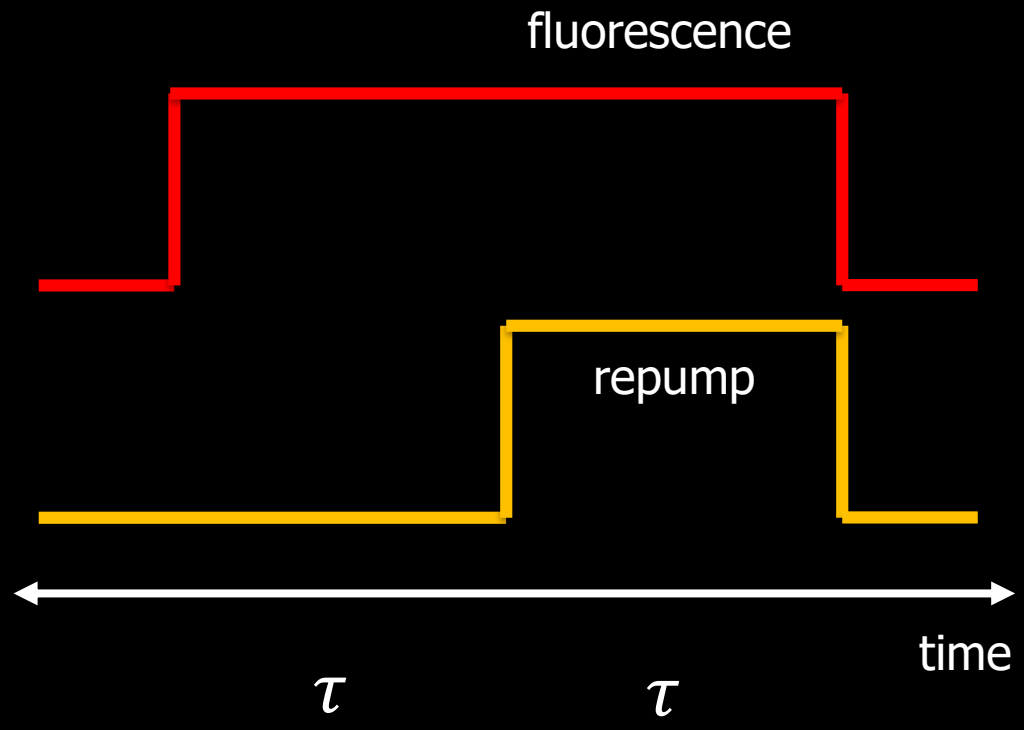


No atom or outside logical states

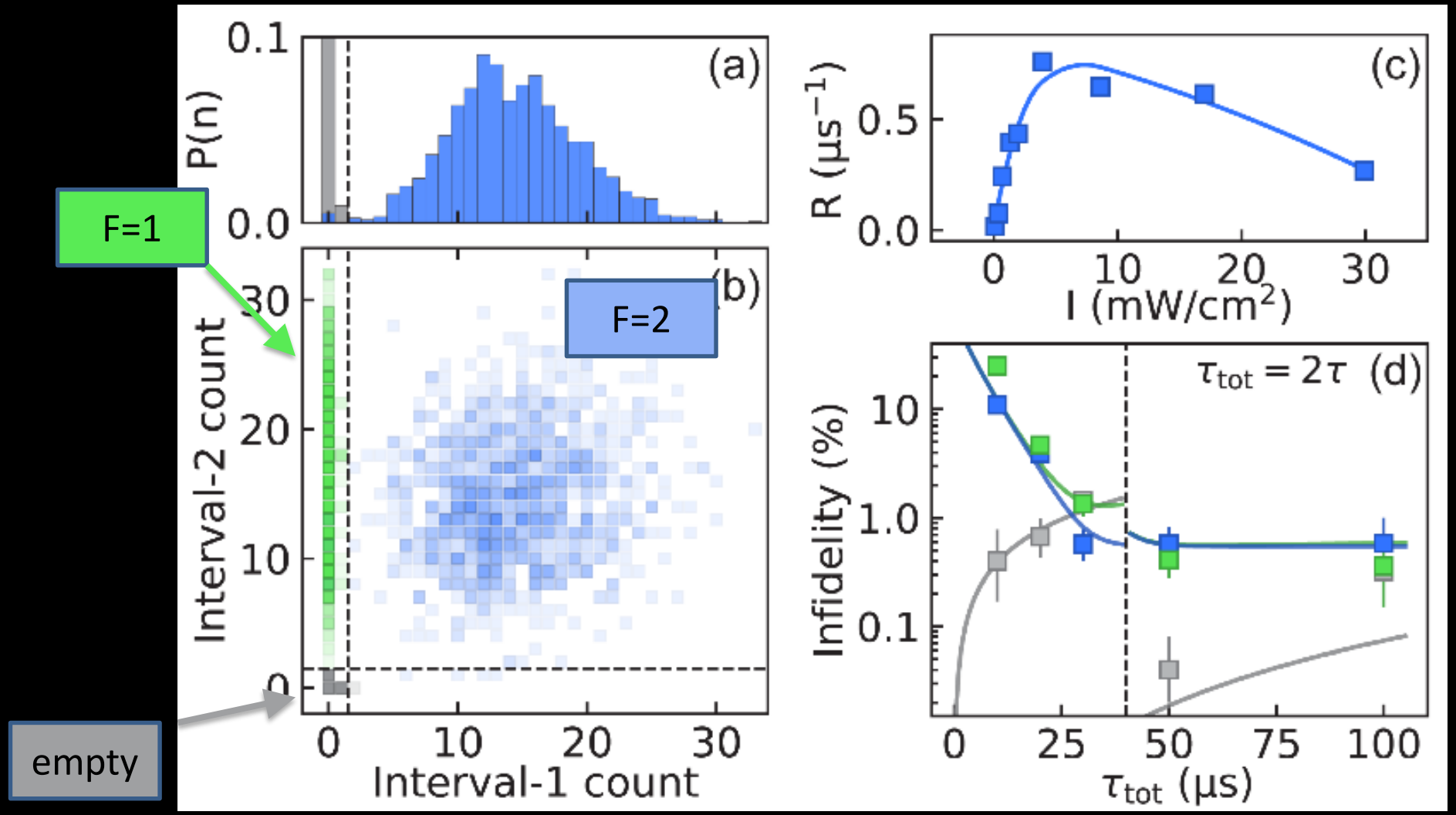


Method 1: (F)luorescence – (R)epump (F)luorescence (FRF)





Method 1: (F)luorescence - (R)epump (F)luorescence (FRF)



Mid-circuit measurement in an atomic tweezer array

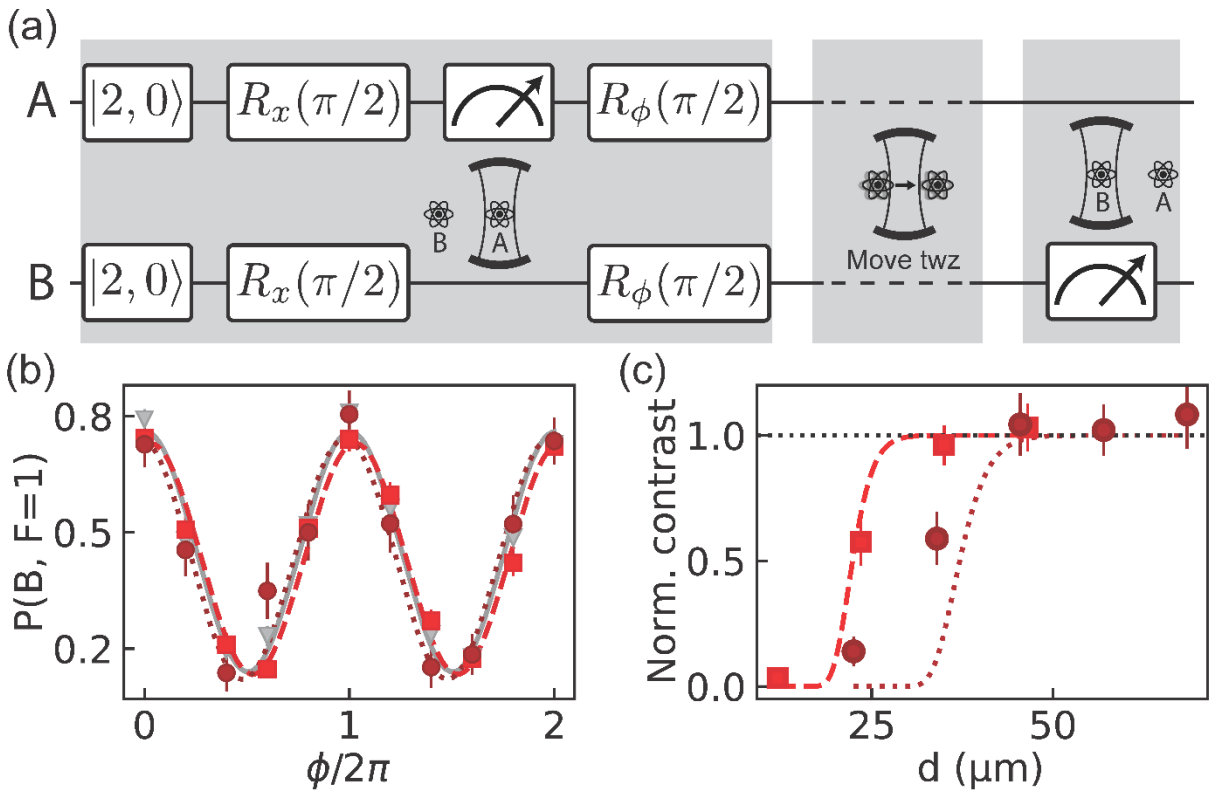
Fast, high fidelity detection of three states:

- No atom (or atom outside logical state basis)
- F=1 hyperfine state (logical $|0\rangle$)
- F=2 hyperfine state (logical $|1\rangle$)

Table I. Measurement infidelity and loss probability

		No atom	F=1	F=2
Fluorescence $2\times(\tau = 25\,\mu s)$	Outcome	low-low	low-high	high-X
	Infidelity	0.04(3) %	0.4(2) %	0.6(2) %
	Loss prob.	n/a	0.2(2) %	1.4(3) %
Transmission $2\times(\tau = 50\,\mu s) + 5\,\mu s$	Outcome	high-high	high-low	low-X
	Infidelity	0.4(1) %	1.1(2) %	0.9(2) %
	Loss prob.	n/a	0.7(3) %	1.4(2) %

excellent recent implementation in fiber cavities by Lukin group



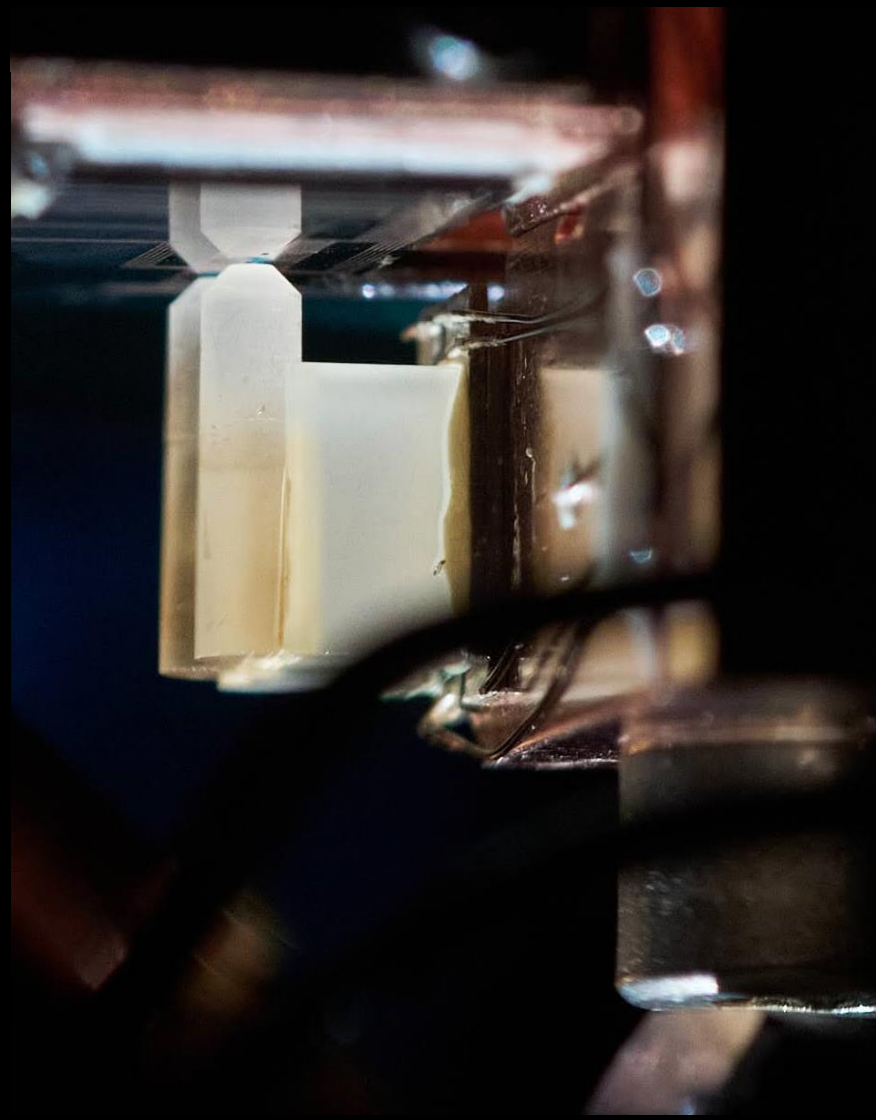
Measurement on portion of atom array does not affect quantum coherence of remainder of array

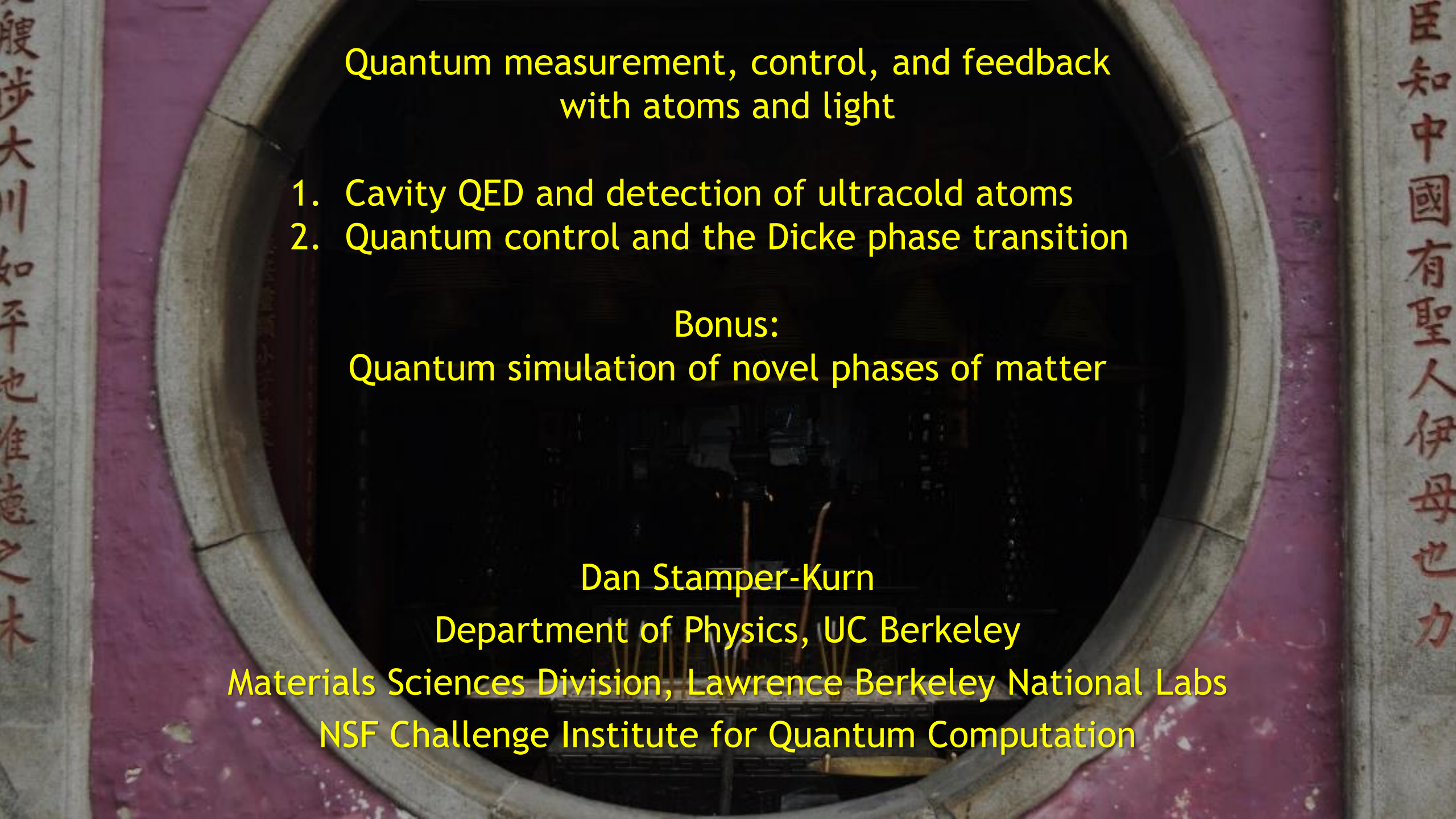
recent mid-circuit operations by Kaufman group, Saffman group, Atom Computing,…

"Mid-circuit cavity measurement in a neutral atom array," Physical Review Letters **129**, 203602 (2022)

Cavity QED and detection of ultracold atoms
Summary

- Light can be used to measure ultracold atomic quantum systems
- Strongly coupled cavity enhances detection sensitivity, minimizes backaction and noise
  - “No wasted information”
- Many different properties can be measured
  - Shown: atom number, position, spin.
  - Others: pair correlation, collective measurements…
- Continuous and real-time measurement
- Cavity is not a passive measurement device
  - Incoherent and coherent backaction
- Cavity is not a closed quantum system





Quantum measurement, control, and feedback with atoms and light

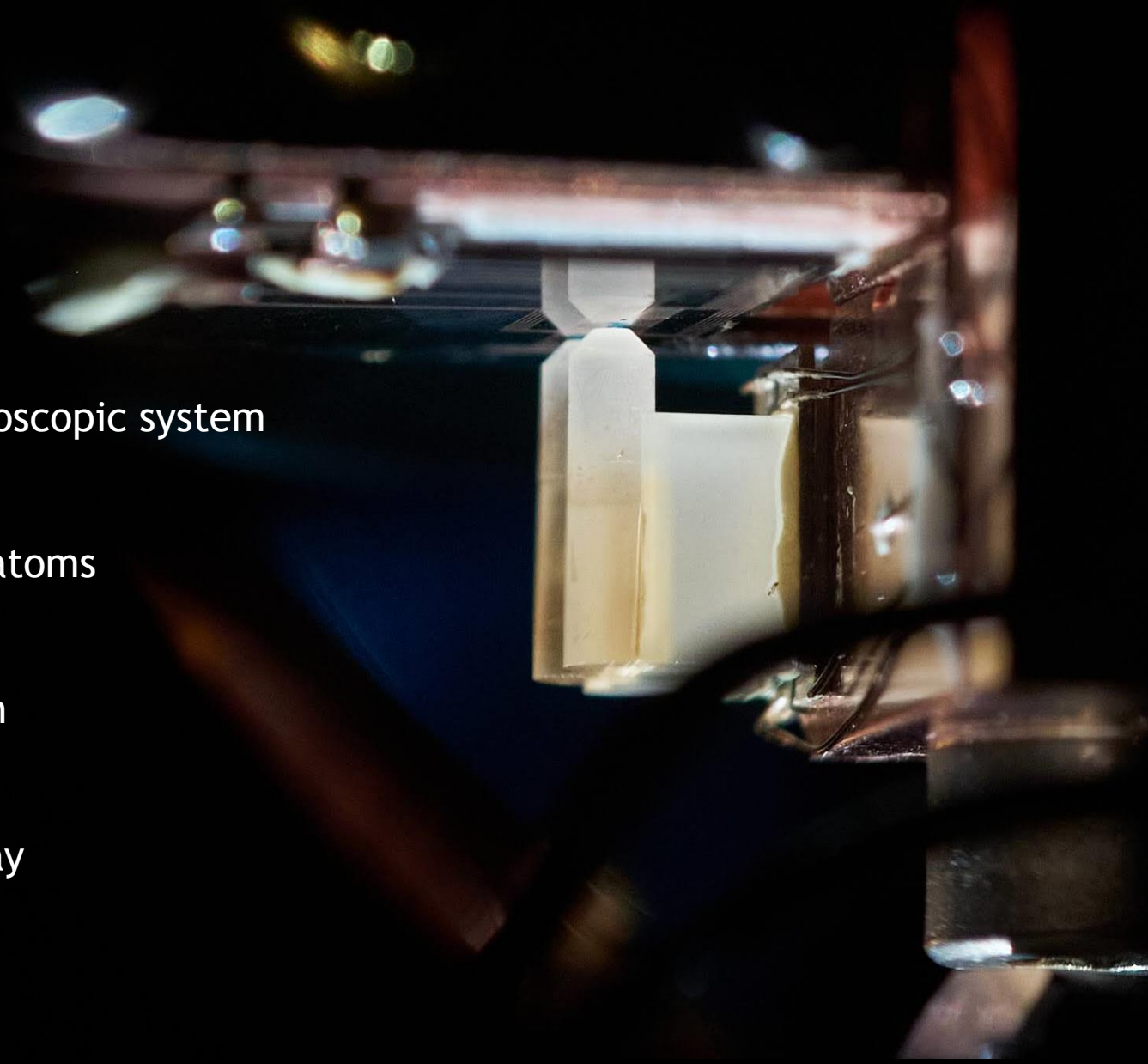
1. Cavity QED and detection of ultracold atoms
2. Quantum control and the Dicke phase transition

Bonus:
Quantum simulation of novel phases of matter

Dan Stamper-Kurn
Department of Physics, UC Berkeley
Materials Sciences Division, Lawrence Berkeley National Labs
NSF Challenge Institute for Quantum Computation

Cavity QED and detection of ultracold atoms

- Primer on cavity QED
- How to position atoms in an optical cavity
- Cavity-enhanced detection of atom number
  - Non-equilibrium thermodynamics in a mesoscopic system
- Cavity-enhanced detection of atomic position
  - Quantum cavity optomechanics with cold atoms
- Cavity-enhanced detection of atomic spin
  - Coherent and incoherent cavity backaction
- Cavity-enhanced detection of single atoms:
  - Mid-circuit measurement in a tweezer array



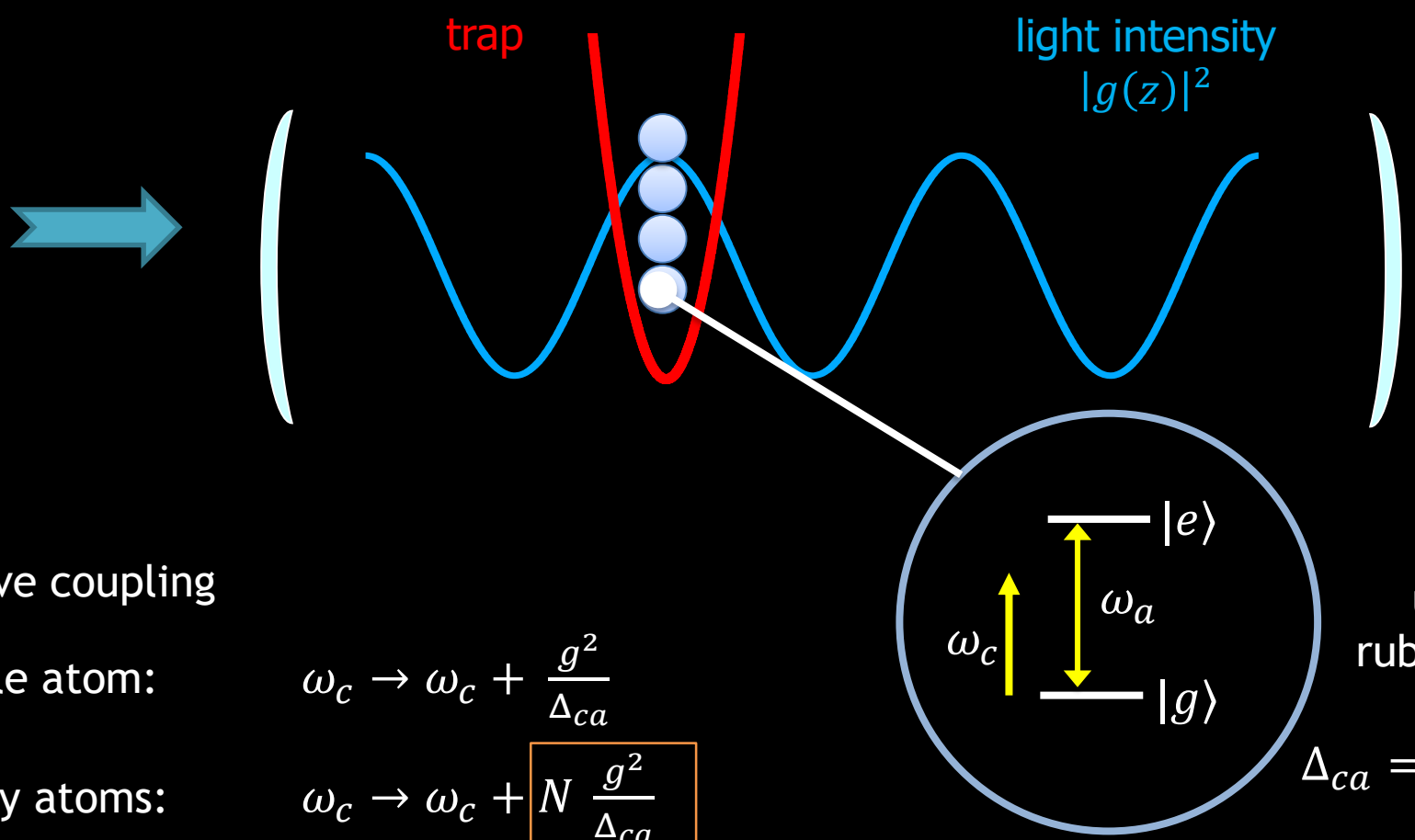
Cavity-enhanced detection of atomic spin:

Coherent and incoherent cavity backaction

"Spin optodynamics analog of cavity optomechanics," PRA **82**, 041804(R) (2010)

"Cavity-assisted measurement and coherent control of collective atomic spin oscillators," PRL **118**, 063604 (2017)

Cavity-enhanced detection of atom number



ultracold rubidium atom

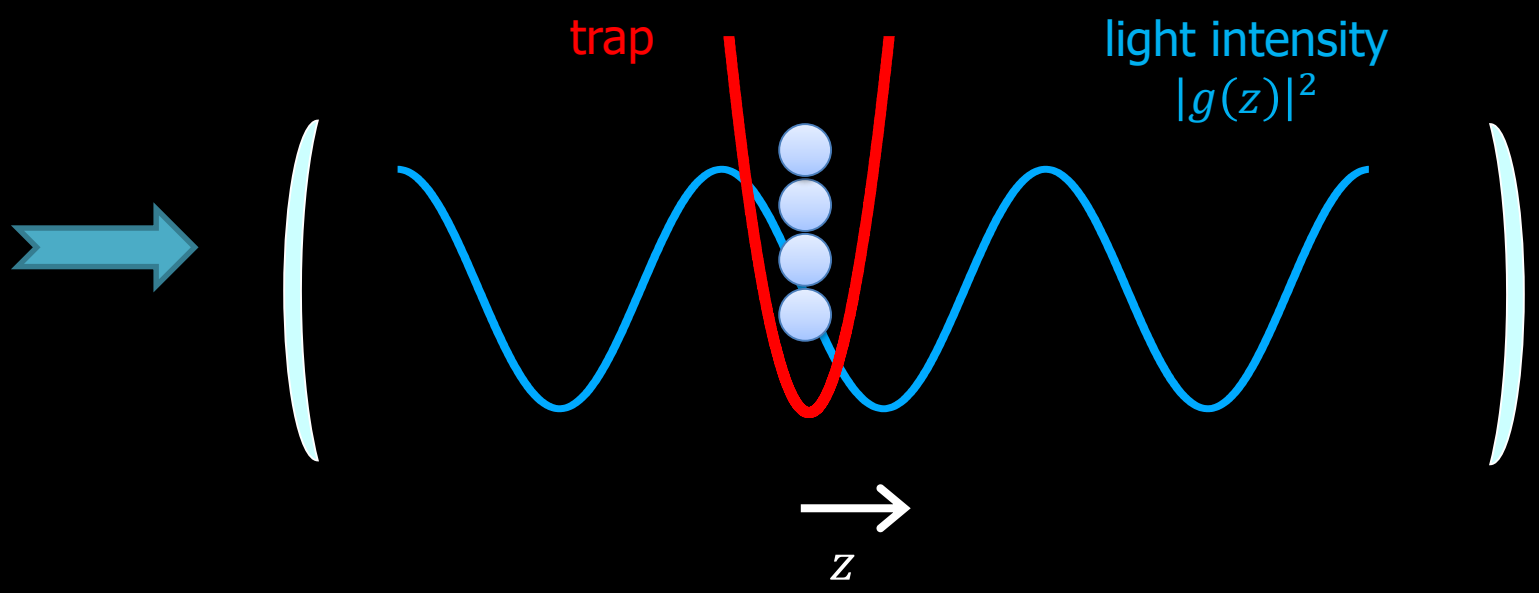
$\Delta_{ca} = \omega_c - \omega_a$

- Dispersive coupling
  - single atom: $\omega_c \rightarrow \omega_c + \frac{g^2}{\Delta_{ca}}$
  - many atoms: $\omega_c \rightarrow \omega_c + \boxed{N \frac{g^2}{\Delta_{ca}}}$

(scalar) shift allows for real-time monitoring (and stabilization) of atom number

"Tracking evaporative cooling of a mesoscopic atomic quantum gas in real time," PRX 11, 041014 (2021)

Cavity-enhanced detection of atomic motion (cavity optomechanics)



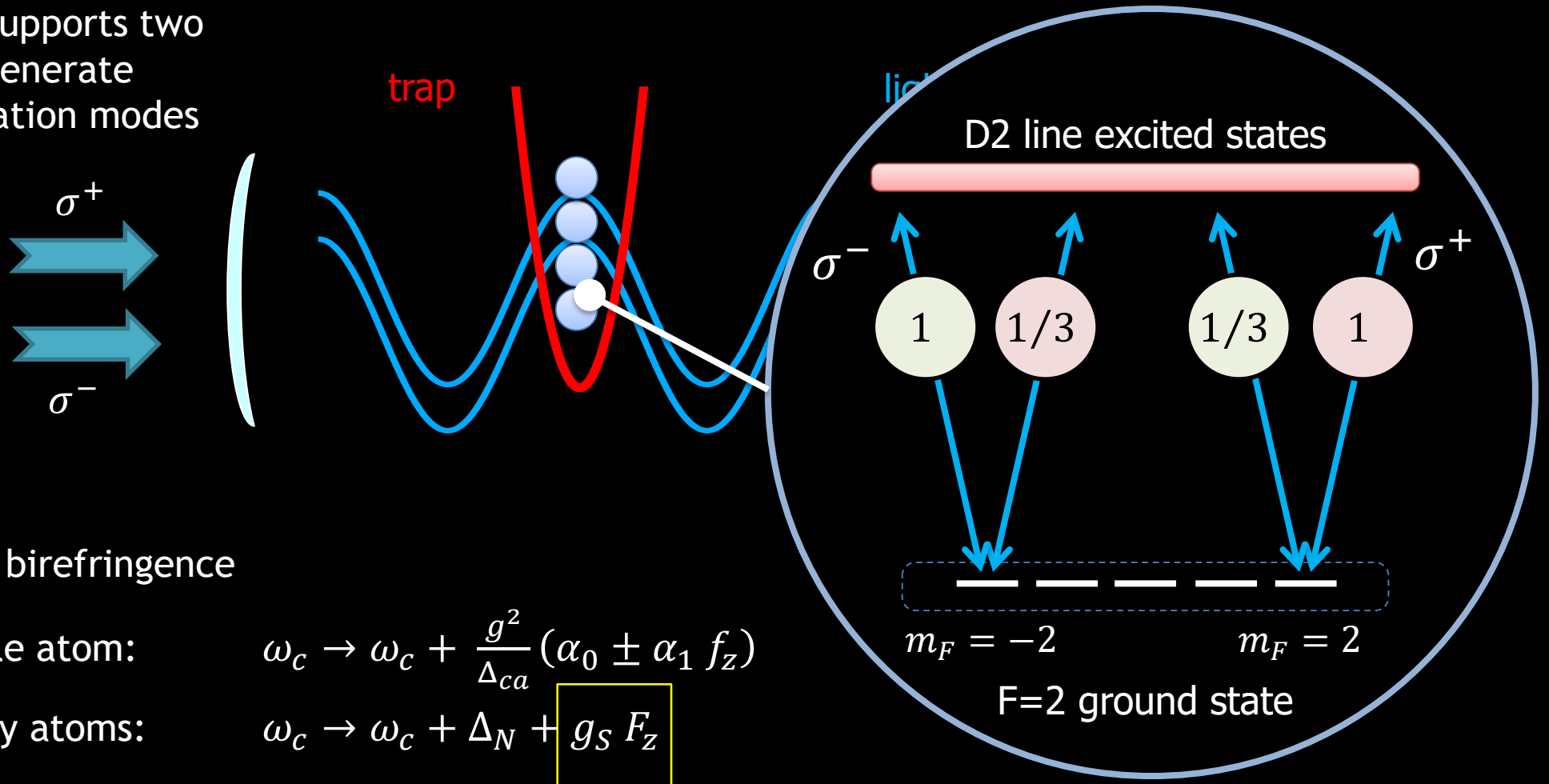
- Dispersive coupling
  - many atoms: $\omega_c \rightarrow \omega_c + \sum \frac{g^2(z_i)}{\Delta_{ca}} \simeq \omega_c + \Delta_N + \boxed{\frac{g_0^2 \sqrt{N}\, k}{\Delta_{ca}} z_{com}}$

Quantum cavity optomechanics with an ultracold-atom mechanical oscillator

"Cavity optomechanics with cold atoms," in Cavity Optomechanics: Nano-and Micromechanical Resonators Interacting with Light (Springer Berlin Heidelberg, 2014).

Atom(s) coupled to light in a cavity

cavity supports two degenerate polarization modes



- Circular birefringence
  - single atom: $\omega_c \rightarrow \omega_c + \frac{g^2}{\Delta_{ca}}(\alpha_0 \pm \alpha_1 f_z)$
  - many atoms: $\omega_c \rightarrow \omega_c + \Delta_N + g_S F_z$

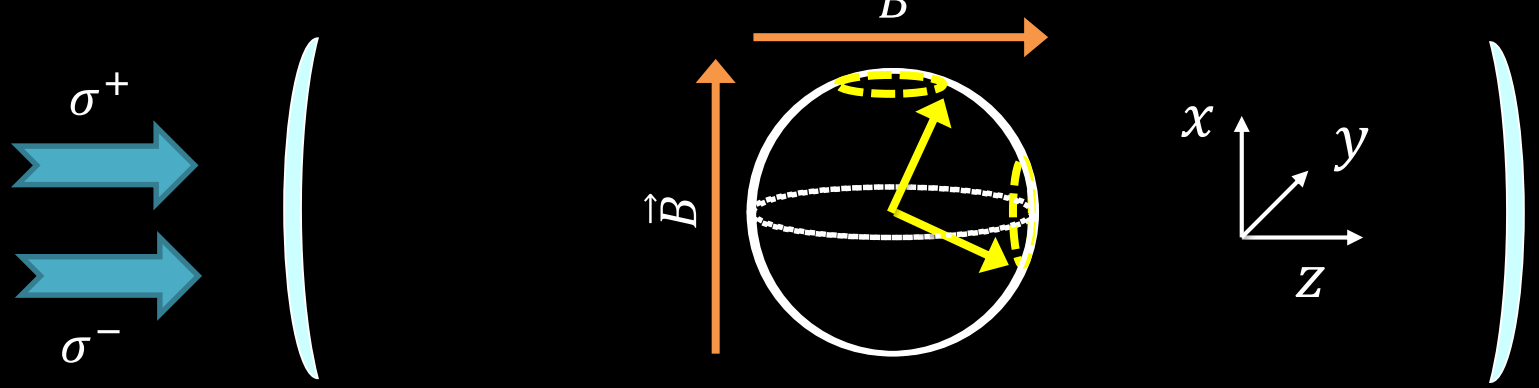
(vector) shift allows for real-time monitoring (and stabilization) of collective atomic spin

"cavity opto-magnonics"

Spin optodynamics analog of cavity optomechanics," PRA **82**, 041804(R) (2010)

Optical spin detection

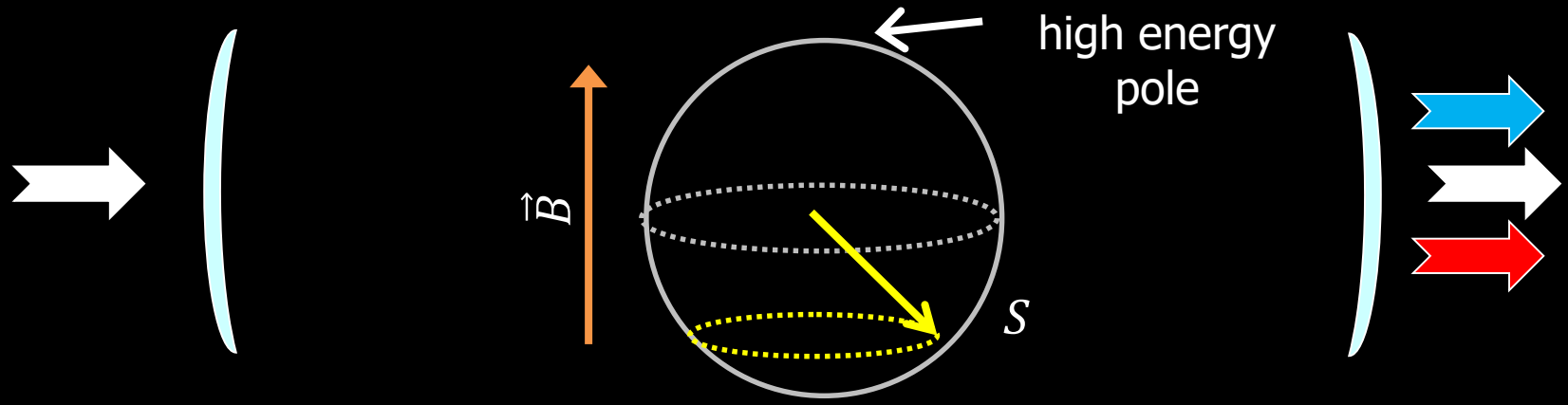
$$H = \gamma \vec{B} \cdot \vec{S}_{coll} \pm \hbar g_S \left(\hat{c}_+^\dagger \hat{c}_+ + \hat{c}_-^\dagger \hat{c}_- \right) \hat{S}_{coll,z}$$

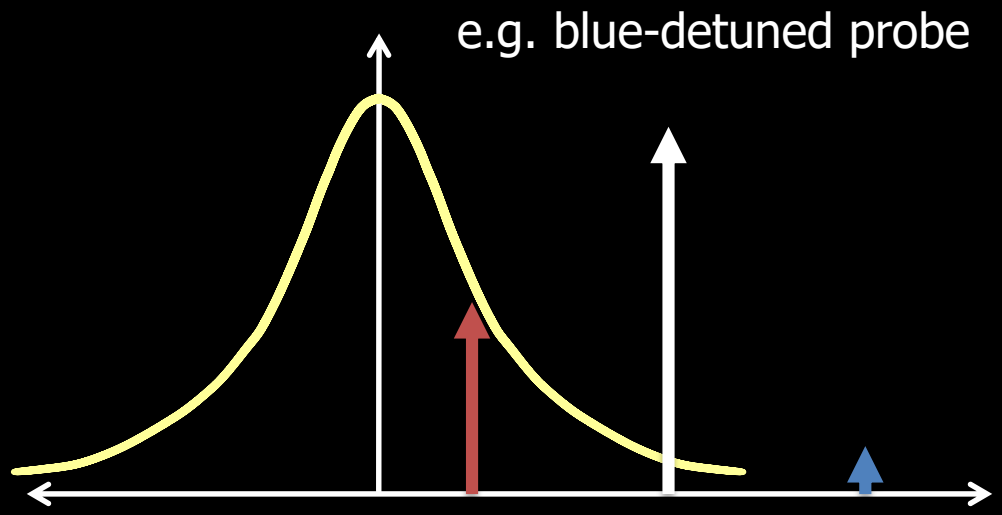


- Longitudinal field:
  - Continuous QND spin detection ($\hat{S}_{coll,z}(t)$ is const. of motion)
  - Measurement back-action does not affect measured signal

- Transverse field:
  - Continuous non-QND spin detection ($\hat{S}_{coll,z}(t)$ is not const. of motion)
  - Back-action enters measured signal ⇒ standard quantum limits
  - Cavity feeds measurement back onto dynamics ⇒ autonomous feedback

Coherent back-action as autonomous feedback



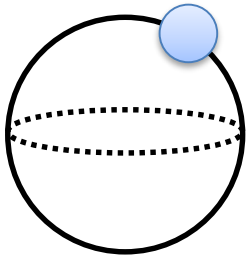


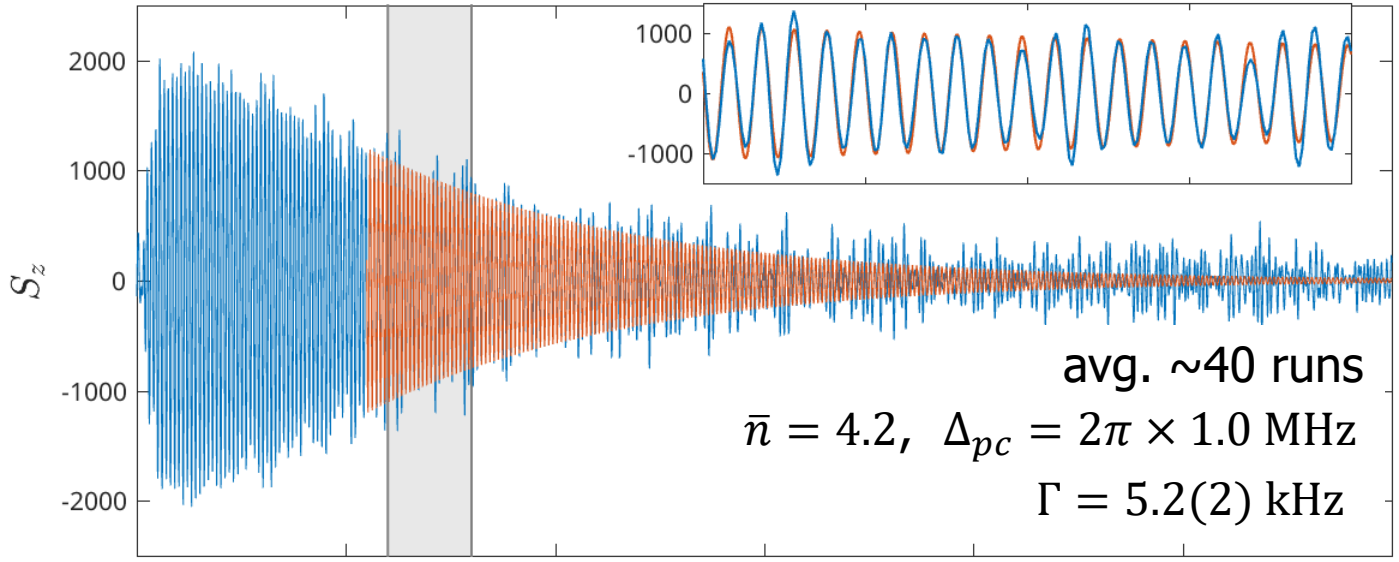
Larmor precession sidebands
cavity promotes anti-Stokes line,
extracts energy

- Dynamics observed through cavity emission:
  - phase coherent signal
  - sideband asymmetry

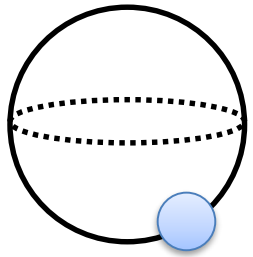
Autonomous feedback cooling toward high-energy pole

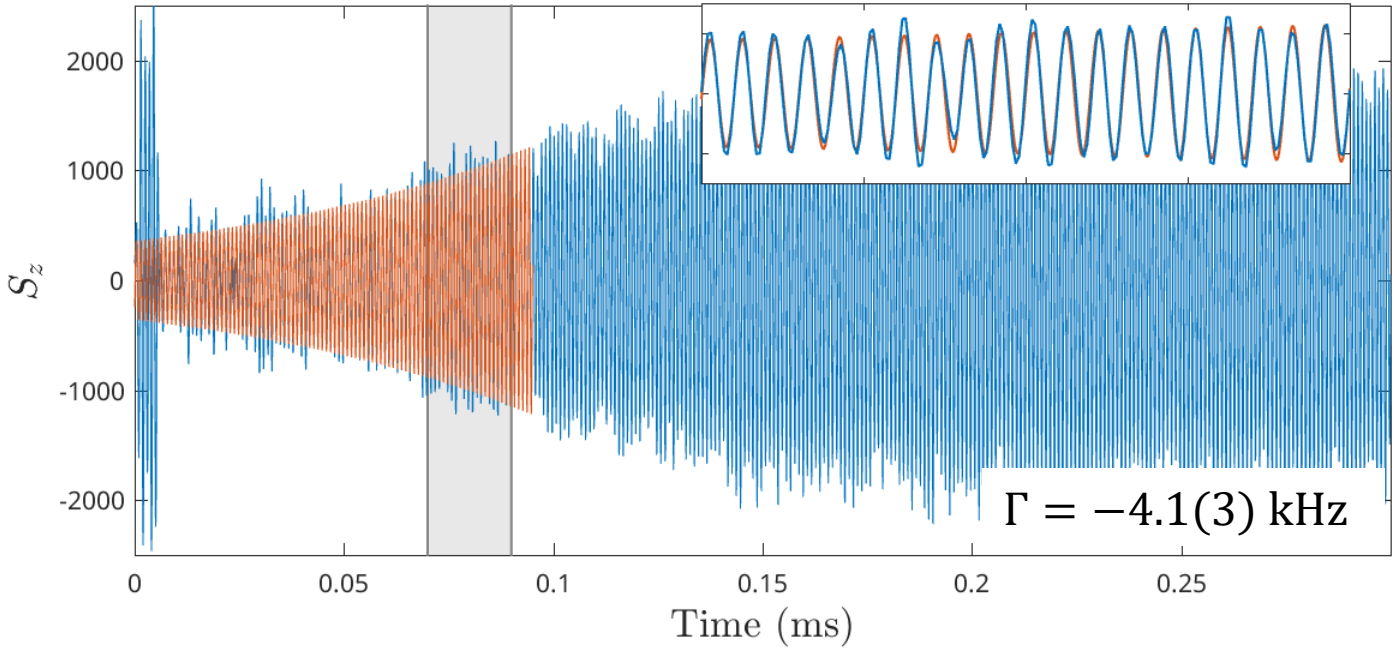
starting near high-energy pole





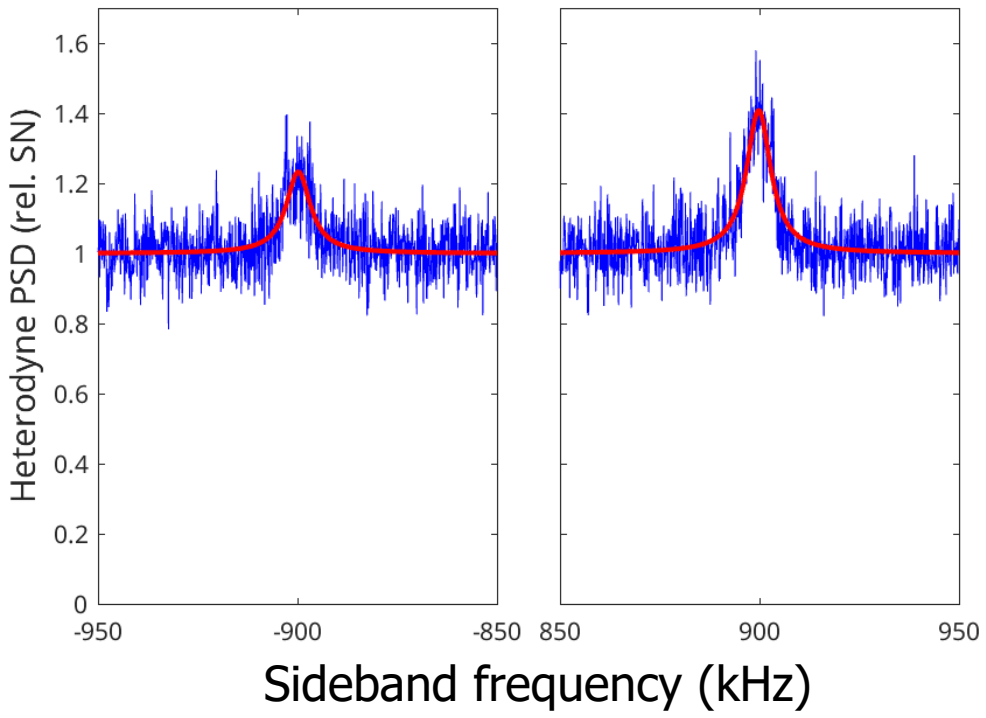
starting near low-energy pole

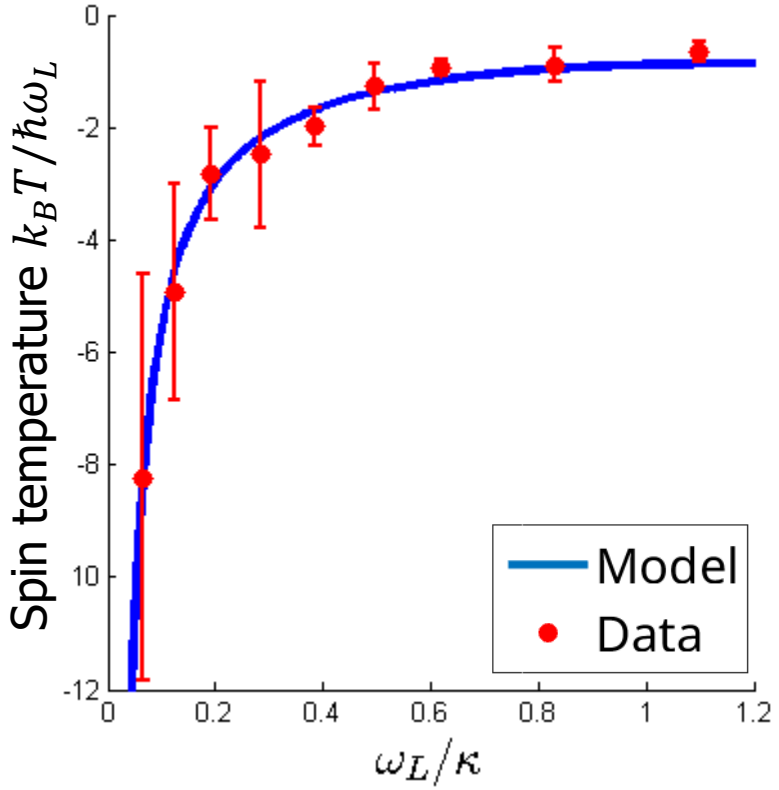




“Cooling” toward high-energy pole

- Sideband asymmetry
  - Cooling to negative spin temperature

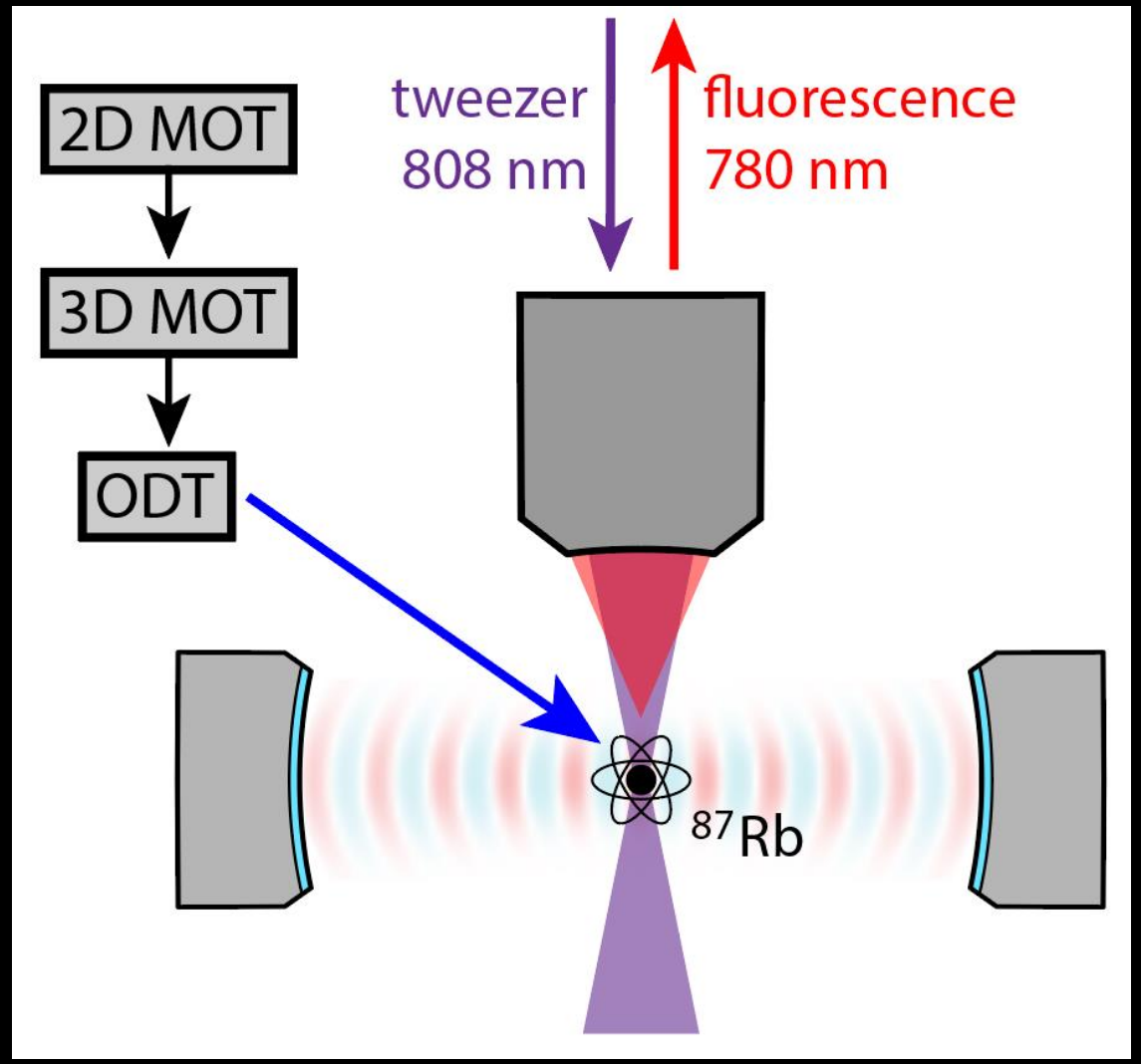




Cavity-enhanced detection of single atoms

"Super-resolution microscopy of optical fields using tweezer-trapped single atoms,"
Physical Review Letters **128**, 083201 (2022)

Cavity QED with a tweezer array (E6)



High-resolution lens

- 1D AOD-generated tweezer array
- Single atom fluorescence imaging
- Mitutoyo 0.5-NA objective
- Detection efficiency $\eta \sim .015$

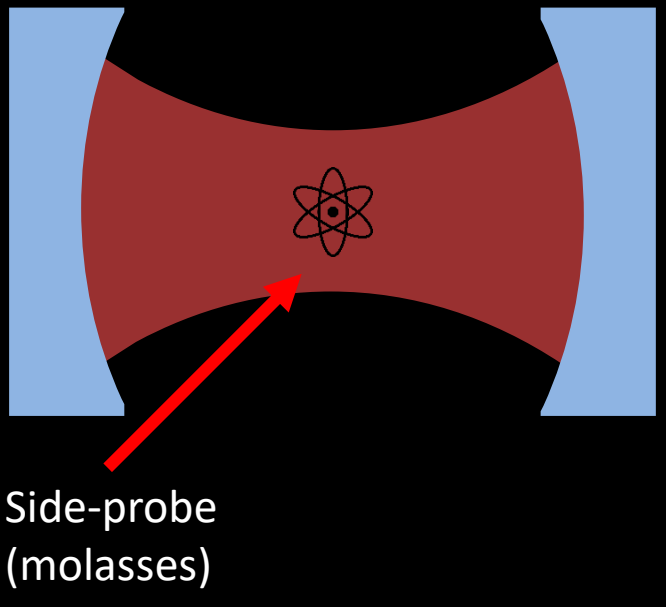
Near-concentric cavity

- Finesse @780 nm: ~15,000
- L ~ 1 cm
- $g_{\max} \sim 2\pi \times 2.7$ MHz
- $\kappa \sim 2\pi \times 1.2$ MHz
- $\Gamma \sim 2\pi \times 6.07$ MHz
- Cooperativity $4g^2/\kappa\Gamma \sim 4$
- Detection efficiency $\eta \sim .25$
- Also high finesse @1560 nm

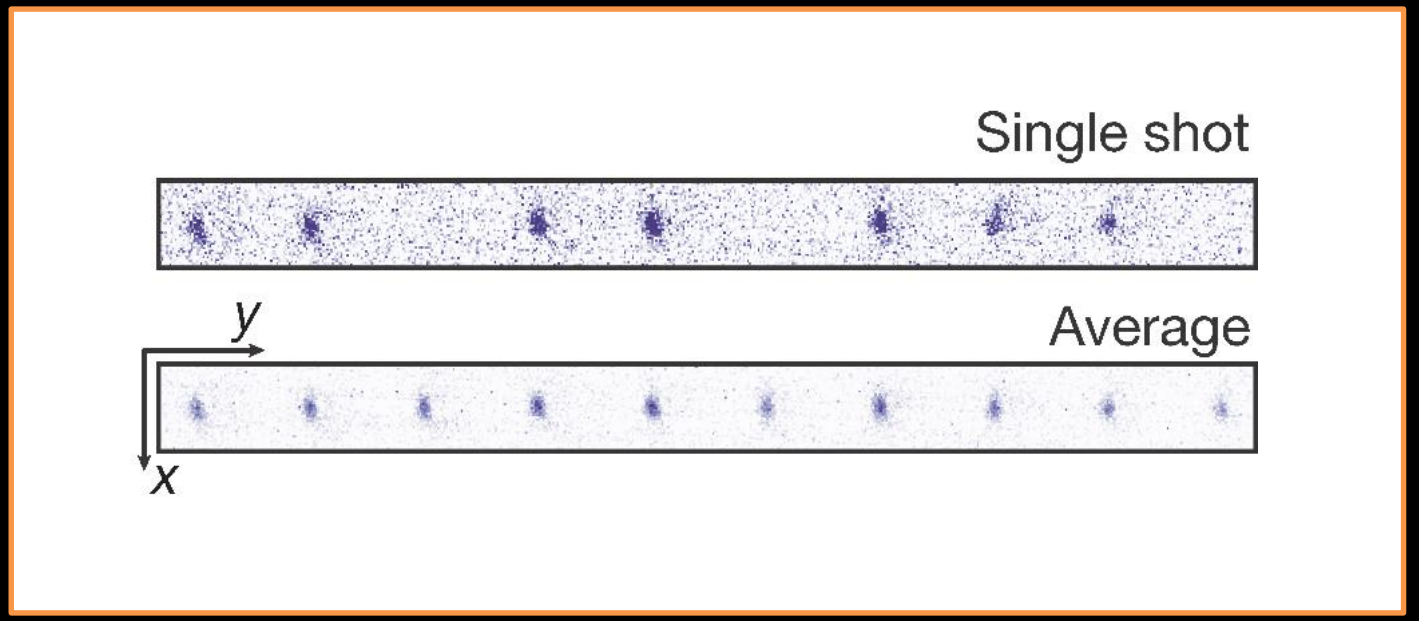
Fluorescence detection

camera

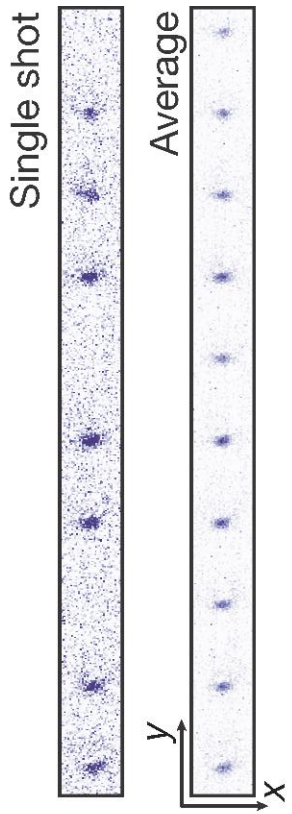


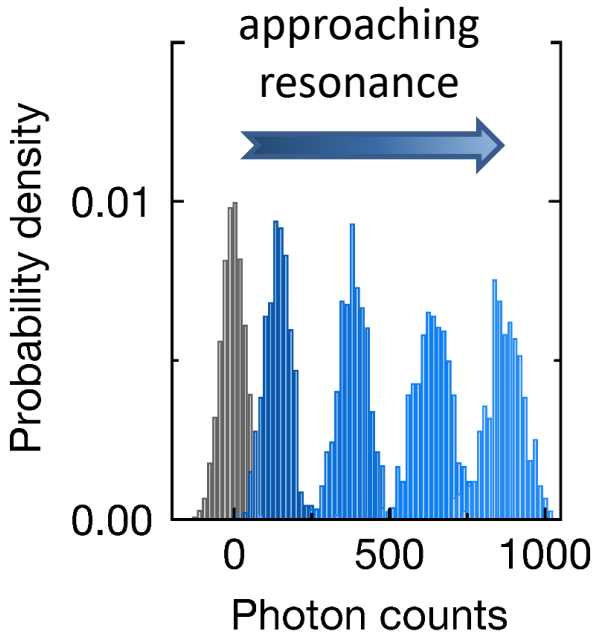


Side-probe
(molasses)



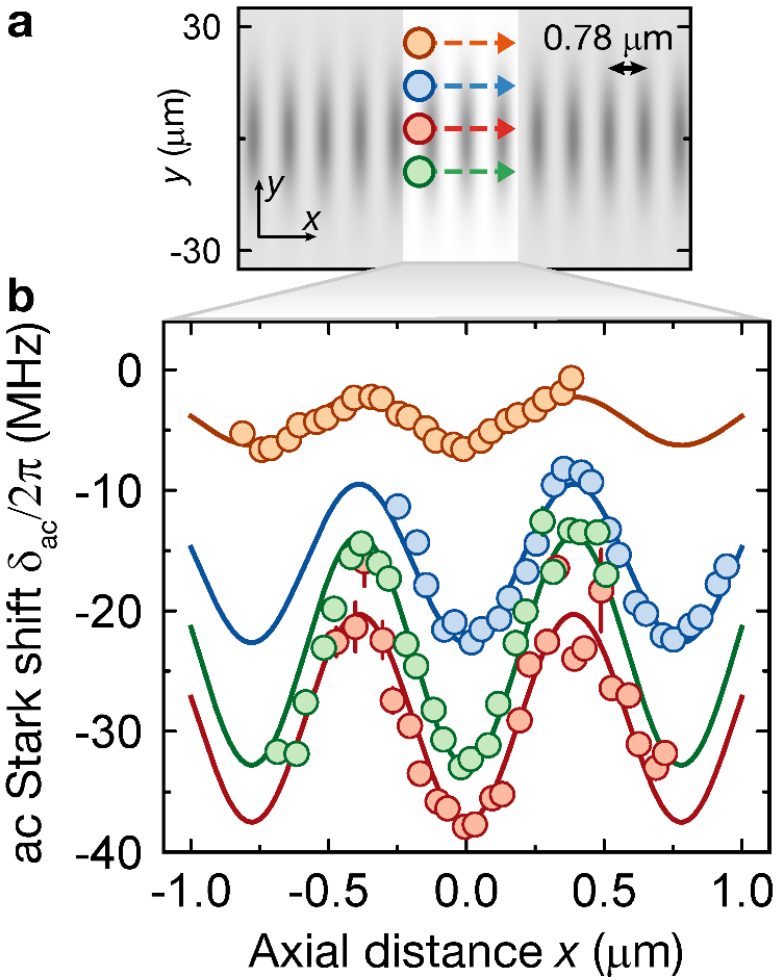
Scanning probe microscopy with single atoms





Fluorescence intensity varies with imaging light detuning

$$\Gamma_{scat} \propto (\omega_L - \omega_0 - \delta_{ac})^{-2}$$



"Sparrow resolution"
$r = 2\,\sigma = 300$ nm

"Super-resolution microscopy of optical fields using tweezer-trapped single atoms,"
Physical Review Letters 128, 083201 (2022)

Mid-circuit measurement in a tweezer array

“cavity QED for tweezers”

“Mid-circuit cavity measurement in a neutral atom array,”
Physical Review Letters **129**, 203602 (2022)

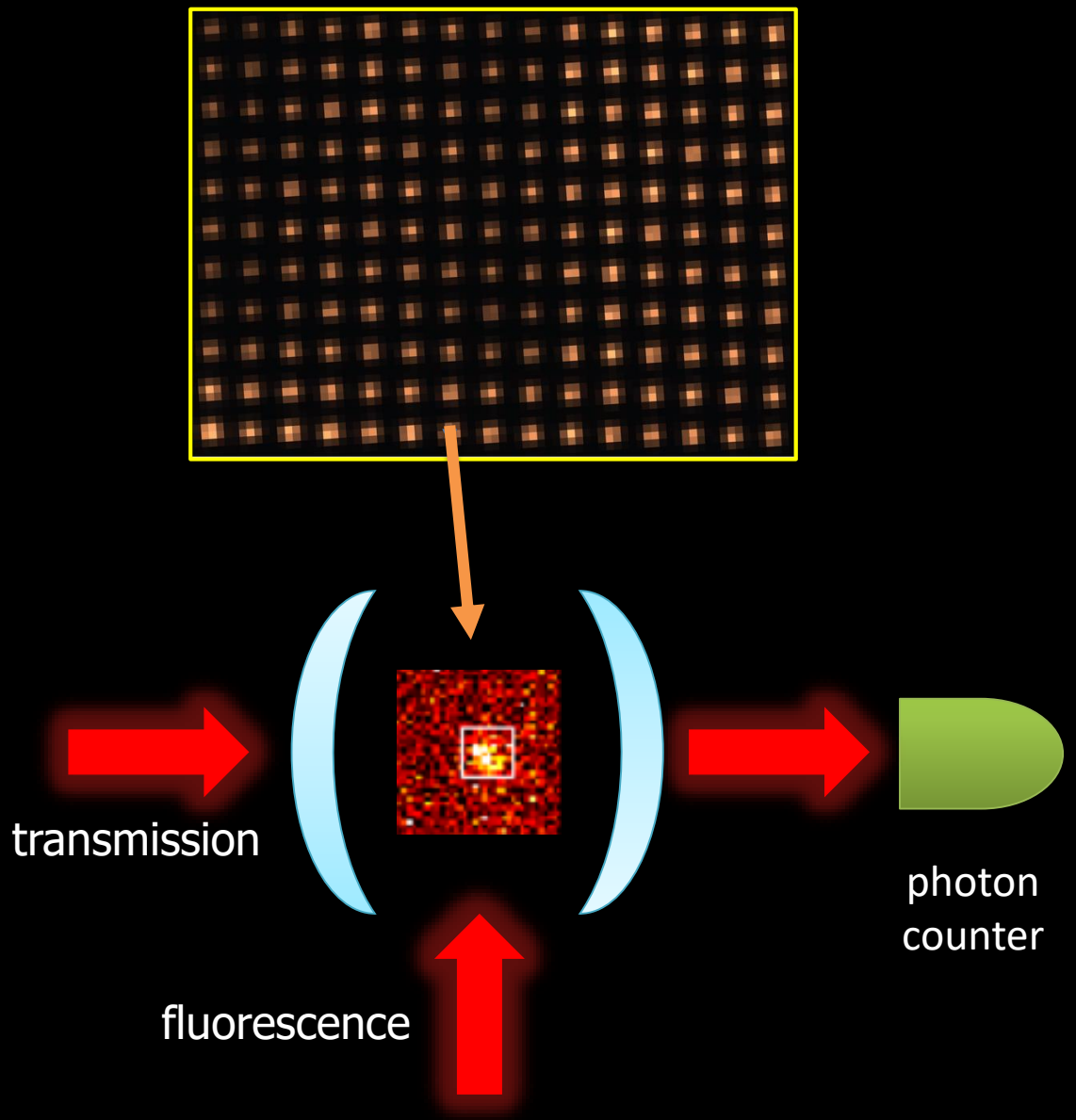
Cavity detection of a single tweezer-trapped atom

Tweezer array experimental sequence:

1. Load tweezers
2. Image filled/empty tweezers
3. Sort
4. Quantum interactions/gates/sensing
5. Image state of each tweezer

Possible improvements:

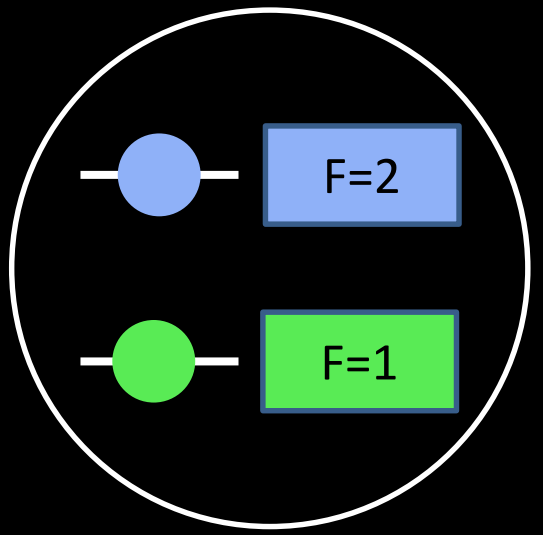
- Faster readout
  - Currently takes 10's of ms. Limits cycle time.
- Atom(s) specific, non-global readout
  - Feedback on live quantum system, error correction.
  - Cluster state quantum computing, sensing



Cavity-based single-atom state detection

Goal: fast, high fidelity detection of three states

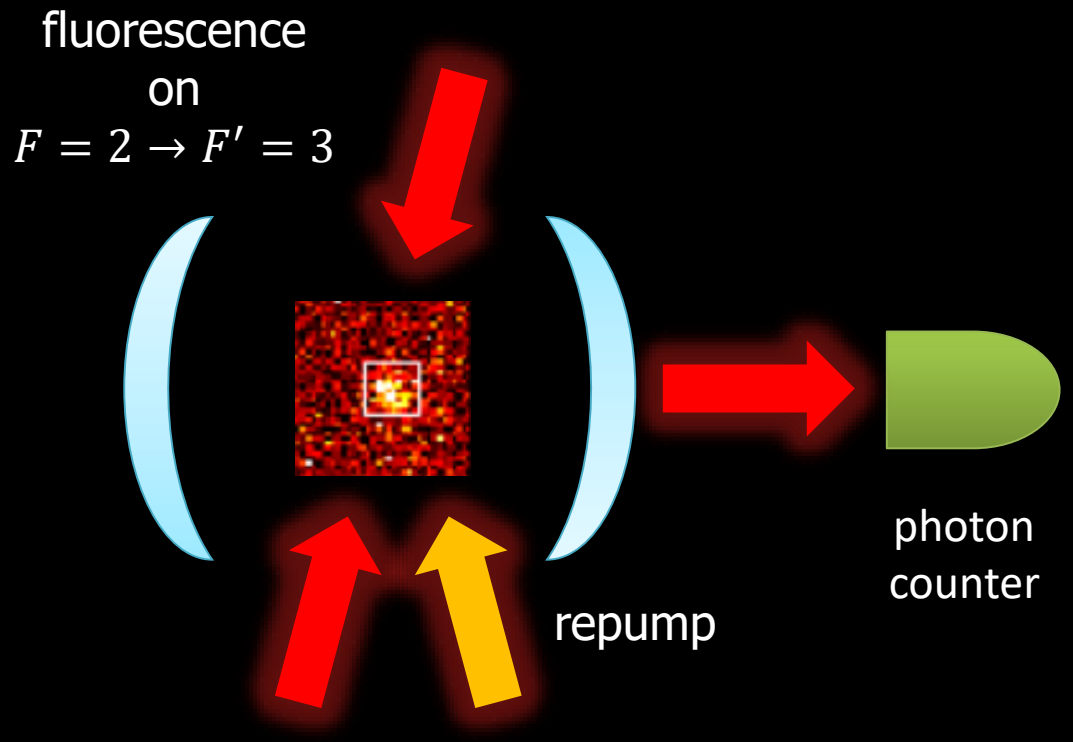
^{87}Rb hyperfine qubit

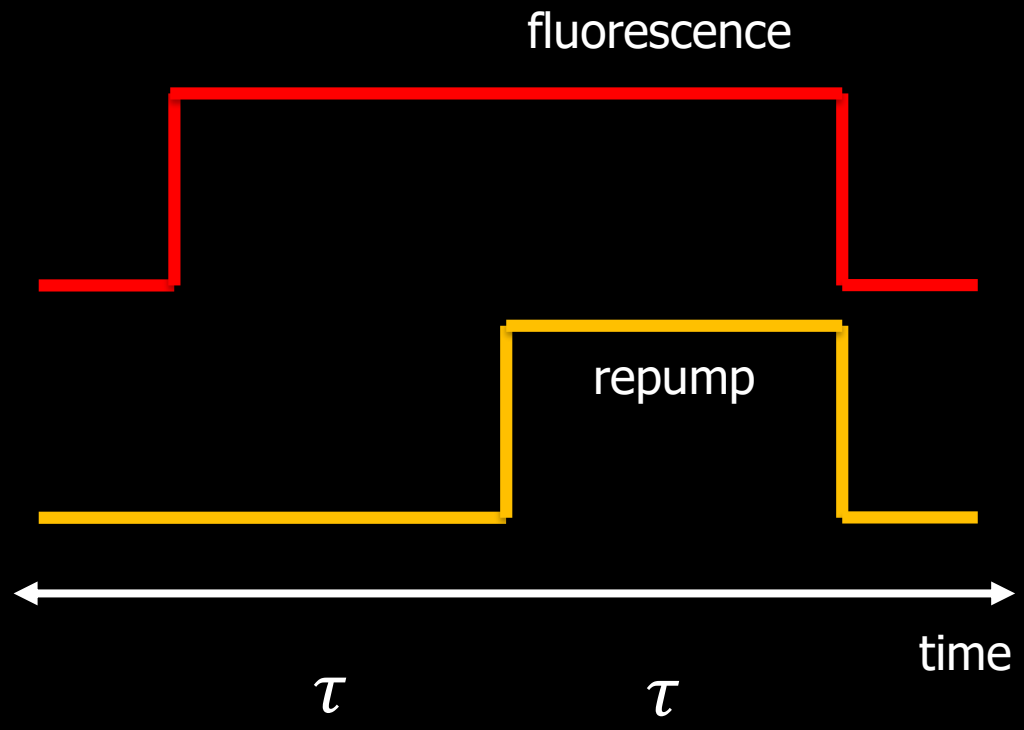


No atom or outside logical states

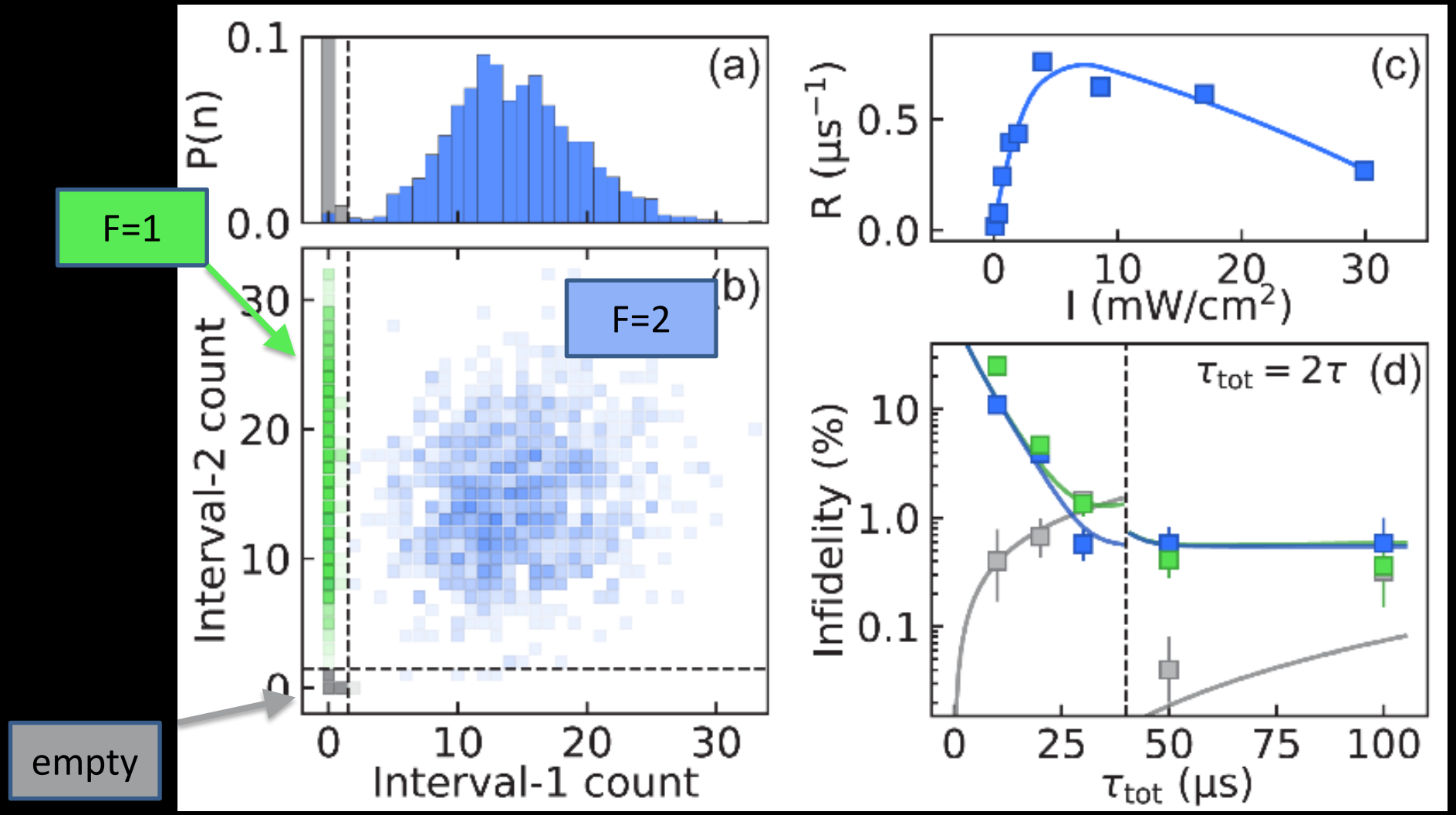


Method 1: (F)luorescence – (R)epump (F)luorescence (FRF)





Method 1: (F)luorescence - (R)epump (F)luorescence (FRF)



Mid-circuit measurement in an atomic tweezer array

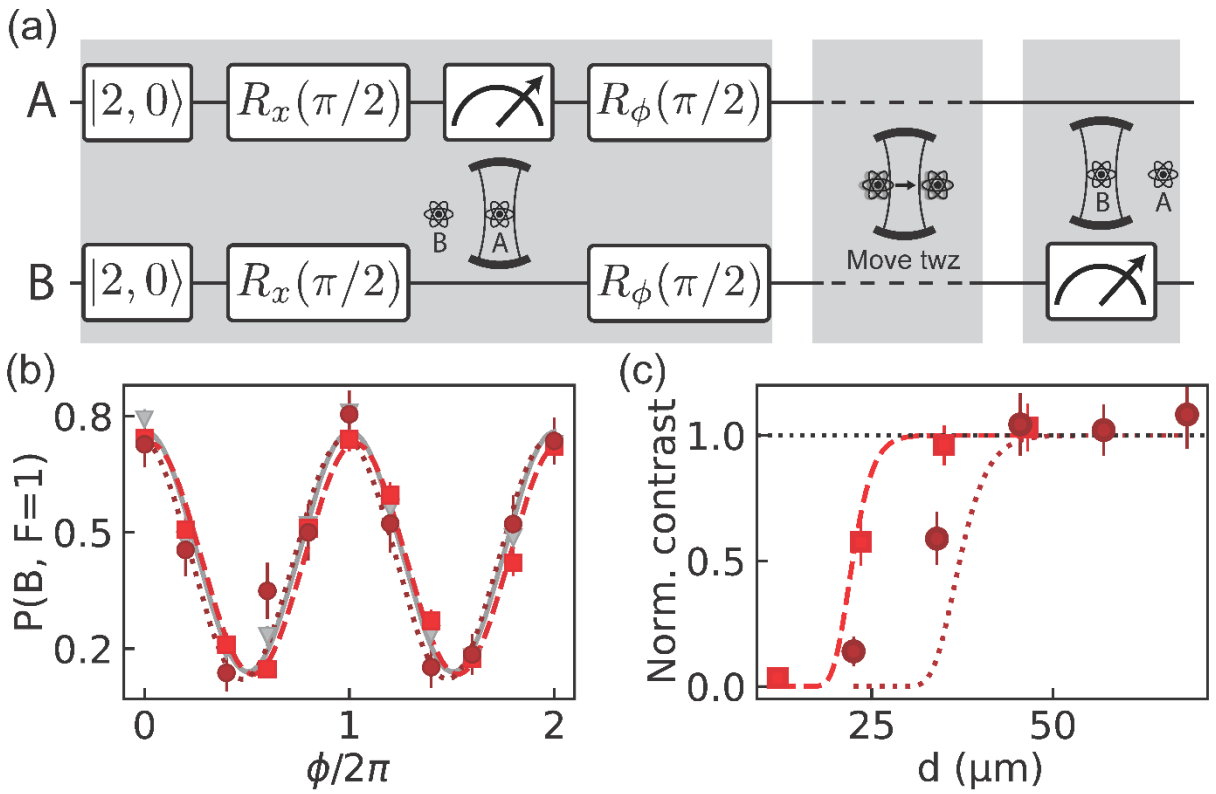
Fast, high fidelity detection of three states:

- No atom (or atom outside logical state basis)
- F=1 hyperfine state (logical $|0\rangle$)
- F=2 hyperfine state (logical $|1\rangle$)

Table I. Measurement infidelity and loss probability

		No atom	F=1	F=2
Fluorescence $2\times(\tau = 25\,\mu s)$	Outcome	low-low	low-high	high-X
	Infidelity	0.04(3) %	0.4(2) %	0.6(2) %
	Loss prob.	n/a	0.2(2) %	1.4(3) %
Transmission $2\times(\tau = 50\,\mu s) + 5\,\mu s$	Outcome	high-high	high-low	low-X
	Infidelity	0.4(1) %	1.1(2) %	0.9(2) %
	Loss prob.	n/a	0.7(3) %	1.4(2) %

excellent recent implementation in fiber cavities by Lukin group



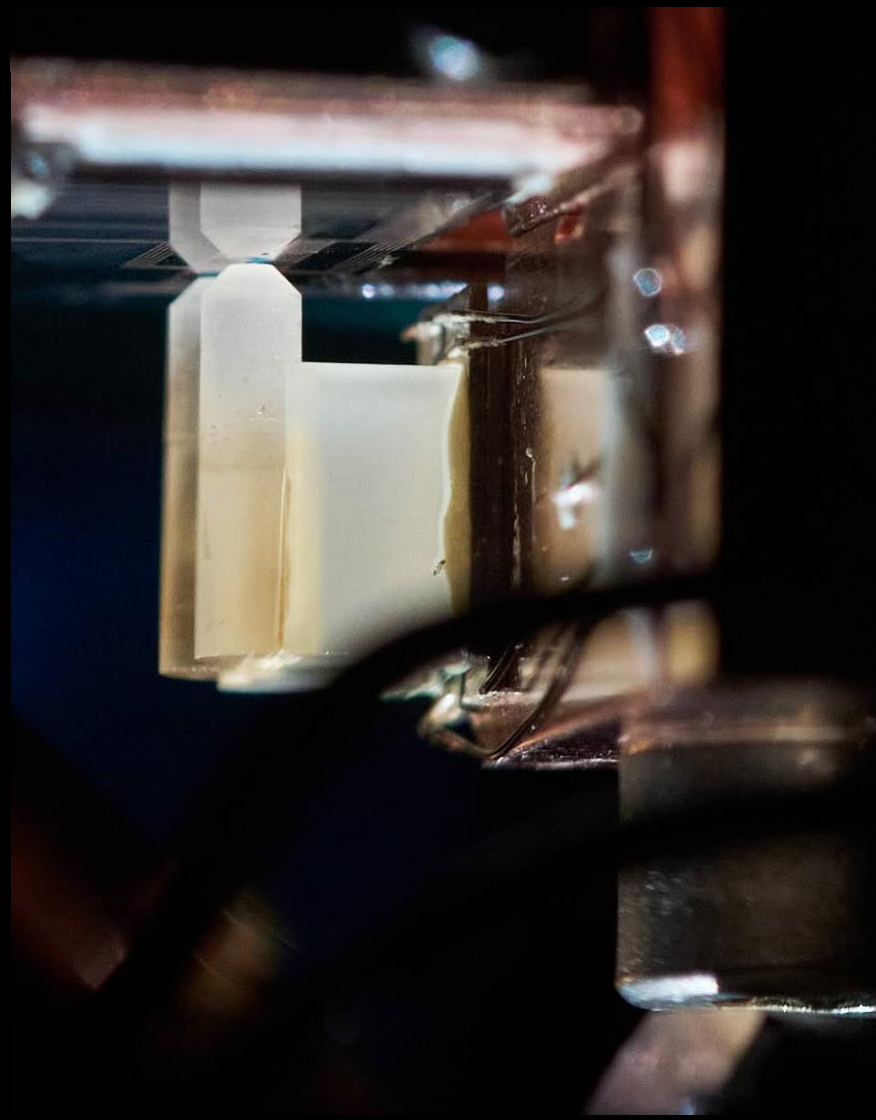
Measurement on portion of atom array does not affect quantum coherence of remainder of array

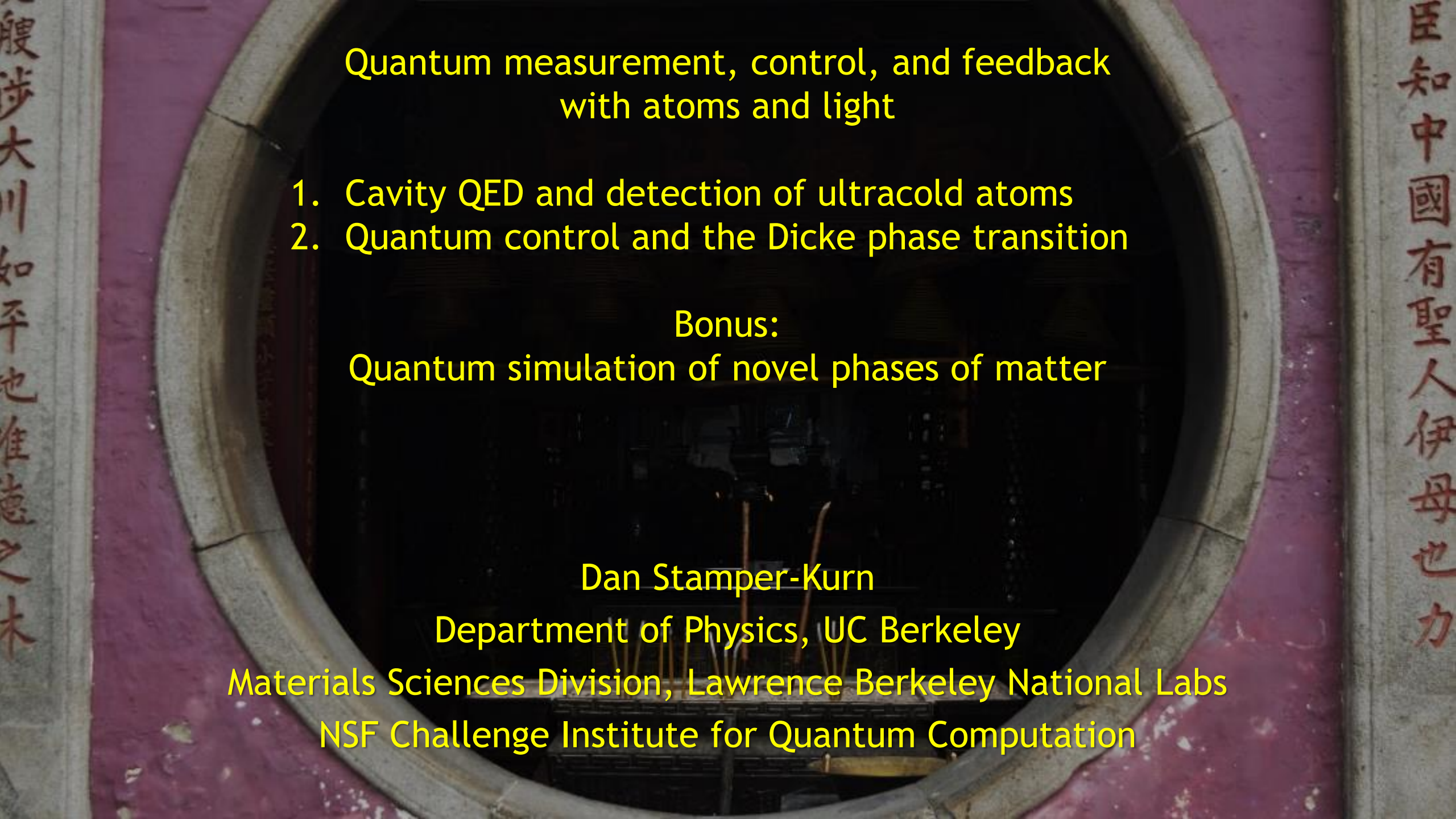
recent mid-circuit operations by Kaufman group, Saffman group, Atom Computing,…

"Mid-circuit cavity measurement in a neutral atom array," Physical Review Letters **129**, 203602 (2022)

Cavity QED and detection of ultracold atoms
Summary

- Light can be used to measure ultracold atomic quantum systems
- Strongly coupled cavity enhances detection sensitivity, minimizes backaction and noise
  - “No wasted information”
- Many different properties can be measured
  - Shown: atom number, position, spin.
  - Others: pair correlation, collective measurements…
- Continuous and real-time measurement
- Cavity is not a passive measurement device
  - Incoherent and coherent backaction
- Cavity is not a closed quantum system



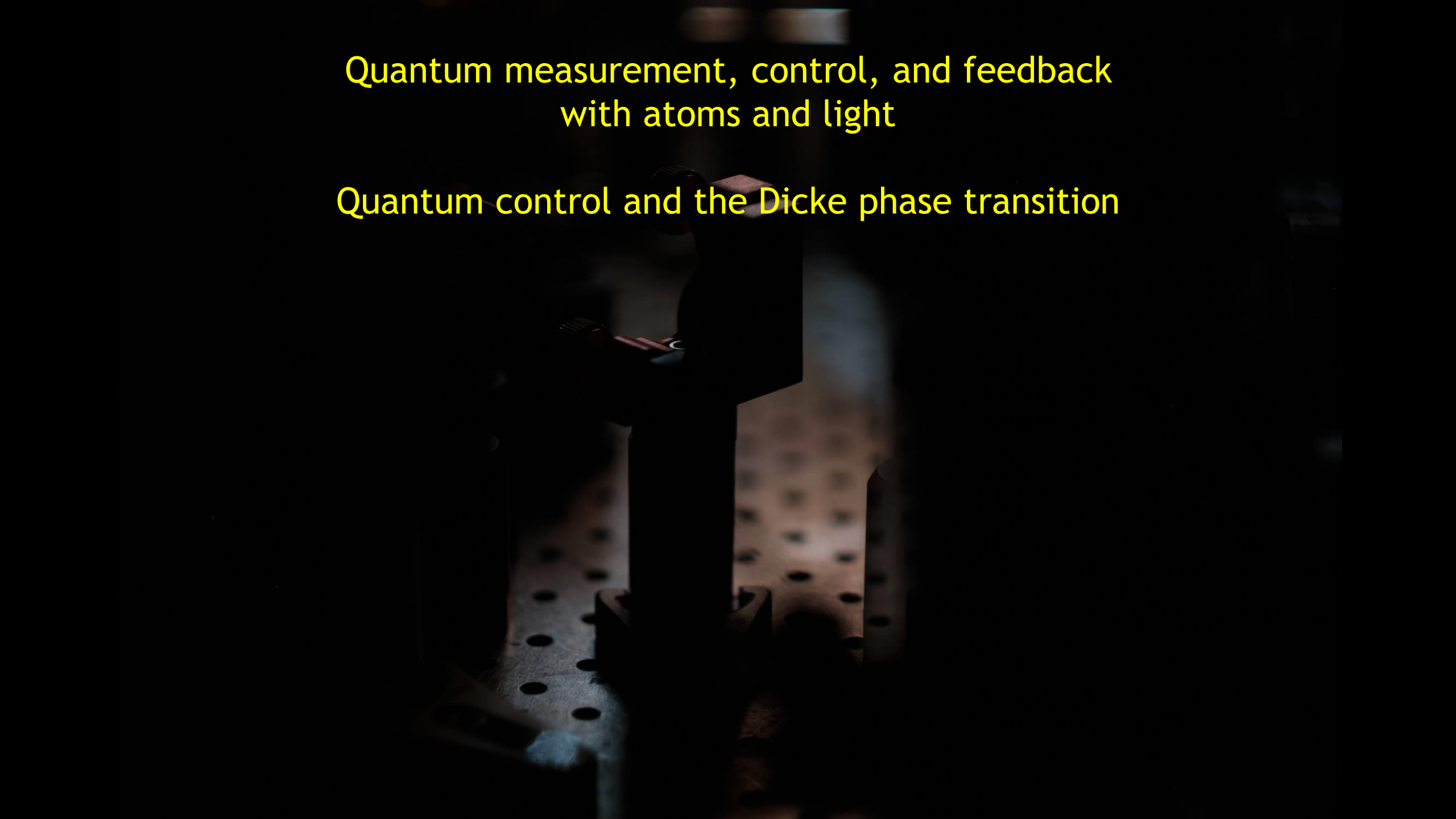


Quantum measurement, control, and feedback with atoms and light

1. Cavity QED and detection of ultracold atoms
2. Quantum control and the Dicke phase transition

Bonus:
Quantum simulation of novel phases of matter

Dan Stamper-Kurn
Department of Physics, UC Berkeley
Materials Sciences Division, Lawrence Berkeley National Labs
NSF Challenge Institute for Quantum Computation



Quantum measurement, control, and feedback with atoms and light

Quantum control and the Dicke phase transition

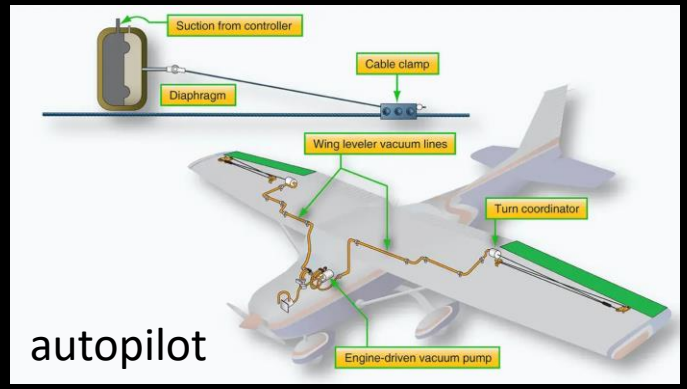
Autonomous feedback stabilization of a quantum spin ensemble

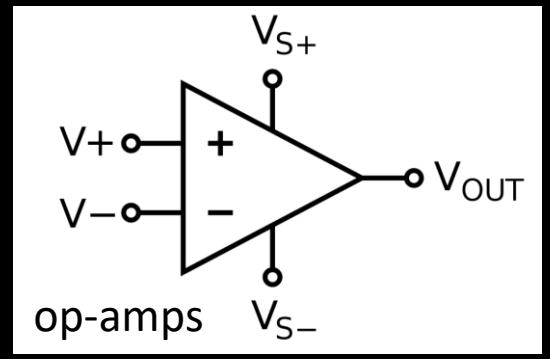
“Autonomous feedback stabilization of a cavity-coupled spin oscillator,”
arXiv:2307.04808

Feedback control of quantum systems

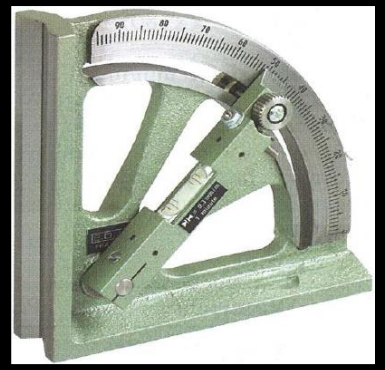
Motivations:

- Robust operation of quantum technologies

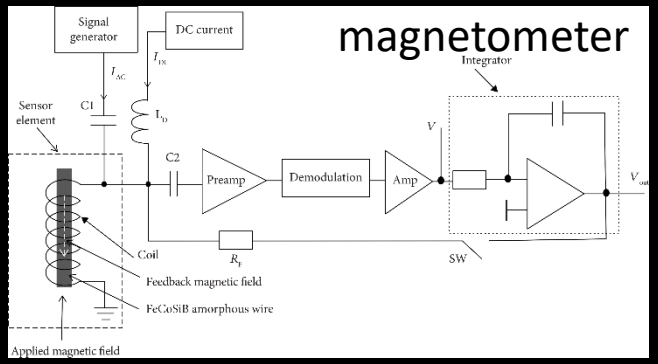




- Sensors with expanded dynamic range

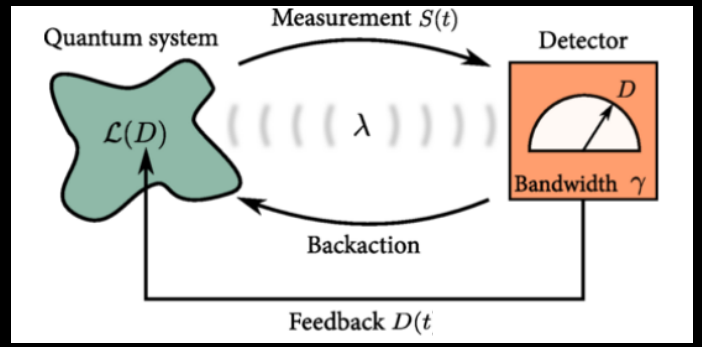


bubble-level inclinometer



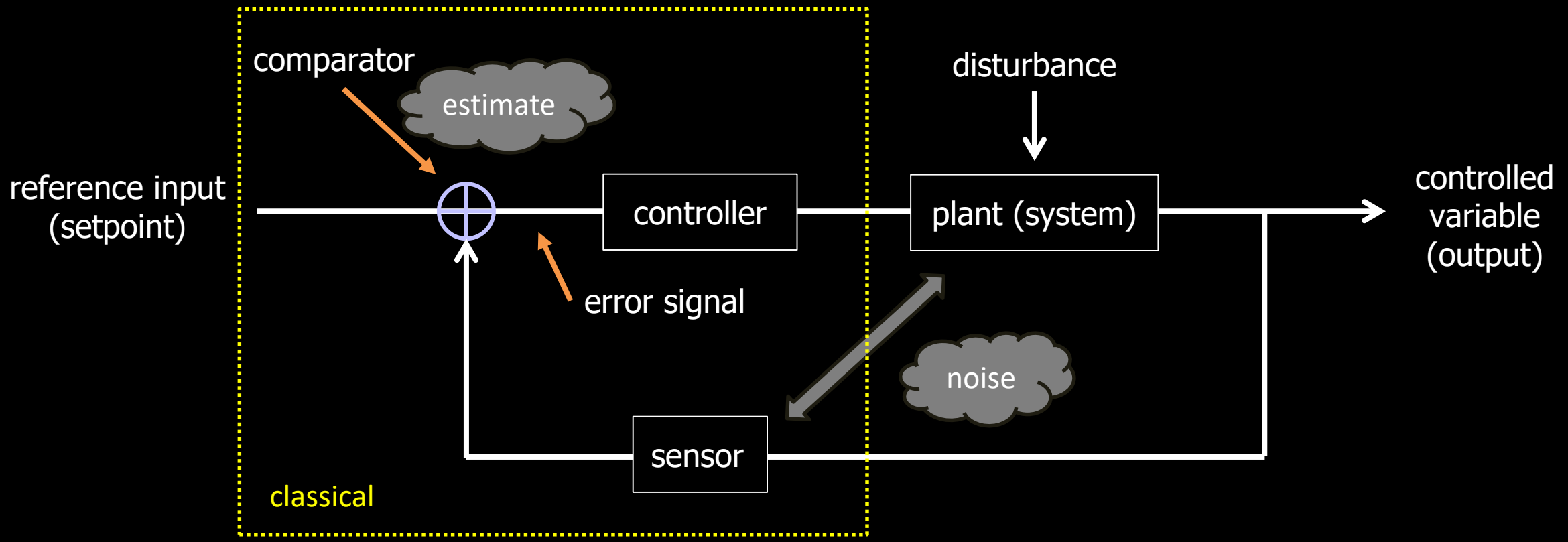
Journal of Sensors 2413408 (2019)

- Fundamental quantum science



PRL **129**, 050401 (2022)

Feedback control of quantum systems



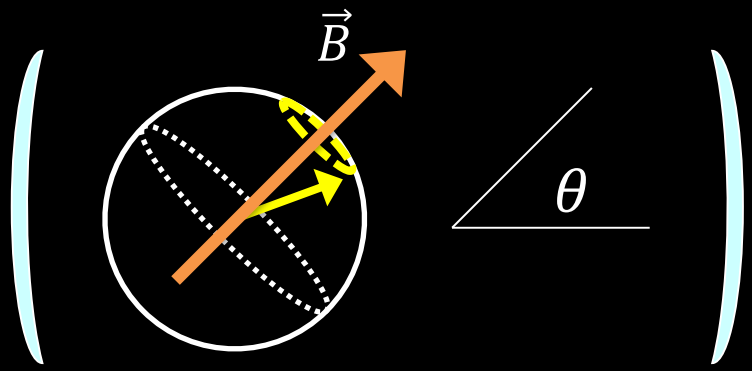
- Measurement-based feedback
  - Mid-circuit measurement and feedback/error correction
- Autonomous (coherent) feedback
  - Stabilization of spin ensemble through cavity backaction

Autonomous stabilization of longitudinal spin (energy)

cavity pump detuning

$\Delta_{set} = \omega_p - \omega_c$

σ^+



magneto-optics
vector ac Stark shift

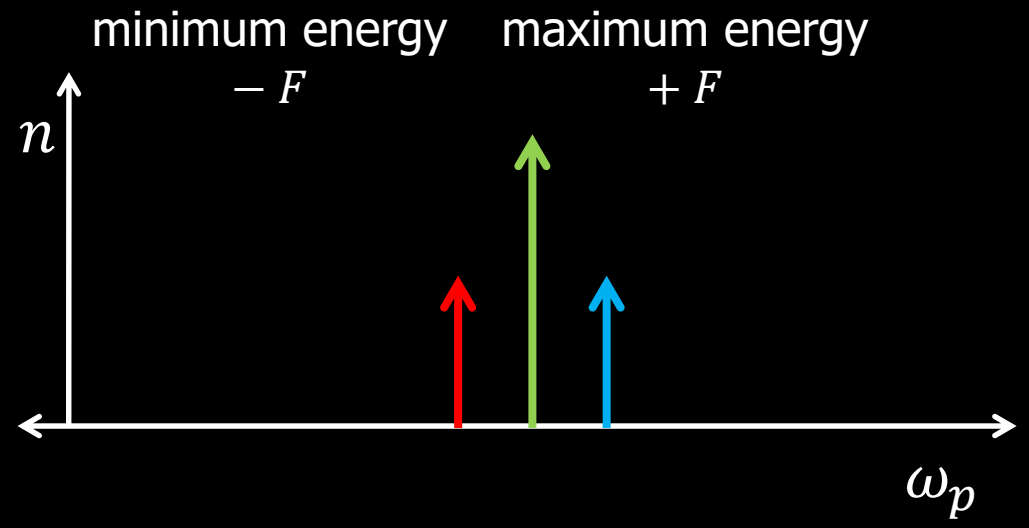
$$\frac{H}{\hbar} = -\Delta_{set}\hat{c}_+^\dagger\hat{c}_+ + \omega_L\hat{F}_\parallel + g_S\,\hat{c}_+^\dagger\hat{c}_+\left(\hat{F}_\parallel\cos\theta + \hat{F}_\perp\sin\theta\right)$$

$\Delta = \Delta_{set} - g_S\hat{F}_\parallel\cos\theta$

"comparator"

"sensor"

"controller"
cavity spin optodynamics
backaction on spin
PRL **118**, 063604 (2017)



Autonomous stabilization of longitudinal spin (energy)

- Set at equator, apply stabilization
- Monitor energy transfer: heterodyne detection of sideband power
- Steady state: measure atomic spin

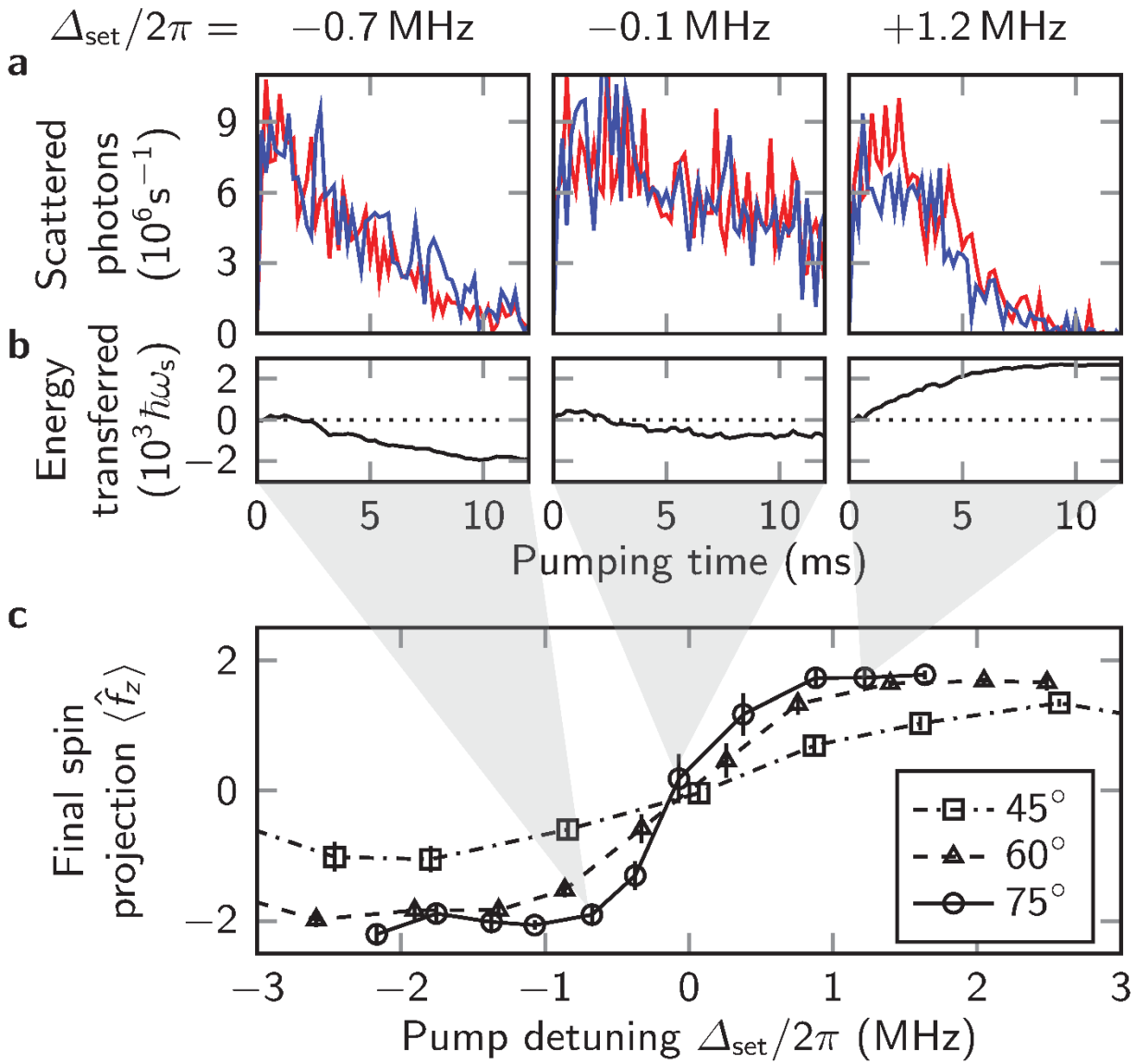
  - demonstrates feedback
  - confirms set-point equation

$$\Delta = \Delta_{set} - g_S \hat{F}_{\parallel} \cos\theta$$

cavity frequency modulation amplitude

$$g_S \, \hat{c}_+^\dagger \hat{c}_+ \, \hat{F}_\perp \sin\theta$$

shallow angle (small $\sin\theta$)
spin dephases before railing



Collective atom-cavity interations

“tweezers for cavity QED”





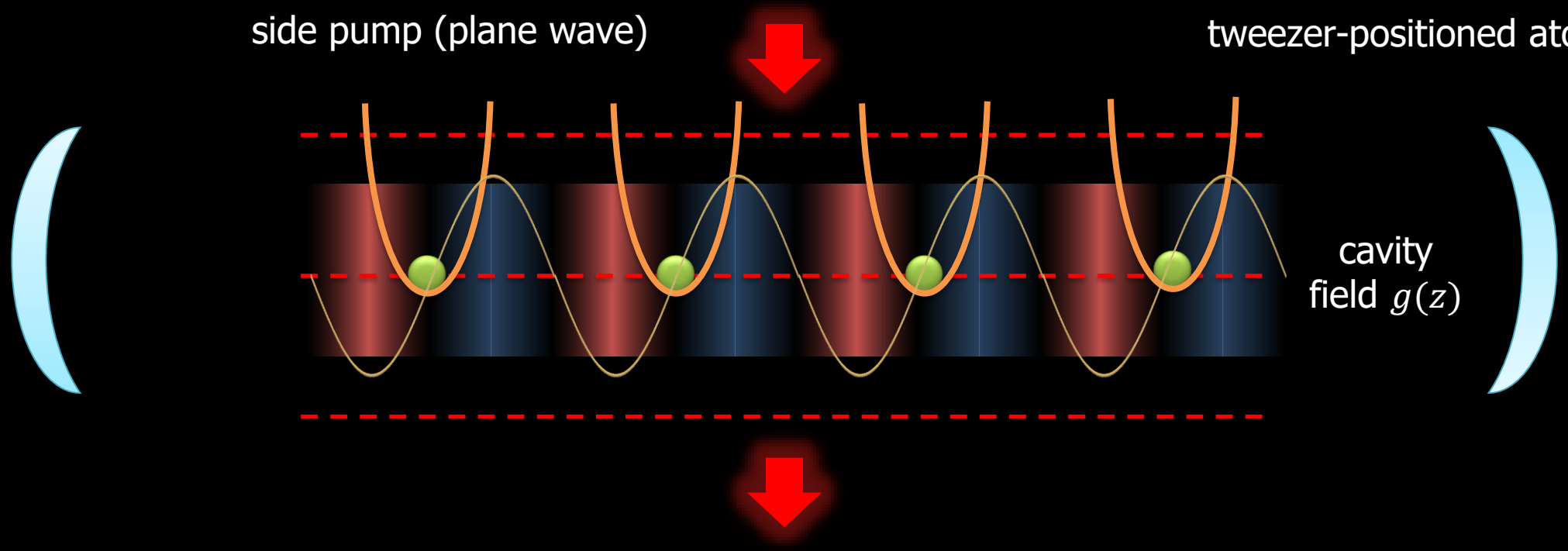


Theory collab.
(Columbia)

Ana Asenjo-Garcia
Stuart Masson
Cosimo Rusconi

“Superradiant and subradiant cavity scattering by atom arrays,”
Physical Review Letters **131**, 253603 (2023)

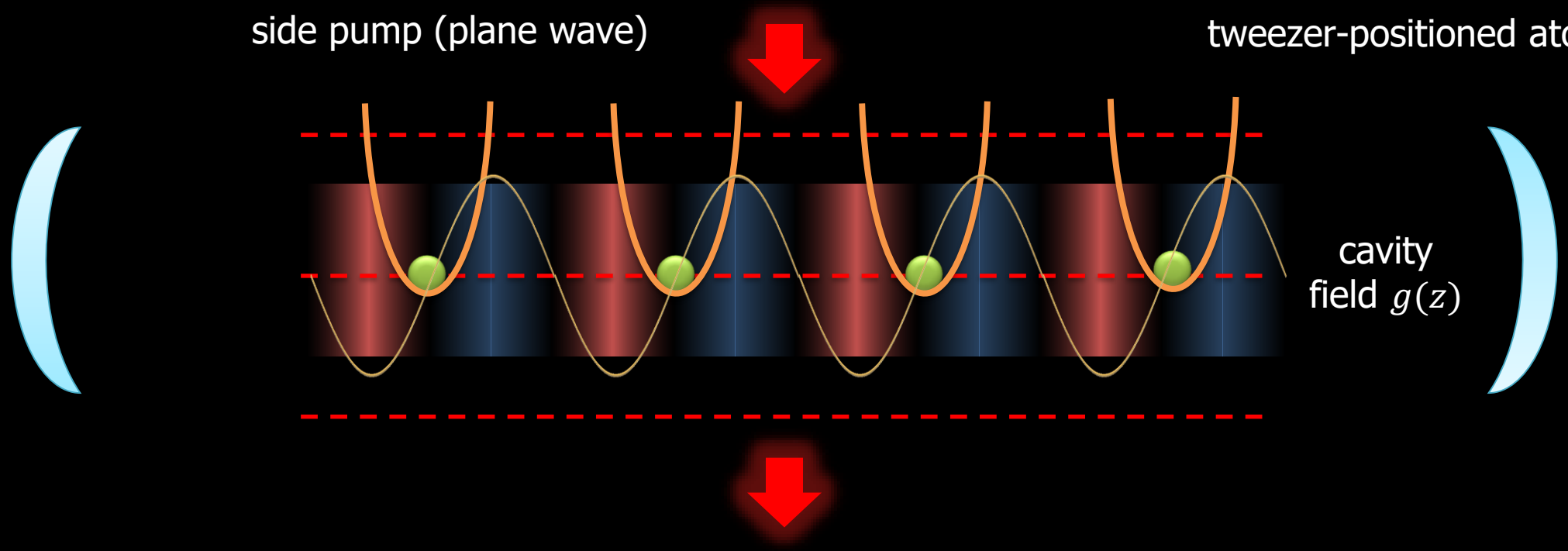
Collective emission and the Dicke phase transition



$$\frac{H}{\hbar} = -\Delta_{pc}\,\hat{c}^{\dagger}\hat{c} + \sum \omega_{z,i}\;\hat{b}_i{}^{\dagger}\hat{b}_i - \frac{1}{\Delta_a}\sum\left(\Omega_i\hat{c}^{\dagger} + \Omega_i^{*}\hat{c}\right)g(\hat{z}_i)$$

- each atom scatters into cavity field

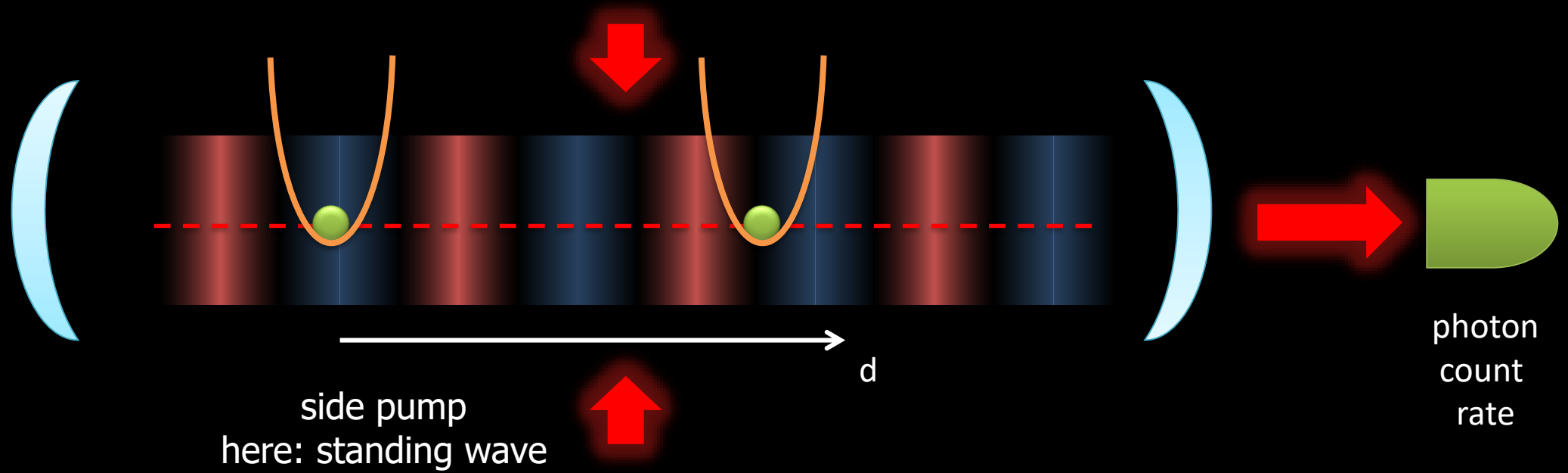
Collective emission and the Dicke phase transition



$$\frac{H}{\hbar} = -\Delta_{pc}\,\hat{c}^{\dagger}\hat{c} + \sum \omega_{z,i}\;\hat{b}_i{}^{\dagger}\hat{b}_i - \frac{1}{\Delta_a}\sum\left(\Omega_i\hat{c}^{\dagger} + \Omega_i^{*}\hat{c}\right)g(\hat{z}_i)$$

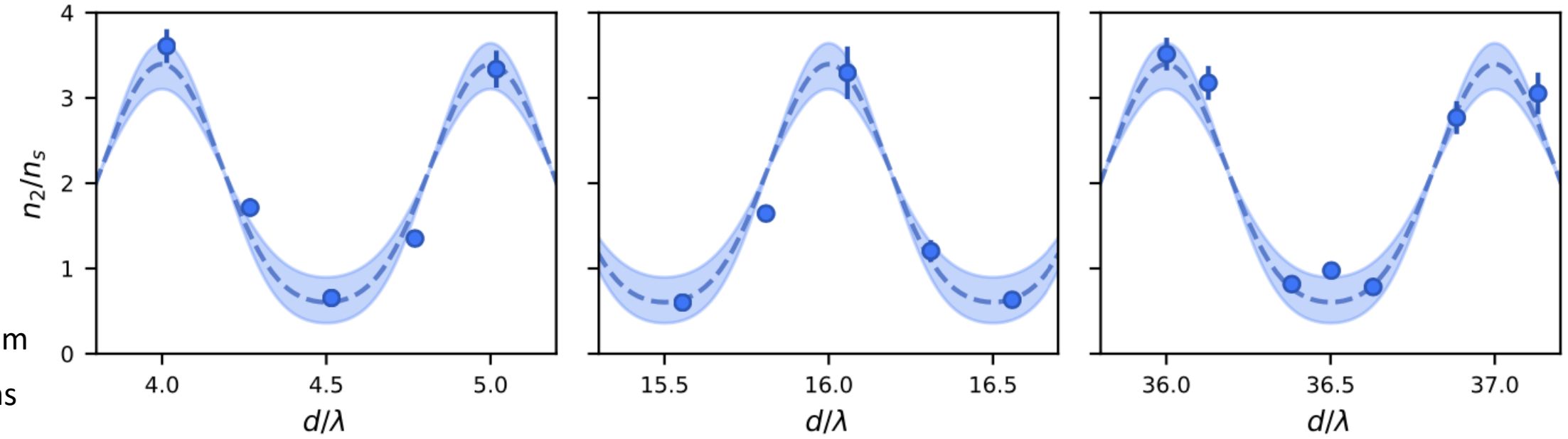
- each atom scatters into cavity field
  - source of collective emission, N^2 scaling of emission intensity

Super- and sub-radiant Rayleigh scattering by two atoms



n_s = single atom

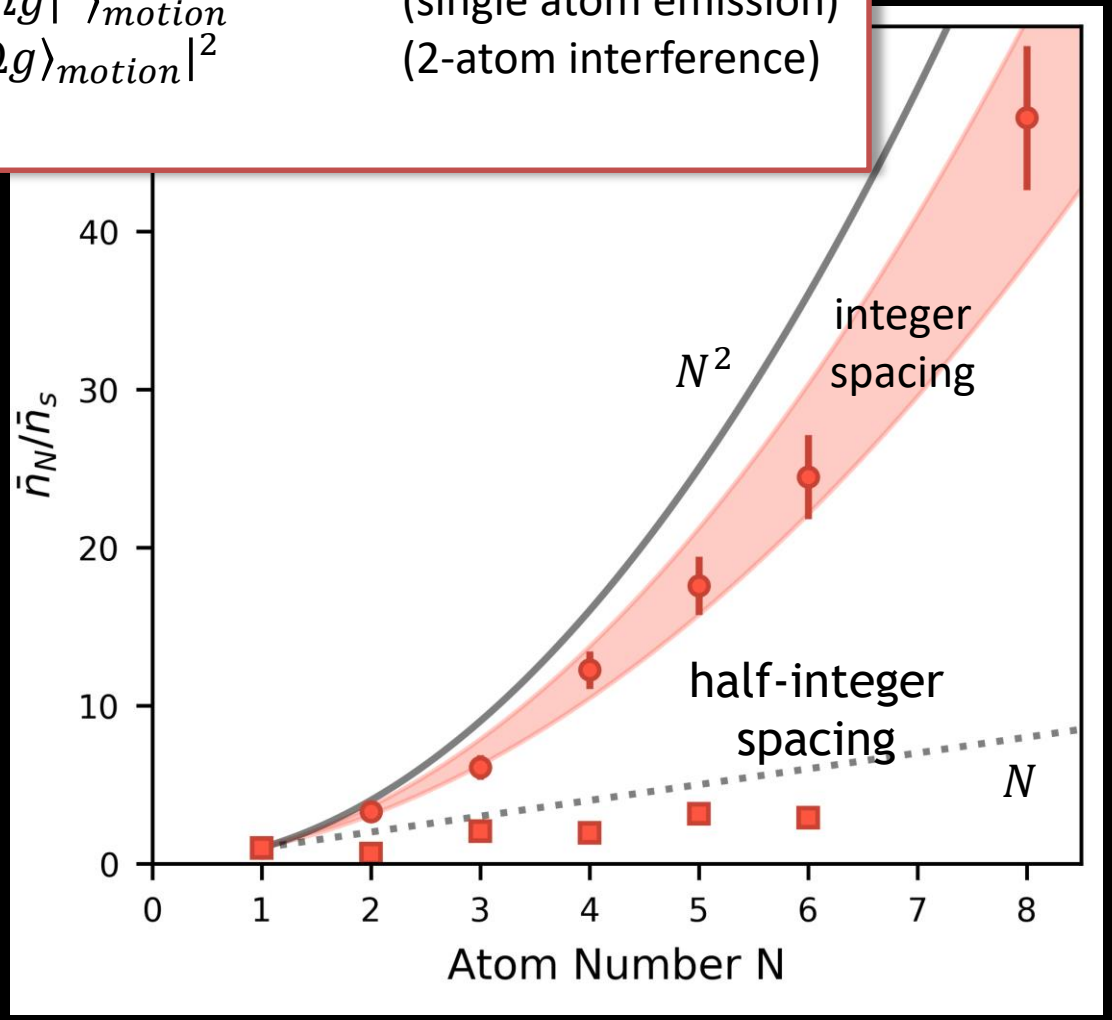
n_2 = two atoms



Collective scattering: N^2 scaling (constructive), even/odd (destructive)

theory: intensity = $A\,N\ + B\,(N^2\ - N)$

$A \propto \langle|\Omega g|^2\rangle_{motion}$ (single atom emission)
$B \propto |\langle\Omega g\rangle_{motion}|^2$ (2-atom interference)



Subtle point:

"Magic detuning"
(-511 MHz from $F = 2 \rightarrow F' = 3$ D2 transition)
multi-level ^{87}Rb atom $\simeq$ two-level atom

- scattering amplitude indep. of hyperfine spin
- Raman transition rate near zero
- only scalar Stark shift
- also occurs for other atoms

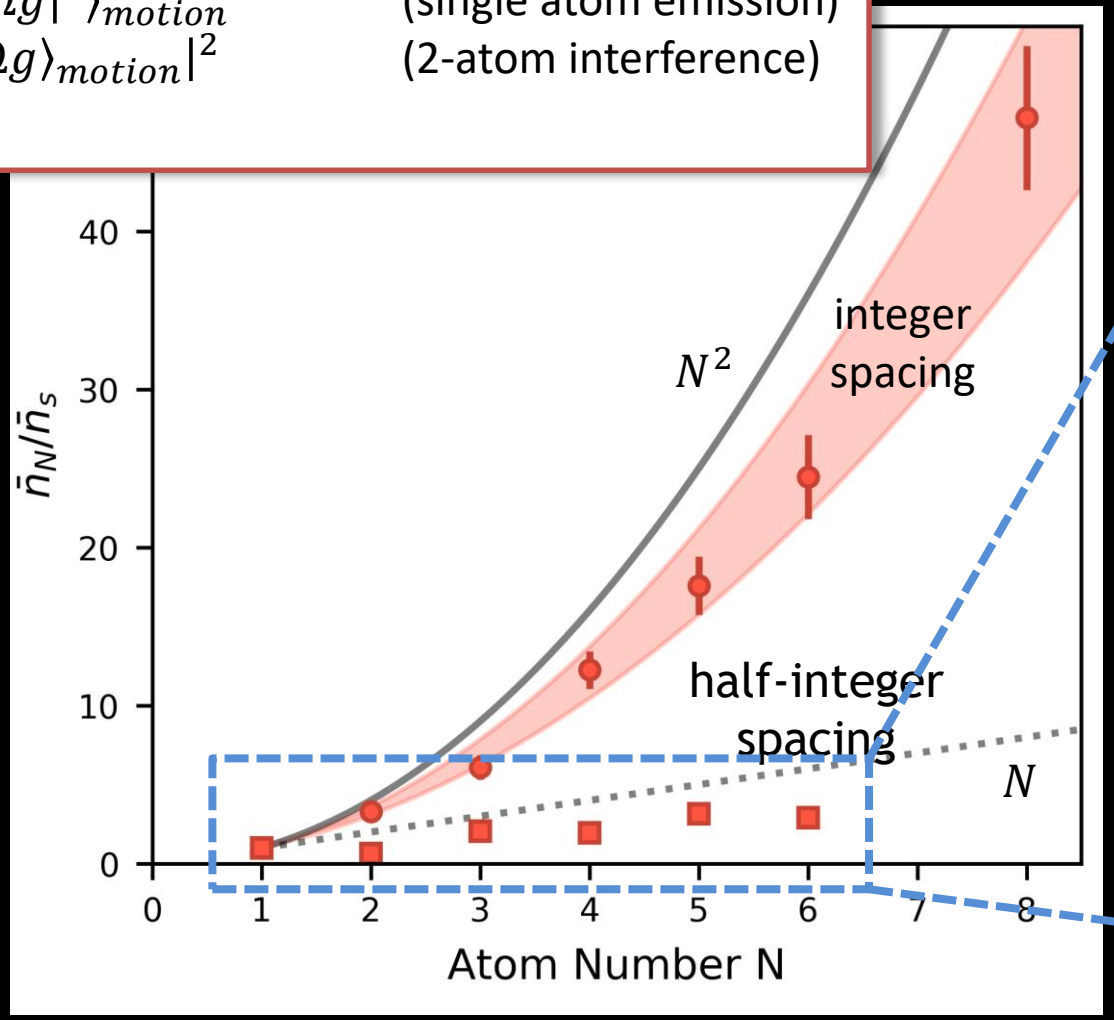
Masson et al., "State-insensitive wavelengths for light shifts and photon scattering from Zeeman states," arxiv:2312.08370

"Superradiant and subradiant cavity scattering by atom arrays," PRL **131**, 253603 (2023)

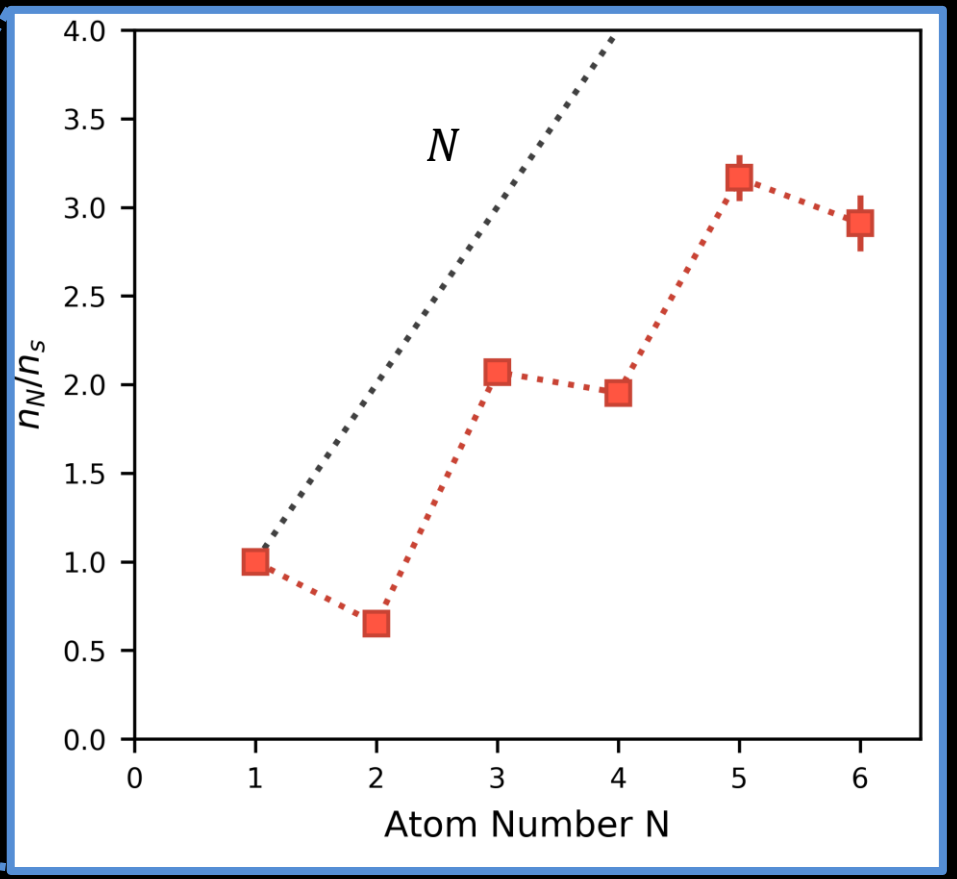
Collective scattering: N^2 scaling (constructive), even/odd (destructive)

theory: intensity = $A\,N\ + B\,(N^2\ - N)$

$A \propto \langle|\Omega g|^2\rangle_{motion}$ (single atom emission)
$B \propto |\langle\Omega g\rangle_{motion}|^2$ (2-atom interference)

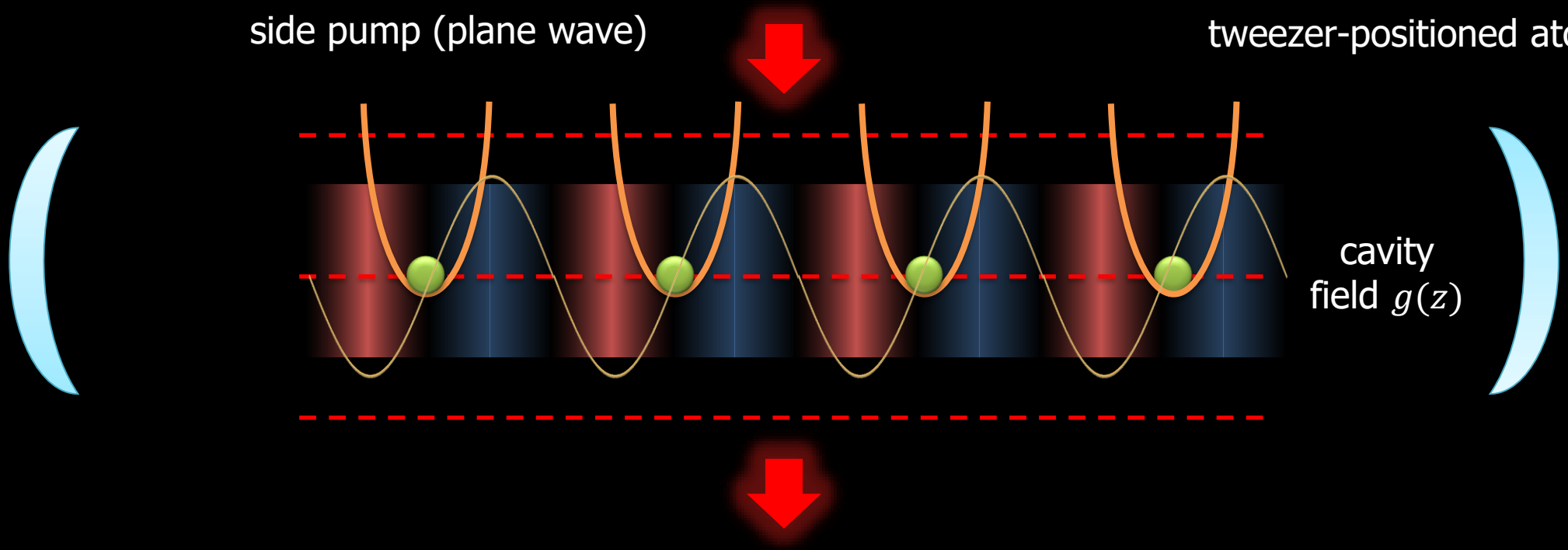


zigzag between even and odd atom number!



"Superradiant and subradiant cavity scattering by atom arrays," PRL **131**, 253603 (2023)

Collective emission and the Dicke phase transition



$$\frac{H}{\hbar} = -\Delta_{pc}\,\hat{c}^{\dagger}\hat{c} + \sum \omega_{z,i}\;\hat{b}_i{}^{\dagger}\hat{b}_i - \frac{1}{\Delta_a}\sum\left(\Omega_i\hat{c}^{\dagger} + \Omega_i^{*}\hat{c}\right)g(\hat{z}_i)$$

- each atom scatters into cavity field
  - source of collective emission, N^2 scaling of emission intensity
- ac Stark shift = optical potential on atoms
  - backaction of self-generated cavity field: symmetry breaking Dicke phase transition
    Black *et al.*, PRL **91**, 203001 (2003); Baumann *et al.*, Nature **464**, 1301–1306 (2010)



visiting with collaborators
Cosimo, Stuart and Ana
New York City, April 8, 2024


eclipse
THROUGH THE EYES OF NASA
NASA
The 2024 Total
Solar Eclipse
through the eyes of NASA
Lunar topography data from NASA's Lunar Reconnaissance Orbiter and the Japan Aerospace Exploration Agency's SELENE lunar orbiter were used to precisely calculate the location of the Moon's shadow for the 2024 total solar eclipse. The planetary positions are from NASA's Jet Propulsion Laboratory Development Ephemeris 421. Earth imagery from NASA's Blue Marble: Next Generation series were used to create the terrain and Earth at night imagery from NASA's Black Marble were used under the eclipse path.
2024 Total Solar Eclipse
Monday, April 8, 2024
Credit: Michala Garrison and the Scientific Visualization Studio (SVS), in collaboration with the NASA Heliophysics Activation Team (NASA HEAT), part of NASA's Science Activation portfolio
Eclipse calculations by Ernie Wright, NASA Goddard Space Flight Center
0 mi 200
0 km 200
2024 Total Solar Eclipse
4:35 PM ADT
3:30 EDT
3:25 EDT
3:20 EDT
3:15 EDT
3:10 EDT
3:05 EDT
2:05 CDT
2:00 CDT
1:55 CDT
1:50 CDT
1:45 CDT
1:40 CDT
1:35 CDT
1:30 CDT
12:30 CST
12:25 CST
12:20 PM CST
2024 Path of Totality April 8, 2024
Along a path about 115 miles wide, the Moon will completely block the Sun in the sky. Totality lasts up to about 4 minutes and 28 seconds depending on the viewer's location within this path.
Outside of this path, viewers within the 48 contiguous U.S. states and many other areas will see a partial solar eclipse (in the shaded areas below).
2024 Maximum Partial Obscuration (%)
2024 Maximum Partial Obscuration (%)
CANADA
UNITED STATES
MEXICO
Pacific Ocean
Atlantic Ocean
Gulf of Mexico
Seattle
Portland
Sacramento
San Francisco
San Jose
Fresno
Bakersfield
Los Angeles
Long Beach
Riverside
San Diego
Las Vegas
Phoenix
Mesa
Tucson
El Paso
Albuquerque
Denver
Aurora
Colorado Springs
Kansas City
Wichita
Oklahoma City
Tulsa
Dallas
Ft. Worth
Arlington
Austin
San Antonio
Houston
Corpus Christi
Chicago
Milwaukee
Detroit
Cleveland
Columbus
Indianapolis
Cincinnati
Louisville
Nashville
Memphis
Atlanta
Jacksonville
Orlando
Tampa
Miami
Coral Gables
Fort Lauderdale
West Palm Beach
Boston
New York
Philadelphia
Baltimore
Washington D.C.
Virginia Beach
Raleigh
Charlotte
Lexington
Omaha
Council Bluffs
St. Louis
Minneapolis
St. Paul
Billings
Great Falls
Boise
Salt Lake City
Las Vegas
Albuquerque
Lubbock
Amarillo
Abilene
Midland
Odessa
Waco
Temple
Killeen
Laredo
Brownsville
Monterrey
Saltillo
Chihuahua
Durango
Mazatlán
Hermosillo
Guaymas
Nogales
Ciudad Juárez
Torreón
Matamoros
Reynosa
Nuevo León
Coahuila
Sonora
Sinaloa
Baja California
Baja California Sur
Tamaulipas
Durango
Chihuahua
Alberta
Saskatchewan
Manitoba
Ontario
Quebec
Nova Scotia
Maine
Vermont
New Hampshire
Rhode Island
Connecticut
New Jersey
Delaware
Maryland
Pennsylvania
New York
Ohio
West Virginia
Virginia
Kentucky
Tennessee
North Carolina
South Carolina
Georgia
Florida
Alabama
Mississippi
Louisiana
Arkansas
Missouri
Illinois
Indiana
Michigan
Wisconsin
Minnesota
Iowa
Nebraska
Kansas
Oklahoma
Texas
New Mexico
Arizona
Nevada
Utah
Colorado
Wyoming
Montana
North Dakota
South Dakota
Idaho
Oregon
Washington
Lake Superior
Lake Michigan
Lake Huron
Lake Erie
Lake Ontario

(Don’t) look up!

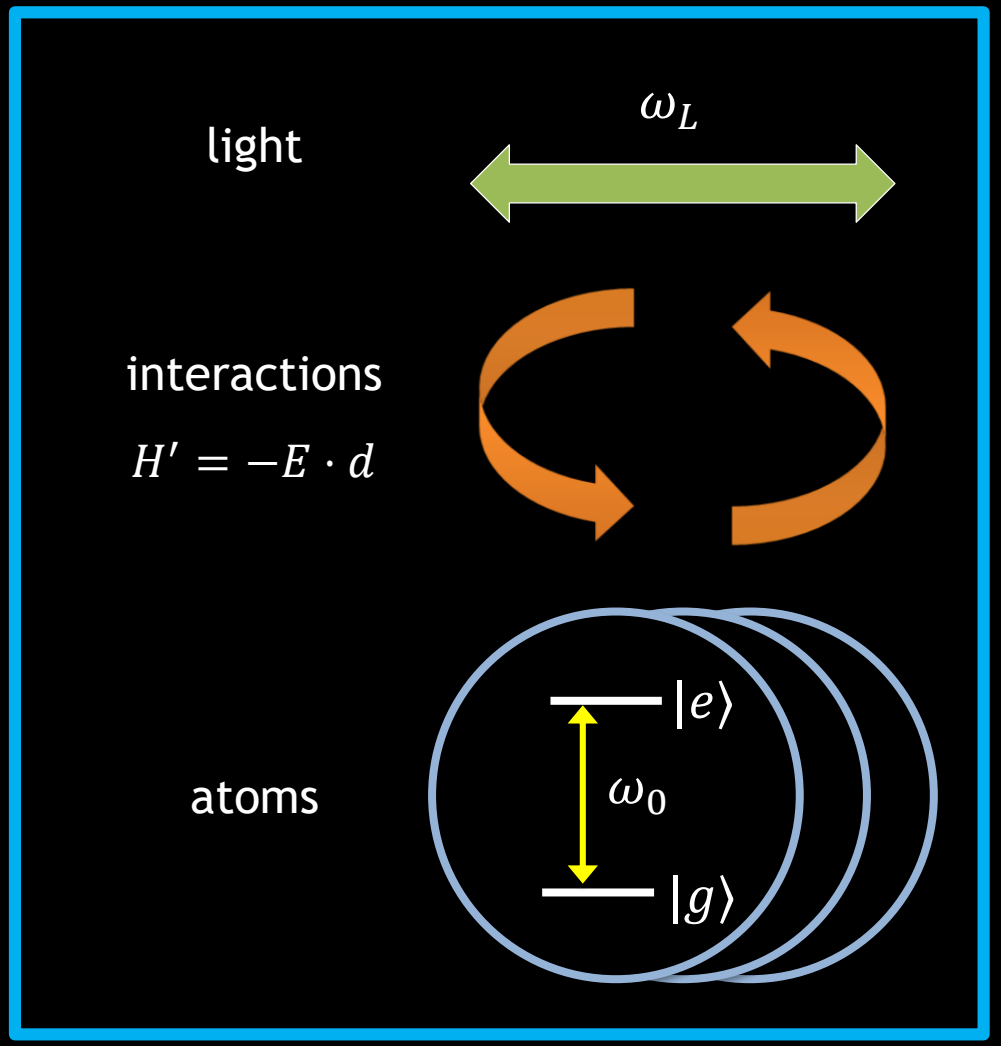


(Don’t) look up!



Nicolas Lefaudeux 2017

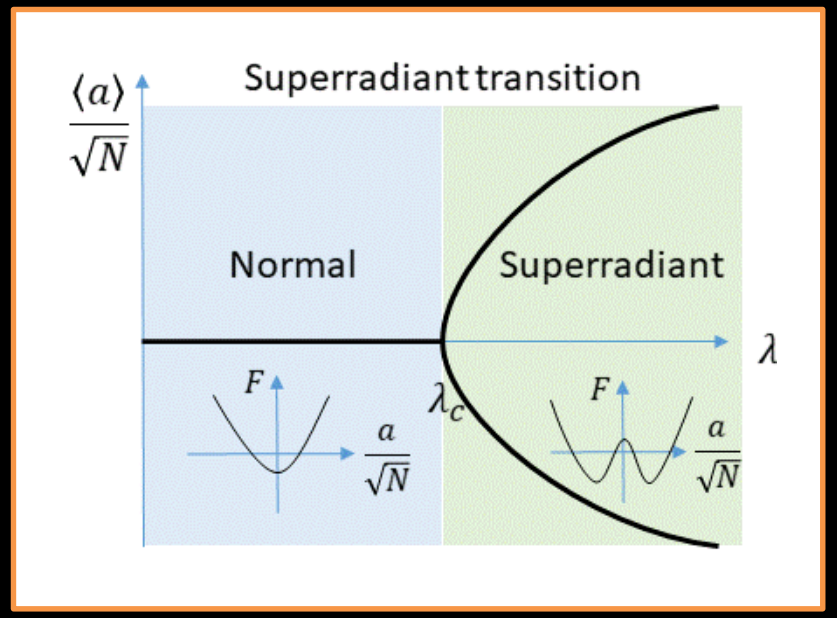
Dicke model



cold ~ $T = 0$ K

$$\frac{H}{\hbar} = \omega_L \hat{c}^\dagger \hat{c} + \sum \frac{\omega_0}{2} \hat{\sigma}_{z,i} - \frac{\lambda}{\sqrt{N}} \left(\hat{c}^\dagger + \hat{c}\right) \sum \hat{\sigma}_{x,i}$$

"... an interesting caricature has been invented by Dicke..."
- Hepp and Lieb, Ann. Phys. 76, 360 (1973)



Roses, DallaTorre,
PLoS ONE 15 , e0235197 (2020)

(Don’t) look up!



Does this occur naturally?

- Look up! Answer is no.

$$\frac{\lambda}{\lambda_c} \sim \sqrt{n\, a_{Bohr}^3}$$

- Realized in driven quantum optical systems
  - Drive lowers effective ω_L
  - Raman transitions lower effective ω_0

Baumann et al: BEC, atomic states of motion
Zhiqiang et al: hyperfine states
here: N atoms, vibrations in tweezer

Nicolas Lefaudeux 2017

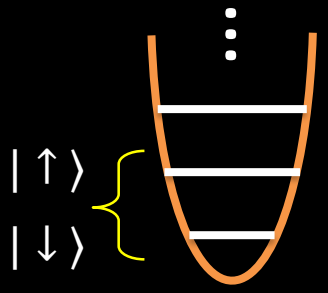
Collective emission and the Dicke phase transition

$$\frac{H}{\hbar} = -\Delta_{pc}\,\hat{c}^{\dagger}\hat{c} + \sum \omega_{z,i}\;\hat{b}_i{}^{\dagger}\hat{b}_i - \frac{1}{\Delta_a}\sum\left(\Omega_i\hat{c}^{\dagger} + \Omega_i^{*}\hat{c}\right)g(\hat{z}_i)$$

1

$$g(\hat{z}_i) = g_0 \sin k\left(\hat{z}_i - z_{0,i}\right) \simeq g_0 k z_{HO}\left(\hat{b}_i{}^{\dagger} + \hat{b}_i\right)$$

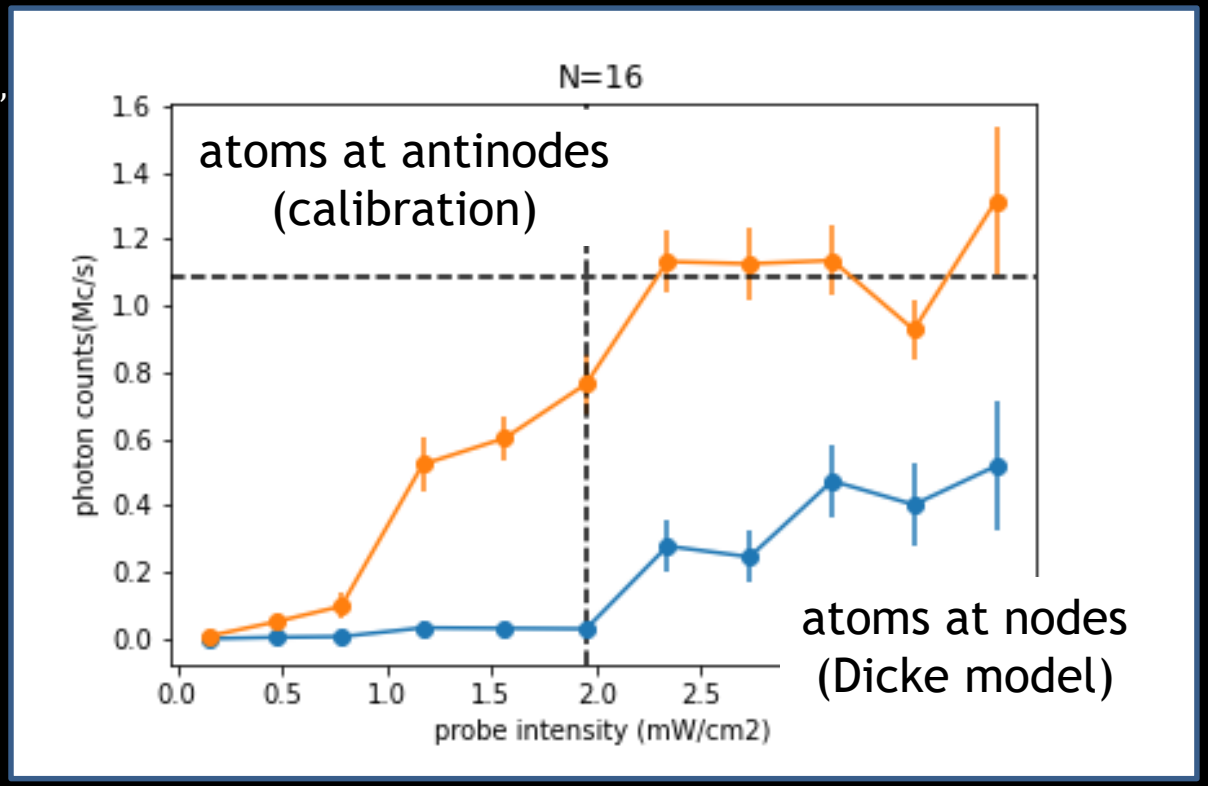
2



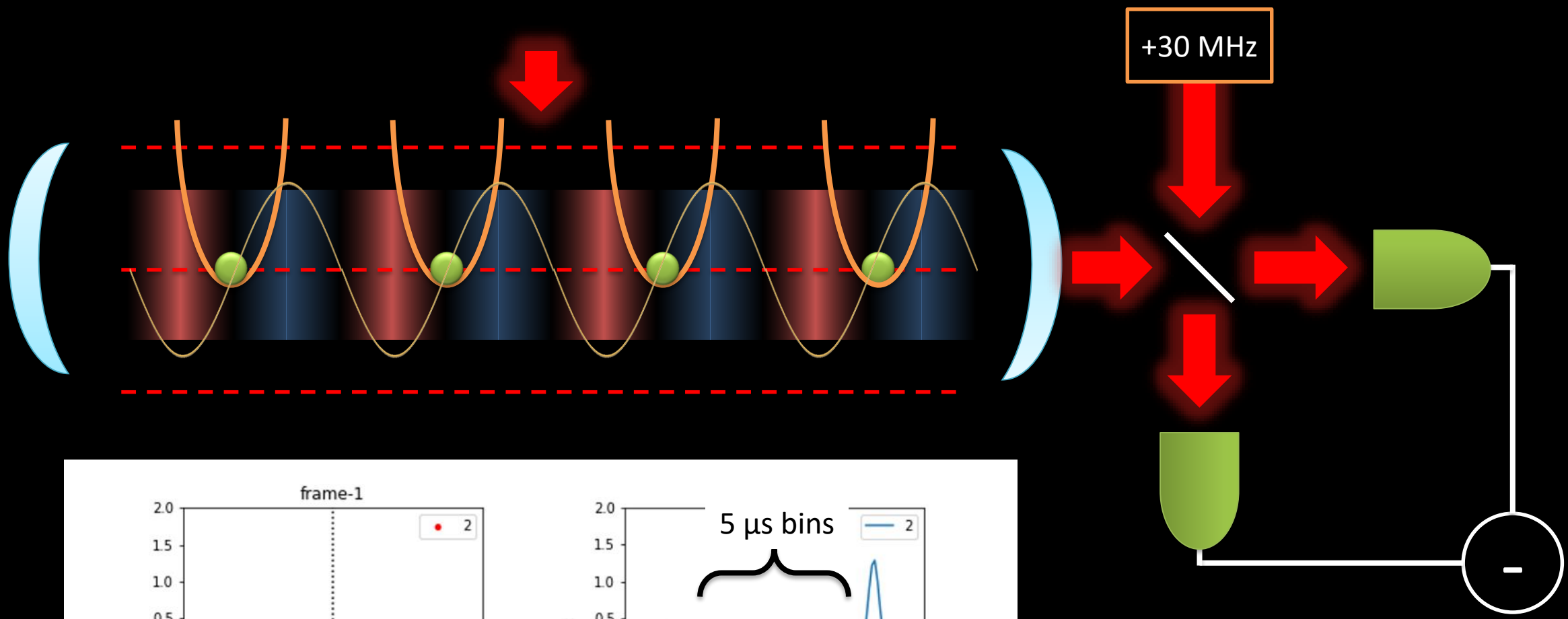
$$\frac{H}{\hbar} = -\Delta_{pc}\,\hat{c}^{\dagger}\hat{c} + \sum \frac{\omega_{z,i}}{2}\hat{\sigma}_{z,}$$

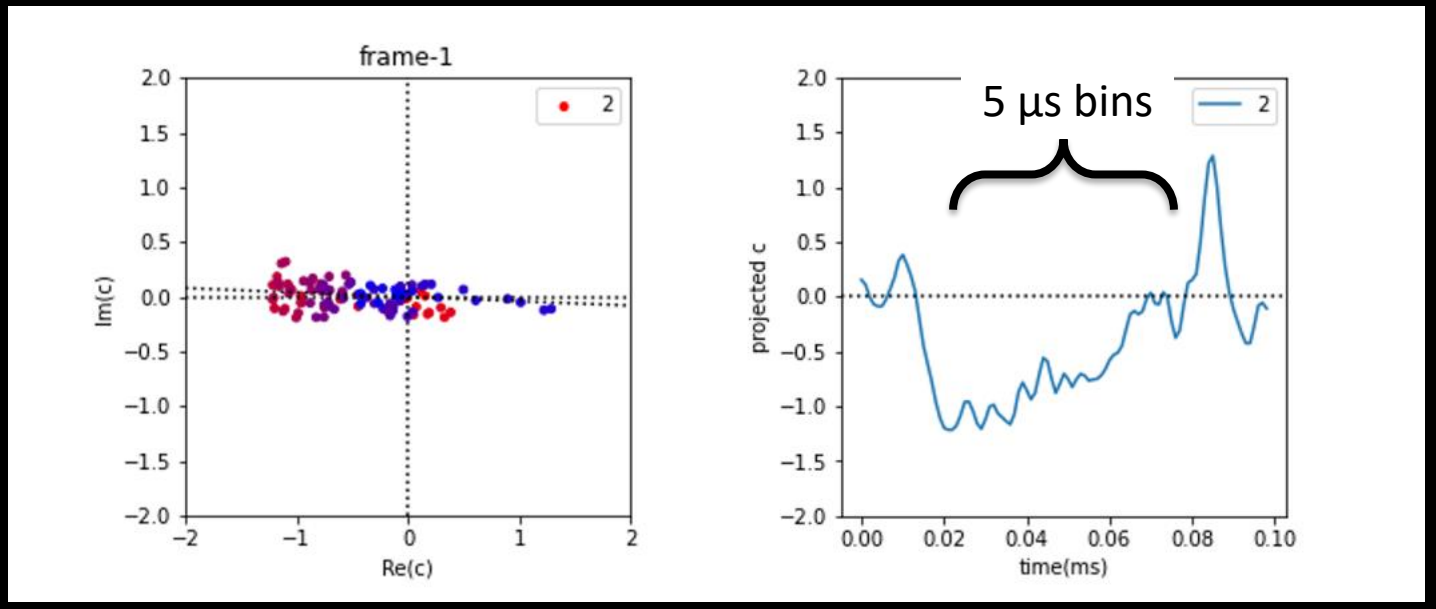
Lots of design parameters!

- strength *and phase* of complex couplings Ω_i
- disorder and explicit symmetry breaking
- time varying parameters
- time/frequency multiplexing of single cavity
- measurement and feedback



Observation of Z_2 symmetry breaking

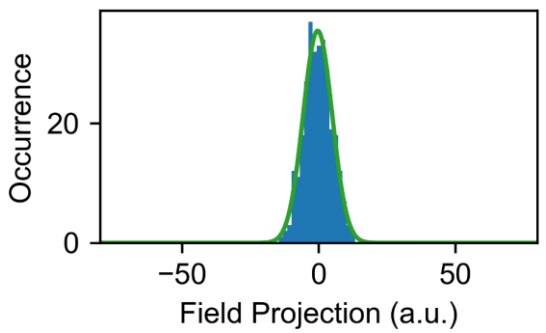


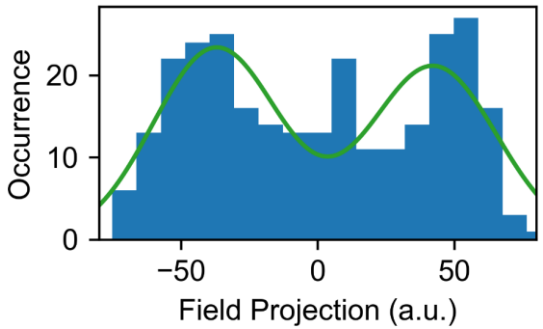


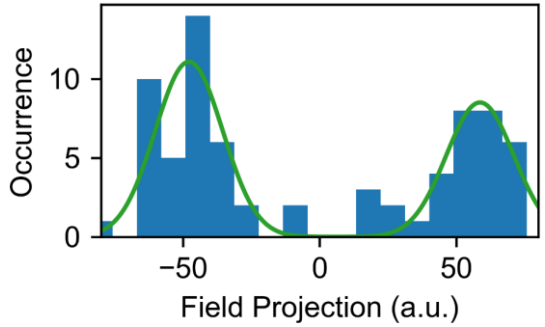
balanced heterodyne receiver.

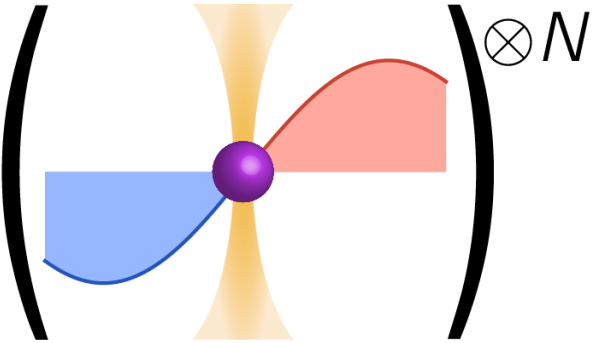
demodulate to get
amplitude and phase of cavity field

Observation of Z_2 symmetry breaking





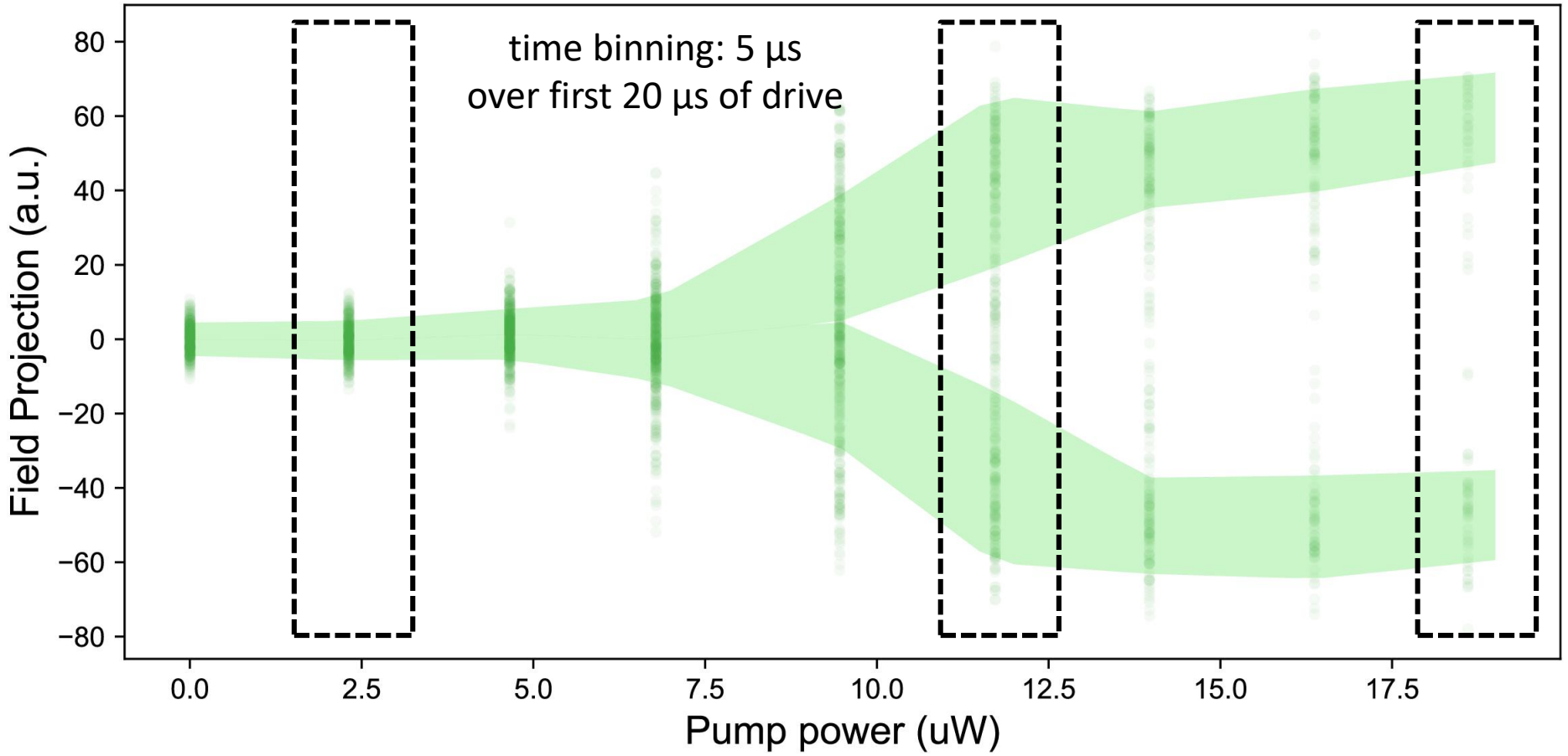




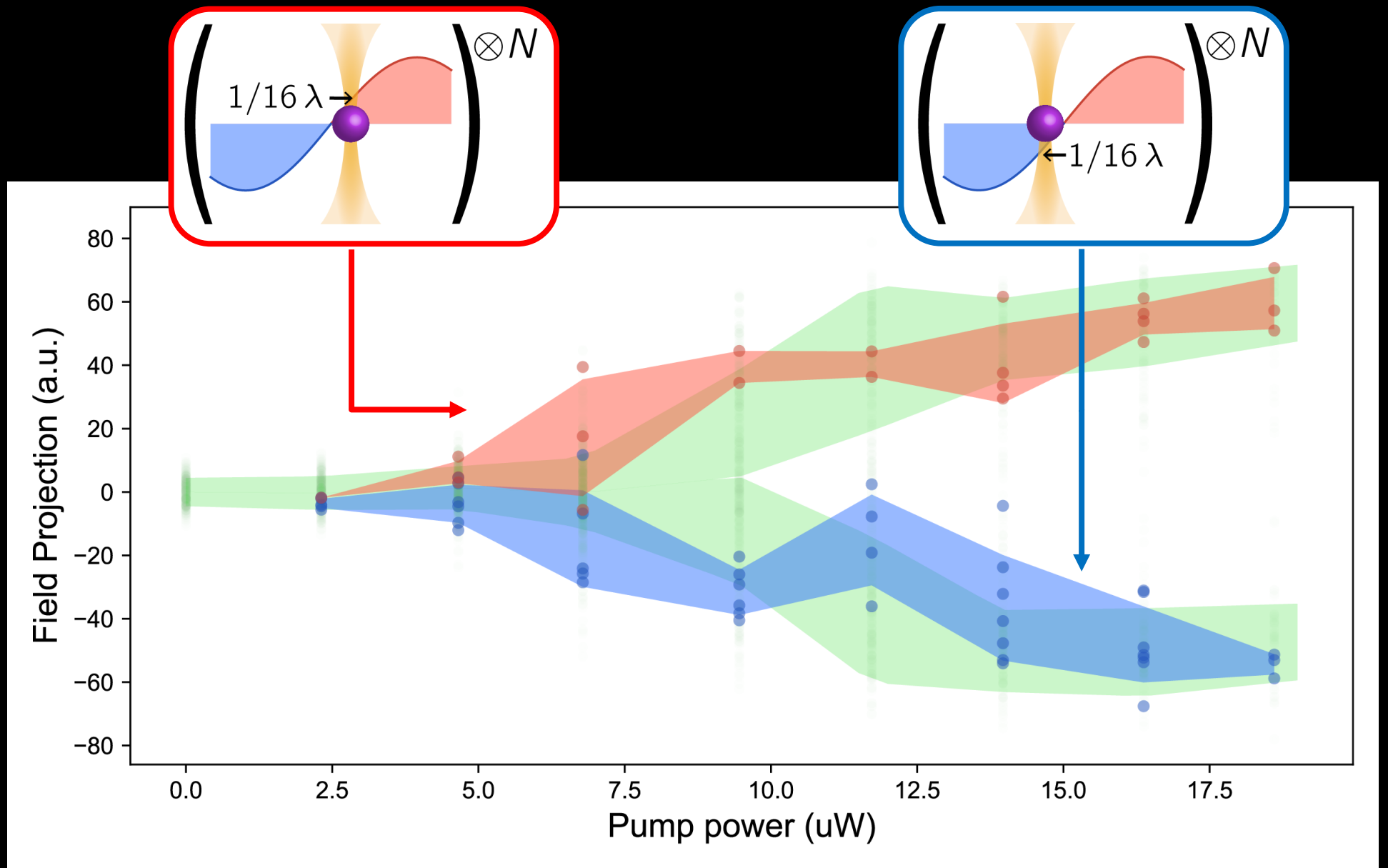
N=20

$\Delta_{ca} = -40\mathrm{MHz},$

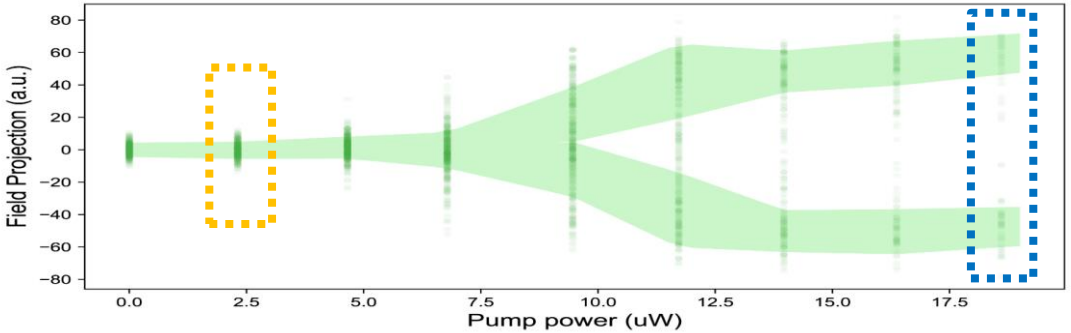
$\Delta_{pc} = -2\mathrm{MHz}$

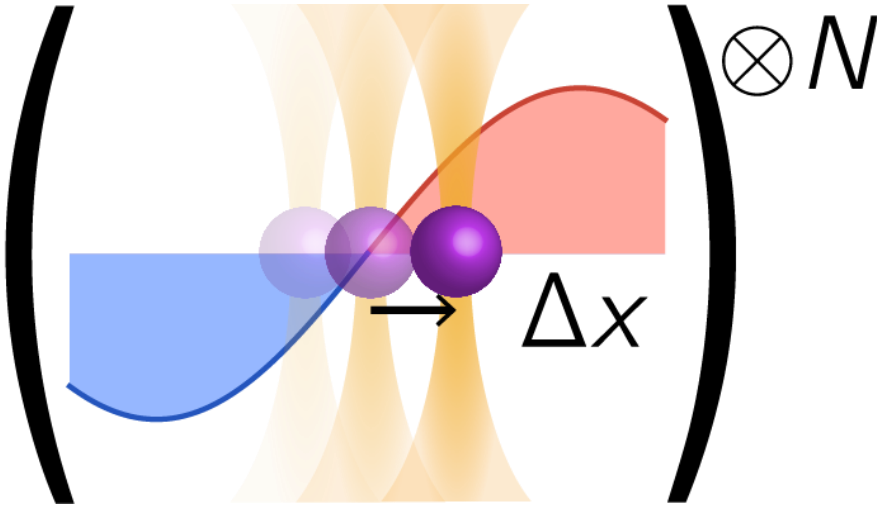


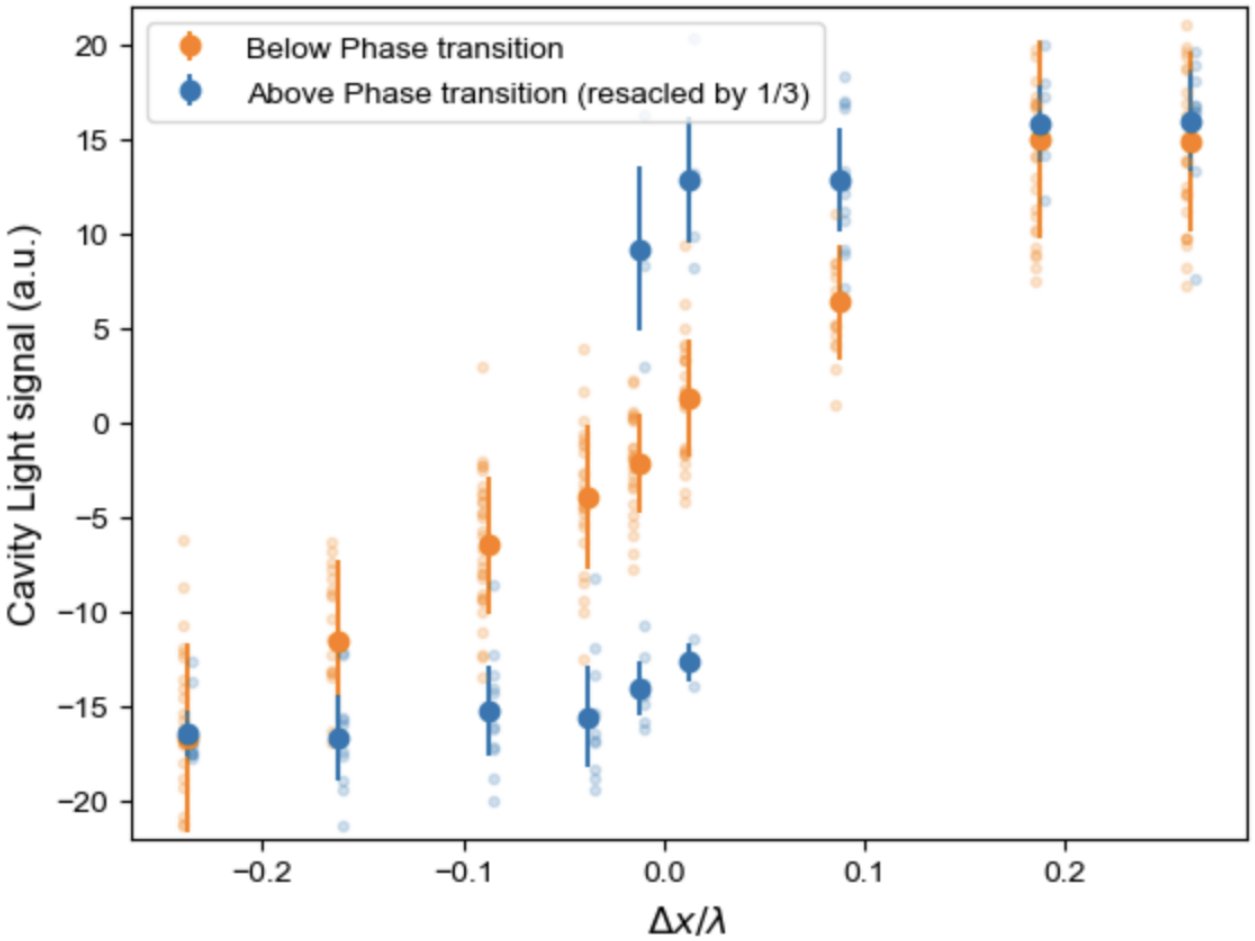
Explicit symmetry breaking



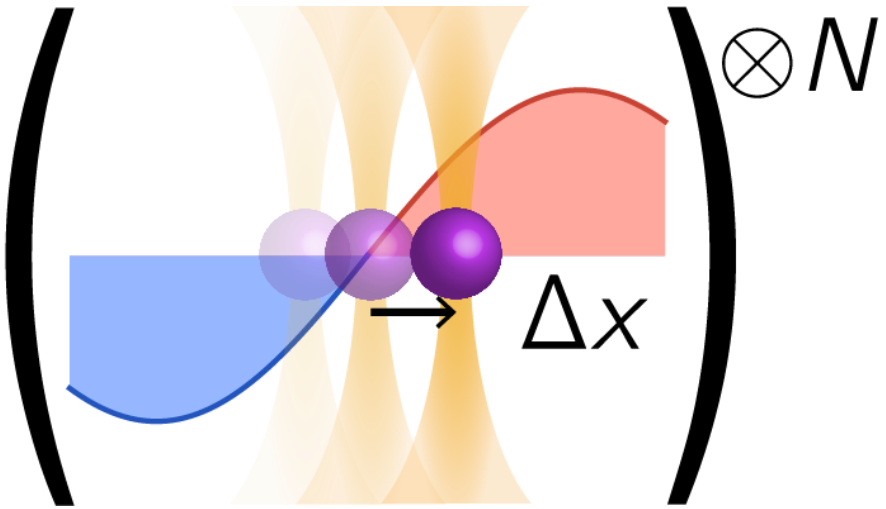
Mechanical susceptibility

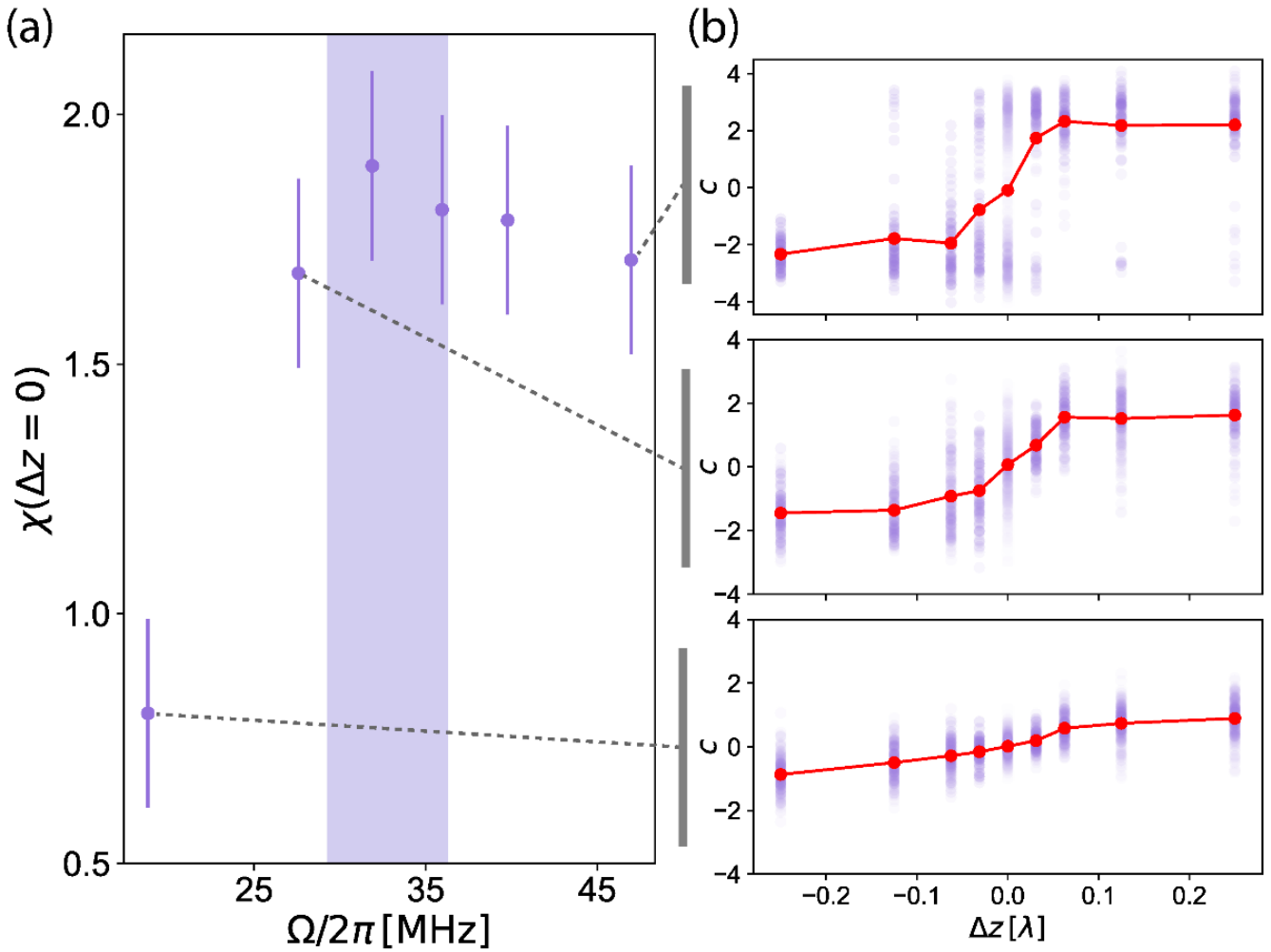






Mechanical susceptibility

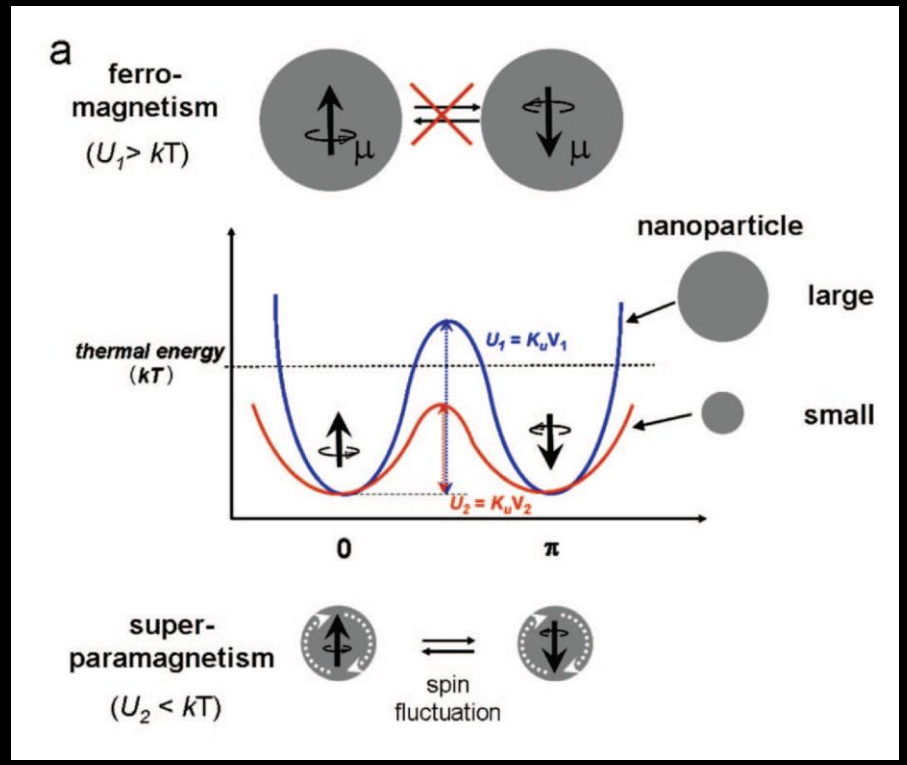


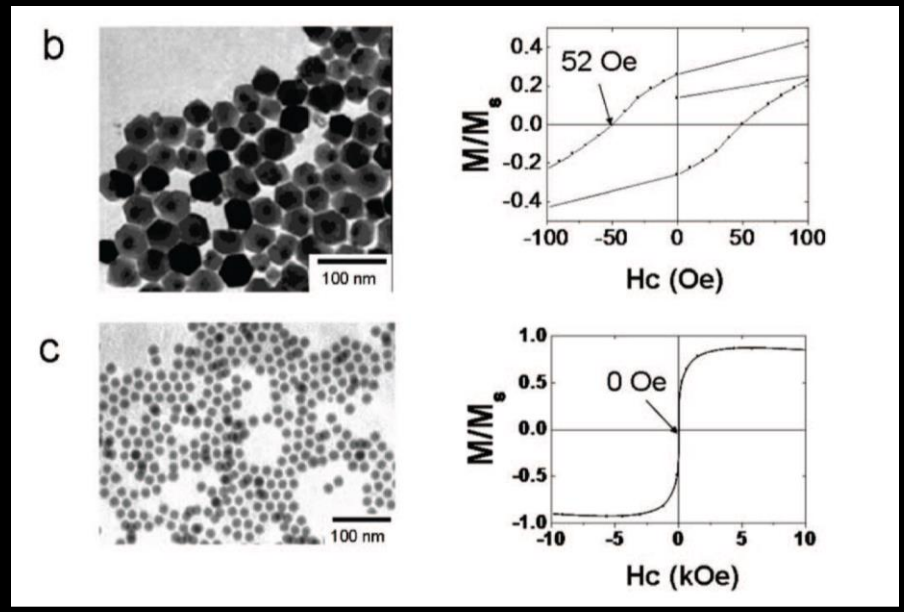


Optomechanics and superparamagnetism

"Phase transitions strictly occur only in the thermodynamic limit"

- e.g. superparamagnetism in nanomagnets
  - relevant to magnetic data storage, biomedical imaging

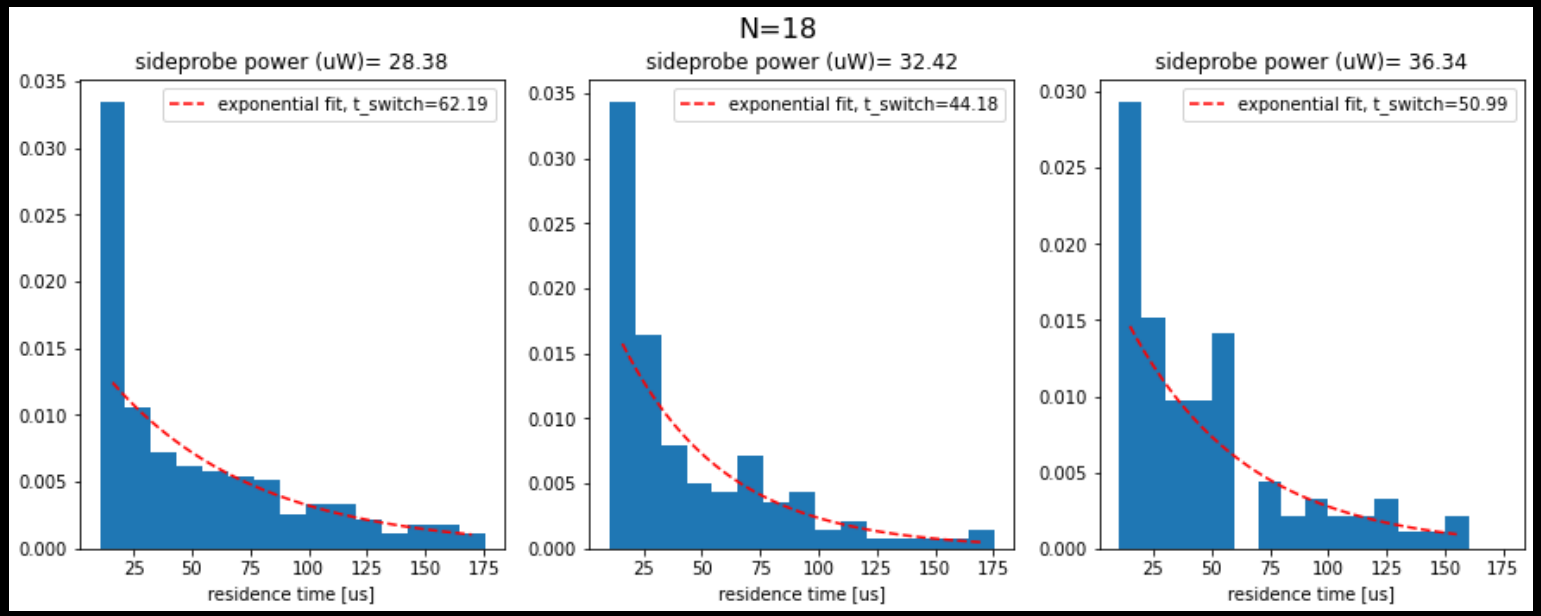


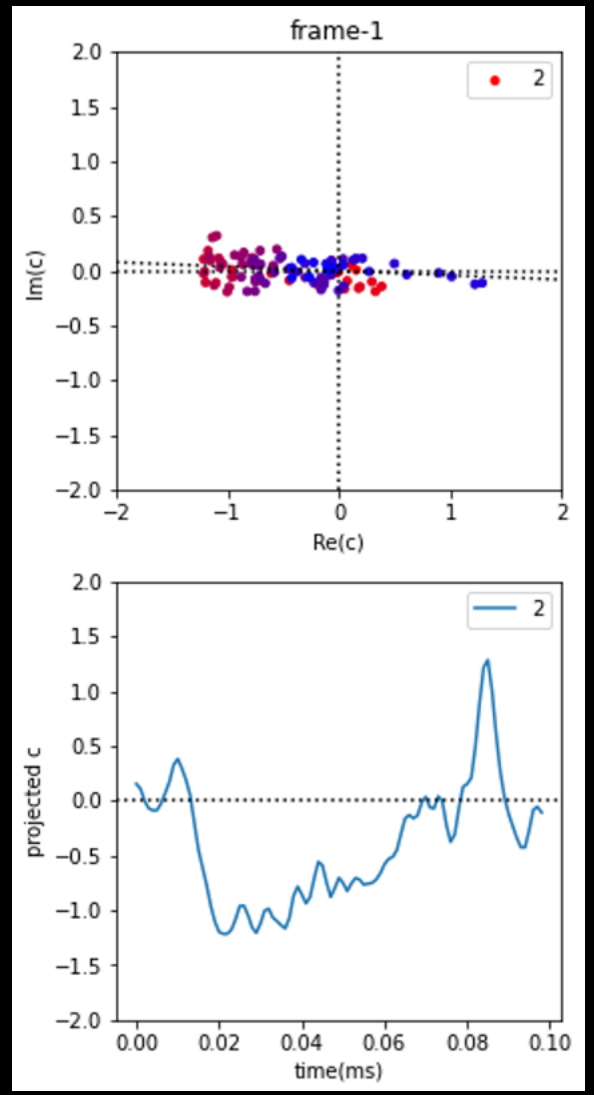


Jun et al., Acc. Chem. Res. **41**, 179 (2008)

Optomechanics and superparamagnetism

- Switching dynamics in meoscopic Dicke model
  - Exponential distribution (Poisson) + rapid switches (over-the-barrier dynamics?)





Next steps

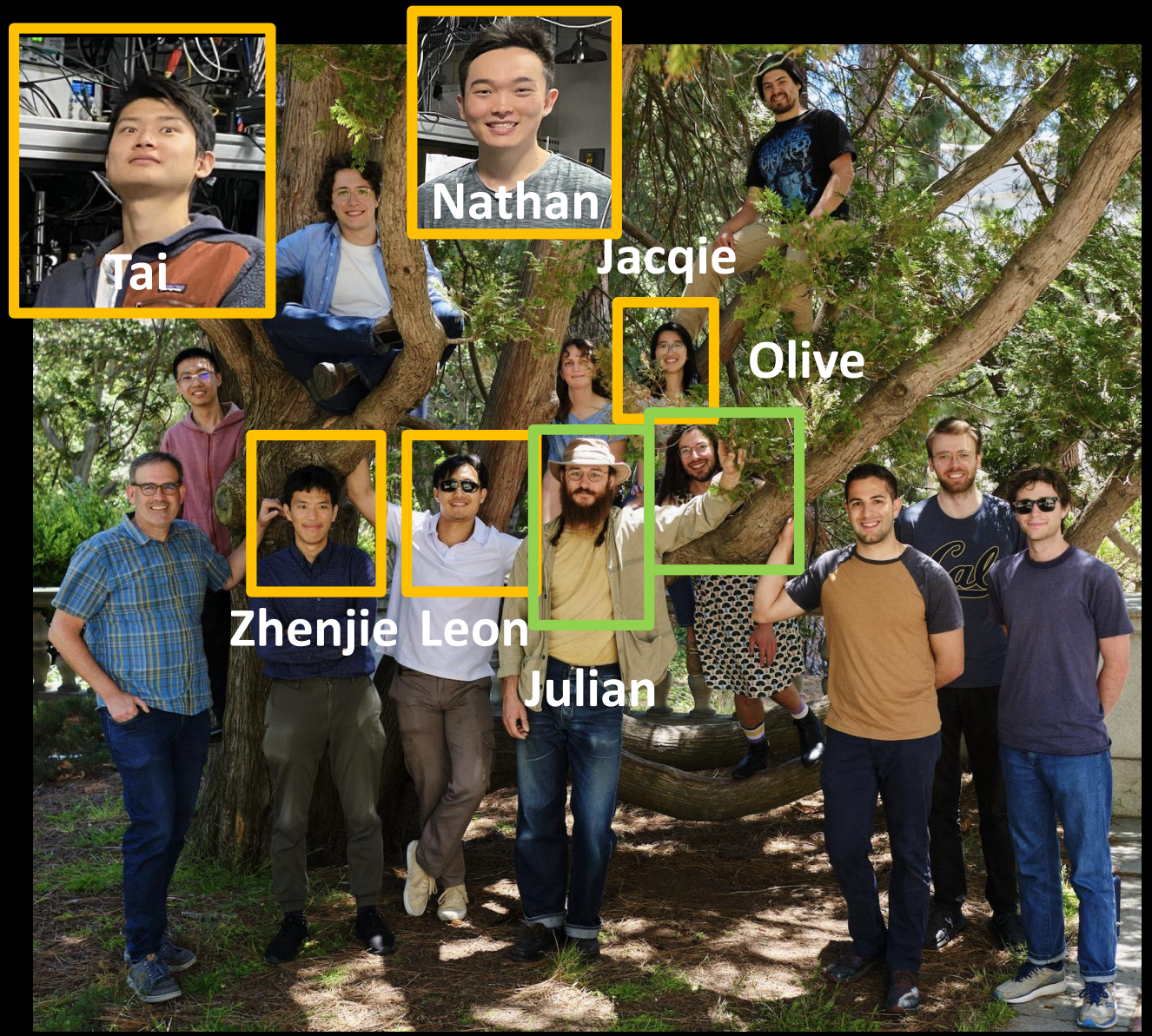
- Mesoscopic signatures in driven-dissipative phase transition
  - Switching dynamics
  - Finite-size scaling
- Quantum optics effects
  - Cavity pulling -> tristability
  - Effects of atomic saturation
  - Limit on N
- Self-organization in the spin sector
  - Schemes for Z2, U(1) symmetry breaking
- Deeper programmability
  - Amplitude and phase control – higher order symmetry breaking
  - Multiple tones – numerical solver

E6 team

Jacquelyn Ho
Leon Lu
Nathan Song
Tai Xiang
Zhenjie Yan

E3 team

Olive Eilbott
Julian Wolf







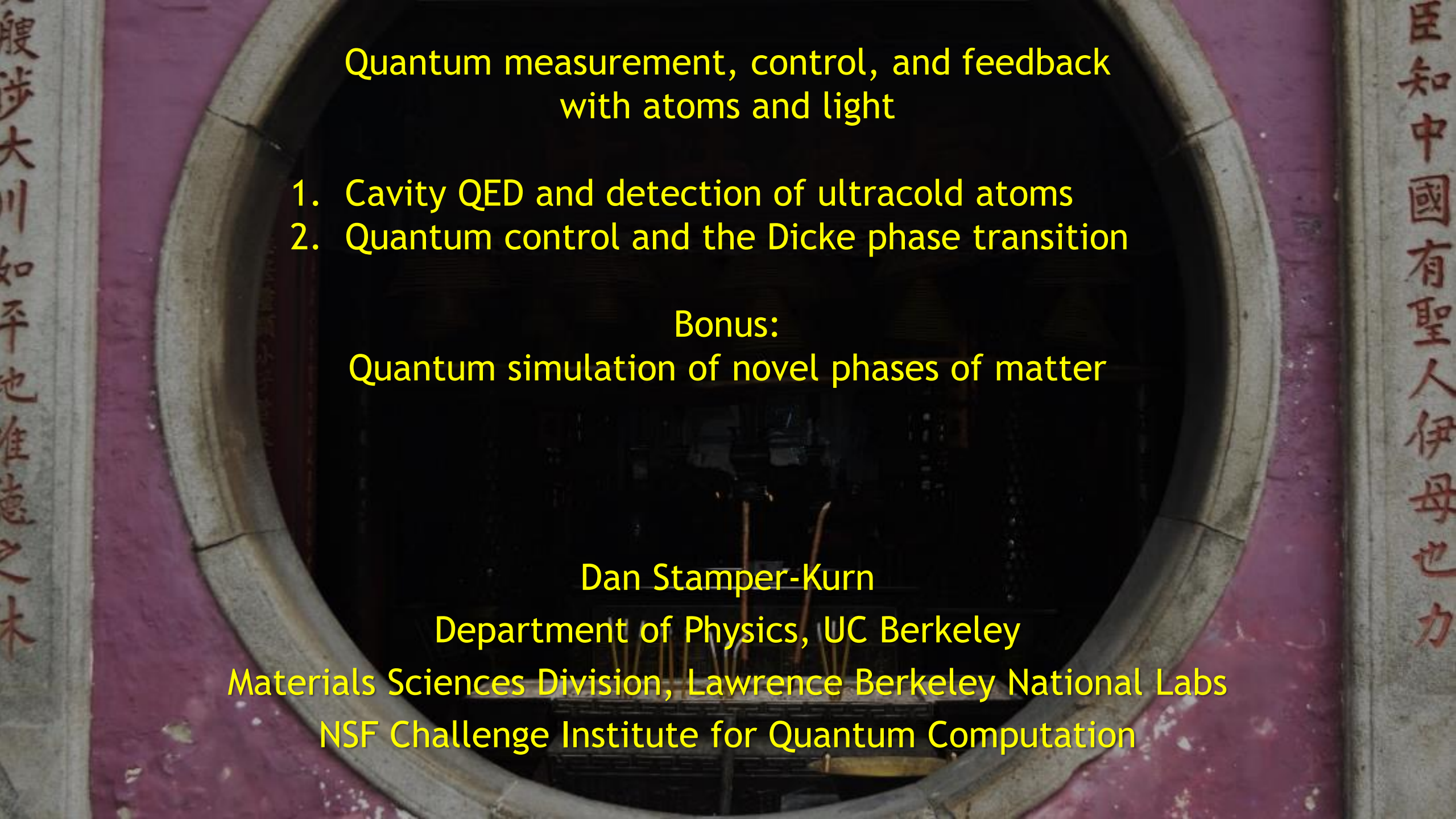


Theory collab. (Columbia)

Ana Asenjo-Garcia
Stuart Masson
Cosimo Rusconi

$$ Thanks! AFOSR, ARO (MURIs and single PI), DARPA, DOE (QSA), NSF, ONR, Heising-Simons

CIQC Challenge Institute for Quantum Computation



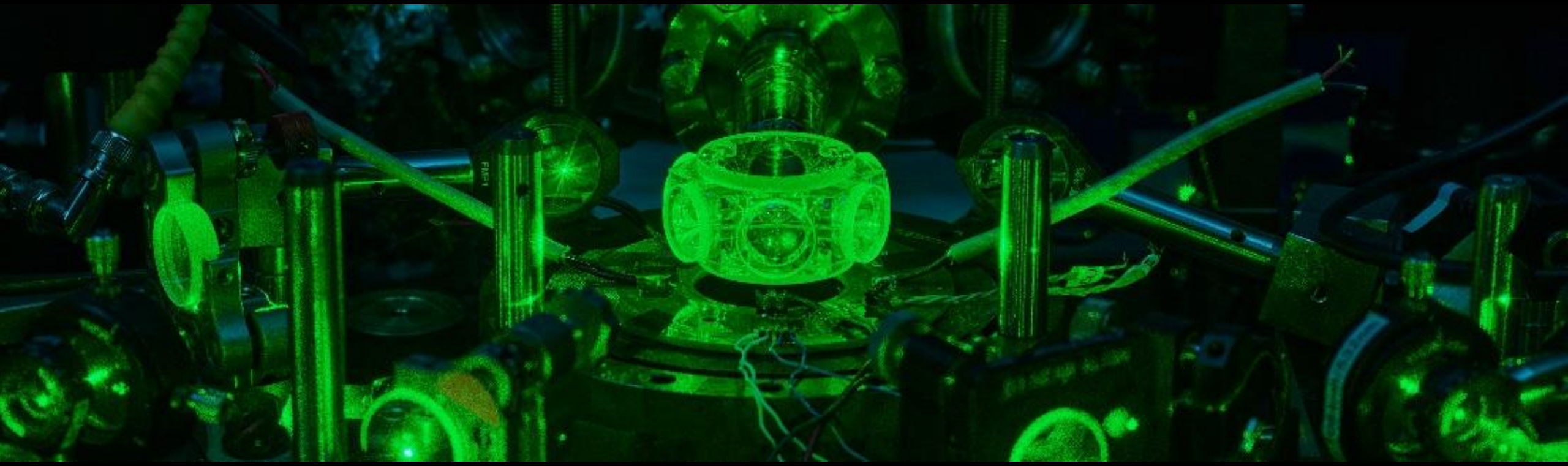
Quantum measurement, control, and feedback with atoms and light

1. Cavity QED and detection of ultracold atoms
2. Quantum control and the Dicke phase transition

Bonus:
Quantum simulation of novel phases of matter

Dan Stamper-Kurn
Department of Physics, UC Berkeley
Materials Sciences Division, Lawrence Berkeley National Labs
NSF Challenge Institute for Quantum Computation

Quantum simulation of novel phases of matter

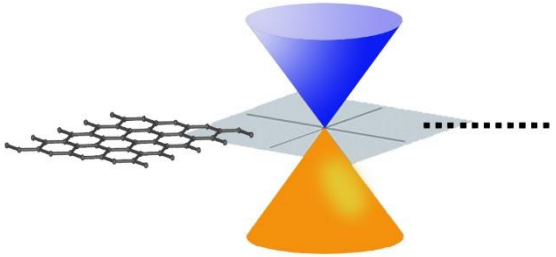


- Quantum gases in non-primitive triangular lattices
  - Navigating through the geometry of band structure
  - Renormalization of band structure in a flat band system
- Laser cooling of transition-metal atoms
  - First laser-cooled gases of titanium

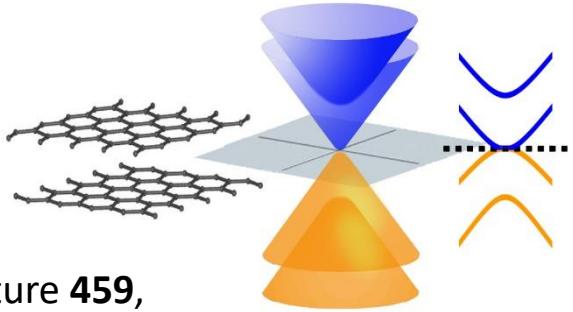
Band structure in 2D materials

- Special features of 2D band structures endow materials of interacting particles with interesting properties

- Examples of late
  - Dirac points (graphene)
    - geometry around Dirac point affects quantum Hall response, scattering (Klein tunneling), etc.
  - Quadratic band touching points (bilayer graphene)
    - unstable to interactions, emergent order, Landau levels
  - Flat bands (magic-angle twisted bilayer graphene)
    - interactions dominate

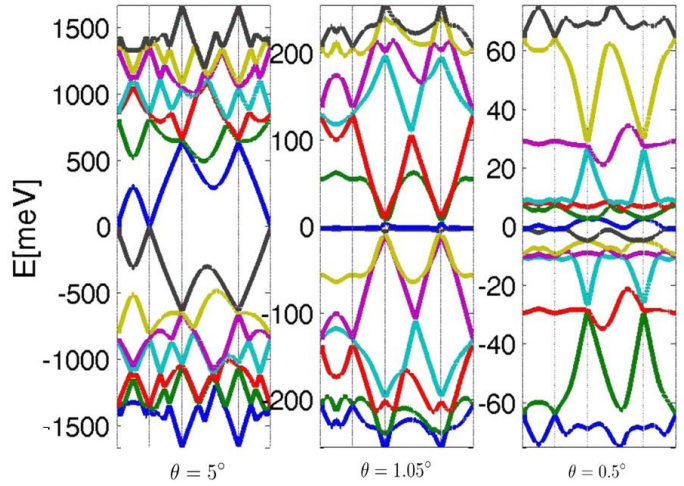


graphene



Nature **459**, 820 (2009)

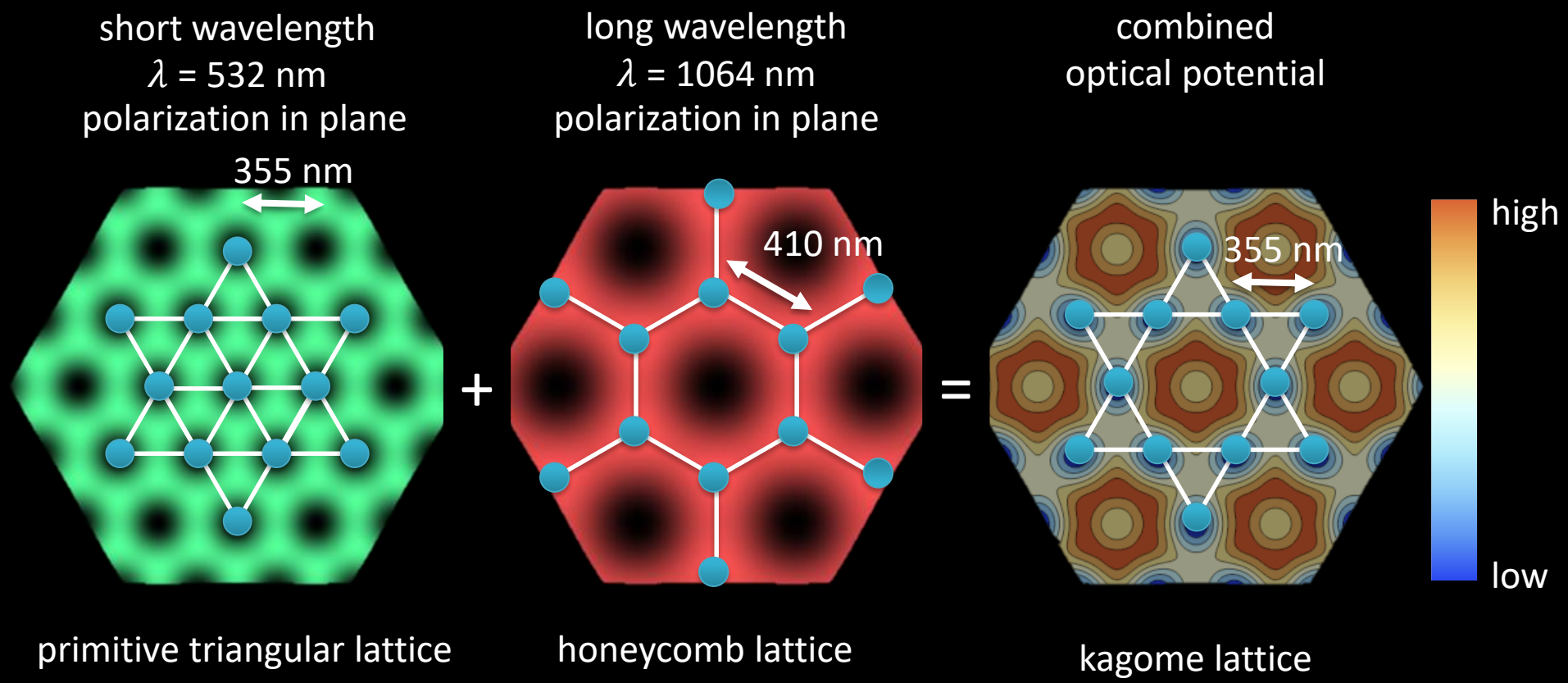
bilayer graphene



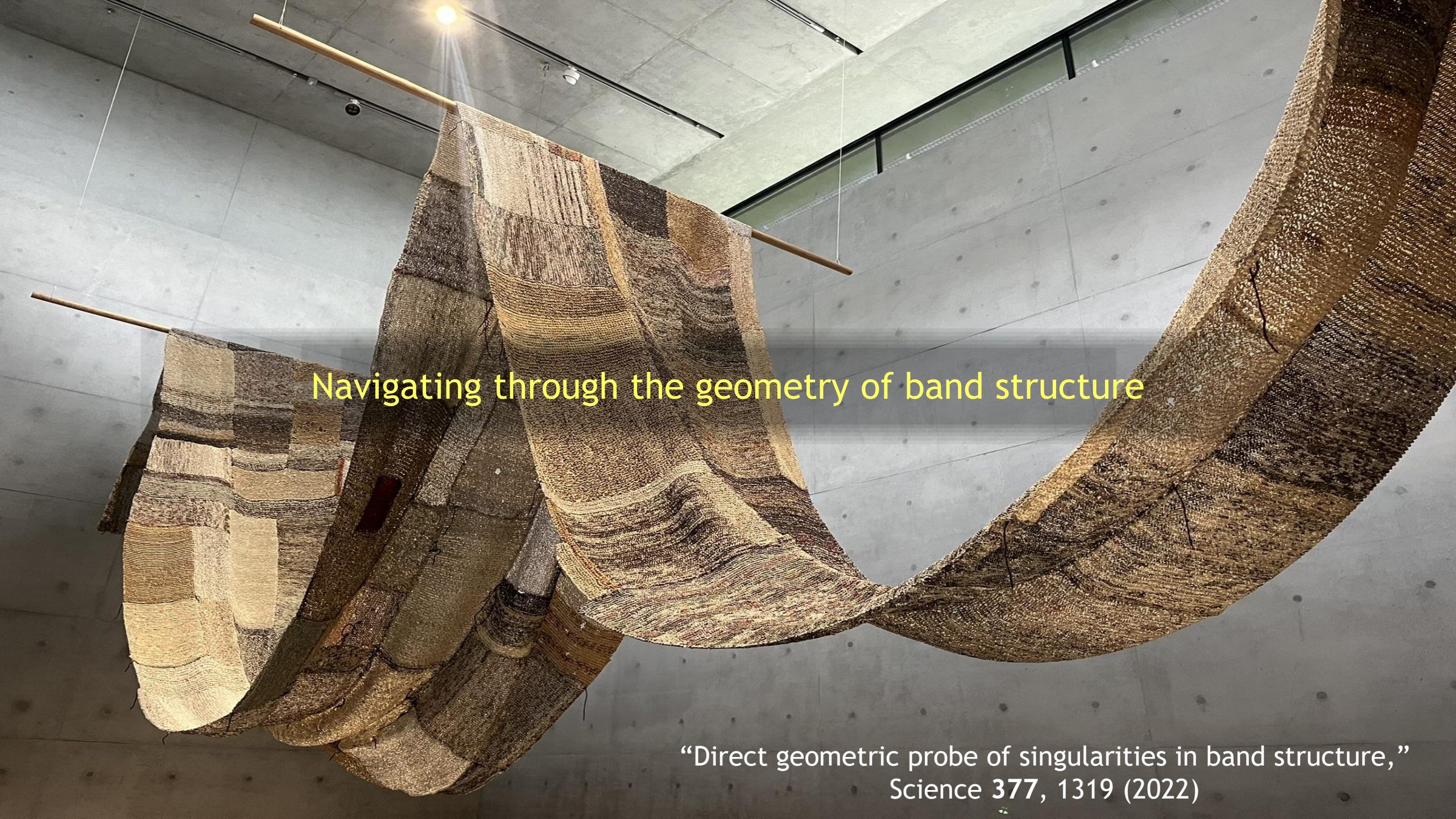
PNAS **108**, 12233 (2011)

twisted bilayer graphene

Triangular lattice with tunable geometry

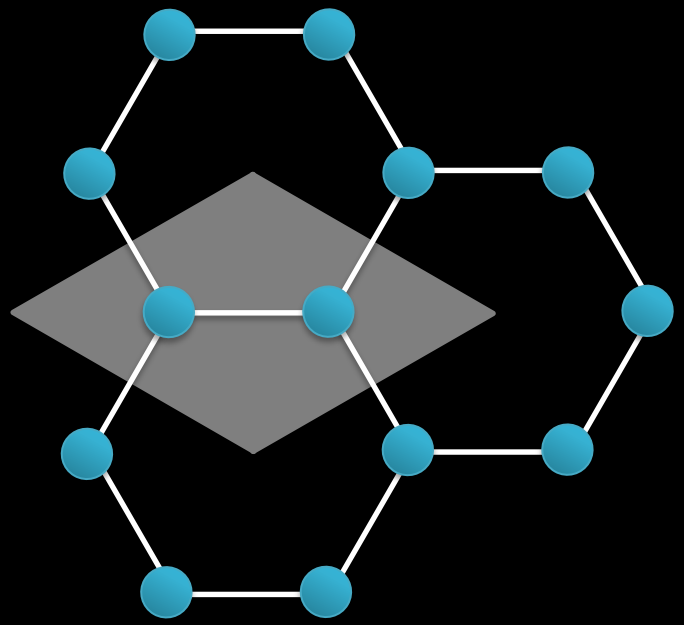


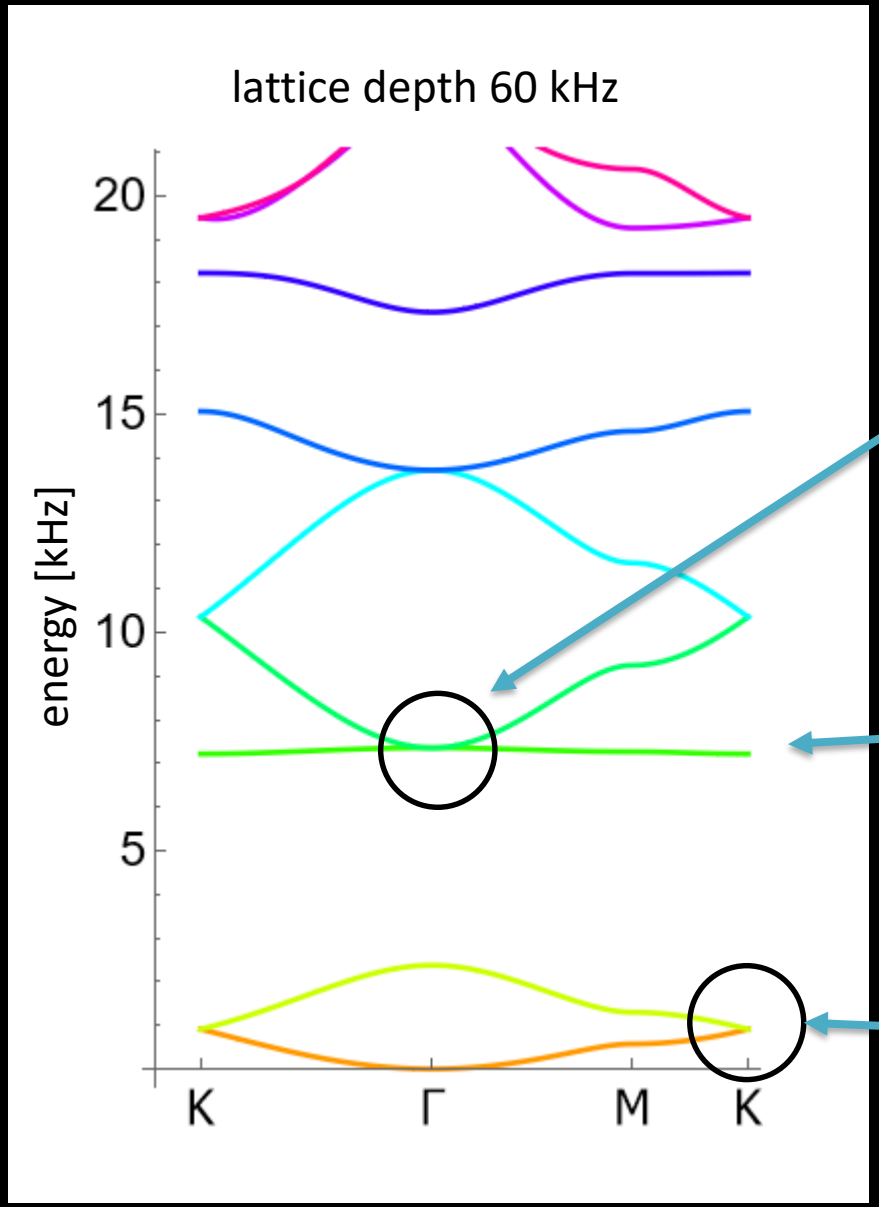
Gyu-Boong Jo et al., "Ultracold atoms in a tunable optical kagome lattice,"
PRL **108**, 045305 (2012)



"Direct geometric probe of singularities in band structure,"
Science **377**, 1319 (2022)

Honeycomb (graphene) lattice

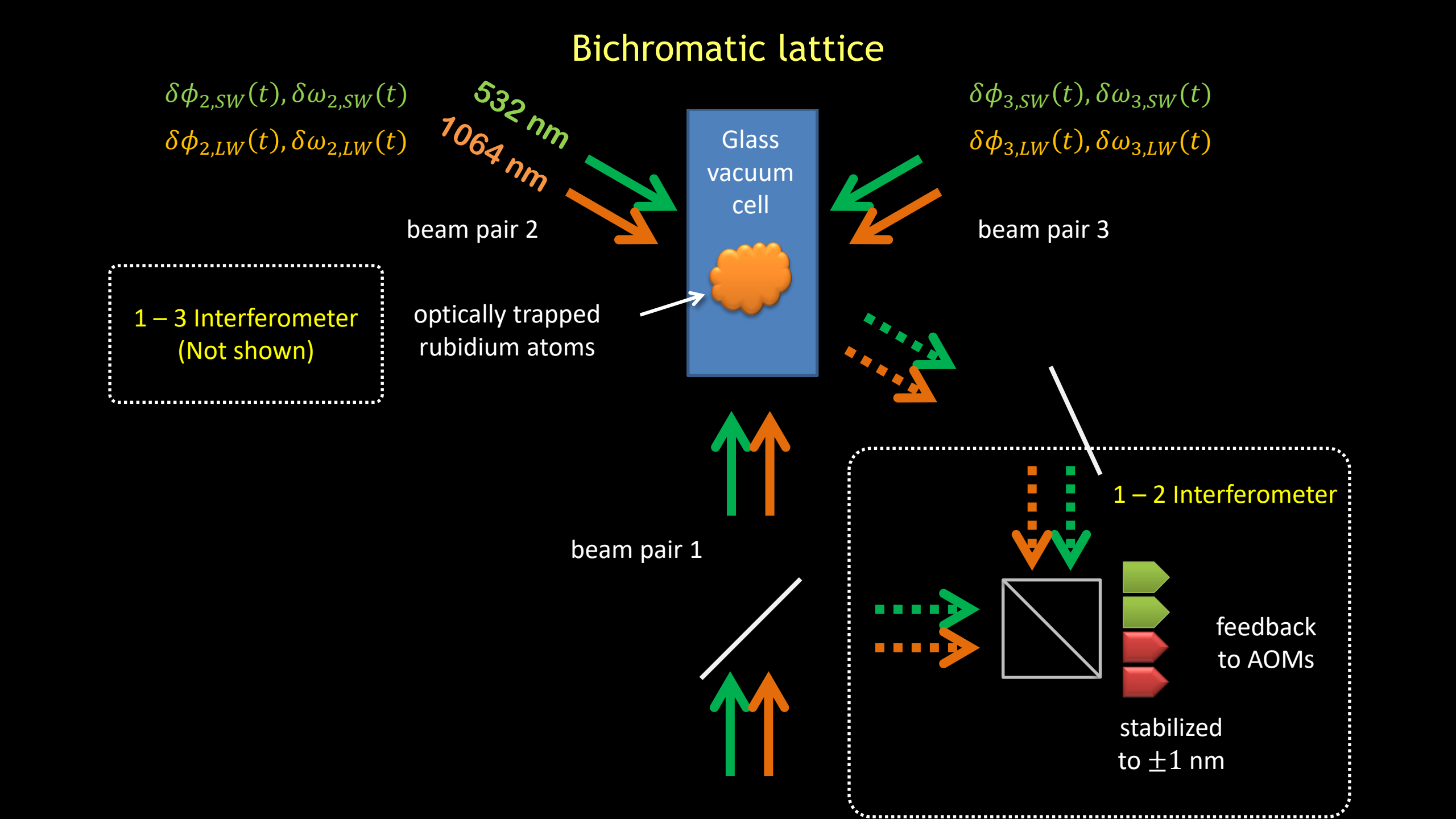




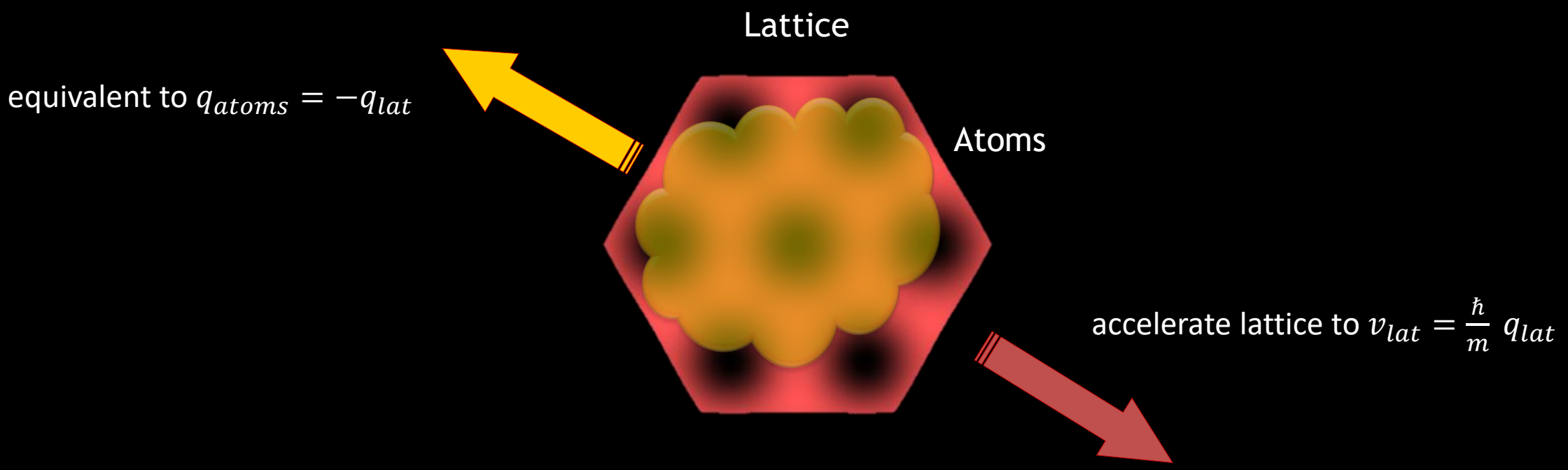
quadratic band-touching point

geometrically frustrated flat band

linear (Dirac) band-touching point


Bichromatic lattice
$\delta\phi_{2,SW}(t), \delta\omega_{2,SW}(t)$
$\delta\phi_{2,LW}(t), \delta\omega_{2,LW}(t)$
532 nm
1064 nm
beam pair 2
Glass vacuum cell
$\delta\phi_{3,SW}(t), \delta\omega_{3,SW}(t)$
$\delta\phi_{3,LW}(t), \delta\omega_{3,LW}(t)$
beam pair 3
1 – 3 Interferometer (Not shown)
optically trapped rubidium atoms
beam pair 1
1 – 2 Interferometer
feedback to AOMs
stabilized to ± 1 nm

Navigating within band structure



- Turn up & then accelerate lattice: prepares atoms in ground state & then drives to $q \neq 0$

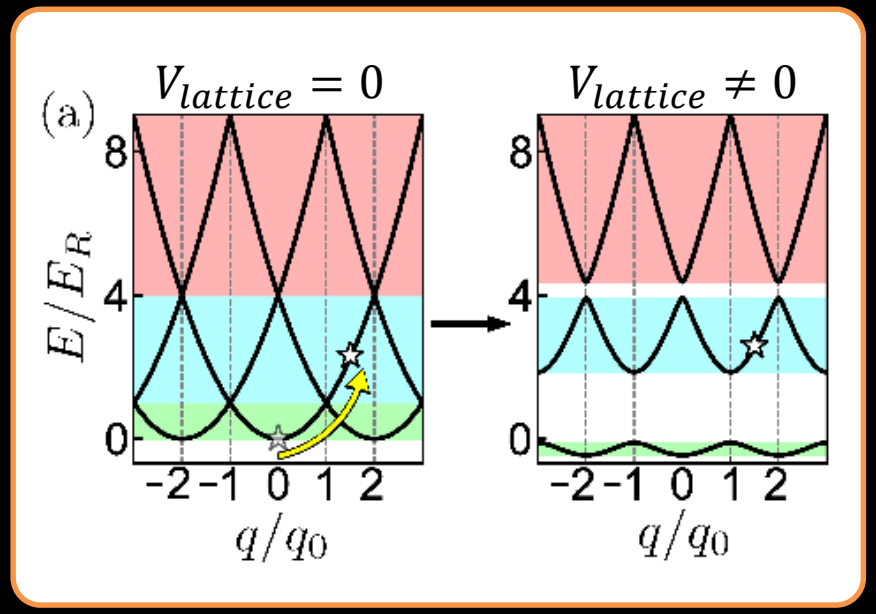
Navigating within band structure

Lattice

equivalent to $q_{atoms} = -q_{lat}$

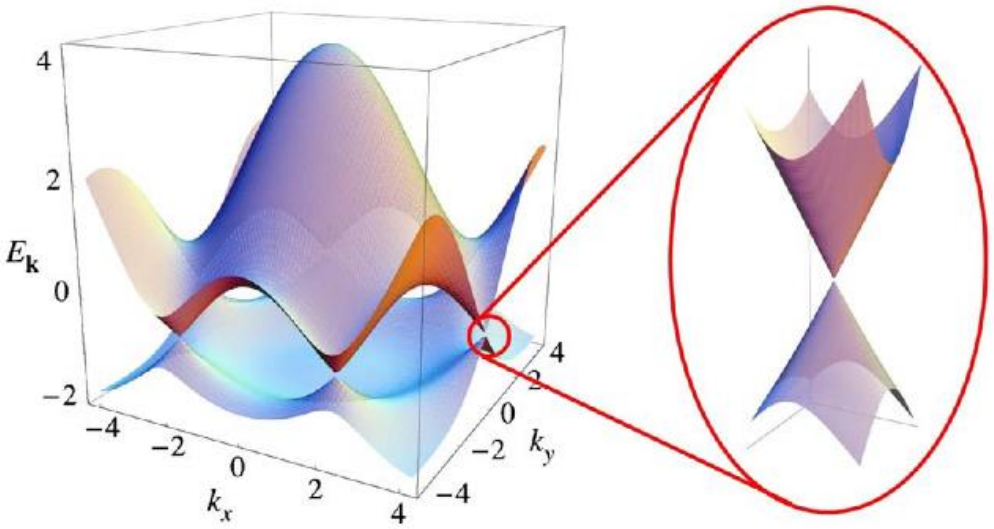
Atoms

accelerate lattice to $v_{lat} = \frac{\hbar}{m} q_{lat}$

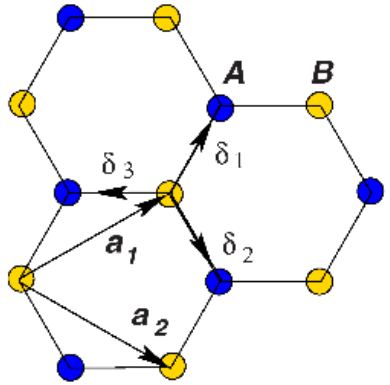


- Turn up & then accelerate lattice: prepares atoms in ground state & then drives to $q \neq 0$
- Accelerate & then turn up lattice: prepares atoms in higher band and $q \neq 0$, “inverse band mapping”

Geometry at a linear band touching point



Castro Neto et al, Rev. Mod. Phys. **81**, 109 (2009)

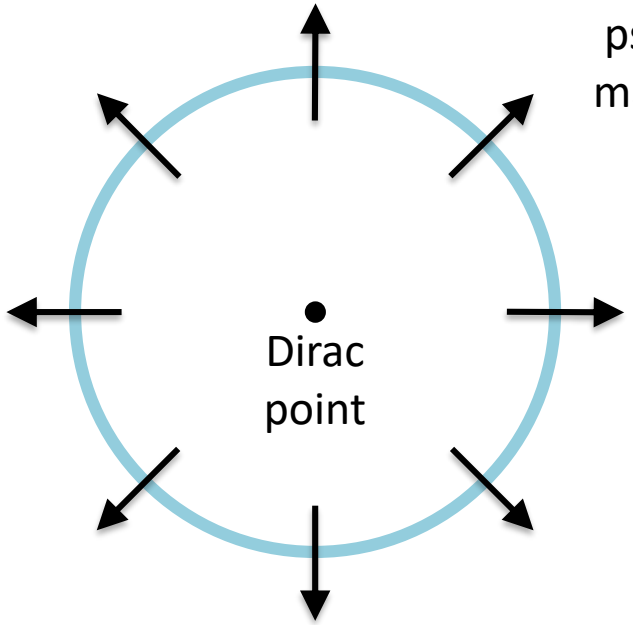


pseudospin:

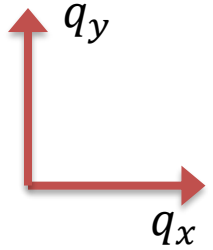
$|A\rangle = |\uparrow\rangle$

$|B\rangle = \xi\,|\downarrow\rangle$

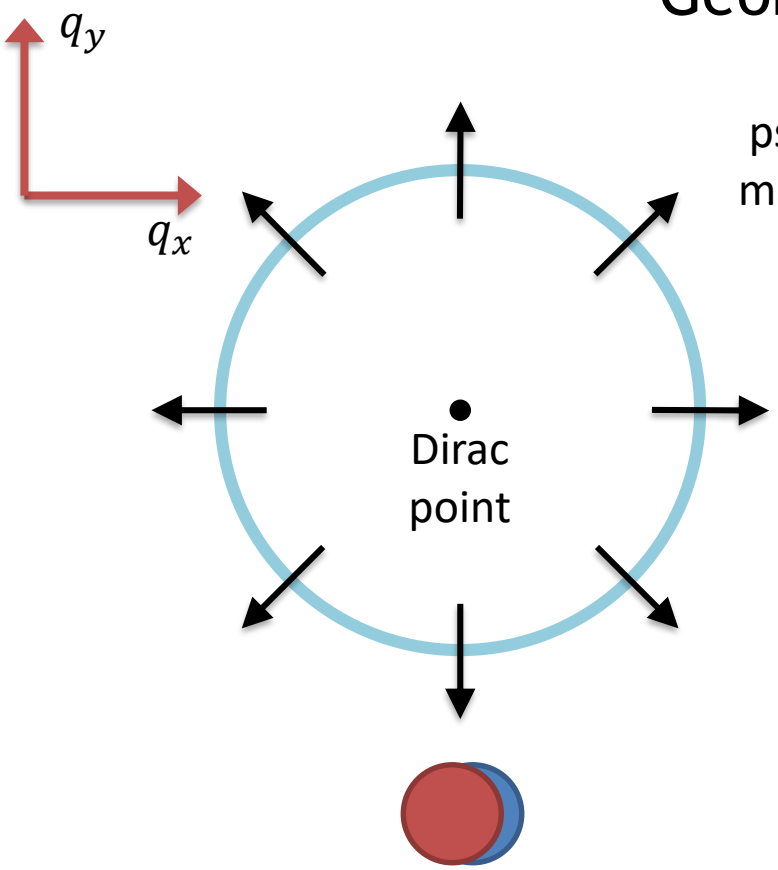
$H = v\,\boldsymbol{\sigma}\cdot(\boldsymbol{q}-\boldsymbol{q_D})$



pseudo-magnetic field



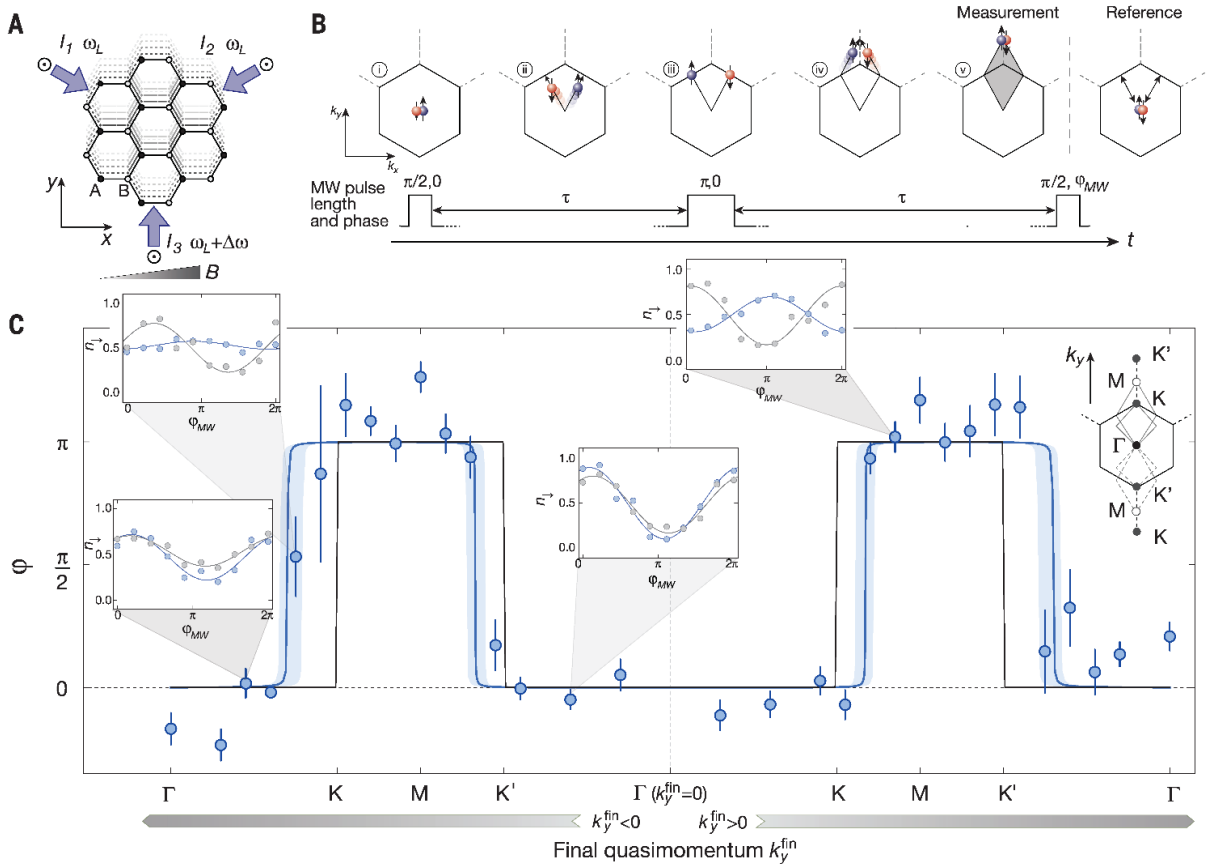
Geometry at a linear band touching point



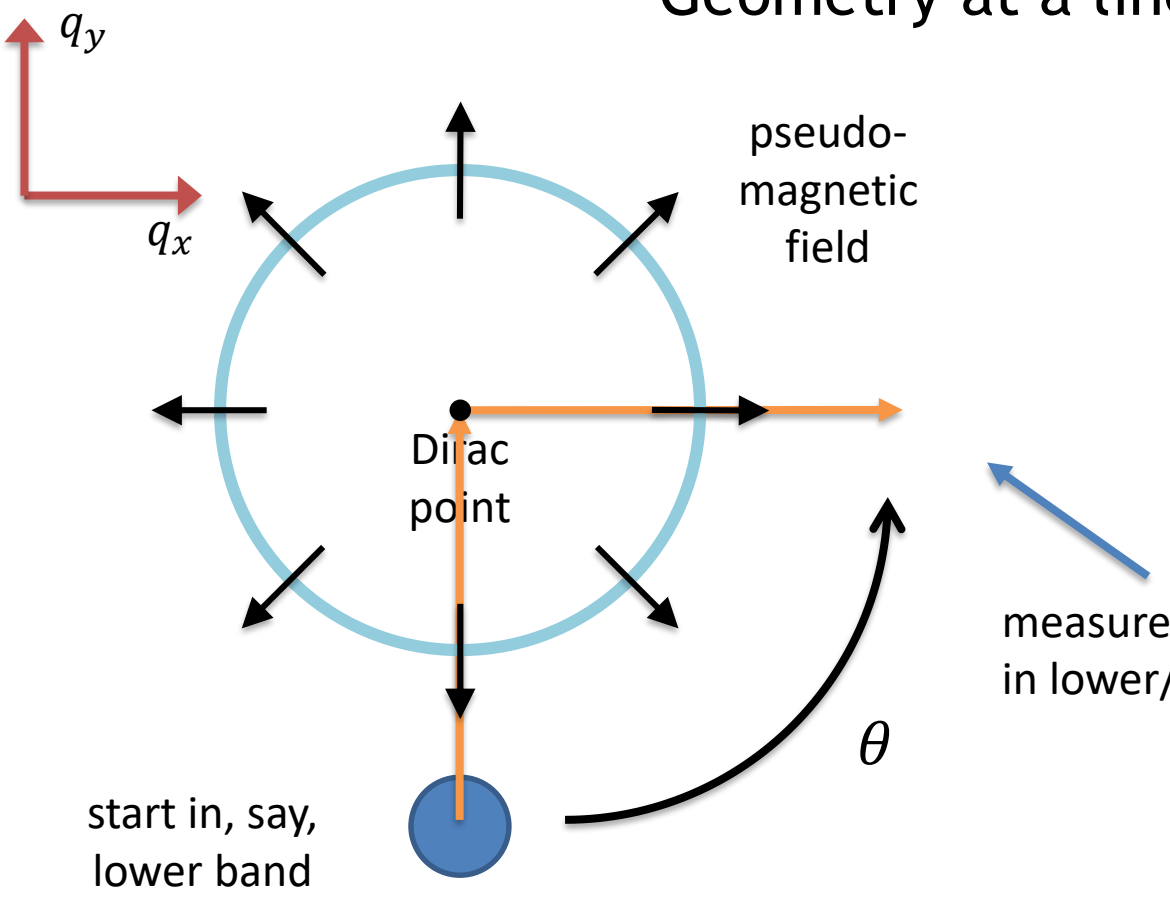
pseudo-magnetic field

How to characterize the singularity at the Dirac point?

1. Measure Berry phase going around Dirac point
   Duca et al (Bloch group), Science 347, 288 (2015)



Geometry at a linear band touching point



How to characterize the singularity at the Dirac point?

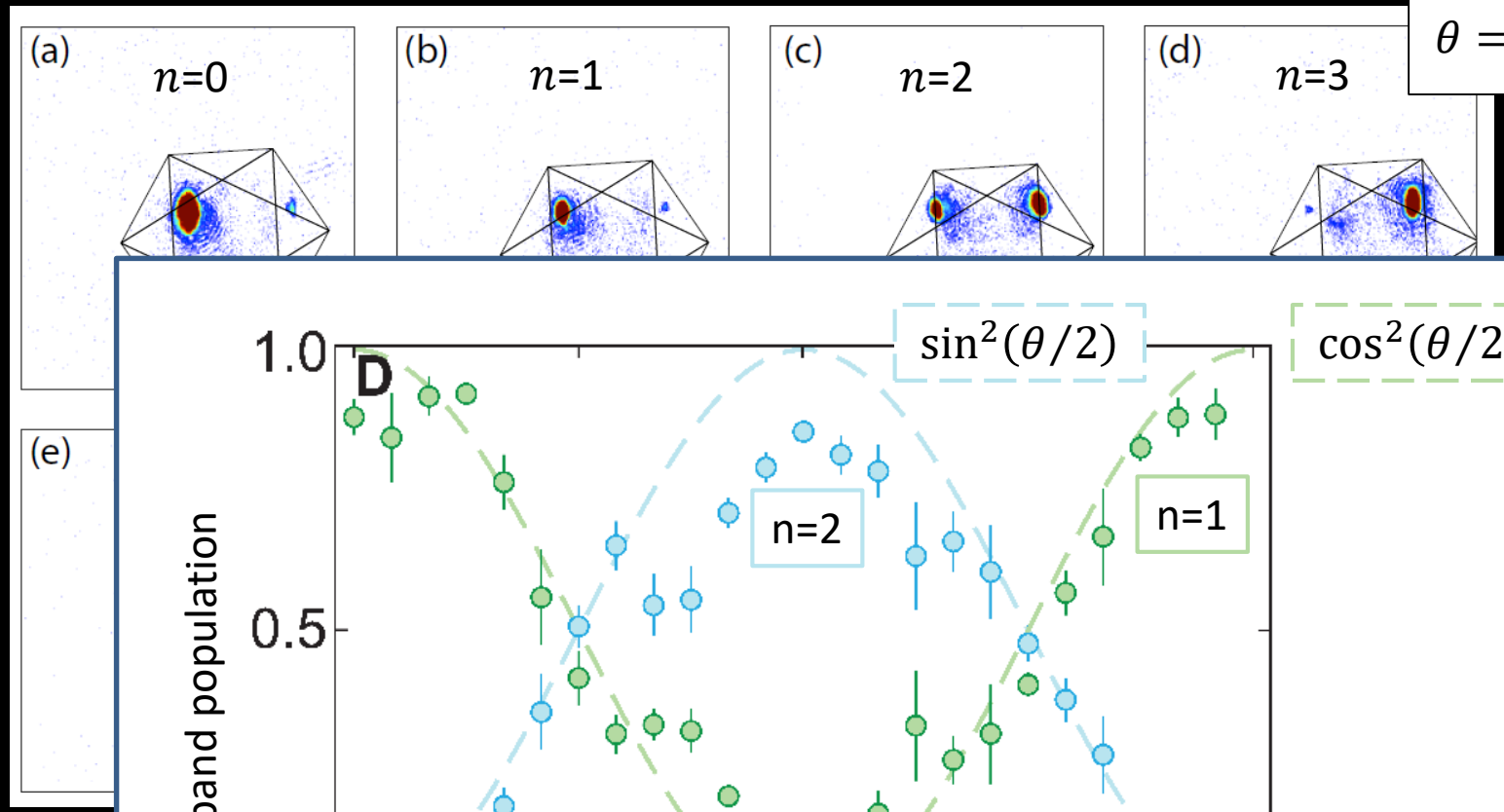
1. Measure Berry phase going around Dirac point
   Duca et al (Bloch group), Science 347, 288 (2015)

2. Measure state rotation (non-Abelian holonomy) going through Dirac point

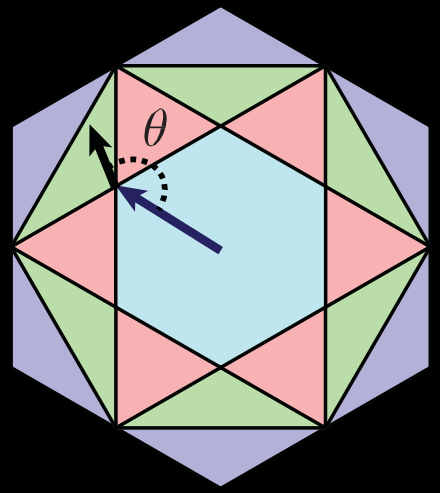
$$P_{lower} = \cos^2(\theta/2)$$

$$P_{upper} = \sin^2(\theta/2)$$

Geometry of Dirac point in honeycomb (IR only) lattice



$$\theta = \frac{\pi}{6} + n\frac{\pi}{4}$$



slowly r
honeycor

slowly ramp down honeycomb lattice (band-mapping)

Probes of Bloch manifold geometry

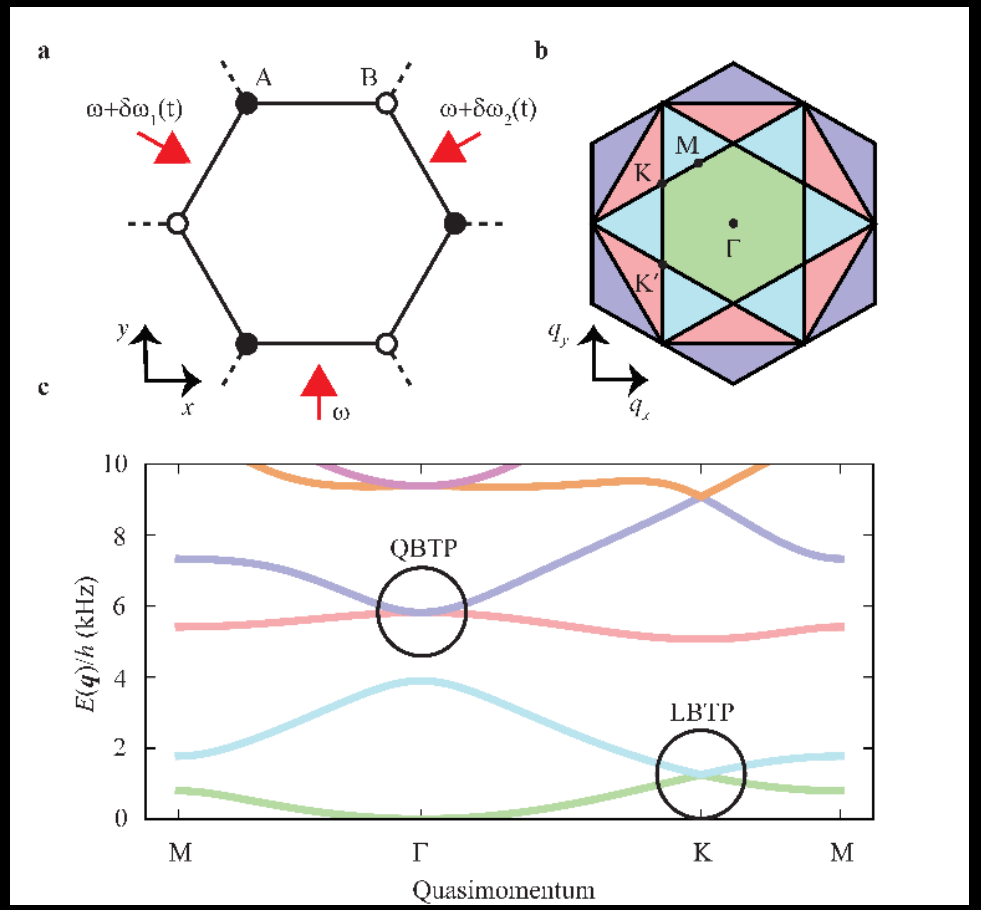
Differential geometry described by non-Abelian Berry connection: $\boldsymbol{A}_{nm}(q) = i\,\langle u_q^n | \partial_q | u_q^m \rangle$

Observable through nonholonomy of parallel transport

- Non-degenerate bands -> Abelian Berry phase nonholonomy produced by diagonal $\boldsymbol{A}_{nn}(q)$
  - Berry phase measurement: Duca et al, Science **347**, 288 (2015)
  - Hall conductivity: Jotzu et al, Nature 515, 237 (2014)
    Aidelsberger et al., Nature Physics 11, 162 (2015)

- Degenerate bands -> Non-Abelian nonholonomy produced by off-diagonal $\boldsymbol{A}_{nm}(q)$ with $n \neq m$
  - Bloch state tomography: Li et al, Science 352, 1094 (2016)
    Tarnowski et al., Nature Comm. 10, 1728 (2019)
  - Transport through singularity: this work

Geometry at a quadratic band touching point



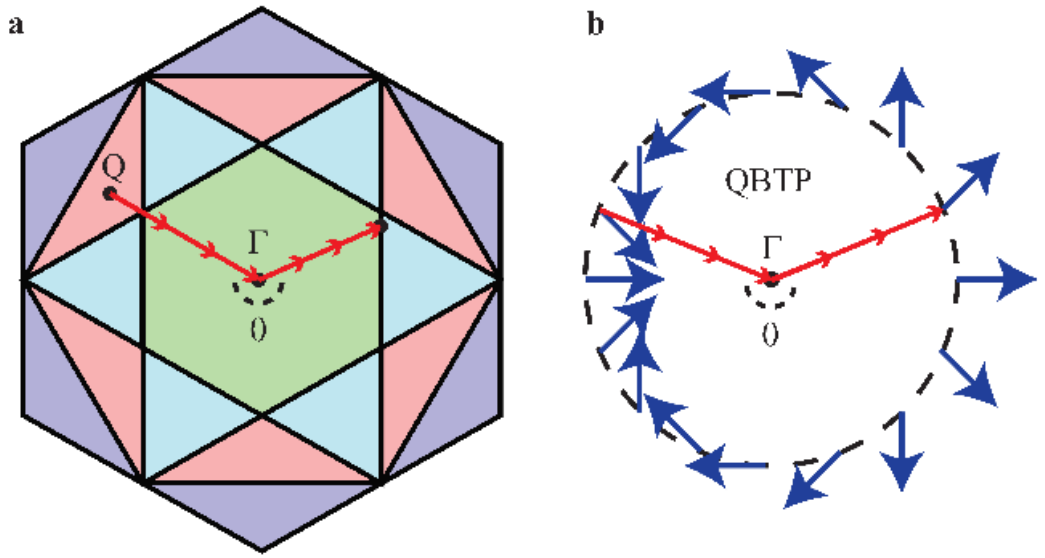
- kagome lattice, twisted bilayer graphene, honeycomb p-bands,…
- implications for materials
  - singular state geometry leads to anomalous Landau level spectrum [Nature **584**, 59 (2020)]
  - instability to nematic or topological phases [PRL **103**, 046811 (2009)]
- singular QBTP carries $\pm 2\,\pi$ Berry phase* that is undetectable by interferometry

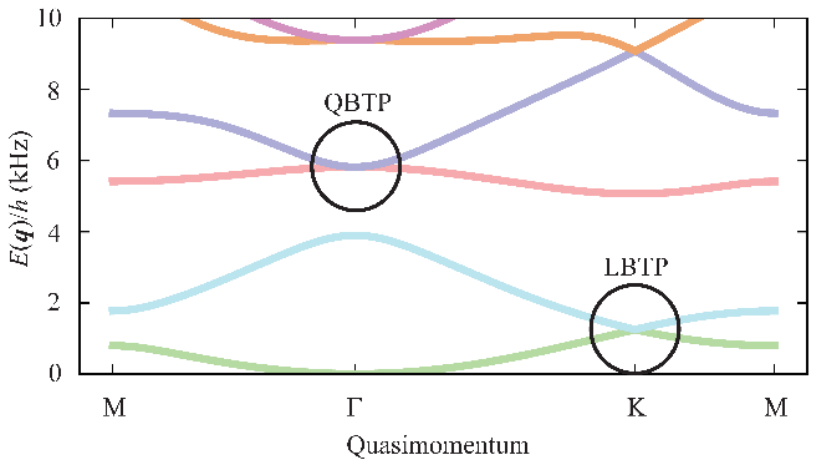
* with typical symmetry assumptions

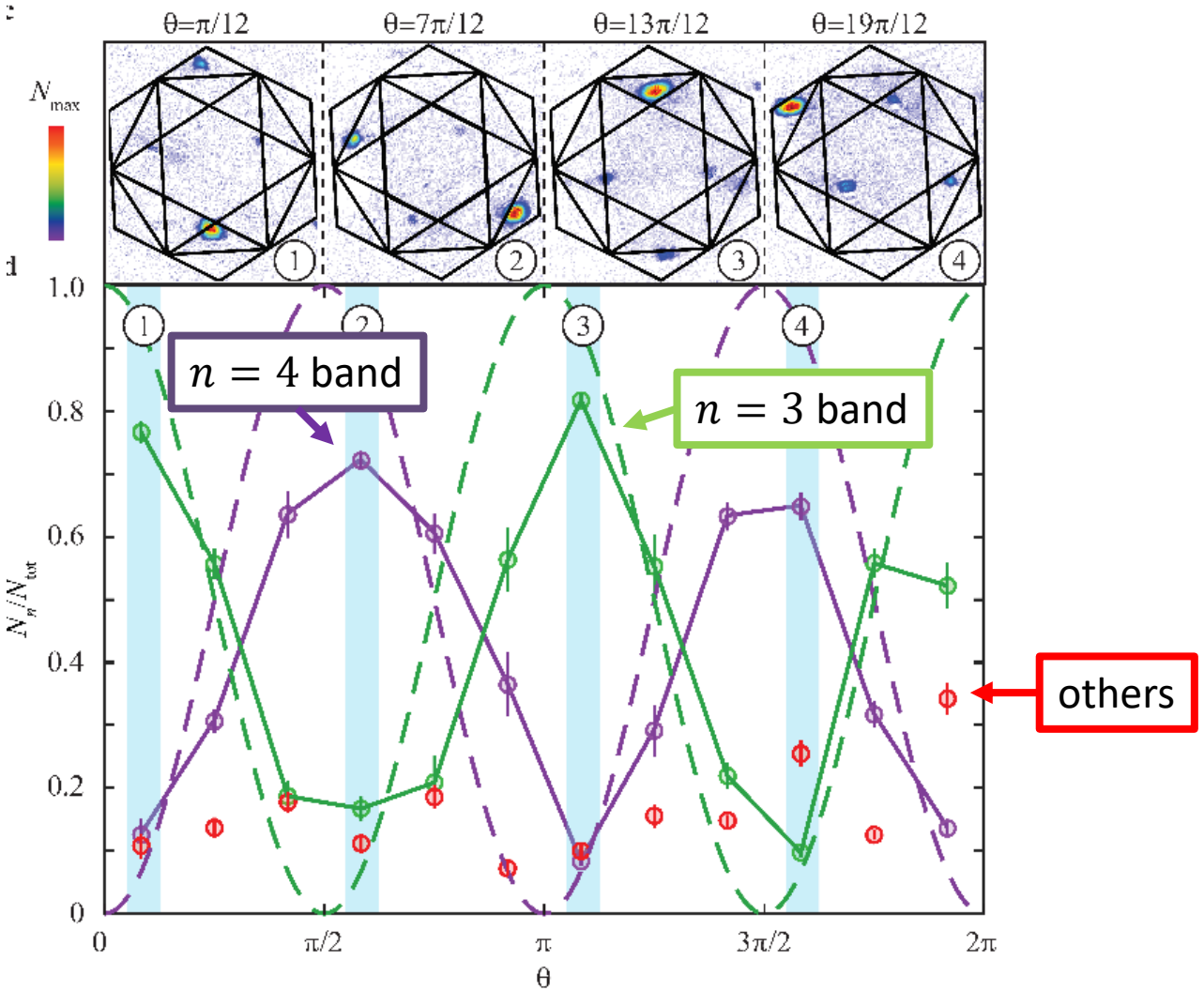
Geometry at a quadratic band touching point

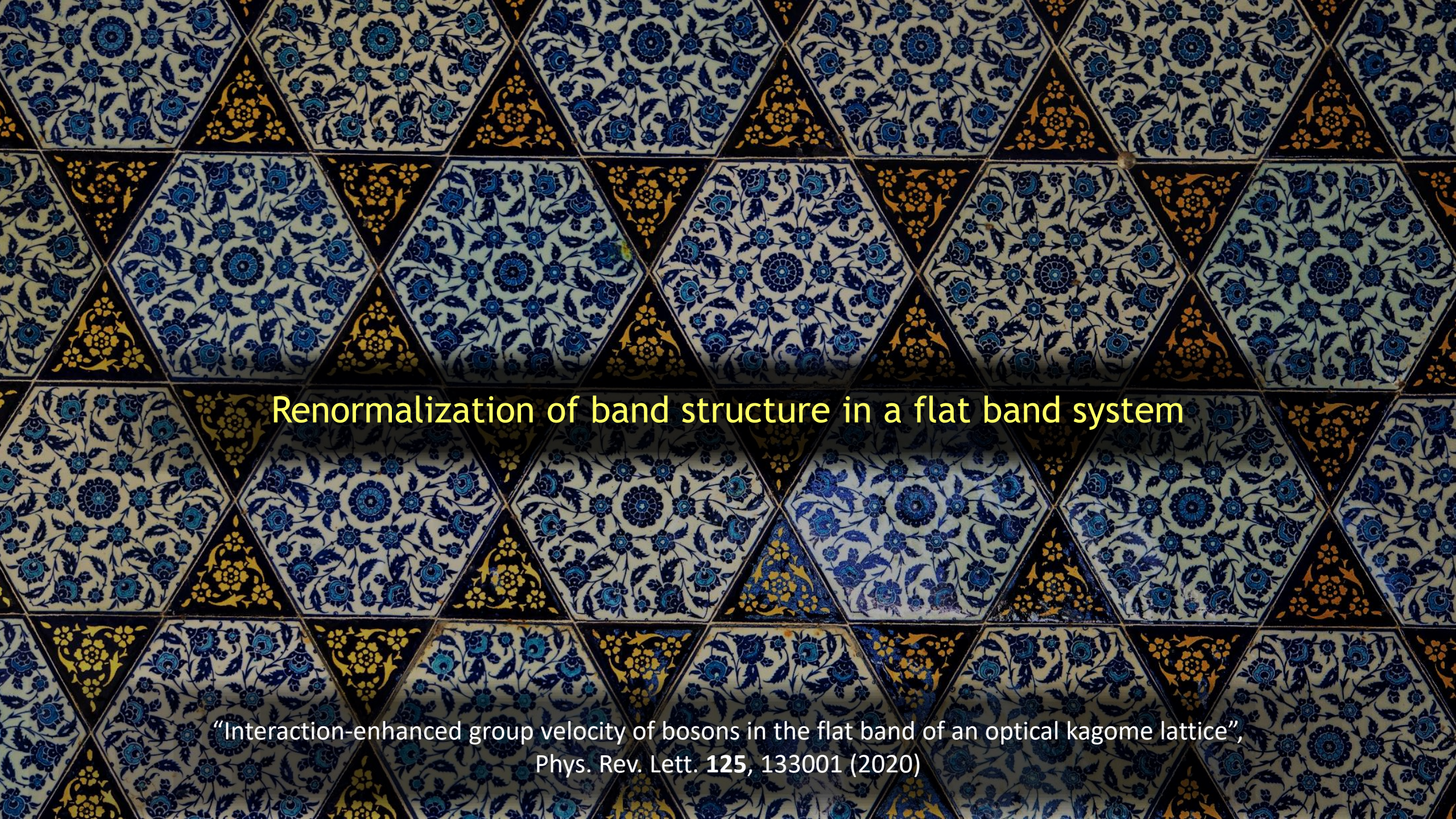
Expected:

$$P_{lower} = \cos^2(\theta)$$
$$P_{upper} = \sin^2(\theta)$$









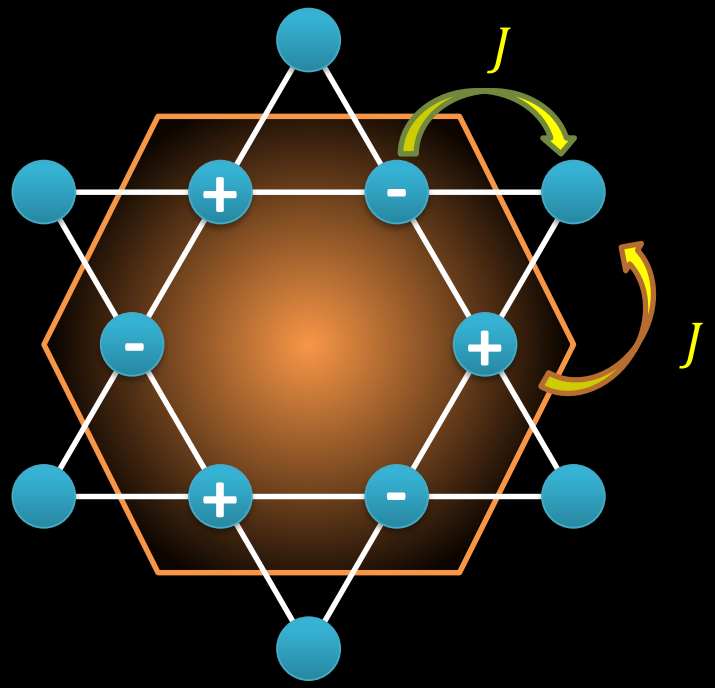
Renormalization of band structure in a flat band system

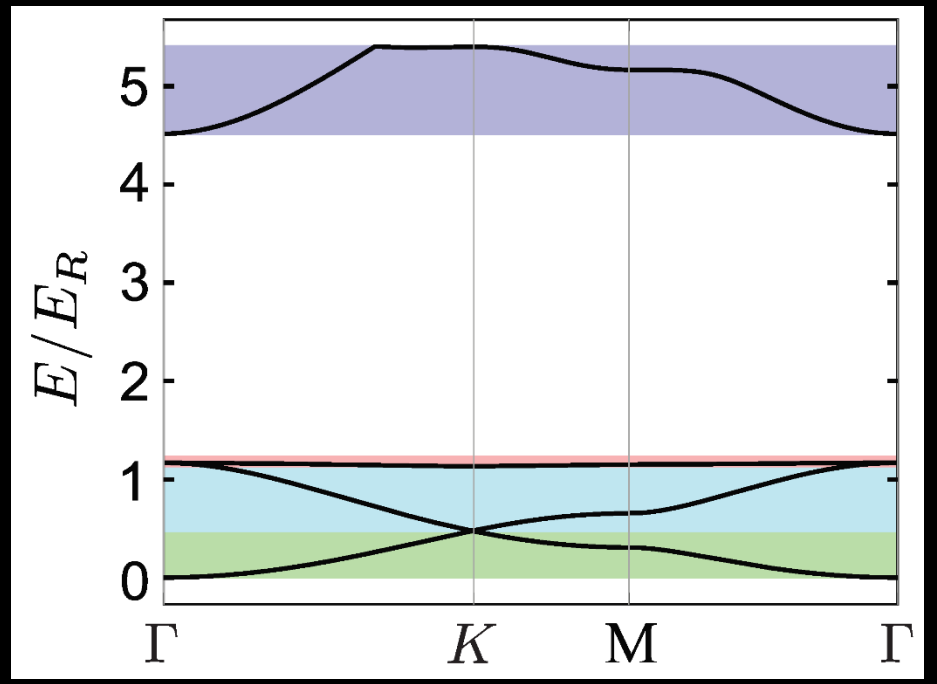
"Interaction-enhanced group velocity of bosons in the flat band of an optical kagome lattice",
Phys. Rev. Lett. **125**, 133001 (2020)

Geometric frustration

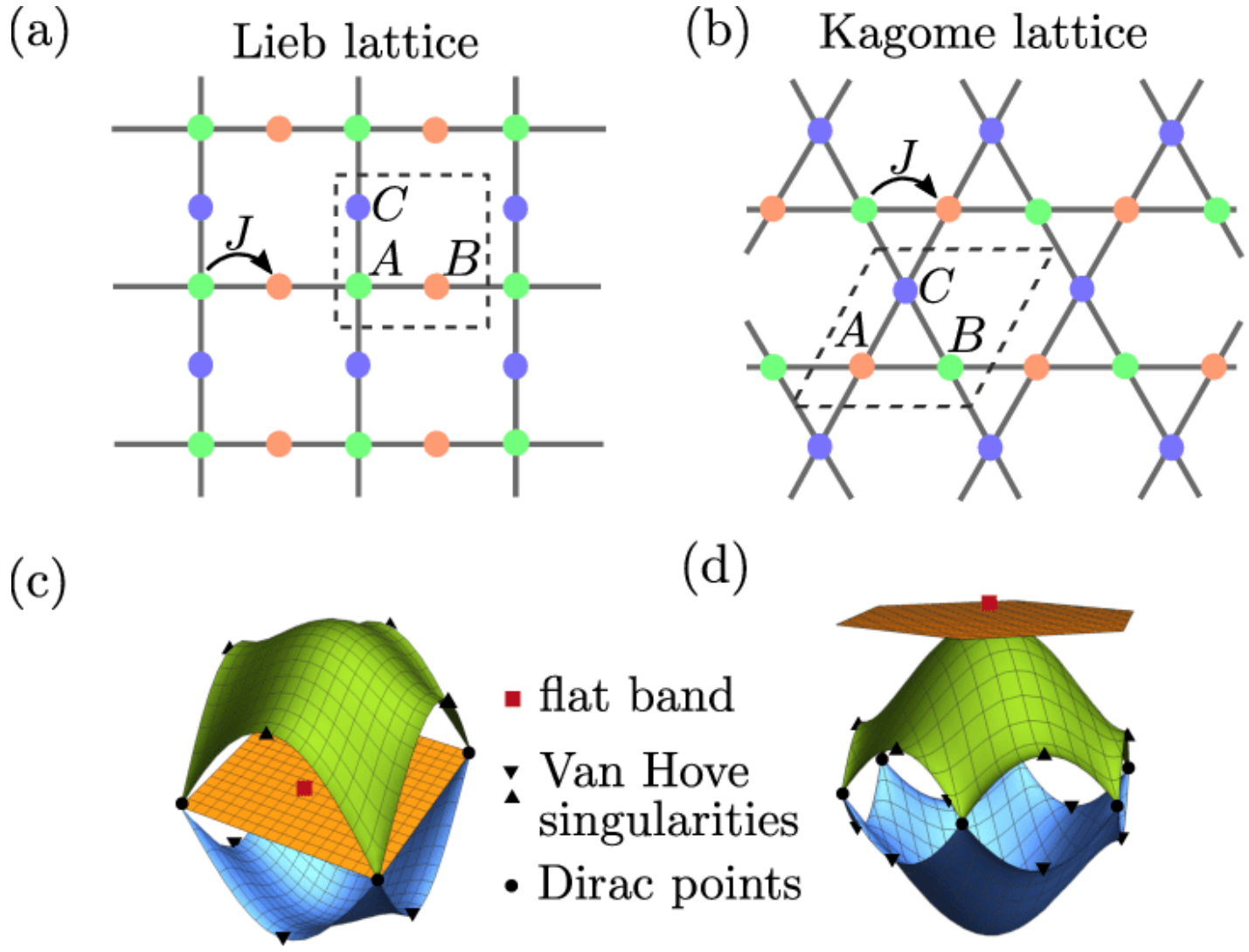
- Route to realizing novel quantum phases of matter
- Focus here on orbital geometric frustration

kagome lattice





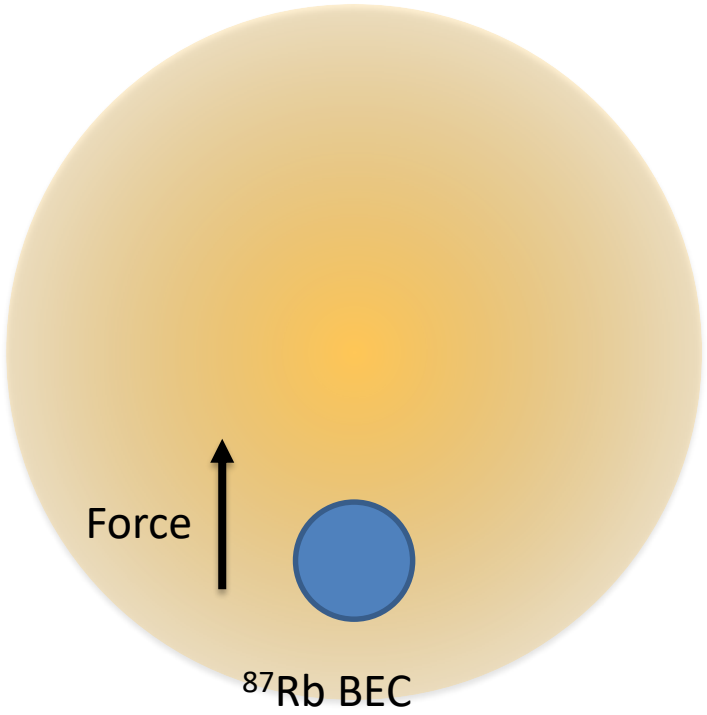
Geometric frustration



Huhtinen… Törmä, et al., Päivi. (2018). “Spin-Imbalanced Pairing and Fermi Surface Deformation in Flat Bands,” PRB **97**, 214503 (2018)

Ozawa, H., et al. "Interaction-Driven Shift and Distortion of a Flat Band in an Optical Lieb Lattice." PRL **118,** 175301 (2017).

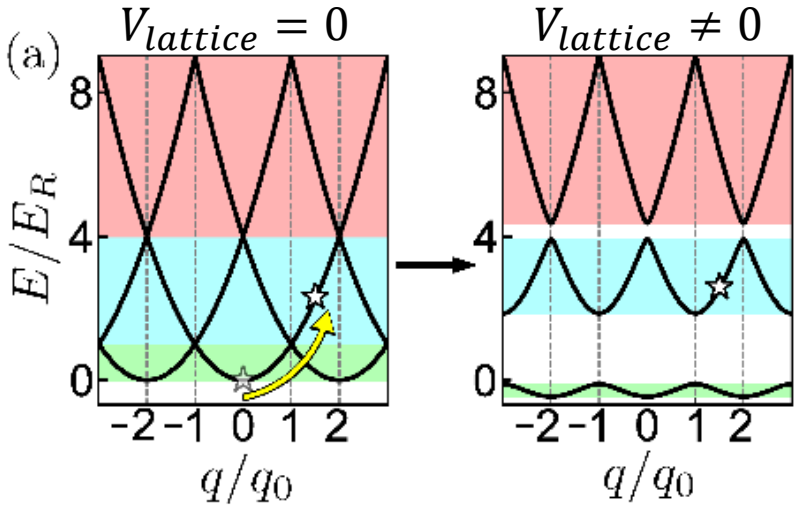
Measuring band structure dispersion



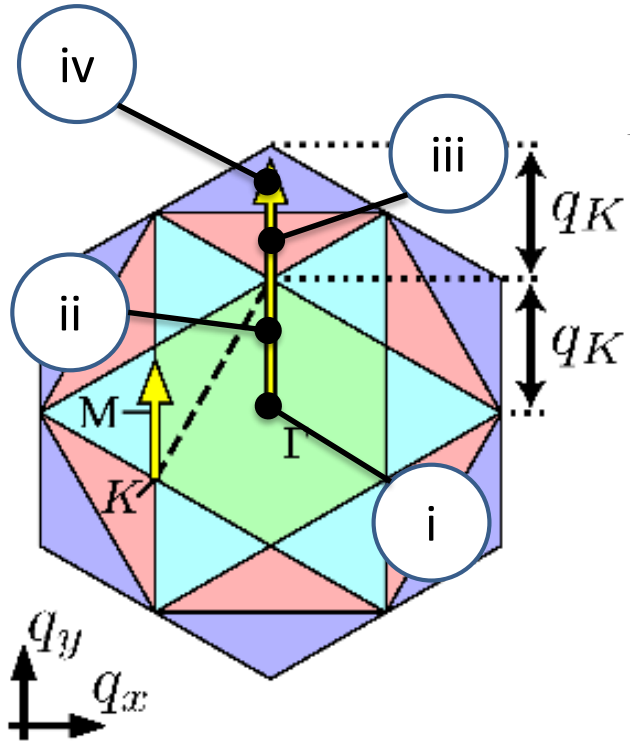
^{87}Rb BEC

N b/w $(0.4 - 22) \times 10^4$

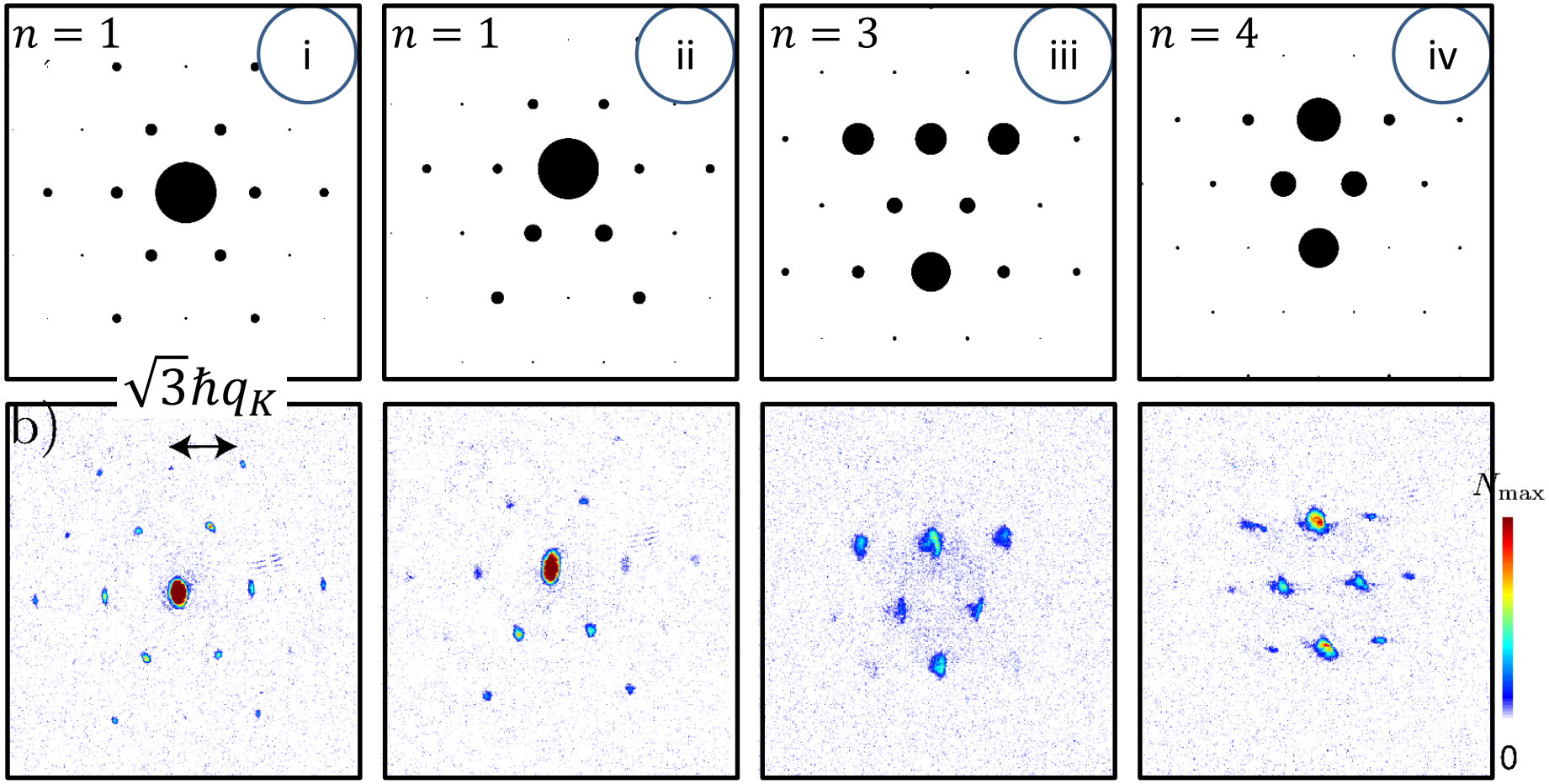
n_0 b/w $(2 - 11) \times 10^{13}$ cm^{-3}



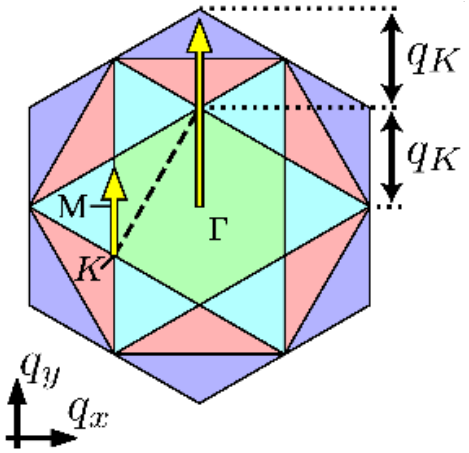
Measuring band structure dispersion

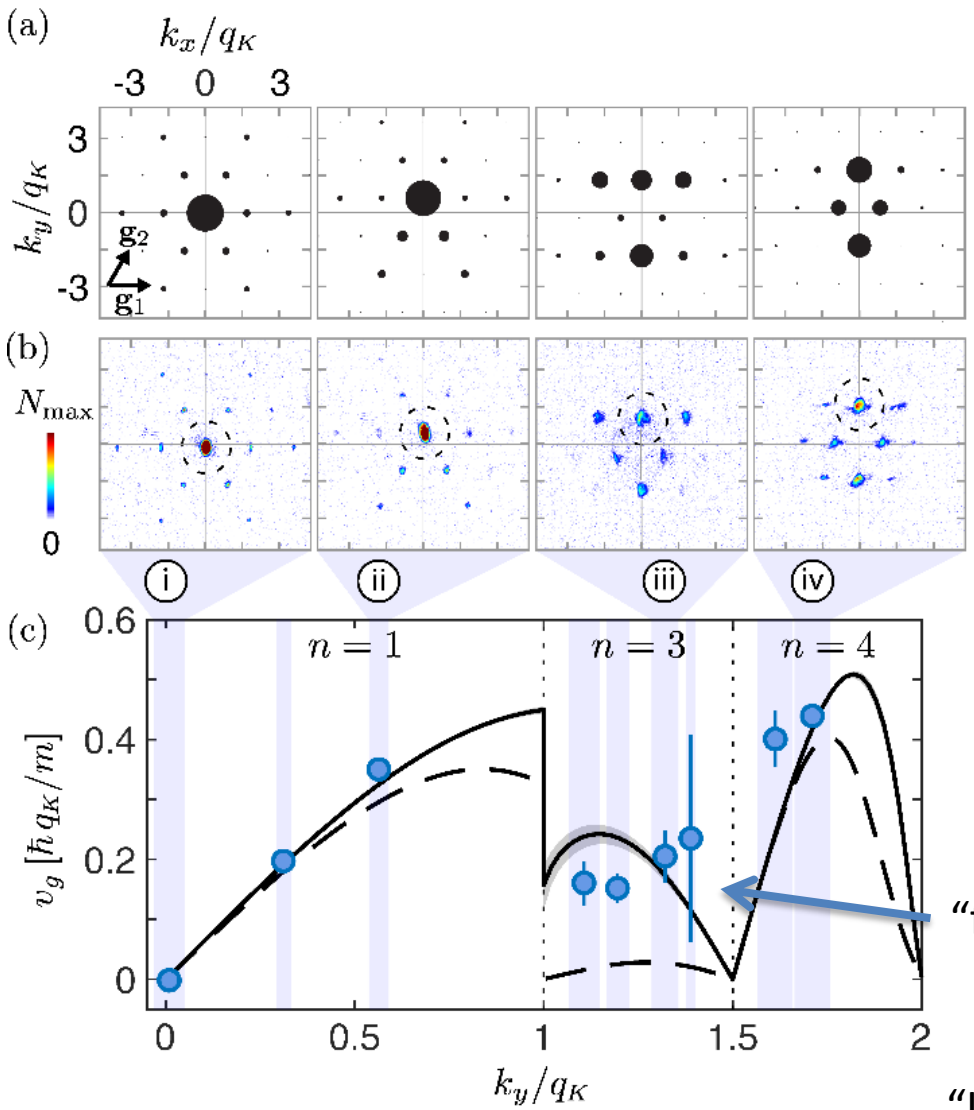


Bloch states in velocity space



Measuring band structure dispersion





Hellmann-Feynman theorem

$$\frac{dE_\lambda}{d\lambda} = \left\langle \psi_\lambda \middle| \frac{dH_\lambda}{d\lambda} \middle| \psi_\lambda \right\rangle$$

$$\boldsymbol{v}_g = \frac{1}{\hbar}\nabla_{\boldsymbol{q}} E_n(\boldsymbol{q}) = \left\langle \psi_\lambda \middle| \frac{\boldsymbol{p}}{m} \middle| \psi_\lambda \right\rangle$$

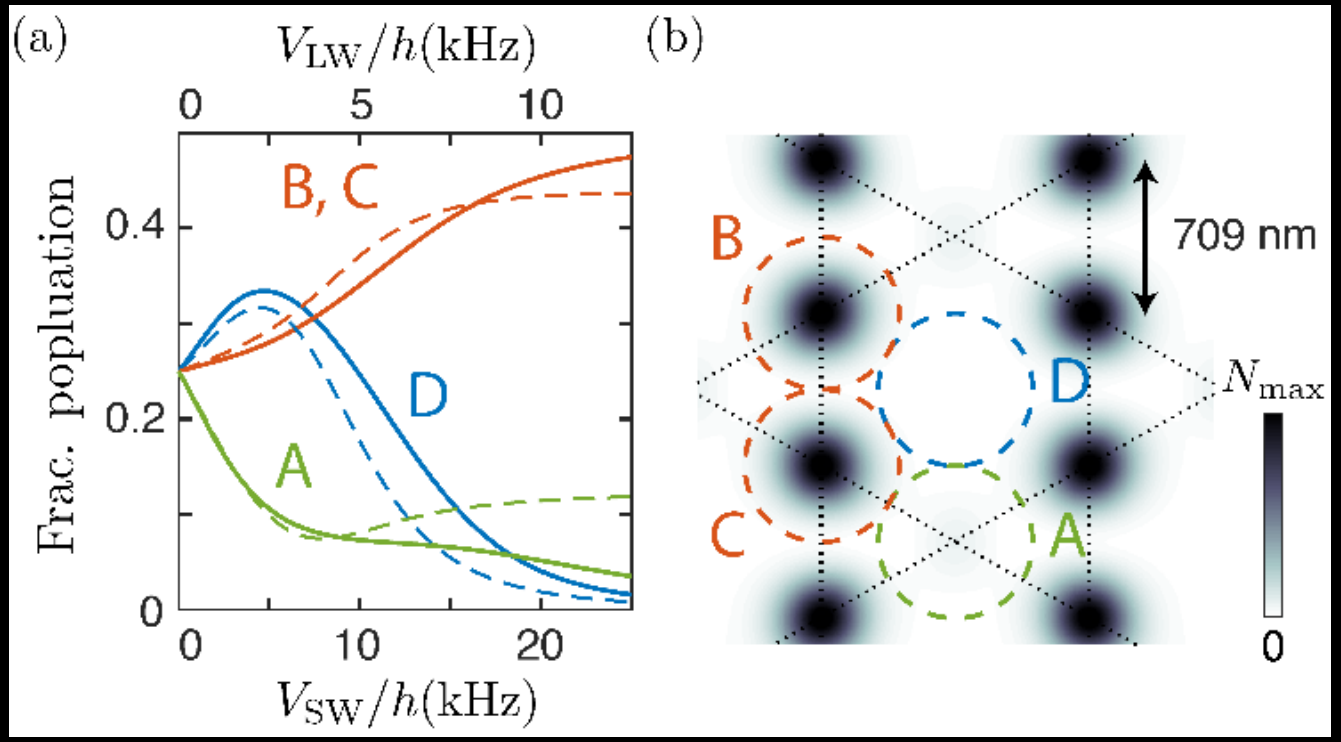
"flat" band of the kagome lattice is not flat!

"Interaction-enhanced group velocity of bosons in the flat band of an optical kagome lattice," Phys. Rev. Lett. **125**, 133001 (2020)

Band structure renormalization

- Interactions among atoms restructure the lattice -> self-consistent band structure
  - Nonlinear Bloch theory… some surprising outcomes:

    “swallowtails,” non-linear Landau-Zener effect, hysteresis, symmetry breaking…

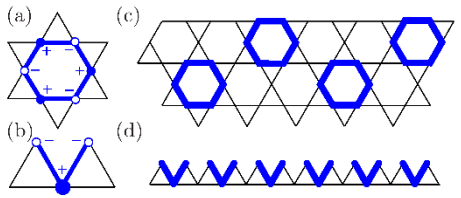


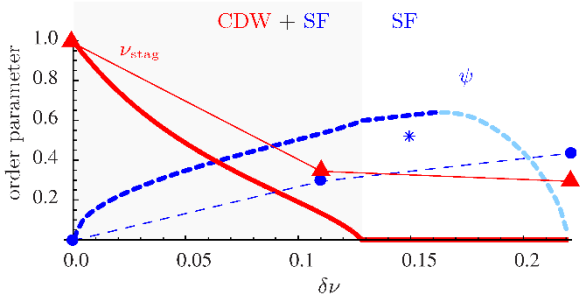
Interacting bosons in a flat band

PHYSICAL REVIEW B **82**, 184502 (2010)

Bose condensation in flat bands

Sebastian D. Huber and Ehud Altman
Department of Condensed Matter Physics, The Weizmann Institute of Science, Rehovot 76100, Isra
(Received 27 July 2010; published 2 November 2010)





PRL **109,** 265302 (2012) PHYSICAL REVIEW LETTERS week ending 28 DECEMBER 2012

Superfluidity of Bosons in Kagome Lattices with Frustration

Yi-Zhuang You, Zhu Chen, Xiao-Qi Sun, and Hui Zhai*
Institute for Advanced Study, Tsinghua University, Beijing 100084, China
(Received 7 August 2012; revised manuscript received 16 October 2012; published 28 December 2012)

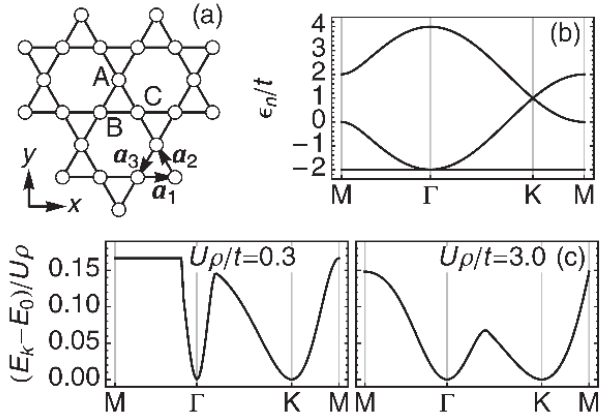


FIG. 1. (a) Kagome lattice, partitioned into A, B, C sublattices. (b) Band structure with inverted hopping sign, where $\Gamma = (0, 0)$, $K = (2\pi/3, 0)$, and $M = (\pi/2, \pi/2\sqrt{3})$. (c) Mean-field energy landscape for different $U\rho/t$. Energy shifted by $E_0 = -2t + U\rho/3$.

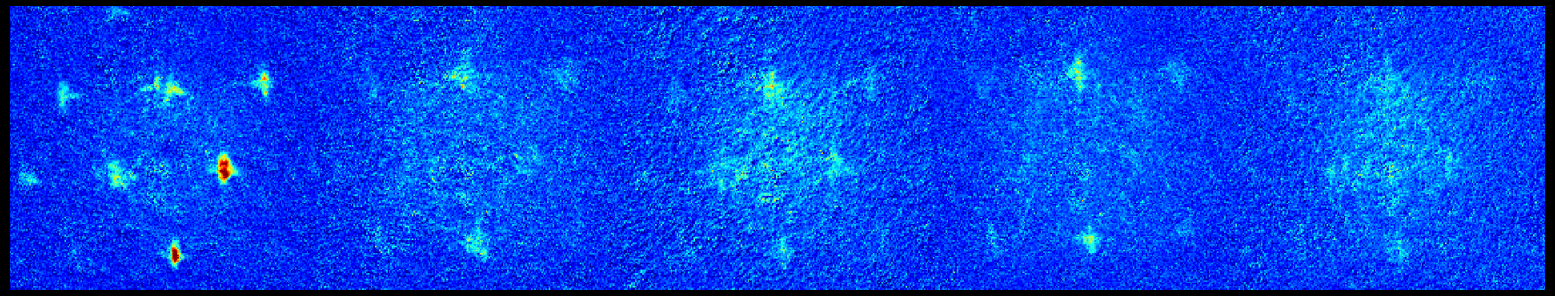
Wigner crystal — lattice supersolid — superfluid

$\nu_{site} = \frac{1}{9}$ $\nu_{site} \sim O\left(\frac{1}{3}\right)$ filling of flat (bottom) band

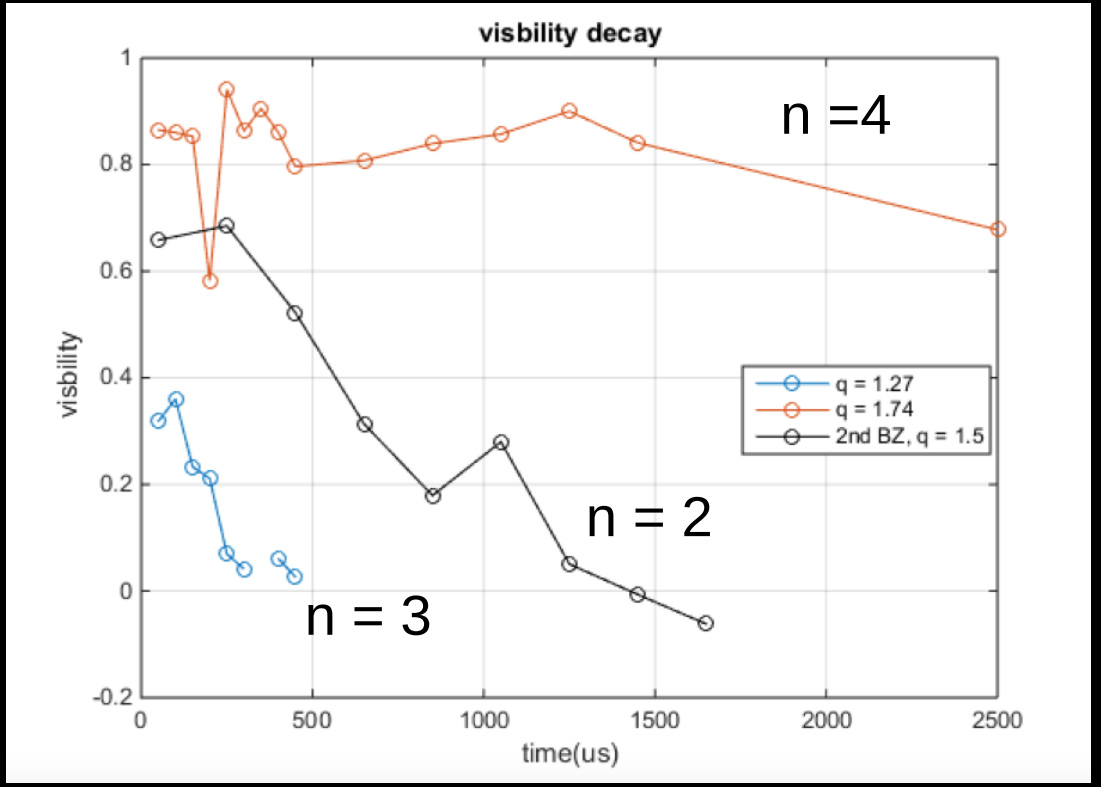
Instability of kagome flat-band population

holdtime (μs) 50 150 250 350 450

3rd band diffraction images

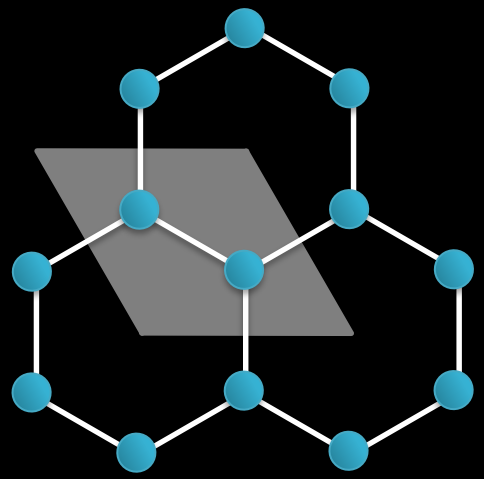


- Atoms are the least stable in the n = 3 band, lifetime ~ 100's μs.

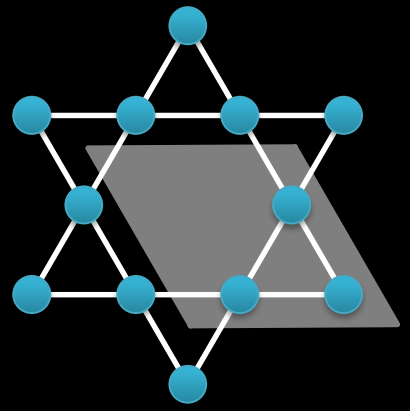


Next steps: fermions in flat bands

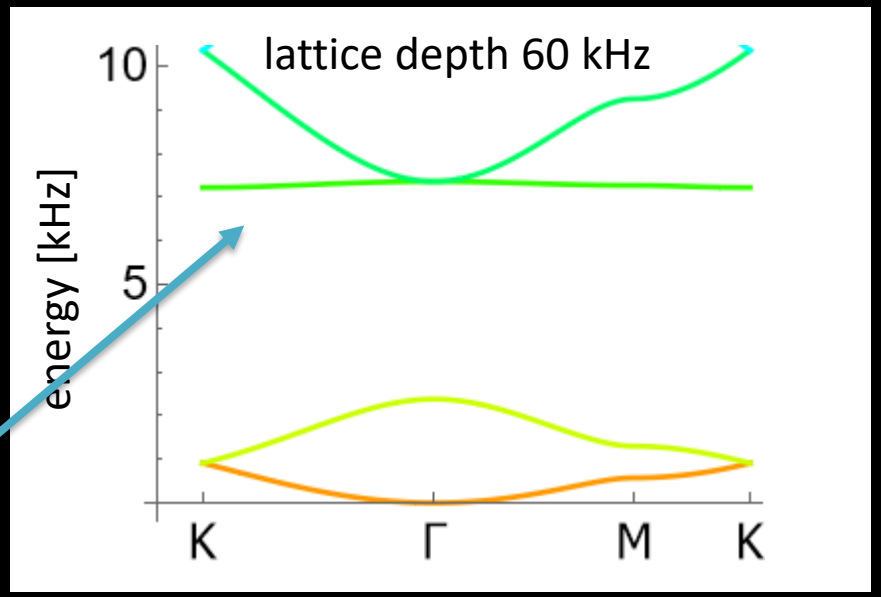
honeycomb lattice

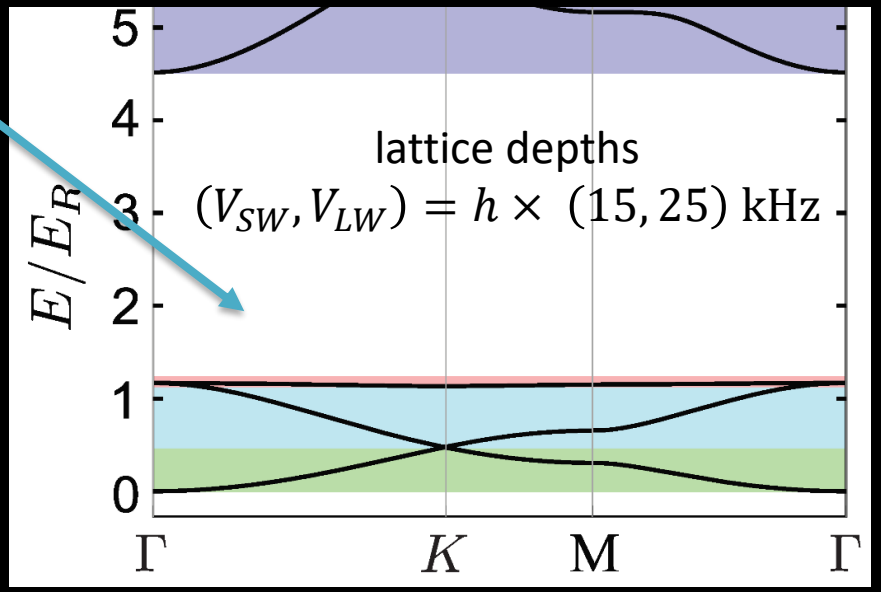


kagome lattice



geometrically frustrated flat bands





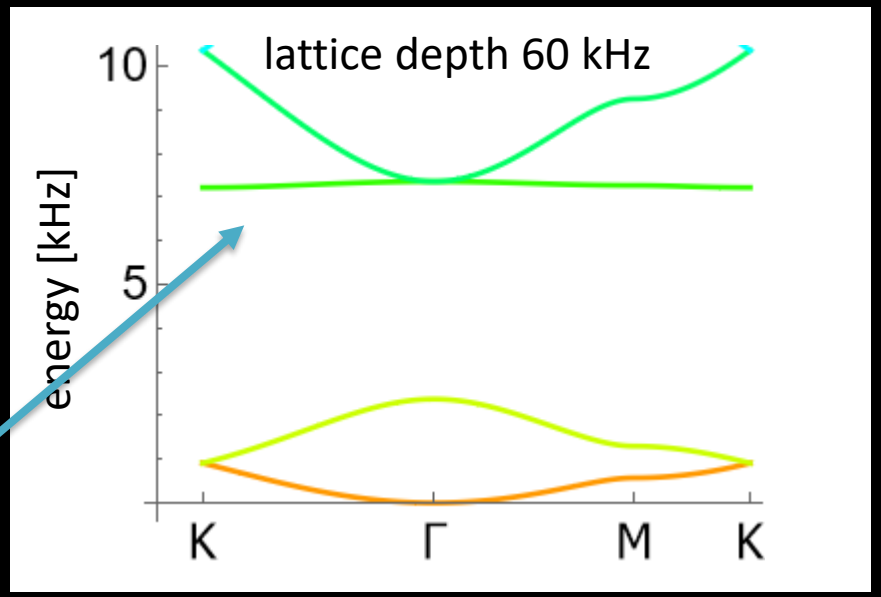
Next steps: fermions in flat bands

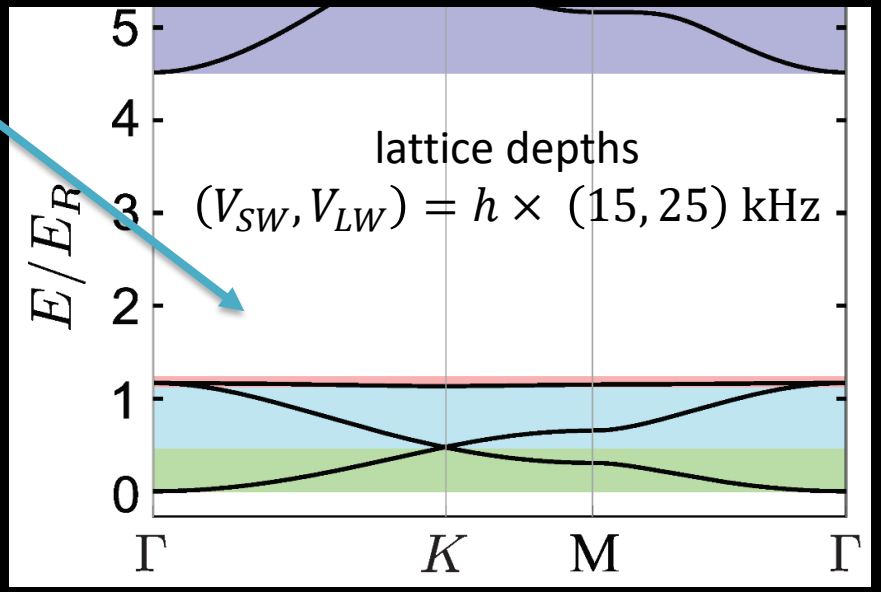
adding ^{40}K atoms (fermions) to our setup

adjust filling to place Fermi energy within flat band

- Weak/non interacting
  - Metal? No Fermi surface
- Repulsive interactions
  - Flat band ferromagnetism
- Attractive interactions
  - “high” temperature superconductor?
  - But… no Fermi surface?

geometrically frustrated flat bands





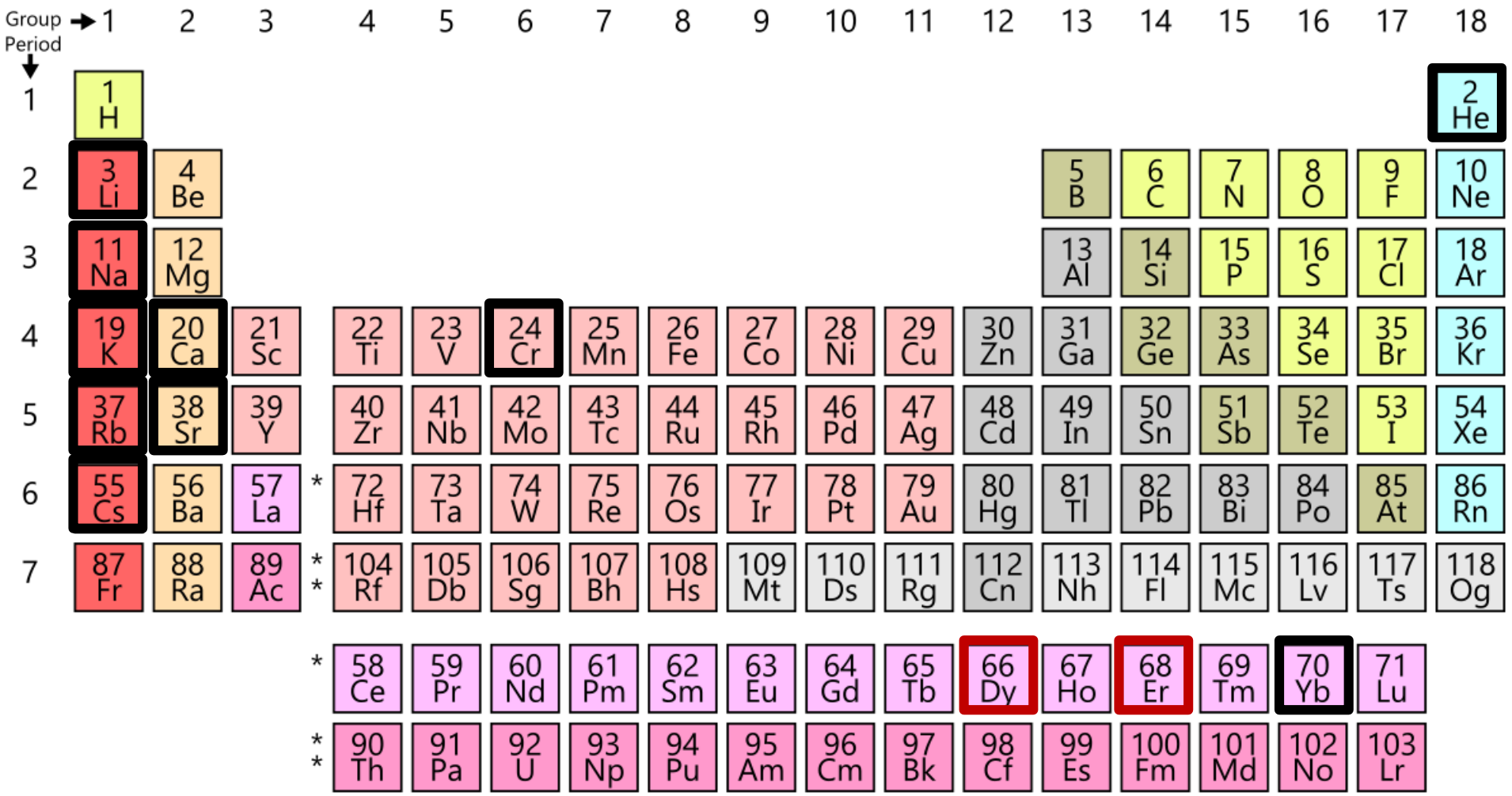
Laser-cooling of transition-metal atoms



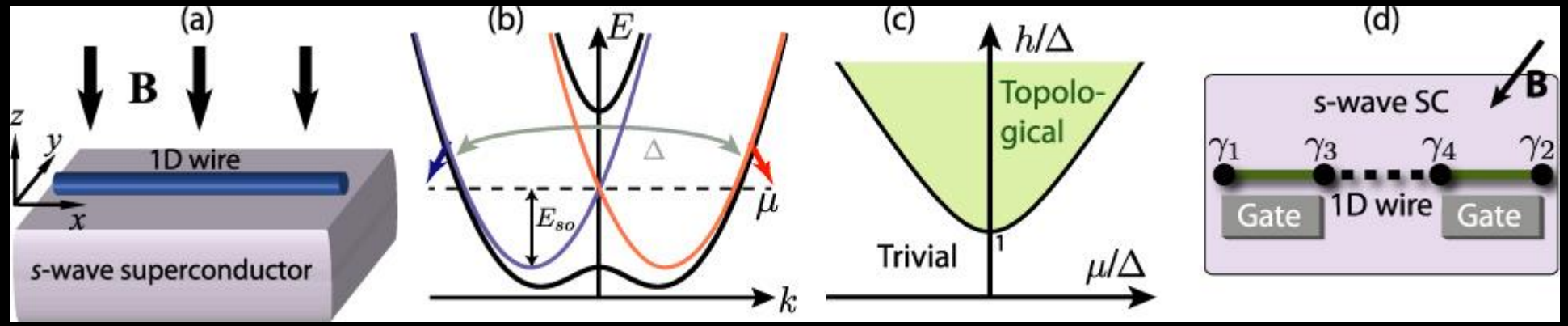
"Laser cooling of transition-metal atoms,"
Phys. Rev. A 102, 053327 (2020)

"Isotope shifts in the metastable a ^5F and excited y $^5G^o$ terms of atomic titanium,"
Phys. Rev. A 103, 032818 (2021)

"Optical telecommunications-band clock based on neutral Ti atoms"
Phys. Rev. A 107, L051102 (2023)


Group
Period
1 2 3 4 5 6 7 8 9 10 11 12 13 14 15 16 17 18
1 H He
2 Li Be B C N O F Ne
3 Na Mg Al Si P S Cl Ar
4 K Ca Sc Ti V Cr Mn Fe Co Ni Cu Zn Ga Ge As Se Br Kr
5 Rb Sr Y Zr Nb Mo Tc Ru Rh Pd Ag Cd In Sn Sb Te I Xe
6 Cs Ba La Hf Ta W Re Os Ir Pt Au Hg Tl Pb Bi Po At Rn
7 Fr Ra Ac Rf Db Sg Bh Hs Mt Ds Rg Cn Nh Fl Mc Lv Ts Og
Ce Pr Nd Pm Sm Eu Gd Tb Dy Ho Er Tm Yb Lu
Th Pa U Np Pu Am Cm Bk Cf Es Fm Md No Lr

Topological superconductors through spin-orbit coupling

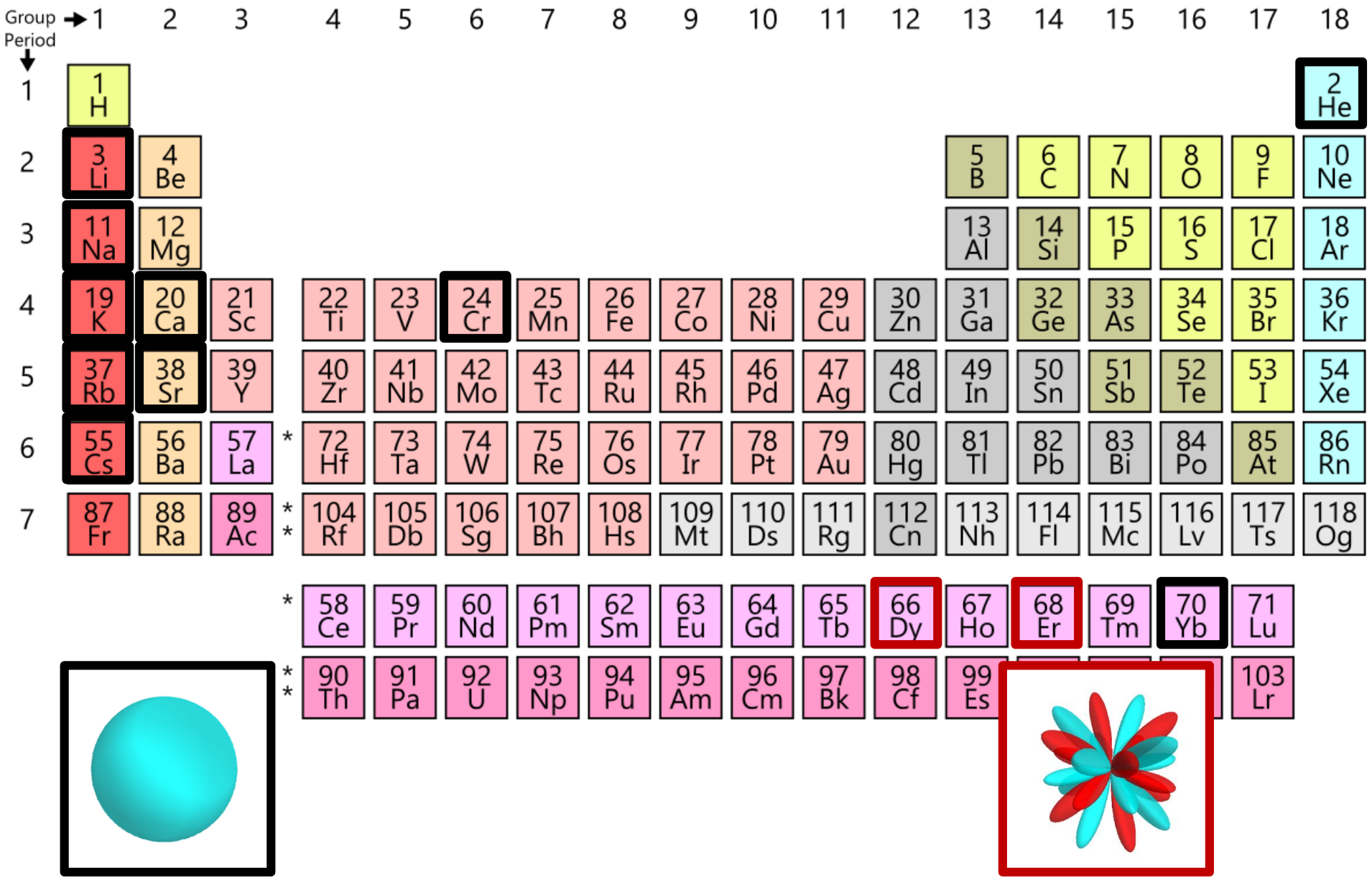


also works in 2D Rashba -> p+ip

figure from Alicea, Rep. Prog. Phys. **75**, 076501 (2012)
Lutchyn, Sau, Das Sarma, PRL **105**, 077001 (2010)
Oreg, Refael, von Oppen, PRL **105**, 177002 (2010)

Necessary ingredients

- fermions
- interactions (s-wave will do)
- spin-orbit coupling
- stable mixtures of 2 or more spin states



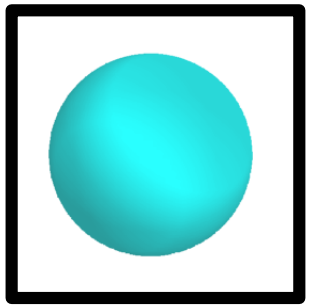
spherical atoms, $L = 0$
(too simple)
isotropic light-atom interaction*

lanthanide atoms, $L \sim 6$ (big)
(too complex)
too magnetic: spin mixtures unstable

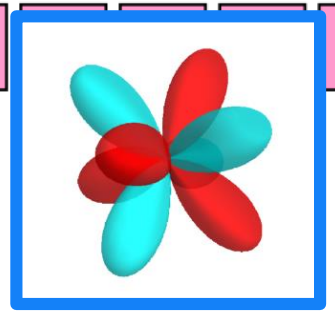
identify a new family of transition-metal elements to be cooled to quantum degeneracy

search for new elements
- bosons and fermions
- can be laser cooled
- $L \neq 0$
- not very magnetic

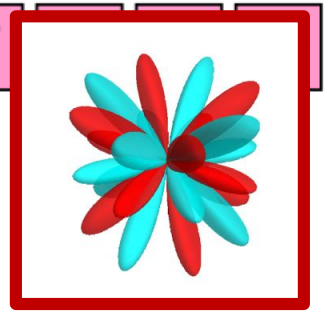
Phys. Rev. A **102**, 053327 (2020)
Phys. Rev. A **103**, 032818 (2021)



spherical atoms, $L = 0$
(too simple)
isotropic light-atom interaction*

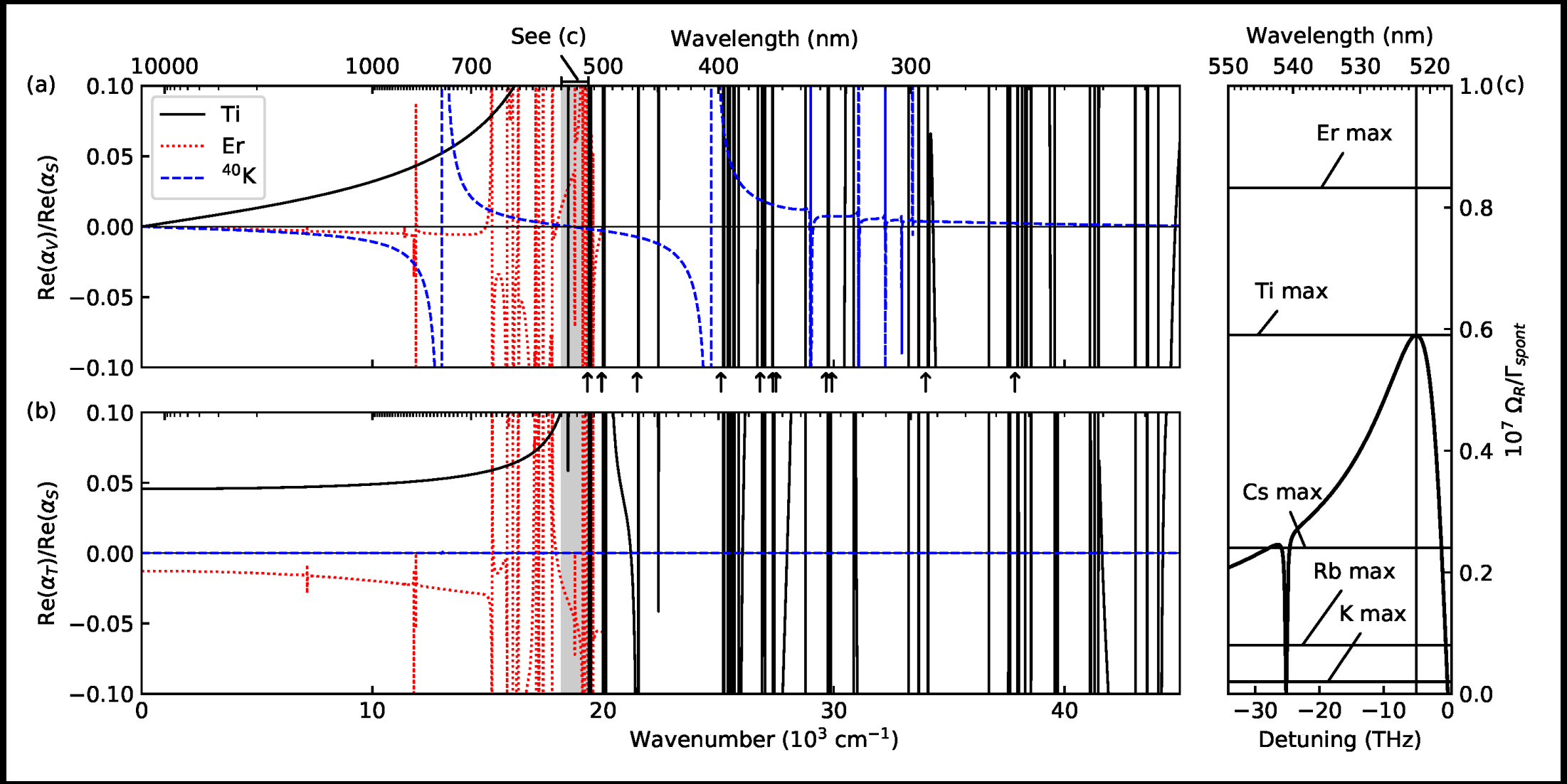


intermediate atoms, $L = 2,3$
(just right)



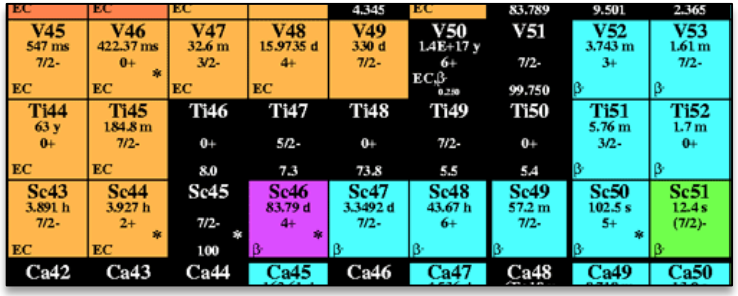
lanthanide atoms, $L \sim 6$ (big)
(too complex)
too magnetic: spin mixtures unstable

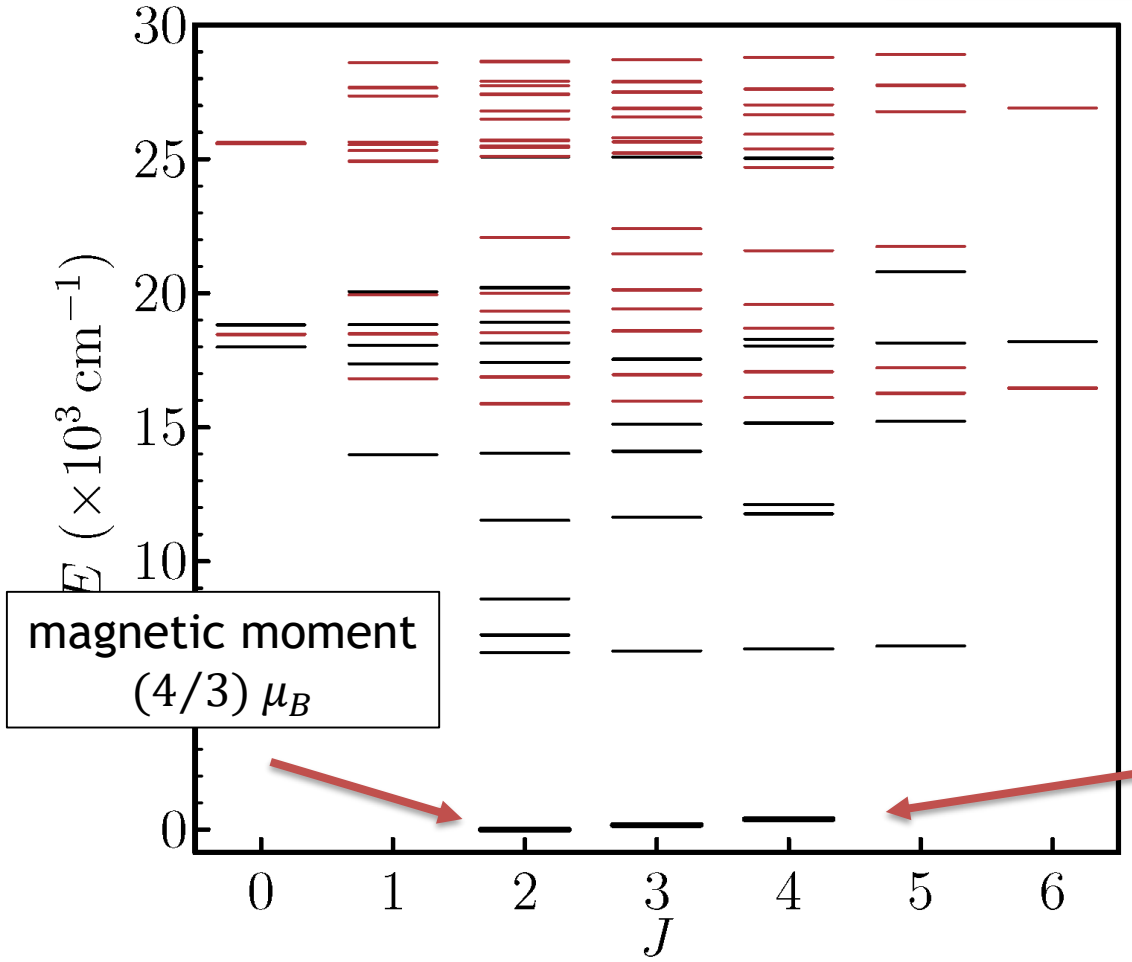
Titanium vs. the alkalis: vector and tensor Stark shift



"Laser cooling of transition-metal atoms," PRA **102**, 053327 (2020)

Scheme for laser cooling titanium

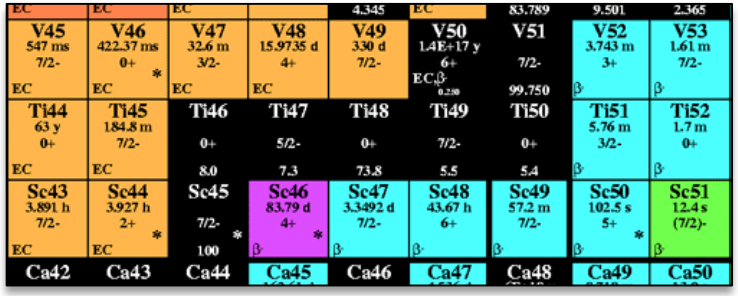


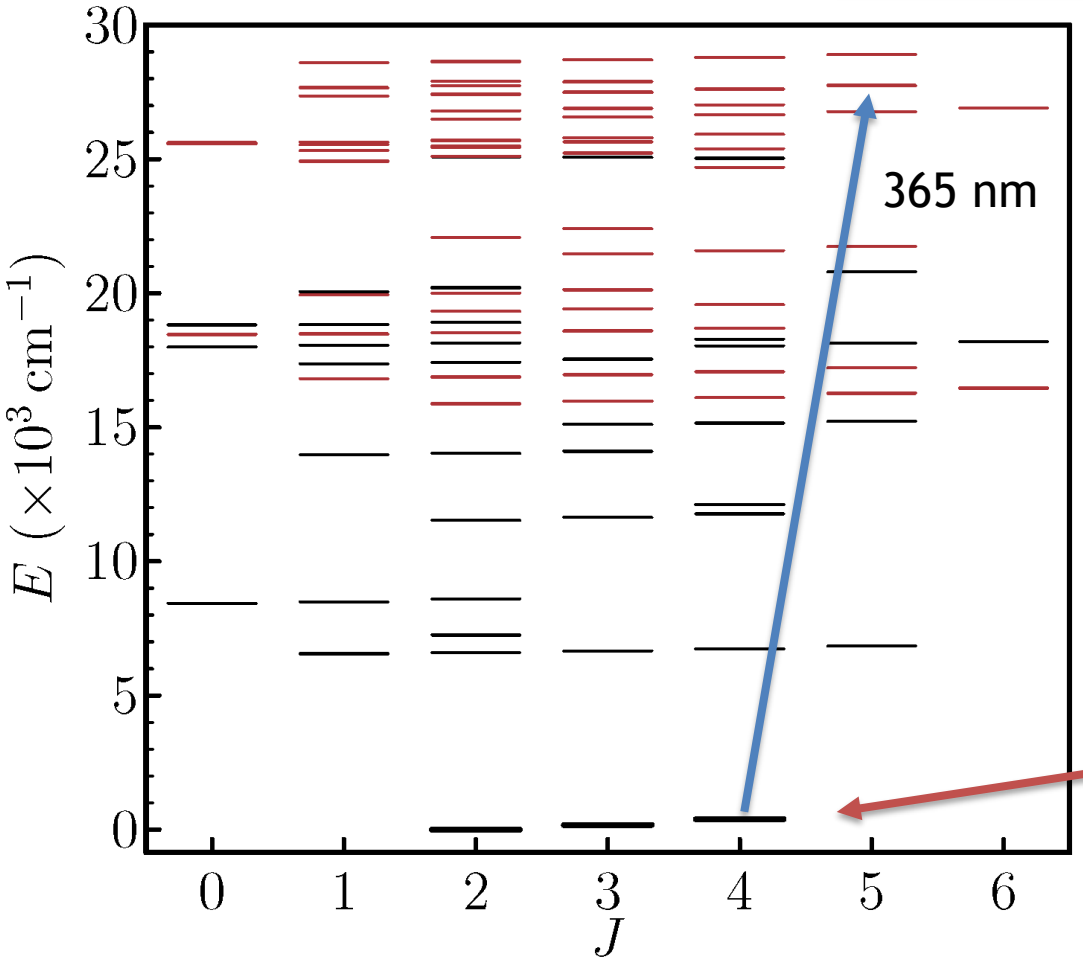


magnetic moment
$(4/3)\ \mu_B$

ground
$3\mathrm{d}^2\ (^3F)4s^2$: $a\ ^3F_J$
(Ca-like)

Scheme for laser cooling titanium





laser cool like Ca?

$3d^2(\ ^3F)4s\ 4p\ (\ ^1P)\colon y\ ^3G_5$

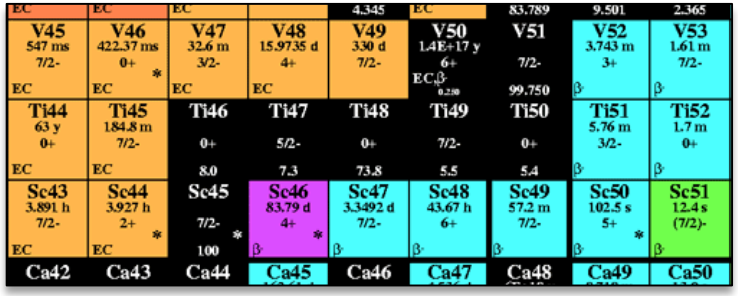
leakage ~ 10^{-1}

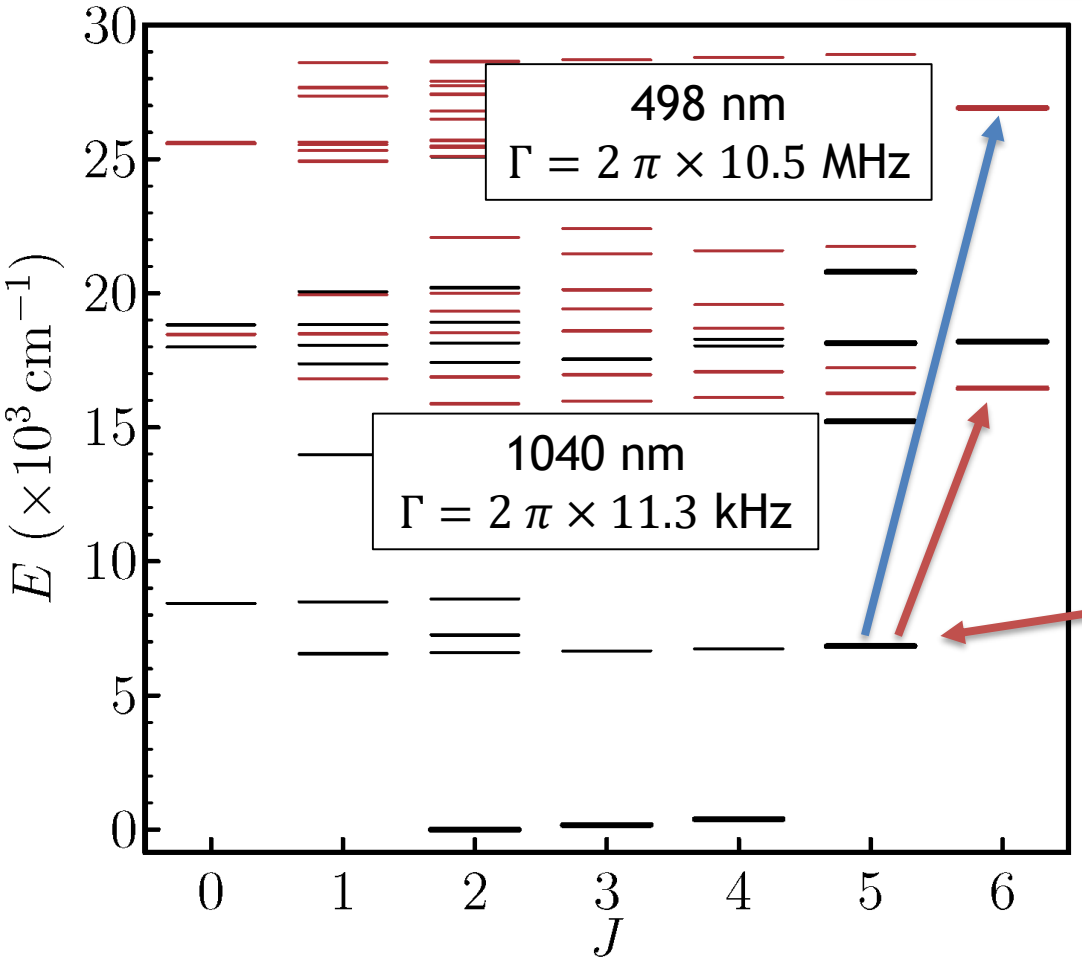
ground

$3\mathrm{d}^2\ (\ ^3F)4s^2\colon a\ \ ^3F_J$

(Ca-like)

Scheme for laser cooling titanium





$3d^3(\,^4F)4p{:}\,y\;^5G_6$

$3d^2(\,^3F)4s\;4p\;(\,^3P){:}\,z\;^5G_6$

metastable
$3d^3(\,^4F)4s{:}\,a\;^5F_5$
(K-like)

Ballpark estimate: leakage ~ 10^{-5}
Safronova: leakage ~ 10^{-7}

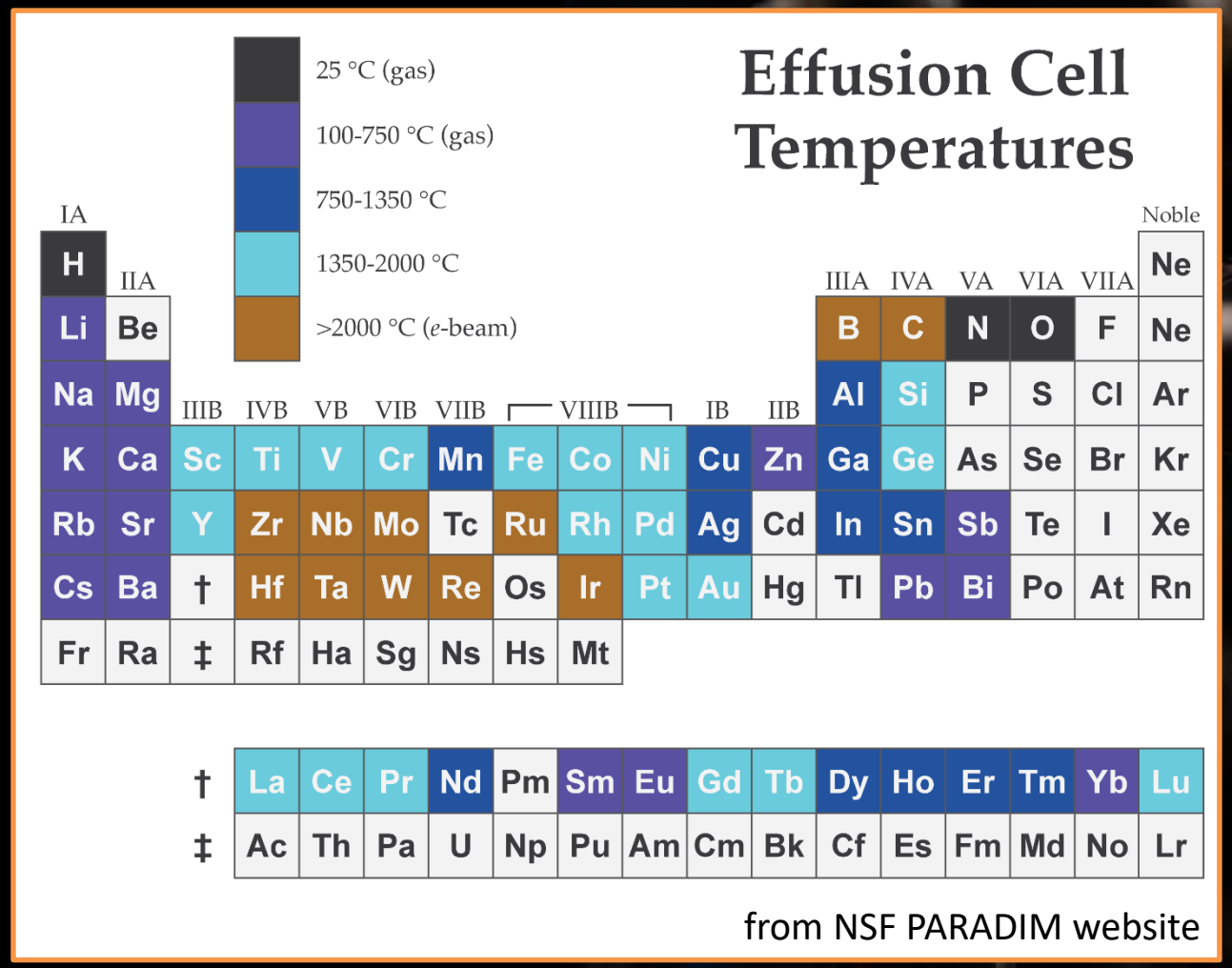
Transition-metal laser-cooling cornucopia

Atom	Ground state		Metastable state				Excited state				
	config.	term	config.	term	energy (cm^{-1})	decay rate (mHz)	config.	term	energy (cm^{-1})	Cooling trans. (nm)	Linewidth ($MHz/2\pi$)
Sc[21–23]	$3d4s^2$	$a^2D_{3/2}$	$3d^2(^3F)4s$	$a^4F_{9/2}$	11677.3121	—	$3d^2(^3F)4p$	$z^4G^\circ_{11/2}$	45761.10(.05)	567.3402(15)	8.6
Y[24–26]	$4d5s^2$	$a^2D_{3/2}$	$4d^2(^3F)5s$	$a^4F_{9/2}$	11532.096	—	$4d^2(^3F)5p$	$z^4G^\circ_{11/2}$	29820.374(13)	546.7986(4)	10.
La[25, 27, 28]	$5d6s^2$	$^2D_{3/2}$	$5d^2(^3F)6s$	$^4F_{9/2}$	4121.572	—	$5d^2(^3F)6p$	$^4G^\circ_{11/2}$	20117.38	625.166	5.86
							$4f5d(^3G^\circ)6s$	$^4G^\circ_{11/2}$	24841.42	406.148	8.9
Ac[29]	$6d7s^2$	$a^2D_{3/2}$	$6d^2(^3F)7s$	$a^4F_{9/2}$	12078.07	—	$6d^2(^3F)7p$	$z^4G^\circ_{11/2}$	33429.76	468.34[c]	—
Ti[30–33]	$3d^24s^2$	a^3F_4	$3d^3(^4F)4s$	a^5F_5	6842.962	—	$3d^3(^4F)4p$	$y^5G^\circ_6$	26910.709(5)	498.3121(3)	10.5
							$3d^24s4p$ [a]	$z^5G^\circ_6$	16458.671(4)	1039.9660(13)	0.0113
Zr[25, 34]	$4d^25s^2$	a^3F_4	$4d^3(^4F)5s$	a^5F_5	5888.93	—	$4d^3(^4F)5p$	$y^5G^\circ_6$	16978.29	468.780[b]	—
							$4d^25s5p$[a]	$z^5G^\circ_6$	27214.89	901.77[b]	—
V[35–40]	$3d^34s^2$	$a^4F_{3/2}$	$3d^4(^5D)4s$	$a^6D_{9/2}$	2424.809(2)	0.017	$3d^4(^5D)4p$	$y^6F^\circ_{11/2}$	25253.457(2)	438.04603(18)	18.3
							$3d^34s4p$[a]	$z^6F^\circ_{11/2}$	18680.070(3)	615.1955(2)	—
			$3d^4(^3H)4s$	$a^4H_{13/2}$	15062.959	—	$3d^4(^3H)4p$	$z^4I^\circ_{15/2}$	37518.445(4)	445.32548(12)	13.
Nb[25, 34, 41]	$4d^4(^5D)5s$	$a^6D_{1/2}$	—	$a^6D_{9/2}$	1050.26	—	$4d^4(^3H)5p$	$y^6F^\circ_{11/2}$	25680.36	405.894[b]	—
							$4d^35s(^5F)5p$	$z^6F^\circ_{11/2}$	20939.92(2)	502.6335(5)[b]	—
			$4d^4(^3H)5s$	$a^4H_{13/2}$	11524.65	—	$4d^4(^3H)5p$	$z^4I^\circ_{15/2}$	33116.36	463.1407	—
Mn[21, 25, 42, 43]	$3d^54s^2$	$a^6S_{5/2}$	—	—	0	0	$3d^5(^6S)4s4p(^3P^\circ)$	$z^6P^\circ_{7/2}$	24802.25	403.076	2.71
								$z^6P^\circ_{5/2}$	24788.05	403.307	2.63
								$z^6P^\circ_{5/2}$	24779.32	403.449	2.51
			$3d^6(^5D)4s$	$a^6D_{9/2}$	17052.29	290	$3d^6(^5D)4p$	$z^6F^\circ_{11/2}$	43314.23	380.780	9.4
			$3d^6(^3H)4s$	$a^4H_{13/2}$	34138.88	—	$3d^6(^3H)4p$	$z^4I^\circ_{15/2}$	58852.60	404.634[c]	—
Tc[44–46]	$4d^55s^2$	$a^6S_{5/2}$	$4d^6(^5D)5s$	$a^6D_{9/2}$	2572.89	—	$4d^6(^5D)5p$	$z^6F^\circ_{11/2}$	30067.29	363.7106	25.0
			$4d^6(^3H)5s$	$^4H_{13/2}$	16553.39	—	$4d^6(^3H)5p$	$^4I^\circ_{15/2}$	42996.15	378.0680	—
Fe[47–49]	$3d^64s^2$	a^5D_4	$3d^7(^4F)4s$	a^5F_5	6928.268	2.0	$3d^7(^4F)4p$	$z^5G^\circ_6$	26874.550(1)	358.22150(4)	16.2
Ru[25, 29, 50]	$4d^7(^4F)5s$	a^5F_5	—	—	0	0	$4d^7(^4F)5p$	$z^5G^\circ_6$	26816.23	349.994	13.7

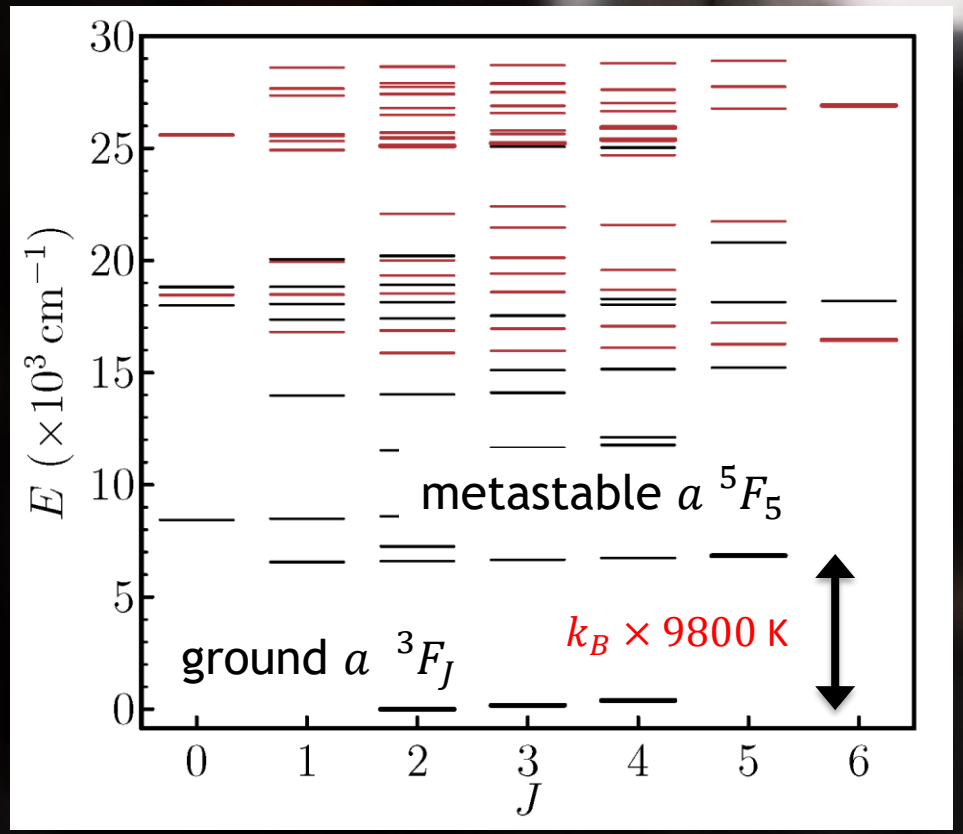
Titanium vs. the alkalis: atomic beams

vapor pressure ~ 10^{-3} mbar
Rb: 400 K
Ti: 1840 K

- How to produce a metastable-state atomic beam?

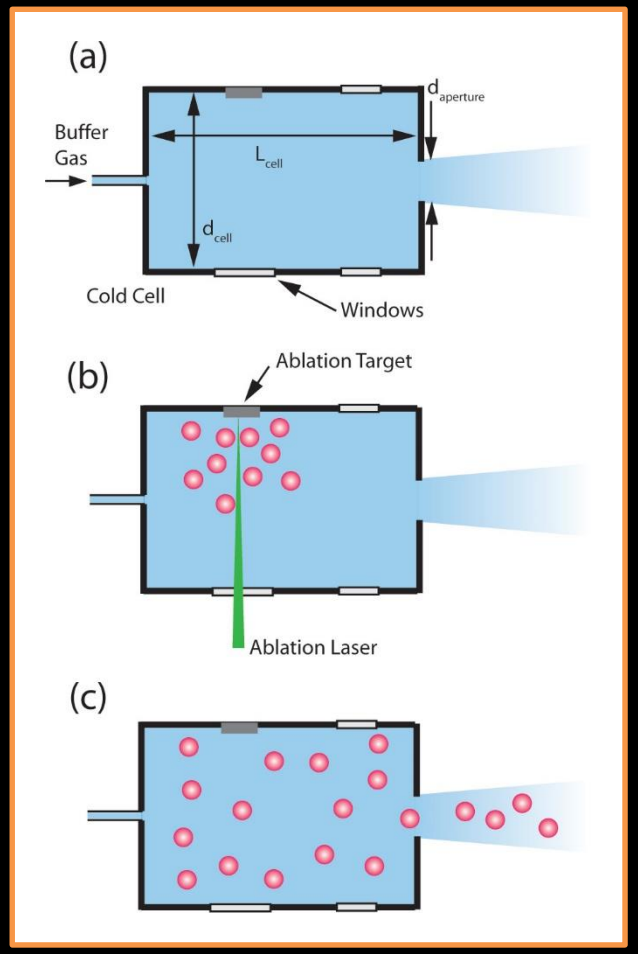


from NSF PARADIM website



Buffer gas beam source

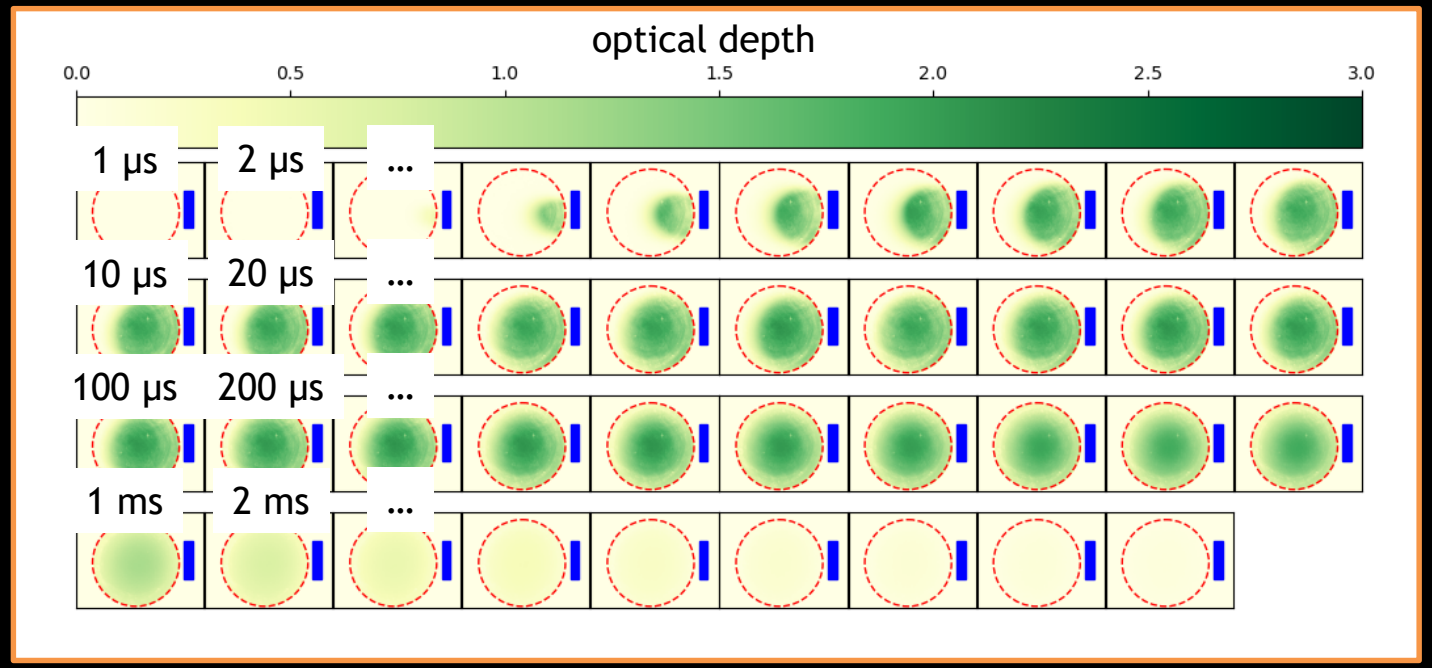
(Cryogenic) buffer gas beam



Hutzler, Lu, Doyle, Chemical Reviews 112, 4803 (2012)

previous: Ti into cryogenic He and Ne
Lu, Hardman, Weinstein, Zygelman, PRA **77**, 06701 (2008)

Many thanks to Jonathan Weinstein (UNR) for getting us started!



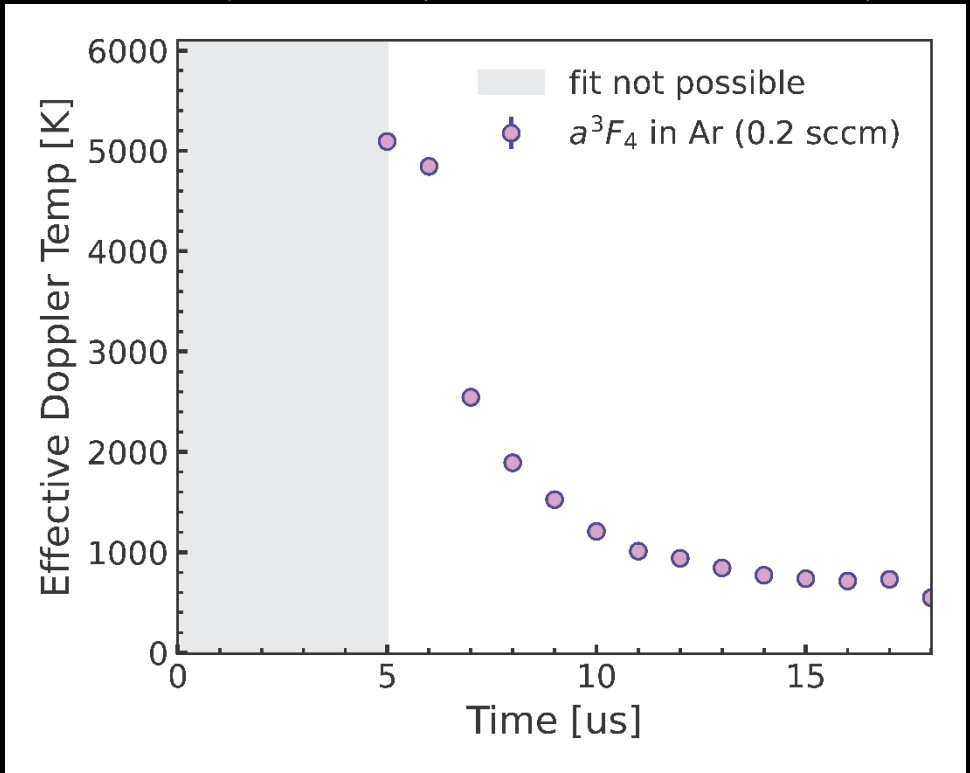
time-resolving expansion and kinetic thermalization of
$a\ ^3F_4$ Ti into room temperature Ar buffer gas

Cold beam of metastable atoms by ablation into buffer gas

very hot plasma ~ 20000 K!

hot neutral ~ 4000 K

cold neutral ~ 300 K

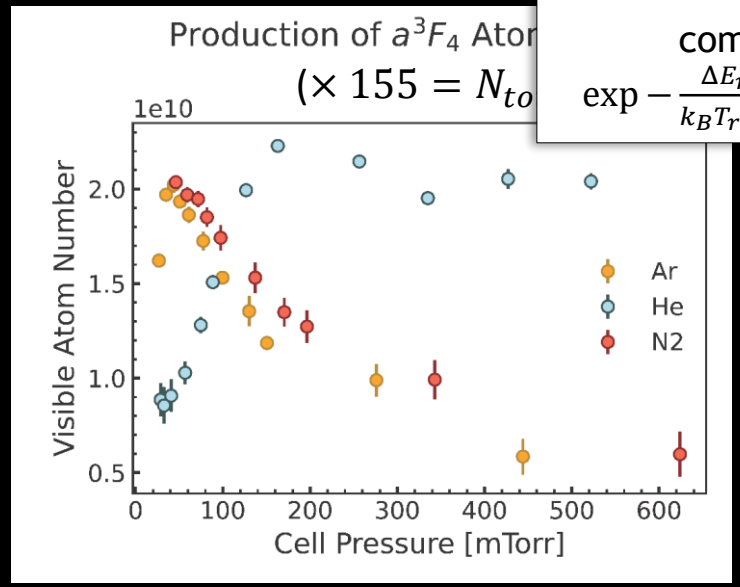


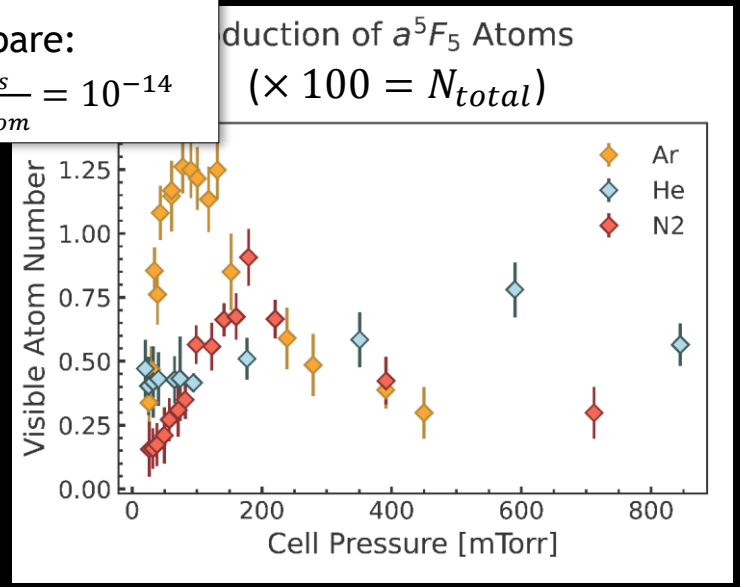
- Is high population of metastable atoms preserved in buffer gas collisions?
  - Fine-structure relaxation slow in cold He-Ti collisions [PRA 77, 06701 (2008)]

about 10% of ground state population!

compare:

$$\exp -\frac{\Delta E_{ms}}{k_B T_{room}} = 10^{-14}$$





we also see metastable atoms emerge as beam from cell

Atomic physics with a titanium-sublimation vacuum pump

is it really this simple?



Agilent Varian Replacement Mini Ti-Ball Source

Condition: New
Part Number: P108787
Warranty: Varian Warranty

Available Now: 1

Sale: $1,227.33

1 Add To Cart

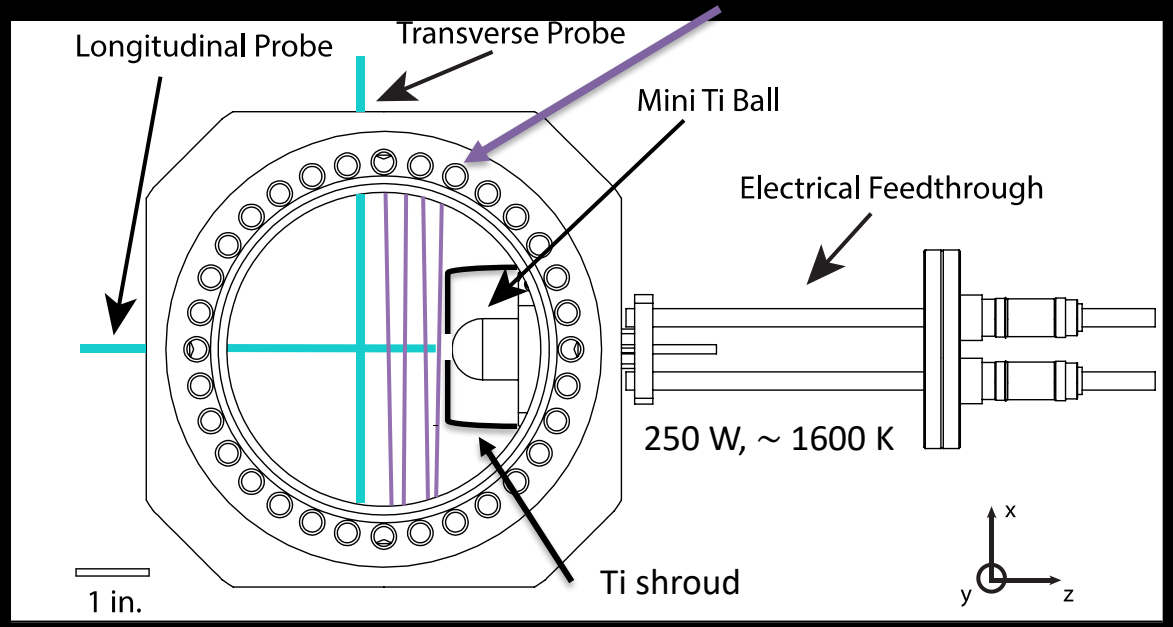
atom beam probes

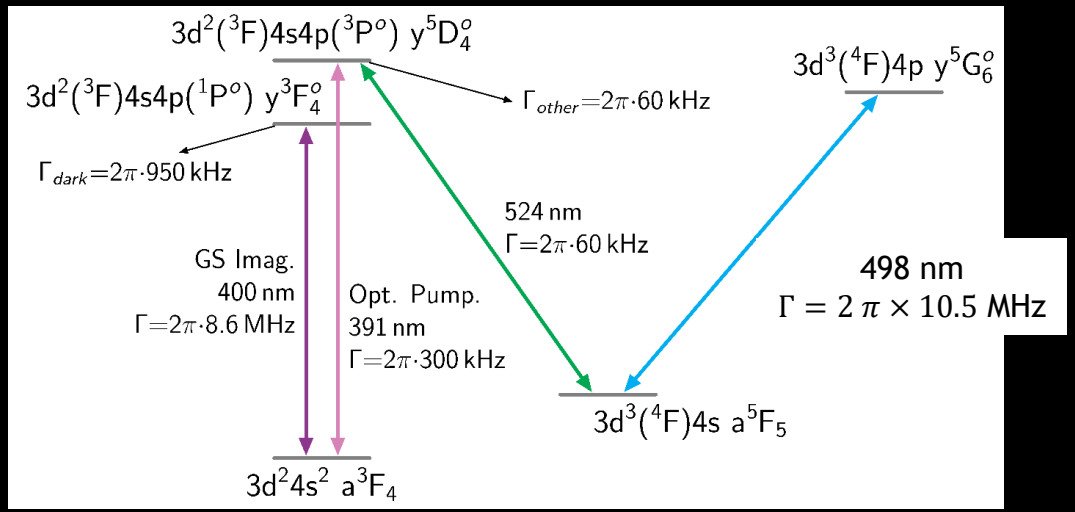
ground: $a\ {}^3F_4 \rightarrow y\ {}^3F_4$ (400 nm)

metastable: $a\ {}^5F_5 \rightarrow y\ {}^5G_6$ (498 nm)

optical pumping

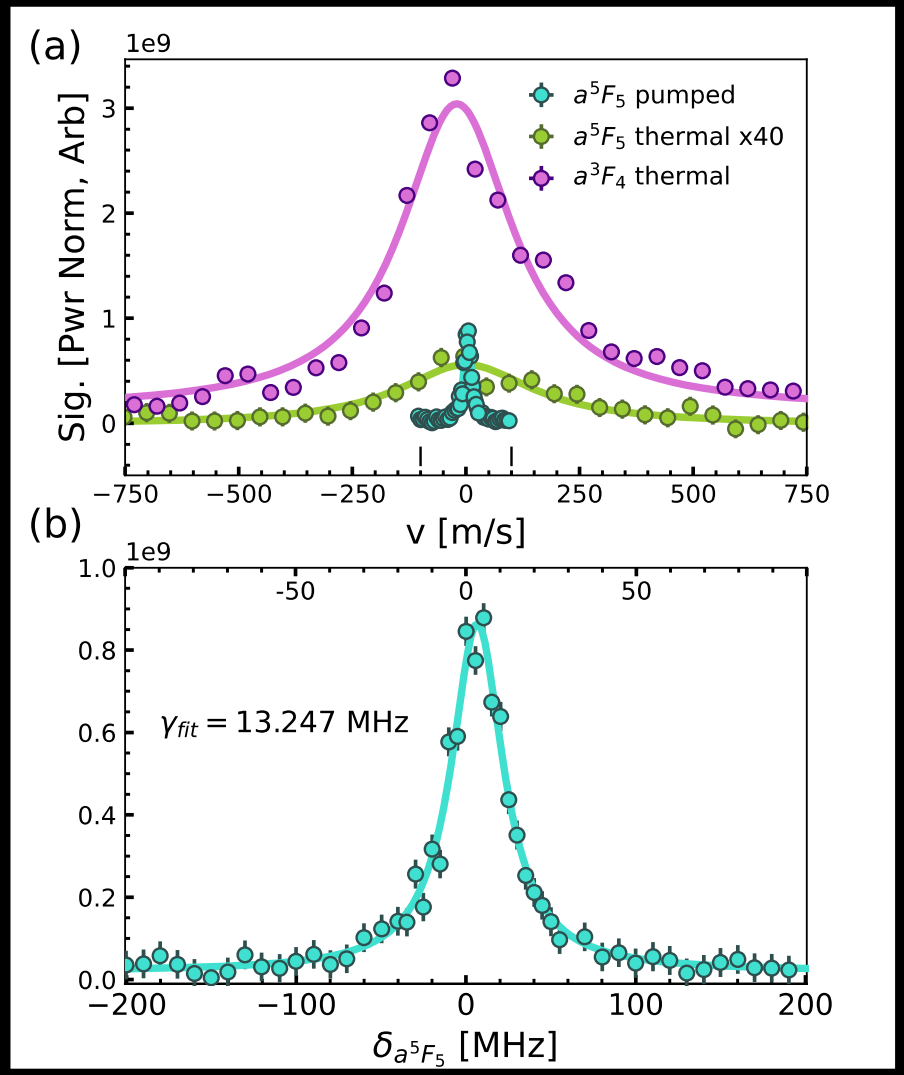
$a\ {}^3F_4 \rightarrow y\ {}^5D_4$ (391 nm)



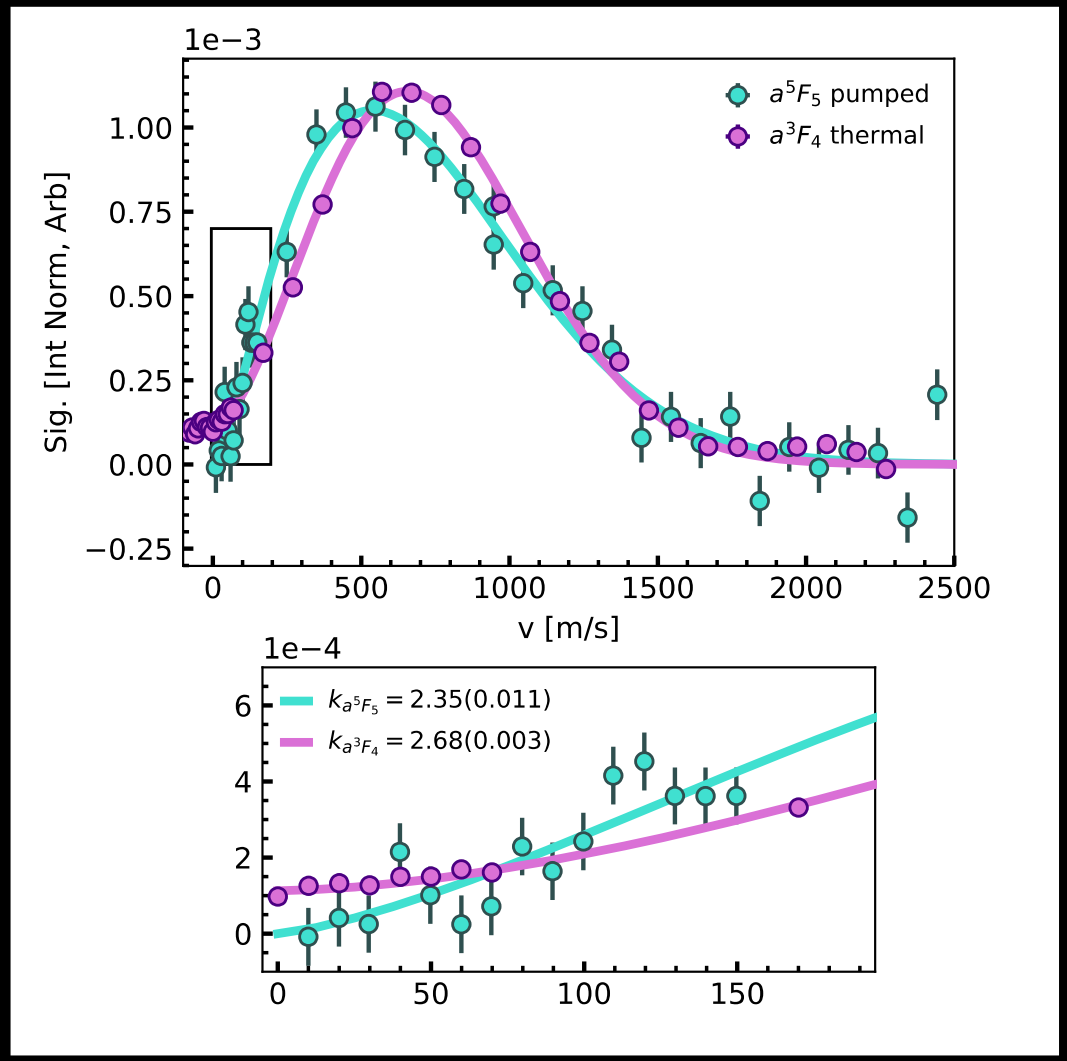


Atomic physics with a titanium-sublimation vacuum pump

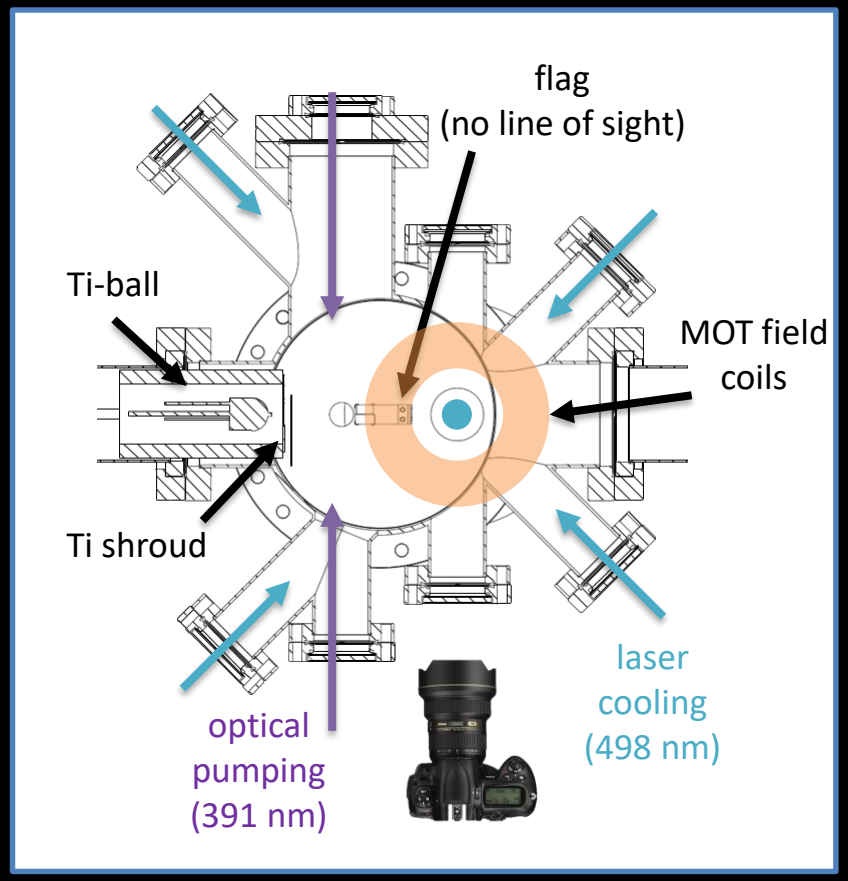
transverse Doppler profiles



longitudinal Doppler profiles



Direct loading of a magneto-optical trap (MOT) from a Ti-sub pump (?)

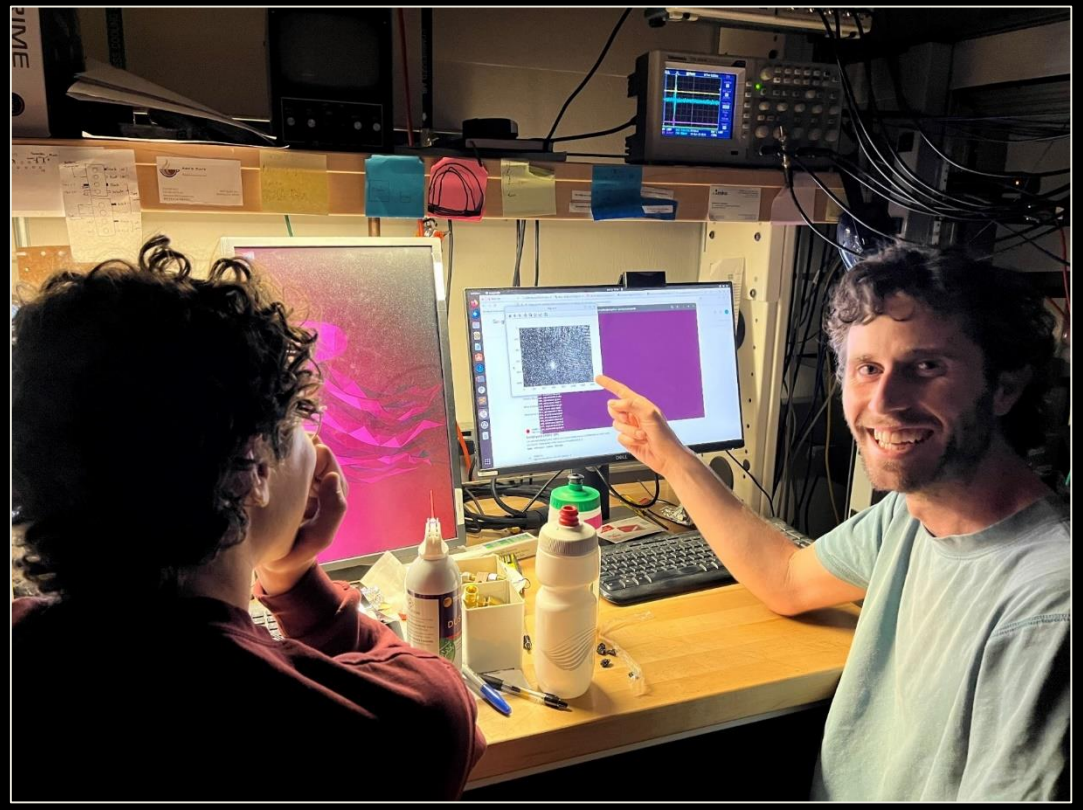


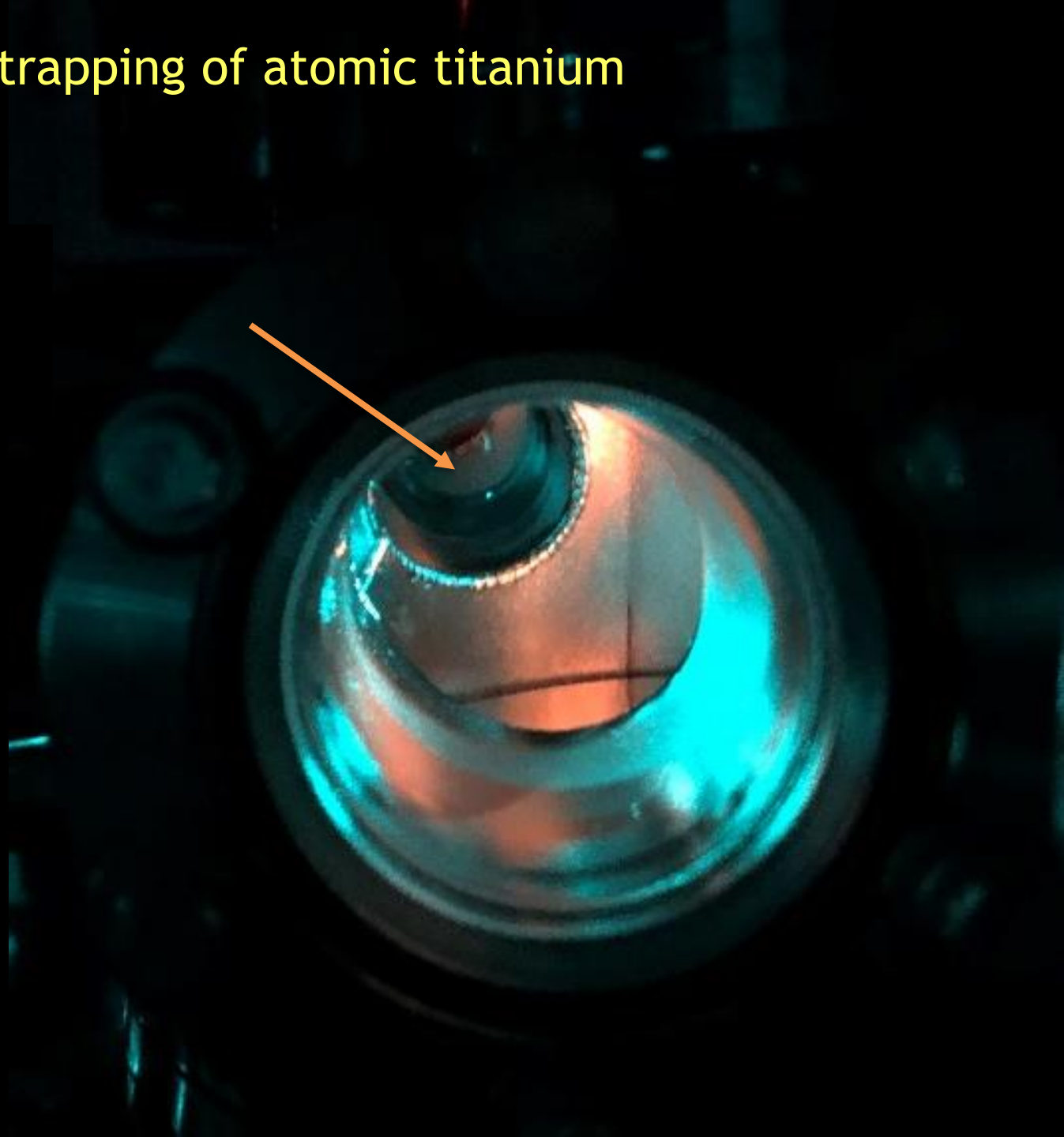
- Try to laser cool and trap the low-velocity tail ($\leq 50\ m/s$?) of a 1600 K thermal distribution ($v_{th} = 750\ m/s$)
- Block direct line of sight

First laser cooling and trapping of atomic titanium

OCTOBER 2023

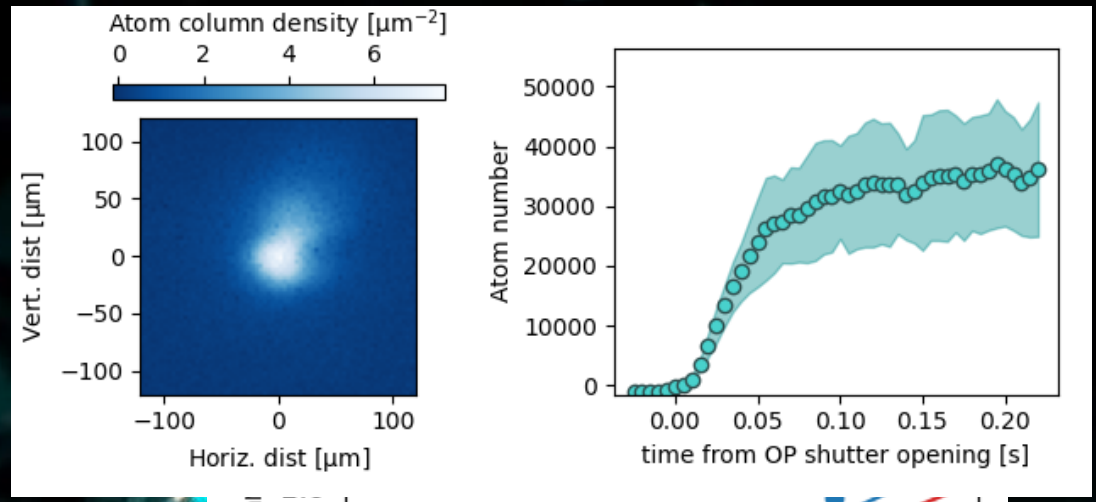
FRIDAY THE 13TH

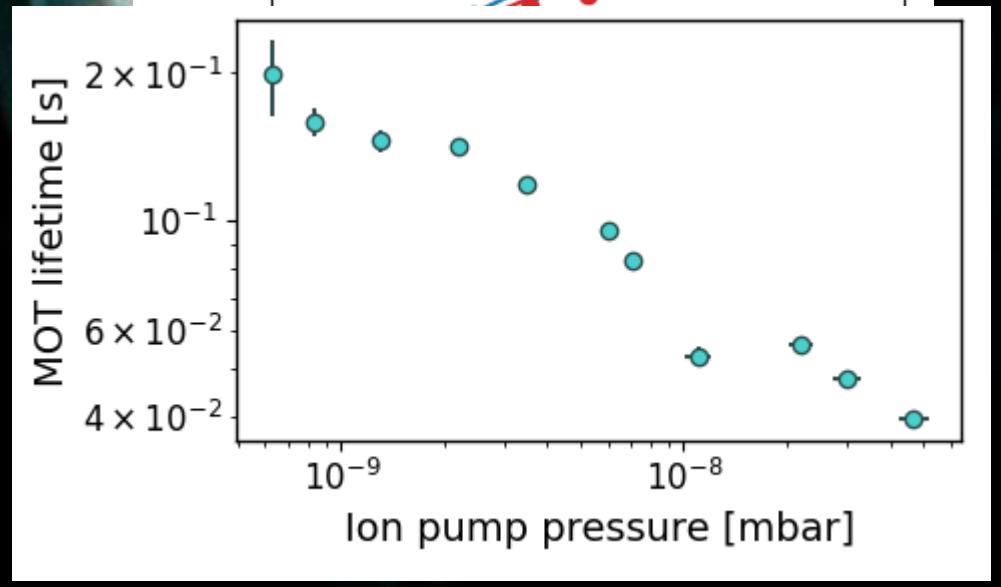




First laser cooling and trapping of atomic titanium

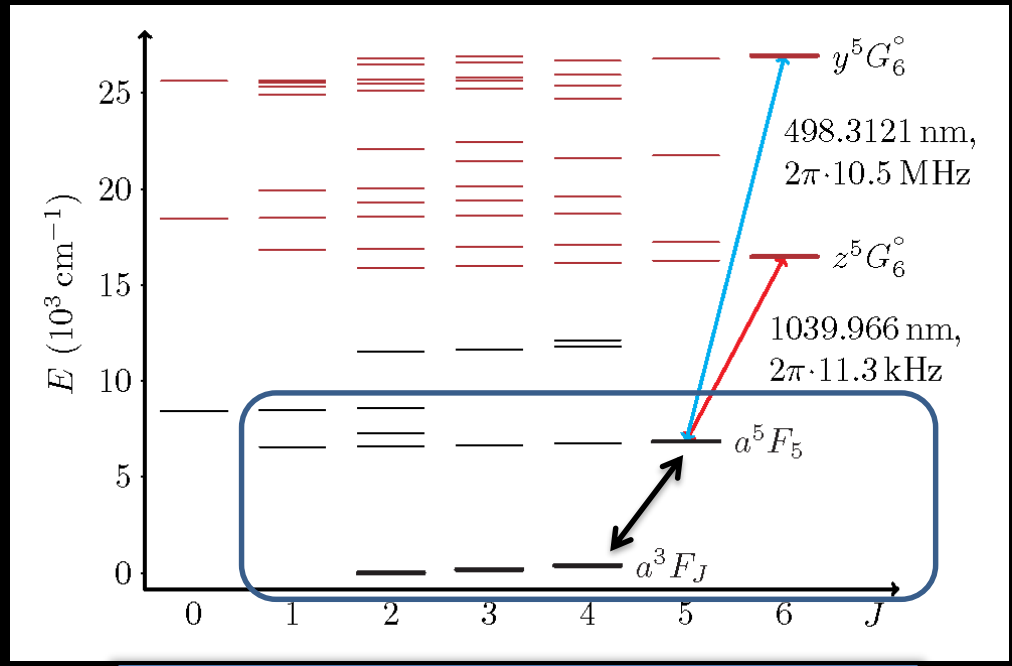
- Magneto-optical trapping achieved separately for three $I = 0$ isotopes: ^{46}Ti, ^{48}Ti, ^{50}Ti
  - based on isotope spectroscopy of laser cooling (498 nm) [PRA **103**, 032818 (2021)] and optical pumping (391 nm) transitions
- Atom number estimate: $N \sim 5 \times 10^4$
  - rudimentary setup, many improvements to come
- Atom temperature estimate: $T \sim 250$ μK (Doppler)
  - polarization-gradient cooling? $T \sim 10$ μK
  - narrow-line MOT? $T \sim 100$ nK (Doppler)
- Lifetime measurement allows for estimated upper bound for leakage out of laser cooling transition: $\leq 2 \times 10^{-6}$
  - also constrains light-induced loss rate: $\beta \leq 2 \times 10^{-11}\ cm^3 s^{-1}$





Some next steps

- Mini Ti-ball MOT
  - Lots of little fixes, characterization
  - Fermionic isotopes
  - First steps toward telecommuncations-band optical clock
  - Ti atoms in optical tweezers
  - Internal state manipulations
- Brighter sources ⇒ more atoms ⇒ quantum gases
  - Ablation-fed buffer gas beam ⇒ 2D MOT
  - Ti-sub beam ⇒ Zeeman slower
- Other transition metals!

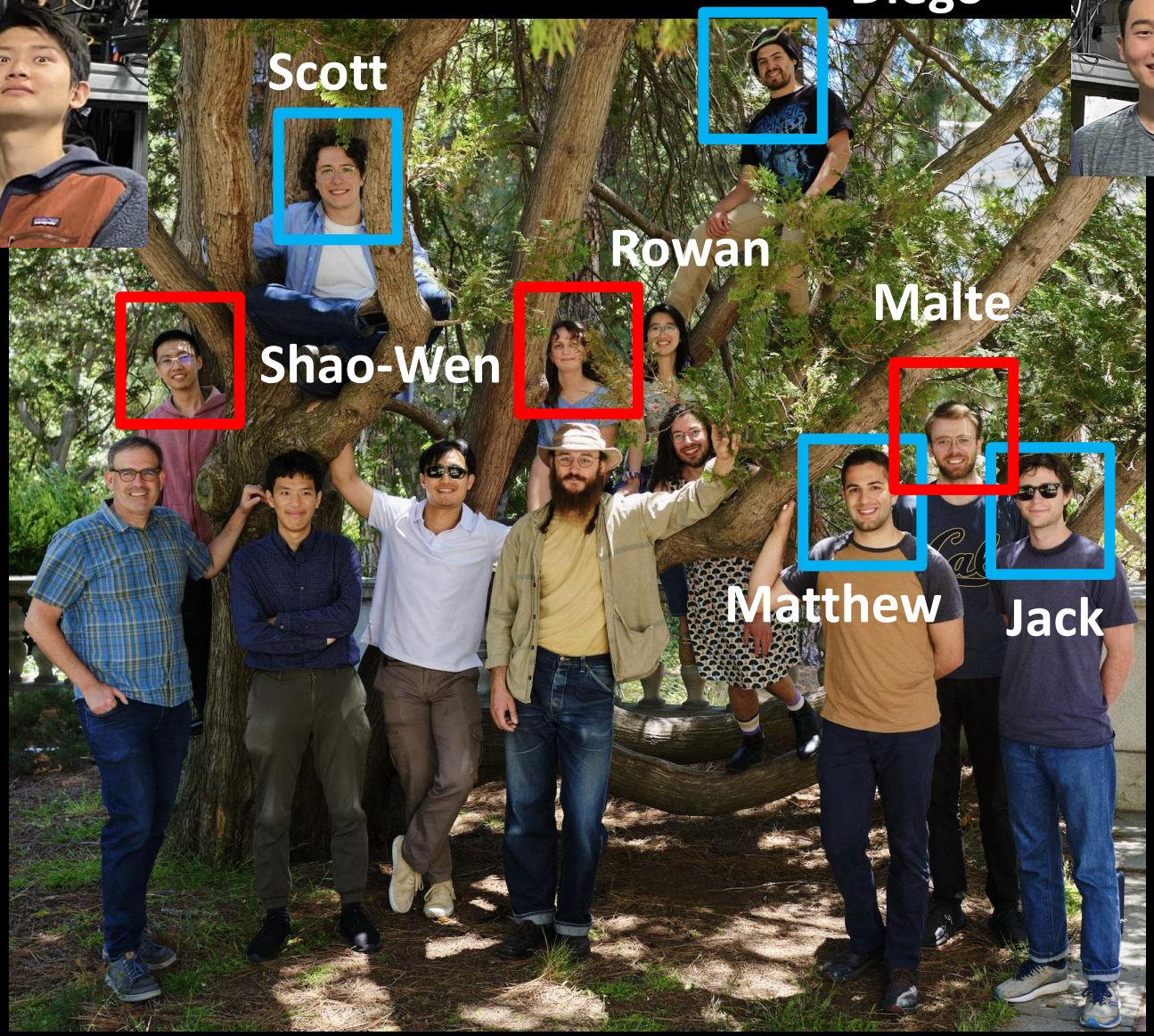


1549 nm wavelength, 240 μHz linewidth

"Optical telecommunications-band clock based on neutral Ti atoms"

Phys. Rev. A 107, L051102 (2023)







E8 team

Scott Eustice
Diego Novoa
Jack Schrott
Matthew Bilotta

E9 team

Shao-Wen Chang
Rowan Duim
Malte Schwarz

$$ Thanks! AFOSR, ARO (MURIs and single PI), DARPA, DOE (QSA), NSF, ONR, Heising-Simons

CIQC Challenge Institute for Quantum Computation